REGULATION OF

NR1/NR2B NMDA RECEPTOR FUNCTION BY THROMBIN

LEUNG HOW WING

B.Sc. (Hons.), NUS

A THESIS SUBMITTED FOR THE DEGREE OF

DOCTOR OF PHILOSOPHY

DEPARTMENT OF PHARMACOLOGY

NATIONAL UNIVERSITY OF SINGAPORE

2010

ACKNOWLEDGEMENTS

First and foremost, I owe my deepest gratitude to my supervisor, Dr Low Chian Ming for allowing me to join his team and giving his support throughout the course of my PhD study. He has, both consciously and unconsciously, taught me many aspects of doing good experiments. I am indebted to his time, his ideas, his advice and his funding for making my PhD experience a stimulating and a fruitful one. I am also thankful for his patience and understanding in giving me a chance to make and learn from my mistakes and giving me room to mature.

Thanks also go out to my co-supervisor Prof Peter Wong Tsun Hon, who has been giving me priceless feedback and rendering assistance whenever needed.

I would also like to express my sincere thanks to the team under Dr Low Chian Ming for their valuable assistance. My keen appreciation goes to Cheong Yoke Ping and Zhang Yi Bin for their technical support and Karen Wee Siaw Ling and Ng Kay Siong for bringing about stimulating discussions, giving helpful suggestions and encouragement. Other past lab members that I have the pleasure to work alongside with are: Dr Rema Vazhappilly, Dr Ng Fui Mee, Dr Vivien Koh and Lim Peiqi, who are always willing to share their technical expertise. I would also like to thank Chen Jing Ting and Noella Anthony for their technical assistance.

I would also like to express my appreciation to our collaborators: Prof Stephen F. Traynelis (Emory University, School of Medicine, Atlanta, GA) for his critical comments in my work; Prof Hiro Furukawa (Cold Spring Harbor Laboratory, Cold Spring Harbor, NY) for providing crucial crystal structure information and insightful views; Dr Yuan Hongjie (Emory University, School of Medicine, Atlanta, GA) for providing technical advice and Dr Zhang Bing (National University of Singapore, Research Centre of Excellence in Mechanobiology, Singapore) for the molecular dynamics simulation.

It is also an honor for me to thank my thesis examiners for their time and interest in my study.

Lastly, I would like to thank my family for their encouragement, patience and understanding. For my parents who took care of my well being and supported me in my pursuits and for my sister who had taken up most of the family responsibilities and allowed me time to concentrate on my study.

This thesis would not have been possible without the support of many people. I hereby thank you all.

TABLE OF CONTENTS

LIST OF PUBLICATIONS

1) Xi-Kai Wee, Kay-Siong Ng, How-Wing Leung, Yoke-Ping Cheong, Kah-Hoe Kong, Fui-Mee Ng, Wanqin Soh, Yulin Lam and Chian-Ming Low. Mapping the high-affinity binding domain of 5-substituted benzimidazoles to the proximal N-terminus of the GluN2B subunit of the NMDA receptor. **British Journal of Pharmacology** 2010, 159:449-461

2) How-Wing Leung, Kay-Siong Ng, Yoke-Ping Cheong, Peter Tsun-Hon Wong, Hiro Furukawa and Chian-Ming Low. Thrombin modifies NMDA receptor sensitivity to ifenprodil and glycine: proteolytic cleavage at lysine 318 of NR2B. (In preparation)

ABSTRACT

1) How-Wing Leung, Peter Tsun-Hon Wong and Chian-Ming Low. A novel clinical implication of thrombin extravasation in the brain: proteolytic cleavage on NMDA receptors. **2nd Taiwan/Hong Kong (CU)/Singapore Meeting of Pharmacologist 2008, Kaoshiung, Taiwan.**

2) Chian-Ming Low, Xi-Kai Wee, Kay-Siong Ng, How-Wing Leung, Yoke-Ping Cheong, Kah-Hoe Kong, Fui-Mee Ng, Wanqin Soh and Yulin Lam. Benzimidazole derivatives bind at sub-nanomolar concentrations to recombinant protein of the NR2B amino-terminal domain of NMDA receptor. **38th Annual Meeting of Society for Neuroscience 2008, Washington DC, USA (*Abstr.* 131.4)**

3) How-Wing Leung, Peter Tsun-Hon Wong and Chian-Ming Low. Regulation of NR1/NR2B NMDA receptor function by thrombin. **37th Annual Meeting of Society for Neuroscience 2007, San Diego, USA. (*Abstr.* 678.16)**

4) How-Wing Leung, Stephen F. Traynelis, Peter Tsun-Hon Wong and Chian-Ming Low. A 30 kDa cleaved fragment from NMDA receptor in mammalian brain by thrombin. **Office of Life Sciences Conference 2007, Singapore.**

SUMMARY

N-methyl-D-aspartate (NMDA) receptor is a subfamily of the glutamate receptors in the central nervous system (CNS) that is involved in the mediation of many physiological activities such as learning and memory. However, overactivation of the NMDA receptors results in excitotoxicity that is often involved in the progression of neuronal cell death in diseases such as ischemic stroke. As such, NMDA receptors are tightly regulated by endogenous mediators.

In particular, the serine protease, thrombin, which is observed in the astrocytes and neurons in the CNS, is involved in modulating the function of the NMDA receptors through the activation of the protease-activated receptor (PAR)-1. Direct interaction with the NMDA receptors by thrombin has yet been fully characterized and determined. The aim of the thesis is, thus, to investigate the possibility of direct interaction between thrombin and the NMDA receptors and the possible effects in the modulation of the NMDA receptors.

In this study, thrombin was observed to interact with the NR2B of the NMDA receptors from rat brain lysate (RBL) and synaptic plasma membrane (SPM) preparations. Based on epitope mapping and the sizes of the fragments (30 kDa fragment and 150 kDa fragment) observed, thrombin was hypothesized to cleave NR2B at the amino terminal domain (ATD). To identify the site of interaction of NR2B with thrombin, the NR2B ATD was expressed as a soluble recombinant fusion protein (MBP-ATD2B) and was subjected to thrombin treatment. N-terminal sequencing of the thrombin-cleaved product deduced the cleavage site to be Lys^{318} at the NR2B ATD. The cleavage site was further confirmed through the absence of cleavage on the MBP-ATD2B(K318A).

Thrombin cleavage studies performed on cortical neuronal culture also demonstrated that thrombin could cleave NR2B expressed in heteromeric NMDA receptors complex. Through two-electrode voltage clamp (TEVC) recordings on *Xenopus laevis* oocytes

expressing NR1/NR2B receptors, it was also observed that a reducing environment, one of the conditions of ischemic stroke, resulted in more efficient thrombin cleavage of NR2B, as demonstrated by a reduction in ifenprodil inhibition. Molecular dynamics simulation based on the NR2B ATD crystal structure also provided an insight into how a reducing environment exposed the Lys^{318} to the extracellular milieu, allowing for interaction with thrombin.

In the final part of the thesis, the various effects of the cleavage were investigated through TEVC recordings. In particular, the deletion construct, with the ATD region up to Lys^{318} removed (NR2B-ΔATD-K318) demonstrated an increase in the ifenprodil IC_{50} and a change in the EC_{50} of glycine and the efficacy of D-cycloserine when co-expressed with NR1. Interestingly, unlike ifenprodil, glycine and D-cycloserine are ligands binding to the NR1 ligand binding domain (LBD) but not the NR2B ATD. These results suggested allosteric modulation of the ATD of NR2 on LBD of NR1 and the importance of the ATD in modulating receptor function.

Taken together, this study had discovered thrombin cleaved NR2B at a specific site at the ATD, which could lead to the alteration of NMDA receptor function. This study had provided an insight on the possible modulation of NMDA receptors through interaction with proteases, in particular, thrombin.

LIST OF TABLES

LIST OF FIGURES

ABBREVIATIONS

AD	Alzheimer's disease
ANOVA	Analysis of variance
ATD	Amino terminal domain
ATIII	Antithrombin III
CNS	Central nervous system
CSF	Cerebrospinal fluid
CTD	Carboxy terminal domain
DIV	Day-in-vitro
DTT	Dithiothreitol
DTNB	5-5-Dithiobis-2-nitrobenzoic acid
EC_{50}	Half maximal effective concentration
eEPSC	Evoked excitatory postsynaptic current
eEPSP	Evoked excitatory postsynaptic potential
EphB	EphrinB receptor
Erk	Extracellular signal-regulated kinase
ER	Endoplasmic reticulum
GAPDH	Glyceraldehyde-3-phosphate dehydrogenase
GFAP	Glial fibrillary acidic protein
IC_{50}	Half maximal inhibitory concentration
ICH	Intracerebral hemorrhage
IgG	Immunoglobulin G
iGluRs	Ionotropic glutamate receptors
LBD	Ligand binding domain
LDLR	Low density lipoprotein receptor
LIVBP	Leucine isoleucine valine binding protein

LRP1	Lipoprotein receptor-related protein
LTP	Long term potentiation
MAGUK	Membrane associated guanylate kinase
MCAO	Middle cerebral artery occlusion
mEPSC	Miniature excitatory postsynaptic current
MMP	Matrix metalloproteinase
MTSEA	2-Aminoethyl methanethiosulfonate hydrobromide
NMDA	*N*-methyl-D-aspartate
OGD	Oxygen-glucose deprivation
PAR	Protease-activated receptor
PD	Parkinson's disease
PKC	Protein kinase C
PN-1	Protease nexin I
P_{OPEN}	Open probability
PPACK	D-Phe-Pro-Arg-chloromethylketone
PSD	Postsynaptic density
PVDF	Polyvinyldine difluoride
RBL	Rat brain lysate
RIPA	Radioimmunoprecipitation assay
SAP	Synapse-associated protein
SDS-PAGE	Sodium dodecyl sulfate polyacrylamide
S.E.M.	Standard error of the mean
SPM	Synaptic plasma membrane
tPA	Tissue plasminogen activator
TEVC	Two-electrode voltage clamp

Chapter 1

Introduction

1 Introduction

1.1 Glutamate receptors

Chemical synapses are the primary sites of communication between nerve cells. They are the specialized junctions where a presynaptic cell releases vesicles loaded with neurotransmitters to the receptors located on the adjacent postsynaptic cell (Lisman et al., 2007; Chen et al., 2008c). There are excitatory and inhibitory neurotransmitters. Glutamate is one of the most common excitatory neurotransmitters and it binds to the glutamate receptors. Glutamate receptors are categorized into two groups namely the ionotropic glutamate receptors (iGluRs) and the metabotropic glutamate receptors (mGluRs). The mGluRs are G-protein coupled receptors. Based on their amino acid sequence, intracellular coupling mechanisms and pharmacological properties, mGluRs are classified into three main groups, Group I (mGluR1 and mGluR5), Group II (mGluR2 and mGluR3) and Group III (mGluR4, mGluR6, mGluR7 and mGluR8) (Fig. 1.1) (Nakanishi, 1992; Niswender and Conn, 2010).

The iGluRs are ligand-gated ion channels. They are structurally distinct from the mGluRs and exist as proteins containing three transmembrane domains. iGluRs are multimeric proteins made up of different subunit stoichiometry. They are pharmacologically categorized into three subclasses, (1) α-amino-3-hydroxy-5-methyl-4-isoxazolepropionic acid (AMPA) receptors (GluR1-4), (2) kainate receptors (GluR5-7, KA-1 and KA-2) and (3) *N*-methyl-D-aspartate (NMDA) receptors (NR1, NR2A-D and NR3A and NR3B) (Fig. 1.1) (Dingledine et al., 1999).

Unlike other ligand-gated ion channels, the NMDA receptors harbor a magnesium (Mg^{2+}) binding site within the channel pore and binding of extracellular Mg^{2+} is strongly voltage dependent (Mayer et al., 1984; Nowak et al., 1984; MacDermott et al., 1986). As a result, activation of the NMDA receptors requires both ligand binding and partial relieve of the voltage-dependent Mg^{2+} block by depolarization. Upon activation, the resulting calcium (Ca^{2+}) flux triggers a variety of intracellular signaling cascades. Hence under physiological conditions, NMDA receptors play a pivotal role in many central nervous system (CNS) functions such as neurological development and in forms of synaptic plasticity that underlie

higher order processes such as learning and memory (Bliss and Collingridge, 1993; Maren and Baudry, 1995; Asztely and Gustafsson, 1996; Lau and Zukin, 2007; Yashiro and Philpot, 2008). However, under conditions when the NMDA receptors are overactivated, they are implicated in neurological disorders such as ischemic stroke, brain trauma and chronic neurodegenerative diseases (Dirnagl et al., 1999; Arundine and Tymianski, 2003). Hence, the NMDA receptors have become the interest of many researchers in search for potential neuroprotective agents.

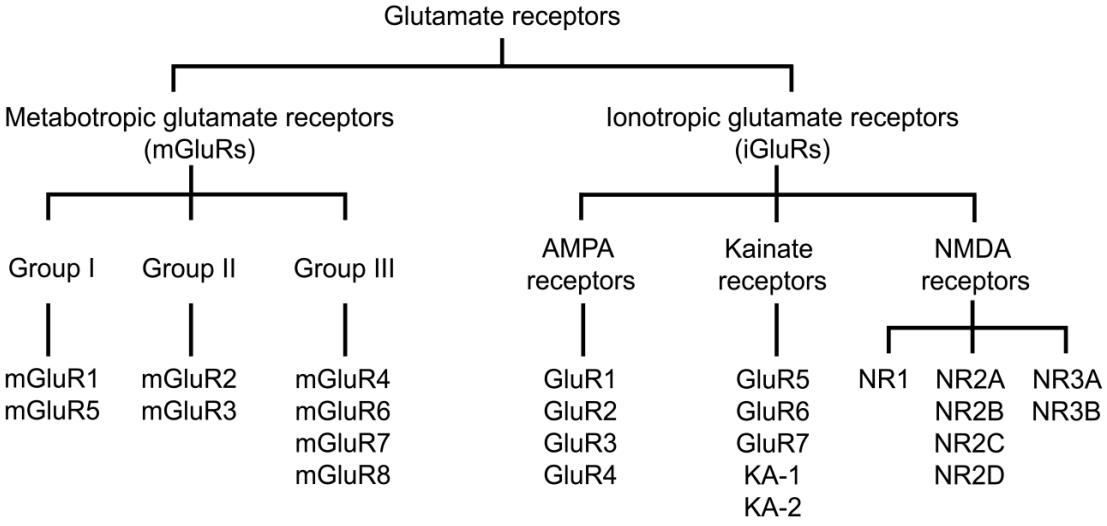

Fig. 1.1. Different subfamilies of the glutamate receptors and their subunits.

1.2 Composition of NMDA receptors

1.2.1 NR1, NR2 and NR3 subunits: regional and temporal expression and biophysical properties of NMDA receptors

Three subunits, namely NR1, NR2 and NR3, have been cloned and studied (Hollmann and Heinemann, 1994; Ciabarra et al., 1995; Nishi et al., 2001; Chatterton et al., 2002). The NR1 is encoded by one gene. From being barely detectable at embryonic day 14 (E14), the mRNA of NR1 gradually increases during development until the third postnatal week. It decreases slightly to adult level and is detected in all neuronal cell types (Laurie and Seeburg, 1994a). The hippocampus, hypothalamus and the olfactory bulb have high expressions of the NR1 (Moriyoshi et al., 1991). The NR1 contains three alternatively spliced exons: exon 5 in the N-terminus (N1 cassette) and exon 21 (C1 cassette) and exon 22 (C2 cassette) in the C terminus. C2 contains an alternative splice site such that part of the C2, including the stop codon, can be spliced out. This produces an alternative C2' cassette and a new reading frame before the next stop codon is reached. The insertion and deletion of different combination of exons result in eight NR1 splice variants (Fig. 1.2). The splice variants give the NMDA receptors different biophysical properties. For example, variants lacking the N1 cassette insertion are more sensitive to proton (H^+) and zinc (Zn^{2+}) whereas variants containing the C1 cassette are modulated by the protein kinase C (PKC) (Tingley et al., 1993; Traynelis et al., 1995; Traynelis et al., 1998; Logan et al., 1999). Variants harboring the C2' cassette have enhanced cell surface expression (Okabe et al., 1999; Standley et al., 2000; Horak and Wenthold, 2009). Expression of the splice variants is temporally distinct. NR1-1 and the NR1-4 account for the greater proportion of adult NR1 mRNA while the NR1-3 mRNA is relatively scarce and is detected only at a low level during the postnatal stage (Laurie and Seeburg, 1994a). Splice variants expression is also regionally unique, for example, the NR1-(1-4)a and NR1-2 splice forms occur homogeneously throughout the brain gray matter but the NR1-(1-4)b are found primarily in the sensorimotor cortex, neonatal lateral caudate, thalamus, hippocampal CA3 cells and in the cerebellar granule cells (Laurie and Seeburg, 1994a; Standaert et al., 1994).

The NR2s are encoded by four different genes producing the four different subunits, NR2A-D. They are 55 to 70 % identical in sequence and are structurally related (Monyer et al., 1992). NR2 has to co-express with the NR1 to be functional NMDA receptors. The mRNA of NR2B and NR2D are found prenatally, while NR2A and NR2C are only detected near birth. NR2A-C peak around postnatal day 20 (P20) while NR2D peaks around P7. After which, all decrease to their respective adult level (Monyer et al., 1994). Most notably, there is a shift in the ratio of NR2B in a prenatal brain to NR2A in a mature adult brain (Sheng et al., 1994; Yashiro and Philpot, 2008). There is also specific spatial expression for NR2 subunits. NR2A and NR2B are most abundantly expressed in the hippocampus CA1 and CA3 pyramidal cells; NR2C are mostly found in the cerebellum and NR2D is prominently expressed in the thalamus (Wenzel et al., 1997). The NR2 subunits endow NMDA receptor complexes with distinct pharmacological and kinetic properties. For example, the order of potency of glycine follows NR2D > NR2C > NR2B > NR2A with the largest ratio between NR2A and NR2D (10-fold) (Chen et al., 2008b). In a similar order, the glutamate potency is the largest between the NR2A and NR2D (7-fold) (Laurie and Seeburg, 1994b; Erreger et al., 2007). Efficacies for the partial agonist D-cycloserine also differ among the NR2 subunits, with NR2B and NR2C having the lowest and the highest efficacy respectively (Sheinin et al., 2001; Dravid et al., 2010). The activation and deactivation of the NMDA receptors are also dependent on the NR2 subunit that is expressed. The peak open probability (P_{OPEN}) for NR2A differs from NR2B by four-fold, contributing to the differences in peak current density (Stern et al., 1992; Chen et al., 1999; Erreger et al., 2005; Gielen et al., 2009; Yuan et al., 2009a). NR2A and NR2B have a slow component of Mg^{2+} unblock that is not found in NR2C and NR2D. As a consequence, NR2C and NR2D respond more quickly to fast depolarization compared to NR2A and NR2B (Clarke and Johnson, 2006). The mean open duration is also dependent on subtypes. For example, NR2A has a overall mean open duration of 35.8 ms while that of NR2D is 1602 ms (Wyllie et al., 1998). Deactivation time is also subunit dependent in the following manner NR2A > NR2B > NR2C > NR2D (Vicini et al., 1998; Wyllie et al., 1998; Chen et al., 1999; Erreger et al., 2005). Besides modulating the

pharmacology and kinetics of the heteromeric NMDA receptors, NR2 also governs the differential binding to modulators and protein. For example, interaction with Zn^{2+} at the extracellular region is subtype specific with NR2A having the highest apparent affinity as evident by the lowest Zn^{2+} half maximal inhibitory concentration (IC_{50}) compared to that of other subtypes (Fayyazuddin et al., 2000; Rachline et al., 2005). Intracellulary, NR2A and NR2B interaction with the PKC at the C-terminal results in the enhancement of the NMDA receptor-mediated Ca^{2+} flux while NR2C and NR2D interaction with the PKC results in suppression of Ca^{2+} flux (Grant et al., 1998). Trafficking of the NMDA receptors from the endoplasmic reticulum (ER) compartment to the cell surface membrane is also mediated by NR2 subunits (Qiu et al., 2009). Reduction/oxidation (redox) action is also dependent on the NR2 subtype identity (Kohr et al., 1994). Considering the differences among the subtypes and their specific temporal and regional characterization, the heterogeneity of the NMDA receptors plays an important role in mediating the numerous functions in the brain. In particular, the shift in the ratio of receptors containing NR2B and NR2A subunits, contributes to the developmental changes in synaptic plasticity and long term potentiation or depression in the brain (Ewald et al., 2008; Yashiro and Philpot, 2008; Cho et al., 2009).

The NR3 are encoded by two genes, resulting in two subunits, namely NR3A and NR3B. NR3A and NR3B are closely related with 47 % identity in sequence homology (Chatterton et al., 2002). The NR3A expression level is high in the postnatal brain and decreases at P12 to adult level (Ciabarra et al., 1995; Sucher et al., 1995; Al-Hallaq et al., 2002; Wong et al., 2002; Low and Wee, 2010). In adulthood, NR3A is detected predominantly in the thalamus, the nucleus of the lateral olfactory tract and the spinal cord (Ciabarra et al., 1995; Sucher et al., 1995). The NR3A also undergoes splicing at the C-terminal with a 60 base pairs insertion, generating two variants, NR3A-1 (shorter variant) and NR3A-2 (longer variant). The NR3A splice variants are also expressed in a regionally and temporally specific manner (Sun et al., 1998). For the NR3B subunit, it starts its expression from P10-P14 and peaks at P21. The level of expression is maintained to adult stage (Fukaya et al., 2005). It is predominantly expressed in the motor neurons in the ventral horn of the

spinal cord and the facial and trigeminal nuclei of the brainstem in the adult nervous system (Andersson et al., 2001; Nishi et al., 2001; Chatterton et al., 2002; Bendel et al., 2005). It is also expressed in the forebrain and cerebellum (Wee et al., 2008). The NR3s are suggested to modulate the NR1/NR2 heteromers by reducing current responses and may also confer the NMDA receptors different sensitivity to Mg^{2+} ions (Das et al., 1998; Matsuda et al., 2002; Matsuda et al., 2003; Tong et al., 2008; Low and Wee, 2010).

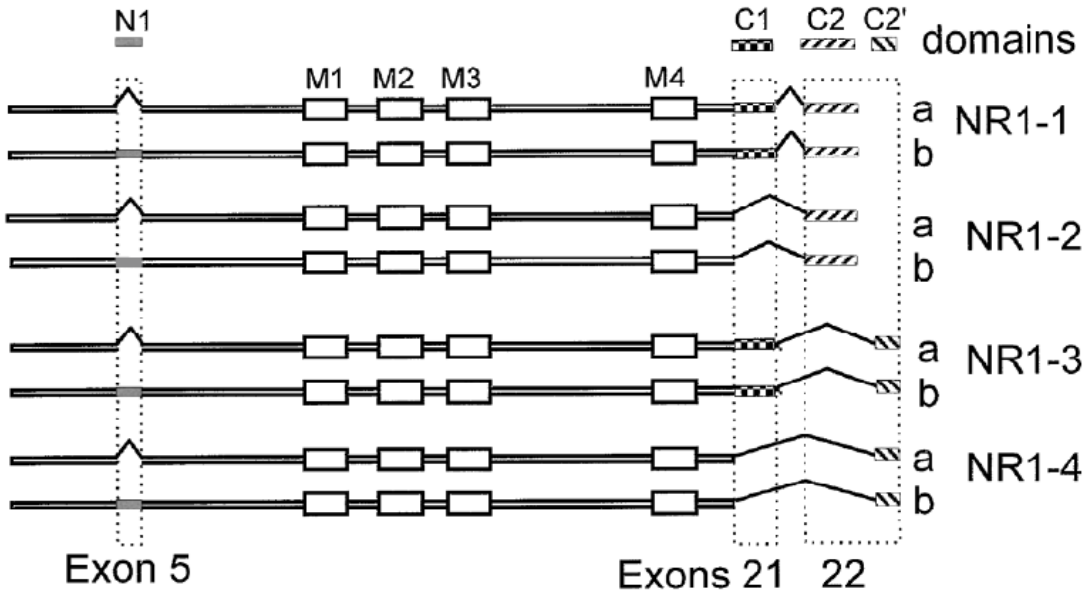

Fig. 1.2. Schematic representation showing the different splice variants of the NR1 subunit. (Adapated from Pharmacological Reviews 1999, 51: 7-61)

1.2.2 Receptor stoichiometry

The NMDA receptors are heteromeric structures made up of the obligatory NR1 subunit in combination with NR2 (NR2A-D) and/or NR3 (NR3A-B). There have been controversies with regards to the stoichiometry of the NMDA receptors. Earlier studies based on the pattern of single-channel conductance states and biochemical investigations have favored the concept that the NMDA receptors are pentameric structures (Brose et al., 1993; Premkumar and Auerbach, 1997; Hawkins et al., 1999). However, recent studies corroborate with the tetrameric structure. Using binomial analysis of the glutamate and glycine dose-response obtained from three receptors populations expressed by different combinations of

wild-type NR1, NR2 and low agonist-affinity mutant NR1, NR2, it is hypothesized that the NMDA receptors follow a tetrameric structure with two glycine binding sites contributed by the NR1 and two glutamate binding sites contributed by the NR2 (Laube et al., 1998). The emergence of the heterodimer NR1-NR2A ligand binding domain protein crystal also fuel the inclination towards a dimer of dimers model (Furukawa et al., 2005). However, one concern with this model is the mismatch between the expected four-fold symmetry of the ion channel pore and the two-fold symmetry required by the dimer of dimers (Mayer, 2006). The recent tetrameric protein crystal structure of the GluR2 gives a glimpse on how this concern can be resolved. The symmetry mismatch is mediated by two pairs of conformationally distinct subunits. Guided by the crystal structure GluR2, luminescence resonance energy transfer (LRET) investigations and cysteine-crosslinking experiments, it is predicted that the NMDA receptor subunits exhibit a 1-2-1-2 pattern, indicative of a dimer of dimers pattern of a tetrameric structure (Sobolevsky et al., 2009; Rambhadran et al., 2010). Studies on the exact subunit composition of the native glutamate receptors are ongoing. Expression of di-heteromeric (e.g. NR1/NR2A) or tri-heteromeric (e.g. NR1/NR2A/NR2B) is regionally and temporally specific (Sheng et al., 1994; Dunah et al., 1998; Tovar and Westbrook, 1999; Dunah and Standaert, 2003; Al-Hallaq et al., 2007; Brothwell et al., 2008). NR3 has also been observed to form diheteromeric receptors (NR1/NR3A or NR1/NR3B) and triheteromeric receptors (Ciabarra et al., 1995; Das et al., 1998; Perez-Otano et al., 2001; Chatterton et al., 2002; Yao and Mayer, 2006; Ulbrich and Isacoff, 2008; Low and Wee, 2010; Pina-Crespo et al., 2010).

1.3 Modular structure of the NMDA receptors

The general topology of the NMDA receptors consists of an amino terminal domain, a ligand binding domain, three transmembrane domains (M1, M3 and M4), a re-entrant loop (M2) and a carboxy terminal domain. The N-terminus is located extracellularly and the C-terminus is at the intracellular region (Fig. 1.3).

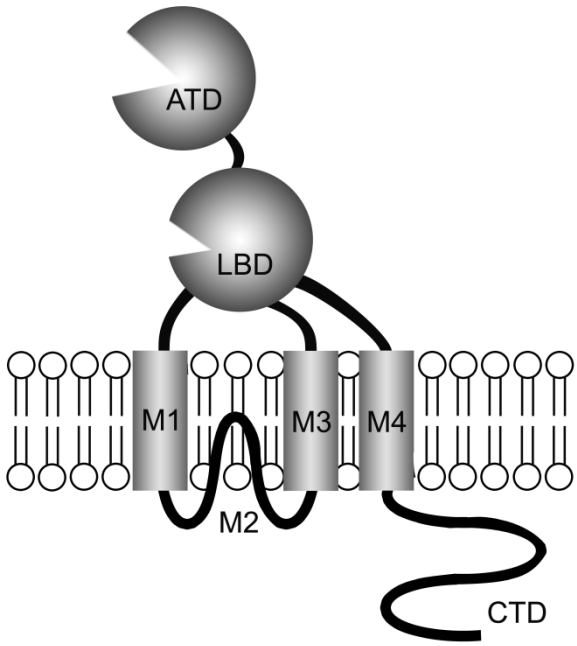

Fig. 1.3. Modular structure of a NMDA subunit. It consists of an amino terminal domain (ATD), a ligand binding domain (LBD), three transmembrane domains (M1, M3 and M4), a re-entrant loop (M2) and a carboxy terminal domain (CTD).

1.3.1 The amino terminal domain (ATD)

The ATD is composed of the first 400 amino acids located extracellularly (Fig. 1.3). It has a weak structure homology with the bacterial amino-acid binding protein, leucine isoleucine valine binding protein (LIVBP) (Masuko et al., 1999; Paoletti et al., 2000; Marinelli et al., 2007). The crystal structure of the monomeric NR2B ATD demonstrates that the ATD has a clamshell-like architecture composed of two domains (R1 and R2). These two domains are connected to each other by three well-structured loops (Karakas et al., 2009). The ATD is an important site for the modulation of the NMDA receptors (Hansen et al., 2010). Depending on the subunit composition, the ATD can modulate the function of NMDA

receptors through interaction with modulators like Zn^{2+}, phenylethanolamine, H^{+}, polyamine and redox agents (Traynelis et al., 1995; Gallagher et al., 1997; Masuko et al., 1999; Fayyazuddin et al., 2000; Low et al., 2000; Choi et al., 2001; Perin-Dureau et al., 2002a; Hatton and Paoletti, 2005; Rachline et al., 2005; Madry et al., 2007a; Han et al., 2008; Gielen et al., 2009; Mony et al., 2009b). The ATD is also involved in the assembly and trafficking of the NMDA receptors (Meddows et al., 2001; Qiu et al., 2009). The ATD of the NR2 participates in the modulation of channel kinetics and the agonist and partial agonist potencies (Madry et al., 2007a; Gielen et al., 2009; Yuan et al., 2009a; Dravid et al., 2010).

1.3.2 The ligand binding domain (LBD)

The LBD is made up of two discontinuous segments, S1 and S2 (Stern-Bach et al., 1994). The S1 is the region between the ATD and M1 and the S2 is the extracellular loop between M3 and M4 (Fig. 1.3). The LBD lies extracellularly. Similar to the ATD, the LBD has a clamshell-like structure and also has a weak structure homology with the LIVBP (Kuryatov et al., 1994; Stern-Bach et al., 1994; Furukawa and Gouaux, 2003). The LBD of the NR1 heterodimerizes with that of the NR2, forming an asymmetric unit. They are arranged in a back-to-back fashion, making various contacts, namely subsite I, subsite II and subsite III (Furukawa et al., 2005). The LBD is the region for agonist binding. For the NR1, the LBD binds to the co-agonist glycine or the endogenous D-serine in the CNS while that of NR2 binds to the agonist glutamate (Shleper et al., 2005). The selectivity of NR1 for glycine is due to Val^{689} (absence of hydroxyl group) and Trp^{731} (presence of indole ring), which preclude hydrogen bonding with γ-carboxylate oxygen of glutamate. Instead, the Arg^{523} and Arg^{732} form hydrogen bond with the α-carboxylate group and the carboxy group of glycine respectively. In particular, Arg^{732} is not present in other iGluRs (Furukawa and Gouaux, 2003). Distinct from the non-NMDA receptors, the presence of Asp^{731}, Glu^{413}, Tyr^{761} and Tyr^{730} in the NR2A allow binding with NMDA (Furukawa et al., 2005). Upon binding to the agonist glutamate and the co-agonist glycine, the closure of the LBD changes in conformation which eventually results in the opening of the ion channel (Kleckner and

Dingledine, 1988; Lerma et al., 1990). Besides modulating the ion channel states (open state, closed state and desensitized state) through ligand binding, the LBD is also considered to be the critical domain in coupling the modulating action of the ATD to the ion channel (Lester and Jahr, 1992; Krupp et al., 1998; Villarroel et al., 1998; Regalado et al., 2001; Zheng et al., 2001; Chen et al., 2004b; Erreger and Traynelis, 2005; Gielen et al., 2008; Zhang et al., 2008).

1.3.3 The transmembrane domain

There are three transmembrane domains, M1, M3 and M4 and a re-entrant loop M2 (Fig. 1.3). M1-4 forms the channel pore of the NMDA receptors. The extracellular vestibule is formed by the M1, M3 and M4 of the NR1 subunit. The pre-M1, pre-M4 and the regions C-terminal to M3 form the superficial part while M3 forms the core of the extracellular vestibule (Beck et al., 1999; Sobolevsky et al., 2002b). The M3 of the NR2 also contributes to the core of the extracellular vestibule but is located more externally to that of NR1, thus resulting in staggering pattern (Sobolevsky et al., 2002a). From the core of the extracellular vestibule, M3 leads to the channel's narrow constriction. Thus, M3 is important in channel gating (Jones et al., 2002; Sobolevsky et al., 2002b; Low et al., 2003; Hu and Zheng, 2005b; Yuan et al., 2005; Chang and Kuo, 2008). The narrow constriction is formed by the non-homologous asparagines at the tip of the re-entrant loop M2. M2 makes up the cytoplasmic vestibule of the channel (Kuner et al., 1996; Wollmuth et al., 1996). Extracellular Mg^{2+} binds to M2 and binding is strongly voltage-dependent (Kupper et al., 1996; Williams et al., 1998; Wollmuth et al., 1998). Upon membrane depolarization and relief from Mg^{2+} block, Ca^{2+} will selectively pass through the pore via electrostatics or coordination chemistry (Dingledine et al., 1999).

1.3.4 The carboxy terminal domain (CTD)

The CTD is the region after the M4 domain (Fig. 1.3). It is the key region for interaction with a large complex of cytoplasmic proteins. These proteins include scaffolding proteins, adaptor proteins, cell adhesion proteins, cytoskeletal proteins and components of signal transduction pathways. The CTD harbors a conserved sequence ESDV (at NR2A and

NR2B) or ESEV (at NR2C and NR2D) which is crucial in binding to a family of proteins known as the membrane associated guanylate kinase (MAGUK) (Hung and Sheng, 2002; McGee and Bredt, 2003; Prybylowski and Wenthold, 2004). Members of MAGUKs which interact with the NMDA receptors include postsynaptic density-95 (PSD-95), synapse-associated protein 97 (SAP97), PSD-93 and SAP102 (Sheng and Pak, 2000; Gardoni, 2008). The CTD of each NMDA receptor subunit binds uniquely to the MAGUKs (Cousins et al., 2008; Zhang and Diamond, 2009). Attachment to the MAGUKs brings about interaction with a wide range of signaling molecules such as neuronal nitric oxide synthase (nNOS), protein kinases and various regulators of small G-proteins (Brenman et al., 1996; Husi et al., 2000; Hung and Sheng, 2002). This makes the CTD of the NMDA receptors subunits critical for modulating the downstream signaling (Kim et al., 1998; Komiyama et al., 2002; Kim et al., 2005; Tu et al., 2010). The CTD also associates with components of cytoskeletal proteins such as α-actinin (a spectrin/dystrophin family of actin-binding proteins), yotiao (a filamentous protein) and myosin regulatory light chain (accessory light chain of the actin-based motor myosin II) (Wyszynski et al., 1997; Lin et al., 1998; Bajaj et al., 2009). The interaction with the cytoskeletal components are important for the trafficking from the nucleus to the PSD and the organization of the NMDA receptors at the PSD (Carlisle and Kennedy, 2005). The CTD also harbors serine/threonine kinases and the protein tyrosine kinases phosphorylation sites (Fig. 1.4) (Dingledine et al., 1999; Chen and Roche, 2007). Phosphorylation regulates NMDA receptors' kinetics, P_{OPEN} and conductances, thereby modulating NMDA receptors funtcions (Wang and Salter, 1994; Xiong et al., 1998; Liao et al., 2001; Krupp et al., 2002). Phosphorylation also regulates the trafficking of the NMDA receptors by modulating their ability to bind to other proteins (Lan et al., 2001; Vissel et al., 2001; Grosshans et al., 2002; Chung et al., 2004; Chen and Roche, 2009; Jeffrey et al., 2009). The type of phosphorylation is also subunit specific (Fig. 1.4). The interaction with various intracellular proteins that are involved in downstream signaling and trafficking makes the NMDA receptors important mediators in long term potentiation (LTP).

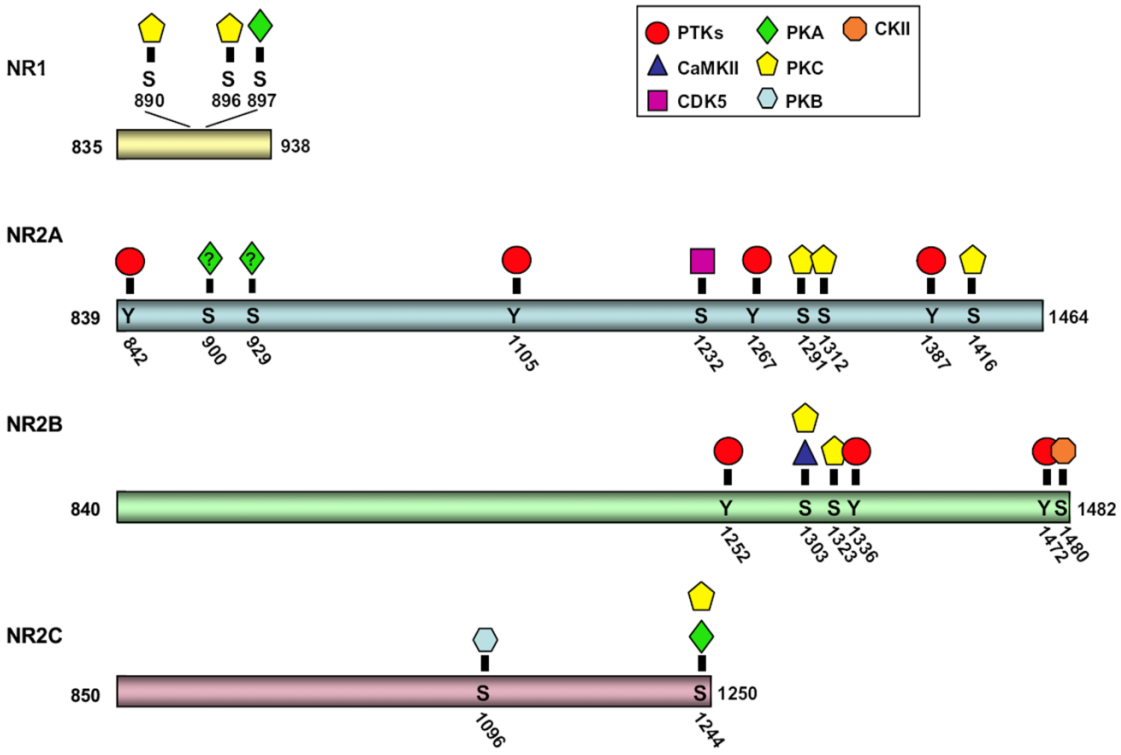

Fig. 1.4. Schematic diagram showing the CTD of NR1 and NR2A-C and their respective phosphorylation sites by different kinases. (Adapted from Neuropharmacology 2007, 53:362-368)

1.4 Activation, relaxation and the endogenous modulators of the NMDA receptors

1.4.1 Activation

Activation of the NMDA receptors requires the binding of the agonist glutamate and the co-agonist glycine or the endogenous D-serine and the relief of the Mg^{2+} channel block. Binding of the agonists is sequential in manner, with each subunit undergoing a conformational change upon binding (Banke and Traynelis, 2003). The conformational changes are related to each other (Gibb and Colquhoun, 1991, 1992; Clements and Westbrook, 1994; Chen et al., 2008b). Conformational changes eventually bring about the opening of the channel pore, allowing the efflux of potassium (K^+) and the influx of sodium (Na^+) and Ca^{2+} (Benveniste and Mayer, 1991; Clements and Westbrook, 1991; Lester et al., 1993; Nahum-Levy et al., 2001; Nahum-Levy et al., 2002). There are three possible consequences upon the binding of agonists; (1) an open state (ion-conducting state) of the receptors, (2) desensitization (long-lived non-conducting state) and (3) the unbinding of agonists (Lester et al., 1990; Lester and Jahr, 1992) . All three can happen with equal probability (Popescu et al., 2004). Considering the numerous conformational changes involved and the dynamics of the NMDA receptors, there are at least three open states and five close states observed in the NR2A-expressing NMDA receptors (Stern et al., 1994; Wyllie et al., 1998). The relative occupancy in the open and the close states determines three discrete modes of activity, i.e. high, medium and low channel P_{OPEN} (Popescu and Auerbach, 2003). The transition among gating modes also determines the relaxation time course (Zhang et al., 2008). Thus within a single activation, the NMDA receptors have multiple conductance level, prolonged periods of intense activity and multiple shut-time components (Cull-Candy and Usowicz, 1987; Jahr and Stevens, 1987; Ascher et al., 1988; Gibb and Colquhoun, 1991; Popescu and Auerbach, 2003). Kinetics of the NMDA receptors are relatively slow compared to other glutamate receptors due to the requirement of multiple conformational changes (contributing to the slow rise time; 7-15 ms) and higher apparent affinity for glutamate (contributing to the slow decay time; 22-4408 ms) (Cull-Candy and Usowicz, 1987; Jahr and Stevens, 1987; Ascher et al., 1988; Lester et al., 1990; Chen et al., 1999; Erreger et al., 2004).

The slow rise time and decay time of the NMDA receptors contribute to the slow component of the excitatory postsynaptic potentials (EPSPs) which makes a dominant contribution to the temporal integration of synaptic inputs (Hestrin et al., 1990; Maccaferri and Dingledine, 2002). Given the pivotal role of NMDA receptors in many physiological and pathophysiological conditions, the NMDA receptors are tightly regulated by extracellular and intracellular factors. Desensitization of the receptors is also crucial in preventing overactivation of the receptors.

1.4.2 Relaxation

Relaxation or the decay of the NMDA receptors has biphasic kinetics. The fast and slow components of decay are due to the occupancy of different close states (Zhang et al., 2008). The close states of the receptors are the result of desensitization. There are three main forms of desensitization; Ca^{2+}-dependent inactivation, glycine-dependent desensitization and glycine-independent desensitization. The composite of the different forms of inactivation and desensitization will determine the overall degree of current flow following activation of the NMDA receptors.

1.4.2.1 Ca^{2+}-dependent inactivation

Ca^{2+}-dependent inactivation results in a decrease in open channel probability following a rise in intracellular Ca^{2+} generated by Ca^{2+} entry through the NMDA receptors or through other routes (Vyklicky, 1993; Tong and Jahr, 1994; Rosenmund et al., 1995; Tong et al., 1995; Rycroft and Gibb, 2004; Wang et al., 2008). Ca^{2+}-dependent inactivation is mediated through an interaction of the CTD with the intracellular proteins and involves the signaling of second messenger systems downstream (Krupp et al., 1999; Rycroft and Gibb, 2004; Wang et al., 2008). This brings about a slower time course of desensitization compared to the other two forms (seconds versus tens or hundreds of milliseconds) (Mayer et al., 1989; Medina et al., 1995). Intracellular Ca^{2+} induces the binding of calmodulin at the CTD of NR1 which affects the interaction of CTD with cytoskeletal proteins such as α-actinin, and this eventually results in the inactivation of NMDA receptors through the translocation of the

receptors (Ehlers et al., 1996; Zhang et al., 1998; Krupp et al., 1999; Lu et al., 2000; Rycroft and Gibb, 2004; Wang et al., 2008). Phosphorylation states at the CTD of the NMDA receptors are crucial in this form of desensitization. Calcineurin, a Ca^{2+}-binding protein, and tyrosine phosphatase dephosphorylate the NR2A receptors, thereby increasing the Ca^{2+}-dependent inactivation while phosphorylation by kinases such as protein kinase A (PKA) and PKC has the opposite effect (Klee et al., 1979; Tong et al., 1995; Westphal et al., 1999; Lu et al., 2000; Krupp et al., 2002; Jackson et al., 2006). The extent of desensitization is NR2 subunit-dependent since NR2A, but not NR2C receptors, is sensitive to Ca^{2+}-dependent inactivation (Krupp et al., 1996; Vissel et al., 2002). Ca^{2+}/calmodulin-dependent protein kinase II (CaMKIIα) also enhances the NR2B desensitization through phosphorylation at the Ser^{1303} and this is dependent on intracellular Ca^{2+} (Sessoms-Sikes et al., 2005).

1.4.2.2 Glycine-dependent desensitization

This refers to the decrement of NMDA receptor currents when the glycine concentration is not saturating and this form of desensitization can be overcome by increasing the concentration of glycine to saturation level (Benveniste et al., 1990; Lerma et al., 1990; Vyklicky et al., 1990). As glycine is a required co-agonist, subsaturating concentration of glycine gives a perceived desensitization of the receptors. It is observed that upon glutamate binding, the apparent affinity of glycine decreases due to negative allosteric coupling between the glutamate binding site at the NR2 and the glycine site at the NR1 subunit (Mayer et al., 1989; Lester et al., 1993). Similarly, NMDA receptors desensitize in an agonist-dependent manner when the glutamate concentration is subsaturating (Nahum-Levy et al., 2001; Nahum-Levy et al., 2002). As the affinity for glycine is subunit dependent, the glycine-dependent desensitization is also subunit-dependent (Kendrick et al., 1998). Modulators affecting the apparent affinity of glycine also influence the glycine-dependent desensitization. Polyamine increases the rate of glycine-dependent desensitization probably through the increase in the apparent affinity for glycine and a decrease in the rate of dissociation for glycine (Benveniste and Mayer, 1993).

1.4.2.3 Glycine-independent desensitization

This refers to the desensitization of the NMDA receptors when the glycine concentration is in saturation and it is independent of Ca^{2+} concentration. The domains involved in this form of desensitization are observed to reside at the pre-M1 domain and the ATD domain (Krupp et al., 1998; Villarroel et al., 1998). NR2A- and NR2B-expressing receptors. Zn^{2+} accelerates the macroscopic desensitization of NR1/NR2A and NR1/NR2B receptors in a dose-dependent manner (Chen et al., 1997). The mechanism behind the Zn^{2+}-dependent desensitization is the allosteric modulation between the ATD and glutamate binding site. Upon binding to glutamate, the apparent affinity for Zn^{2+} increases. This shifts the relaxation of the macroscopic current to a new equilibrium. Higher degree of desensitization is observed with higher concentration of glutamate. Similar interaction between the ifenprodil binding site and glutamate binding site is observed in NR1/NR2B receptors (Zheng et al., 2001). Similarly, it is also observed that in the presence of Zn^{2+}, the half maximal effective concentration (EC_{50}) of glutamate decreases, probably due to the decrease in glutamate affinity (Erreger and Traynelis, 2005). Zn^{2+}-dependent desensitization is subunit-dependent, i.e. NR2A and NR2B are significantly desensitized but not NR2C since Zn^{2+} binds with different affinity to these receptors (Chen et al., 1997; Paoletti et al., 1997; Kendrick et al., 1998). However, this is in contrast with results from Hu and Zheng (2005) where they observed glycine-independent desensitization is not dependent on the above mentioned sites but on the residues in the lurcher motif of NR1 or NR2A (Hu and Zheng, 2005a). The highly conserved lurcher motif located at the M3 is important for channel gating (Kohda et al., 2000; Taverna et al., 2000; Jones et al., 2002). Mutants in the lurcher motif cause a reduction in glycine-independent desensitization and a slower deactivation time constants (Kohda et al., 2000; Hu and Zheng, 2005b). Other pore mutants such as Met^{823} in the M4 domain of NR2A and Asn^{598} in the M2 of NR1 also affect the desensitization and channel gating (Ren et al., 2003; Chen et al., 2004a). Thus the change in desensitization may be accounted for by a change in gating rate. There is also a type of desensitization that is independent of the agonist, Ca^{2+} and Zn^{2+} but related to the interaction with PSD-95. The

interaction with PSD-95 modulates the localization of the NMDA receptors and is important in modulating the desensitization changes during development (Li et al., 2003; Sornarajah et al., 2008).

1.4.3 Endogenous modulators

In view of their involvement in various physiological and pathophysiological conditions, the NMDA receptors are tightly regulated by desensitization and extracellular factors such as H^+, Mg^{2+}, Zn^{2+}, polyamine and a redox environment. NMDA receptors are also regulated intracellularly. Such modulators include kinases, phosphatases and scaffolding proteins. Phosphorylation can alter the channel properties. It can also modulate the interaction between the NMDA receptors with scaffolding proteins thereby regulating the localization of NMDA receptors (van Zundert et al., 2004; Gardoni and Di Luca, 2006; MacDonald et al., 2006; Groc et al., 2009).

1.4.3.1 Modulation by H^+

An increase in the exttracellular concentration of H^+ can suppress the NMDA-activated current. H^+ is a non-competitive ligand as it does not affect the affinities of the agonists (Tang et al., 1990). Inhibition by H^+ has no effect on the unitary conductance or individual open dwell times. Rather, H^+ inhibition is voltage-insensitive and decreases the opening frequency of NMDA receptors, thereby reducing the P_{OPEN}, without altering the time course of desensitization or deactivation (Traynelis and Cull-Candy, 1990; Banke et al., 2005). It is NR1 splice variant-specific with splice variants containing the positively charged residues at the C-terminus end of exon 5, shielded from the tonic H^+ inhibition (Traynelis et al., 1995). It is also dependent on the NR2 subunit with NR2C as the least and NR2B and NR2D as the most sensitive to H^+. IC_{50} of H^+ for NR2B and NR2D is ~pH 7.4, indicating that under normal condition, half of the NMDA receptors will be under tonic inhibition (Traynelis et al., 1995; Low et al., 2003). The physical binding sites to H^+ are dispersed in several regions, including the linker between M3 and S2 of the NR1 and the linker between S2 and M4 of NR2 (Low et al., 2003). The ATD of the NR2 is also involved in fine-tuning the

sensitivity to H^+ (Gielen et al., 2009). Proton inhibition is tightly coupled to the movement of the gating pore (Kashiwagi et al., 1997; Traynelis et al., 1998; Jones et al., 2002; Sobolevsky et al., 2002a; Low et al., 2003; Banke et al., 2005). Modulation of H^+ sensitivity appears to be a common downstream mechanism for a number of the NMDA receptors' allosteric modulators (see below). Thus H^+ acts as an intrinsic protective mechanism when the H^+ concentration is high during hypoxic/ischemic conditions (Giffard et al., 1990; Kaku et al., 1993).

1.4.3.2 Modulation by Mg^{2+}

Mg^{2+} ion binds at a site located at the channel pore of the NMDA receptors thus Mg^{2+} binding effectively blocks the conductance of the NMDA receptors (Kuner et al., 1996; Williams et al., 1998; Yuan et al., 2005). As there is an electric field due to the membrane potential across the plasma membrane, the association and dissociation of Mg^{2+} is sensitive to changes in the membrane potential (Ascher and Nowak, 1988; Jahr and Stevens, 1990; Premkumar and Auerbach, 1996; Vargas-Caballero and Robinson, 2004). Negative membrane potential favors Mg^{2+} binding and thus Mg^{2+} dissociates from its binding site upon membrane depolarization (Wollmuth et al., 1998; Vargas-Caballero and Robinson, 2004). The Mg^{2+} block of the NMDA receptors is therefore voltage-dependent. Upon depolarization, Mg^{2+} can be driven through the channel pore making it a permeant channel blocker (Mayer and Westbrook, 1987; Ascher and Nowak, 1988; Wollmuth et al., 1998). There are two components of Mg^{2+} unblock; a slow component (of several milliseconds) and a fast component (of less than 1 ms) (Spruston et al., 1995; Vargas-Caballero and Robinson, 2003; Kampa et al., 2004; Vargas-Caballero and Robinson, 2004; Clarke and Johnson, 2006). The slow unblock is dependent on NR2, resulting in different sensitivity to Mg^{2+} blockade (Monyer et al., 1992; Ishii et al., 1993; Monyer et al., 1994; Clarke and Johnson, 2006). However, NR3A and NR3B are insensitive to Mg^{2+} block (Chatterton et al., 2002).

1.4.3.3 Modulation by Zn^{2+}

Zn^{2+} inhibits the peak glutamate-evoked current responses in a non-competitive manner (Chen et al., 1997; Fayyazuddin et al., 2000; Rachline et al., 2005). Zn^{2+} inhibits by binding to two sites, namely (1) a high affinity, voltage-independent site and (2) a low affinity, voltage-dependent site (Williams, 1996; Chen et al., 1997; Paoletti et al., 1997; Traynelis et al., 1998). The high affinity Zn^{2+} inhibition is attributable to the slow dissociation of Zn^{2+} from its binding site (Paoletti et al., 1997). Using electrophysiological techniques and analysis based on the crystal structure of ATD, Zn^{2+} is characterized to bind to the cleft of the ATD to mediate the high affinity inhibition (Choi and Lipton, 1999; Fayyazuddin et al., 2000; Low et al., 2000; Paoletti et al., 2000; Karakas et al., 2009). However, binding affinity differs among the NR2 subunits with the IC_{50} spanning more than three orders of magnitude: from low nM for NR2A receptors, to 1 μM for NR2B receptors and ≥ 10 μM for NR2C and NR2D receptors (Chen et al., 1997; Paoletti et al., 1997; Traynelis et al., 1998; Rachline et al., 2005). The high affinity of Zn^{2+} binding to the ATD of NR2A is due to the presence of His^{42} and His^{44} in NR2A which are not conserved in the NR2 subunits (Chen et al., 1997; Choi and Lipton, 1999; Low et al., 2000). Although Zn^{2+} binds with high affinity to the ATD of NR2A, the voltage-independent inhibition on NR2A is incomplete. However, the incomplete Zn^{2+} inhibition is not observed in the other NR2 subunits (Rachline et al., 2005). The partial incomplete inhibition by Zn^{2+} on NR2A is suggested to be due to the effect of H^+. Zn^{2+} inhibition is enhanced in the presence of H^+. The saturating Zn^{2+} cannot completely inhibit due to non-saturating H^+ concentration under physiological condition (Traynelis et al., 1998; Low et al., 2000). Factors affecting the H^+-inhibition, like the exon 5 of NR1 splice variant, would thus, affect the voltage-independent Zn^{2+}-inhibition (Traynelis et al., 1998). Besides H^+, voltage-independent Zn^{2+} inhibition is also allosterically regulated by other modulators or ligands. Glutamate binding on the LBD of NR2 has a positive allosteric modulation on Zn^{2+} binding to the ATD of NR2A. This also mediates the fast desensitization of NR2A-expressing NMDA receptors (Zheng et al., 2001). Channel inhibition by Zn^{2+} through the ATD is a demonstration of the transduction of signal from the ATD to the LBD by conformational

movement (Gielen et al., 2008). Although the binding site for Zn^{2+} is at the ATD, tyrosine kinase phosphorylation at the CTD can also modulate the Zn^{2+} inhibition at the ATD (Zheng et al., 1998). For the low affinity, voltage-dependent Zn^{2+}-inhibition, it involves the binding of Zn^{2+} to a region near the channel pore (Christine and Choi, 1990). Unlike the voltage-independent Zn^{2+} inhibition, the voltage-dependent Zn^{2+}-inhibition shows no subunit specificity (Paoletti et al., 1997). The voltage-dependent block may work in a similar way as the Mg^{2+} channel block. However, Zn^{2+} can permeate more easily than Mg^{2+}, thus the voltage dependent block of Zn^{2+} is lower than that of Mg^{2+} (Legendre and Westbrook, 1990; Paoletti et al., 1997). Indeed, the inhibition by Zn^{2+} is observed to protect neurons from excitotoxic insults that are induced by glutamate or NMDA (Choi and Koh, 1998; Cote et al., 2005). Despite the understanding on the inhibition by Zn^{2+}, it is still controversial whether Zn^{2+} inhibits NMDA receptors in a tonic or phasic manner (Vogt et al., 2000; Kay, 2003; Izumi et al., 2006; Kay, 2006). More studies have to be carried out to understand how Zn^{2+} regulates the NMDA receptors in the CNS.

1.4.3.4 Modulation by polyamine

Polyamines are polybasic aliphatic amines that are positively charged at physiological pH. The endogenous polyamines are synthesized from ornithine, a byproduct of the urea cycle. In the CNS, they are released by neurons and/or glial cells (Masuko et al., 2003). Polyamine produces three different effects on the NMDA receptors, (1) a voltage-dependent block, (2) a glycine-dependent potentiation and (3) a voltage- and glycine-independent potentiation (Rock and Macdonald, 1995; Williams, 1997b; Mony et al., 2009a). These effects are not observed in NR2C and NR2D (Williams, 1995). High concentration of polyamine promotes the voltage-dependent block of the NMDA receptors with the block being more pronounced at hyperpolarized potentials. Block by polyamine is mediated by the interaction with residues from the M3 of NR1 and NR2B, the S2 of NR1 and the linker between M1 and M2 of NR2 (Kashiwagi et al., 1996; Kashiwagi et al., 1997; Jin et al., 2008). Polyamine binding at the opening of the pore impedes ion flow and causes a decrease in the

unitary conductance and the average open duration that is distinct from the voltage-dependent Mg^{2+} block (Brackley et al., 1990; Rock and Macdonald, 1992a, b; Williams, 1997a). Inhibitory effects are similar in both NR2A and NR2B (Williams, 1994; Sharma and Reynolds, 1999). However, low concentration of polyamine results in the stimulation of the NMDA receptors (Brackley et al., 1990; Rock and Macdonald, 1992a; Mony et al., 2009a). Polyamine increases the NMDA receptors' affinity for glycine (McGurk et al., 1990; Ransom and Deschenes, 1990). Increase in the affinity of glycine decreases the rate of development of glycine-dependent desensitization and the rate of dissociation of glycine from the NMDA receptors. However, the rate for dissociation of NMDA is not reduced (Benveniste and Mayer, 1993). This results in the glycine-dependent stimulation by polyamine. This form of stimulation is observed in both NR2A- and NR2B-expressing receptors (Williams, 1994). Voltage- and glycine-independent stimulation is unique to NR2B subunits (Williams, 1994; Sharma and Reynolds, 1999). This form of stimulation causes an increase in the channel opening frequency but no change in average open time or amplitude. Polyamine can also potentiate the steady-state current (i.e. the desensitized response) in a dose-dependent manner. The desensitization onset rate is affected by polyamine (Lerma, 1992; Rumbaugh et al., 2000). Polyamine binds to the ATD of NR1 and NR2B (Williams, 1995; Masuko et al., 1999; Han et al., 2008). Site of binding on NR2B is distinct from that of ifenprodil, a NR2B-specific drug (Gallagher et al., 1996; Kew and Kemp, 1998; Han et al., 2008). It is also observed that polyamine stimulation involves the interplay with proton through a relief in proton inhibition (Williams et al., 1995; Kashiwagi et al., 1996). Polyamine, being positively charged, acts like the exon 5 insert of the NR1 splice variants, relieving H^+ inhibition. Thus, polyamine stimulation is not effective on NR1-(1-4)b splice variants as proton inhibition is relieved by the positive residues contributed by the exon 5 insert (Durand et al., 1993; Traynelis et al., 1995). Even when NR1-(1-4)b/NR2B is co-expressed, this form of stimulation does not occur (Durand et al., 1993; Williams, 1994; Zheng et al., 1994). In view of the various effects of polyamine acting on the different subtypes of NMDA receptors, the effects of polyamine vary widely between individual neurons due to the different NMDA receptors expressed on

different neurons (Williams et al., 1990; Lerma, 1992; Rock and Macdonald, 1992a, b; Benveniste and Mayer, 1993; Araneda et al., 1999).

1.4.3.5 Modulation by redox activity and S-nitrosylation

Certain cysteine residues are observed to be sites for redox modulation. Cysteine contains a thiol side chain which is able to form disulfide bond with neighboring cysteines during oxidized condition or remains as thiols in reduced condition. Several pairs of disulfide bonds are observed in the ATD and the LBD crystal structure (Table 1.1) (Furukawa and Gouaux, 2003; Karakas et al., 2009). Three of the disulfide bonds are redox modulation sites with two of them from the ATD and one of them located at the LBD (Table 1.1) (Choi et al., 2001). Upon reduction of these disulfide bonds by the reducing agent dithiothreitol (DTT), NMDA receptors are potentiated whereas oxidation by 5-5-dithiobis-2-nitrobenzoic acid (DTNB) decreases the magnitude of response (Aizenman et al., 1989; Tang and Aizenman, 1993). Reduction of the disulfide bond increases the open dwell time and open frequency of NR1/NR2A receptors but only increases the open frequency of NR1/NR2B and NR1/NR2C receptors (Brimecombe et al., 1997; Brimecombe et al., 1999). Upon DTT reduction, NR1/NR2A potentiates with three kinetic components. The disulfide bond between Cys^{87} and Cys^{320} of NR2A is involved in the fast component and that between Cys^{79} and Cys^{308} of NR1 underlies the intermediate component. These two components are only observed in NR1/NR2A and are reversible by washout of reducing agents. The Cys^{86} and Cys^{321} of NR2B are homologous to these residues and are observed to form disulfide bond based on the analysis of the crystal structure of the NR2B ATD (Table 1.1). Thus it is possible that Cys^{86} and Cys^{321} also mediate the redox action (Brimecombe et al., 1999; Karakas et al., 2009). Cys^{744} and Cys^{798} of NR1 mediate the persistent component that are observed in all NR2 subunits when expressed with NR1 (Kohr et al., 1994; Sullivan et al., 1994; Brimecombe et al., 1999; Choi et al., 2001). Although these cysteines are not physically involved in the binding of modulators such as polyamine, H^+ and Zn^{2+}, their redox status are crucial for their modulation on the NMDA receptors (Tang and Aizenman, 1993; Sullivan et al., 1994; Gozlan

and Ben-Ari, 1995; Choi et al., 2001; Kaye et al., 2007; Karakas et al., 2009). This could indicate that the disulfide bridges formed between these cysteines are important in maintaining structural configuration of the receptors and the reduction in the disulfide bond leads to conformational changes that affect the sensitivity of the receptors to such modulators.

The free thiol groups of cysteines can also form S-nitrosothiol in the presence of nitric oxide (NO) (Ignarro, 1990). NO interacts and S-nitrosylates predominantly the Cys^{399} of NR2A, decreasing the number of channel openings and resulting in a down regulation of evoked current. This acts as an important neuroprotection during NMDA-induced excitotoxicity (Lei et al., 1992; Lipton et al., 1993; Kim et al., 1999; Lipton et al., 2002). Cys^{399}, which is not conserved among the NR2 subunits, lies in the linker region. The linker region is important for determining the differential channel kinetics of NR2-expressing NMDA receptors (Gielen et al., 2008; Yuan et al., 2009a). This may explain the uniqueness of NR2A compared to other NR2 subunits. The other three pairs of cysteines involved in redox action can only be S-nitrosylated when they are in the free thiol forms (i.e. their reduced state) (Table 1.1) (Aizenman and Potthoff, 1999; Kim et al., 1999; Choi et al., 2000).

In view of the above, cysteines act as important redox switches and respond to the external environment. For example, under physiological circumstances, an oxidized state of the Cys^{744} and Cys^{798} of NR1 is required for light stimulation (Leszkiewicz et al., 2000; Leszkiewicz and Aizenman, 2002). Under pathological circumstances such as stroke, when the level of oxygen is low and reducing condition is favored, free thiol forms would likely be predominant (Yager et al., 1991; Anderson et al., 1999; Chen and Shi, 2008). As such, hypoxia enhances S-nitrosylation involving Cys^{744} and Cys^{798} of NR1. The disulfide bond is susceptible to reduction and may induce other critical sites such as Cys^{399} or itself to be more readily nitrosylated by NO and eventually leads to neuroprotection via nitrosylation of the NMDA receptors (Takahashi et al., 2007). Redox modulatory sites are also involved in modulating pain transmission and epileptic activity (Quesada et al., 1996; Laughlin et al., 1999). This makes these three pairs of disulfide bonds (Cys^{79} and Cys^{308}; Cys^{744} and Cys^{798} of

NR1 and Cys[87] and Cys[320] of NR2A) and the conserved disulfide bond between Cys[86] and Cys[321] important modulators during hypoxic condition like stroke.

NMDA receptor subunits	Domains	Cysteines/ disulfide bond pairs		Crystal structure	Redox action	S-nitrosylation
NR1	ATD	79	308		✓	✓*
NR2A		87	320		✓	✓*
NR2B		86	321	✓		
NR2A	Linker between ATD and LBD	399			✓	✓
NR1	LBD	420	454	✓		
		436	455	✓		
		744	798	✓	✓	✓*

Table 1.1. Crucial cysteines in the NMDA receptor subunits. These cysteines are located in different domains of the NMDA receptor subunits. From the available crystal structure and electrophysiological experiments, they, with exception to Cys[399], are observed to form disulfide bonds and are involved in redox action and/or S-nitrosylation. Cyan and gray indicate the respective homologous residues. ✓ indicates involvement and ✓* indicates S-nitrosylation only when in free thiol forms.

1.5 NMDA receptors and excitotoxicity in stroke

Although the NMDA receptors are tightly regulated by various endogenous modulators, overactivation often leads to excitotoxicity. Overactivation occurs in disease states such as stroke. Stroke is the rapidly developing loss of brain functions due to a disturbance in the blood supply to the brain, usually caused by bleeding or blocked blood vessels. It is broadly categorized into two types based on their causes. Hemorrhagic stroke is caused by the rupture of blood vessels, resulting in bleeding in the brain. Ischemic stroke is caused by local thrombosis or embolism, resulting in a transient or permanent reduction in blood flow (Donnan et al., 2008). This results in a lack of glucose and oxygen supply, disrupting the homeostasis and the ionic gradients in the brain. The loss of membrane potential causes the neurons and glia to depolarize, releasing neurotransmitters into the synaptic cleft (Dirnagl et al., 1999; Besancon et al., 2008). Glutamate, one of the neurotransmitters that is released, becomes accumulated in the synaptic cleft. This results in the overactivation of the NMDA receptors and the uncontrolled influx of Na^+ and Ca^{2+}. The influx of Na^+ is responsible for the early necrotic events. Ca^{2+} entry results in the delayed neurodegenerative injuries through the activation of cytoplasmic and nuclear events (Fig. 1.5) (Dirnagl et al., 1999; Szydlowska and Tymianski, 2010). At the centre of the perfusion deficit, cells are killed rapidly. However, between the infarct core and the unaffected brain tissue is the penumbra. This is an area of constrained blood flow and partially preserved energy metabolism. Without treatment, this area proceeds to infarction due to ongoing excitotoxicity (Baron, 2001; Markus et al., 2004). Thus this area is a prime area for neuroprotection (De Silva et al., 2010). Many drugs targeting the NMDA receptors are developed to salvage the penumbra and prevent the spread of cell death. There are several regulatory sites of the NMDA receptors that are targeted; (1) the glutamate binding site, (2) the glycine binding site, (3) the site within the channel lumen where Mg^{2+} and phencyclidines bind and (4) the ATD. However, many of these drugs are not successful in clinical trials (Green and Shuaib, 2006).

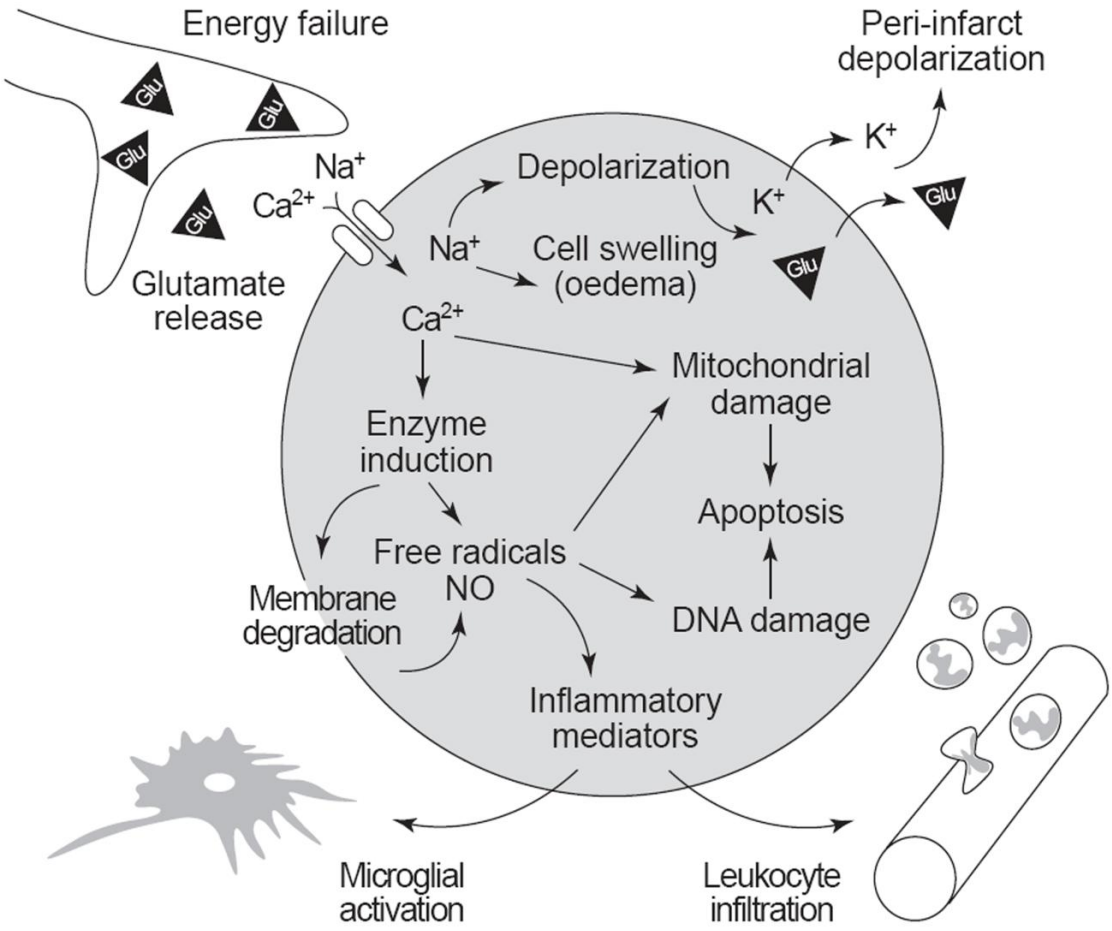

Fig. 1.5. An overview of pathophysiological mechanisms in ischemic stroke. Glu indicates glutamate. NO indicates nitric oxide. The lack of oxygen and glucose disturb the homeostasis which eventually lead to the excessive release of glutamate. Overactivation of glutamate receptors leads to uncontrolled influx of Na^+ and Ca^{2+} postsynaptically, causing membrane depolarization, cell swelling, enzyme induction and mitochondrial damage. These processes eventually lead to cell death. (Adapted from Trends in Neurosciences 1999, 22: 391-397)

1.5.1 Competitive antagonists

Antagonists targeting the agonist or the co-agonist binding sites are likely drug candidates (Fig. 1.6). However, competitive antagonists discriminate poorly between the NMDA subtypes and result in the generalized inhibition of NMDA receptors (Paoletti and Neyton, 2007). Classical competitive antagonists on the glutamate binding site are the phosphono derivatives of short-chain (five to seven carbons) amino acids such as D-2-amino-5-phosphonopentanoic acid (AP5) and D-2-amino-7-phosphonoheptanoic acid (AP7) (Dingledine et al., 1999). Selfotel is one such drug targeting the glutamate binding site. However, it is terminated in phase III stroke clinical trial due to an increase in mortality,

possibly due to neurotoxicity (Davis et al., 1997; Davis et al., 2000). Quinoxaline-2,3-dione (e.g. trisubstituted 5-nitro-6,7-dichloro-qinoxaline-2,3-dione (ACEA-1021)), quinolin-2(1H)-ones, benzazepine (e.g. 3-hydroxy-1h-1-benzazepine-2,5-diones (HBAD)), kynurenic acid (e.g. 7-chlorokynurenic acid (7CKA)) and substituted indole-2-carboxylates derivatives target the glycine binding site (Swartz et al., 1992; Kulagowski et al., 1994; Keana et al., 1995; Woodward et al., 1995; Di Fabio et al., 1997; Dingledine et al., 1999). Of which, gavestinel, an indole-2-carboxylate, is developed and tested in clinical trials. Gavestinel does not improve the outcome of stroke (Lees et al., 2000; Haley et al., 2005; Warach et al., 2006). As glycine binding is dependent on the NR2 subunit, some of the glycine site competitive antagonists are more potent in certain types of NR2 subtypes. For example, the dichloro-tetrahydroquinoline-2-carboxylic acid derivative (CGP 61594) is more effective for NR1/NR2B receptors (Honer et al., 1998).

1.5.2 Channel blockers

Channel blockers have similar binding site as Mg^{2+} and are usually uncompetitive antagonists (Fig. 1.6). They bind to the NMDA receptors only during transmitter-activated state and exhibit a use-dependent and a voltage-dependent blockade. Examples of such channel blockers are ketamine, phencyclidine, memantine and 5-methy-10,11-dihydro-5H-dibenzocyclohepten-5,10-imine maleate (MK-801) (Wong et al., 1986; Huettner and Bean, 1988; Yuan et al., 2005; Johnson and Kotermanski, 2006). Binding of open channel blockers results in the dissociation of the agonists and the subsequent closing of the NMDA receptor channel. Dissociation of the channel blocker is generally slow and is dependent on the channel blocker binding site in the pore. The deeper it binds in the channel pore, the longer it will be trapped. As a result, phencyclidine and MK-801, which are suggested to bind deep within the channel pore, are not successful as drug candidates owing to their neuropsychiatric and pathological side effects (Lipton, 1993; Dravid et al., 2007). In contrast, memantine which has partial trapping in closed channel, is thus the only NMDA receptor antagonist approved as a drug (in Alzheimer's disease) by the Food and Drug Administration (FDA)

(Blanpied et al., 1997; Winblad and Poritis, 1999; Reisberg et al., 2003; Tariot et al., 2004). Memantine also provides positive outcome in animal stroke model, but it is ineffective in the treatment of stroke in human trials (Chen et al., 1992; Chen et al., 1998; Lipton, 2006). Rather, memantine has beneficial effects for recovery from stroke (Orgogozo et al., 2002). Moreover, other channel blockers such as Aptiganel, Remacemide and AR-R15896AR are ineffective in stroke clinical trials either due to a lack of positive stroke outcome or the occurrence of high mortality rates (Cregan et al., 1997; Dyker and Lees, 1999; Albers et al., 2001; Lees et al., 2001; Diener et al., 2002). Novel alternatives such as the N-alkylglycine and the amino-alkylcyclohexanes derivatives are thus explored (Planells-Cases et al., 2002; Gilling et al., 2007).

1.5.3 Non-competitive antagonists

These are ligands that block NMDA receptors in voltage-independent manner without causing significant reduction in agonist potency. One such group of drugs is the phenylethanolamine. A typical phenylethanolamine is ifenprodil. Ifenprodil is highly subunit specific, binding to only the NR2B-expressing receptors. Ifenprodil has two binding sites. The low affinity, voltage-dependent site is at the ion channel pore. The high affinity, voltage-independent binding site is located at the hydrophobic pocket in the cleft of the NR2B ATD (Fig. 1.6) (Williams, 1993; Perin-Dureau et al., 2002a; Karakas et al., 2009). Ifenprodil stabilizes an agonist-bound state that has a low P_{OPEN} (Kew et al., 1996; Fischer et al., 1997). It has allosteric effects on the polyamine on NMDA receptors but more importantly is the allosteric effects on H^+ (Kew and Kemp, 1998). Ifenprodil binding also causes a larger fraction of the receptors to be protonated at physiological pH and the potency of ifenprodil increases at low pH (Mott et al., 1998; Williams, 2001). Considering that NR2B-expressing receptors are involved in mediating excitotoxicity, ifenprodil represents a good drug lead (Chen et al., 2008a; Liu and Chen, 2008). Second generation of ifenprodil analogues, such as eliprodil and traxoprodil (CP101606 and RO25,6981 respectively), which have greater selectivity for NR2B are developed. However, they fail in stroke clinical trials due to side effects or a lack of

efficacy (Nikam and Meltzer, 2002; Gogas, 2006). Besides phenylethanolamine-like drugs, non-phenylethanolamine-like analogues are also selective for NR2B receptors and act as non-competitive antagonists. A few of such drugs that have emerged are hydroxyl-benzimidazoles, benzamidine, dihydroimidaoline, 4-aminoquinolines and 2- and 4- aminopyridine (Pinard et al., 2002; Alanine et al., 2003; Buttelmann et al., 2003; Claiborne et al., 2003; McCauley et al., 2004). However for most of them, the site of action is largely unknown but possibly resides at the ATD due to some structural similarities with the phenylethanolamine (Layton et al., 2006; Wee et al., 2010).

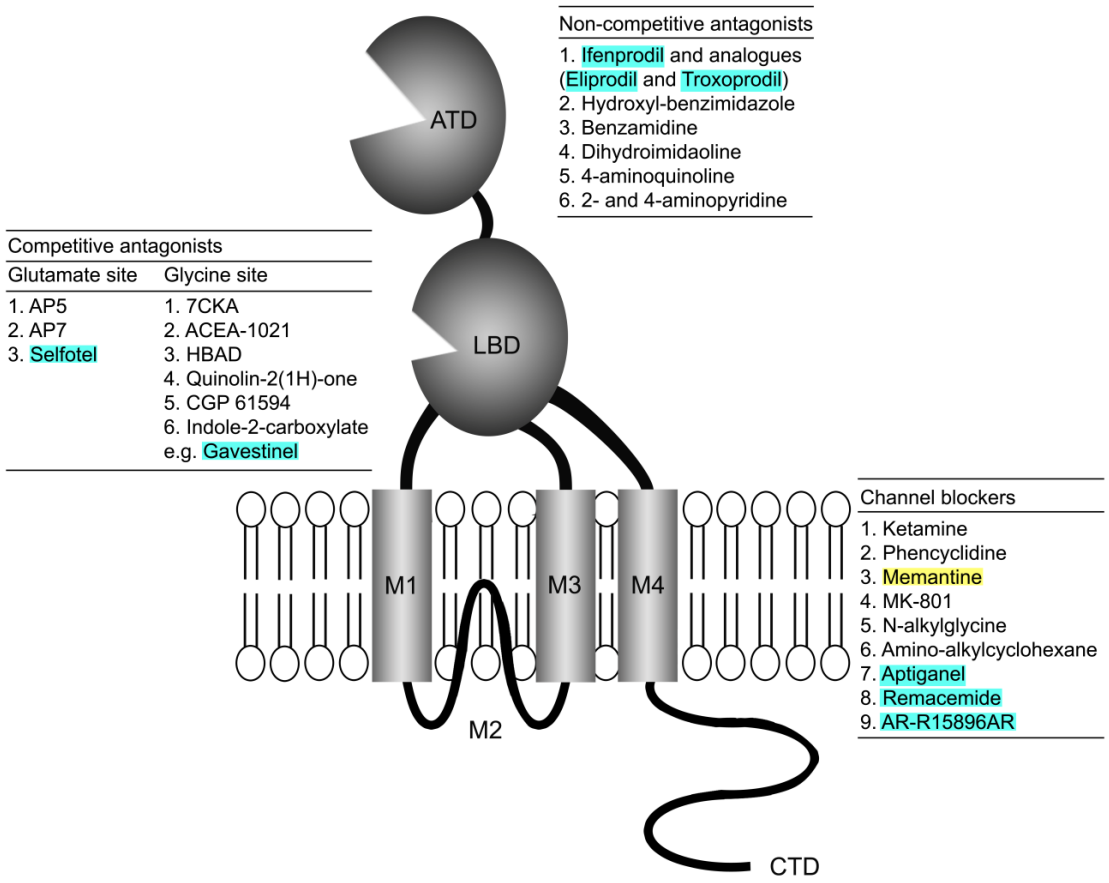

Fig. 1.6. Diagram showing the different domains of the NMDA receptors which the antagonists target to. Cyan indicates drugs that have undergone clinical trials but have failed. Yellow indicates the only NMDA receptor-targeting drug that is approved for use in Alzheimer's disease by FDA.

1.6 Thrombin

1.6.1 In coagulation cascade

To date, tissue plasminogen activator (tPA) is the only FDA approved drug for treating ischemic stroke. It has a therapeutic window of three hours (h) and works by the activation of plasminogen to plasmin (Disorders and Stroke rt-PA Stroke Study Group, 1995). Plasmin is responsible for dissolution of the clot. Unlike plasmin, thrombin is involved in forming the clot through the conversion of soluble fibrinogen to insoluble fibrin (Mosesson, 2005). tPA, plasmin and thrombin are serine proteases involved in the coagulation cascade, which determines the blood hemostasis. Upon vascular damage, tissue factor (TF), a transmembrane protein, becomes exposed to factor VII (FVII). The activated FVII (FVIIa) complexes with TF forming TF-FVIIa, triggers the coagulation cascade and results in the formation of the prothrombinase complex (FVa, FXa, Ca^{2+} and anionic phospholipid). FXa cleaves prothrombin after Arg^{320} and generates meizothrombin. This is cleaved again after Arg^{271} to liberate active thrombin (35.5 kDa) (Nesheim et al., 1979; Krishnaswamy et al., 1987; Brufatto and Nesheim, 2003; Davie and Kulman, 2006). In addition to its involvement in forming the fibrin clot, thrombin also cleaves and activates G-protein coupled protease-activated receptors (PAR)-1, -3 and -4 to promote platelet activation and mediate inflammatory responses (Ossovskaya and Bunnett, 2004; Steinhoff et al., 2005; Martorell et al., 2008).

1.6.2 Structure and action of thrombin

Thrombin has a light chain linked by a single disulfide bond to a heavy chain which, itself, contains three intrachain disulfide bonds (Fig. 1.7). Upon prolonged standing in solution, α-thrombin is autolytically converted to β-thrombin through cleavage at Arg^{62}-Ile^{63} and Arg^{73}-Asn^{74} in the heavy chain (Fig. 1.7). β-thrombin is converted to γ-thrombin through cleavage at Arg^{123}-Glu^{124} and Lys^{154}-Gly^{155} (Fig. 1.7) (Boissel et al., 1984). Catalytic activities measured by chromogenic substrates are roughly similar among thebse three species but β- and γ-thrombin are less active towards physiologic macromolecules such as fibrinogen

(Chang, 1986; Hofsteenge et al., 1988; Bovill et al., 1995; Davie and Kulman, 2006). The catalytic site (His^{43}, Asp^{99} and Ser^{205}) is conserved among serine proteases and is important for the charge relay system (Kraut, 1977; Davie and Kulman, 2006). Thrombin cleaves at the scissile bond (P1-P1') following basic residues. (For subsequent discussion, the terms P4, P3, P2, P1, P1', P2' and P3' will describe the substrate peptide amino acid positions relative to the P1–P1' bond and S4, S3, S2, S1, S1', S2' and S3' correspond to that on the thrombin.) The Asp^{199} lies at the bottom of the primary specificity pocket and interacts with the basic residues in the P1 of the substrates (Davie and Kulman, 2006). Thrombin specificity extends beyond P1 and the kinetic behavior for cleavage is largely contributed by the side chain of the surrounding amino acids of P1 on the substrates (Table 1.2) (Lottenberg et al., 1983; Le Bonniec et al., 1991; Le Bonniec et al., 1996; Backes et al., 2000; Marque et al., 2000; Petrassi et al., 2005). The restricted specificity compared to trypsin (a typical serine protease) is due to the presence of two protruding loops, a 60 loop and a γ-loop, which partially occlude the substrate binding cleft of thrombin. The 60 loop usually makes contacts with hydrophobic residues at the amino terminal end of scissile bond while the γ-loop determines specificity of residues at the carboxy terminal end of the scissile bond (Bode et al., 1989; Dang et al., 1997; Davie and Kulman, 2006). There are two other surface regions, exosite I and II, located at opposite ends of the substrate binding groove at the heavy catalytic chain, which confer the exceptional specificity of thrombin towards macromolecular substrates (Davie and Kulman, 2006). The exosite I and exosite II interact with negatively charged groups of thrombin substrates. Exosite I, also known as the fibrinogen-binding exosite, exists only in α-thrombin as this region is cleaved off in β- and γ-forms (Tsiang et al., 1995; Pechik et al., 2004). Exosite II is also known as the heparin-binding exosite (Sheehan and Sadler, 1994; Li et al., 2004).

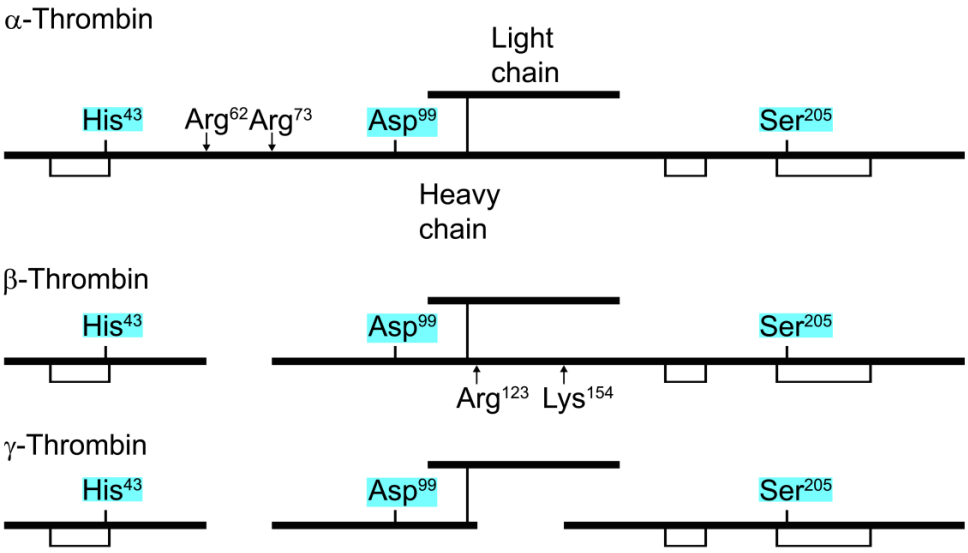

Fig. 1.7. Autolysis of thrombin. Cleavage sites are indicated by arrows. Light chain is linked to the heavy chain through a disulfide bond. Disulfide bonds on the heavy chain are indicated by ⌴. The catalytic triad is highlighted in cyan. The fragments of β-thrombin and γ-thrombin are held together by noncovalent forces. Some polypeptide are lost in the process, which causes different binding capabilities among the α-, β-, and γ- thrombin.

Thrombin ▼

NH_2...P4—P3—P2—P1—P1'—P2'—P3'...COOH

	P4	P3	P2	P1	P1'	P2'	P3'
Side chain preference	Aliphatic			Basic		Non-acidic Bulky Hydrophobic	Postively charged Non-acidic No Pro
Amino acids	Iso Val Leu Ala Pro	X	Pro	Arg Lys	Ser	Phe	Arg Lys

Table 1.2. Preferred amino acids for thrombin cleavage. The terms P4, P3, P2, P1, P1', P2' and P3' describe the substrate peptide amino acid positions relative to the P1-P1' bond. Thrombin cleaves at the bond between P1 and P1'. Amino acids are represented by their three-letters amino acid code. X indicates the site can be any amino acids.

1.6.3 Localization and regulation in the brain

In addition to the prothrombin that is released from the liver into the blood stream, prothrombin mRNA is also expressed in neuronal and glial cells (Niclou et al., 1994; Arai et

al., 2006). Prothrombin is distributed in the olfactory bulb, cortex, colliculus superior and inferior, corpus striatum, thalamus and hippocampus of the brain (Dihanich et al., 1991). The prothrombin activator, FX, is also expressed in the brain (Shikamoto and Morita, 1999). It is likely that the action of thrombin in the CNS becomes more prominent under pathological condition when the blood brain barrier is disrupted and thrombin-activating factors, prothrombin and thrombin extravasate into the brain parenchyma (Sinnreich et al., 2004; Sokolova and Reiser, 2008). In support of this, levels of prothrombin and thrombin are observed to be augmented in patients with neurodegenerative disorders, such as Parkinson's disease (PD), human immunodeficiency virus encephalitis, Alzheimer's disease (AD), ischemic and hemorrhagic stroke (Riek-Burchardt et al., 2002; Boven et al., 2003; Karabiyikoglu et al., 2004; de Castro Ribeiro et al., 2006; Grammas et al., 2006; Ishida et al., 2006; Cuomo et al., 2007; Hua et al., 2007).

Under physiological condition, thrombin is regulated by the serine protease inhibitor (serpin) superfamily (Pike et al., 2005). In the brain, antithrombin III (ATIII) and protease nexin I (PN-1) are serpins that are expressed in neurons and various glial cell subtypes at different developmental stages (Choi et al., 1990; Deschepper et al., 1991; Mulligan et al., 1991; Mansuy et al., 1993; Smirnova et al., 1996; Kury et al., 1997; Niclou et al., 1998; Docagne et al., 1999). However, during pathological condition, their levels do not increase with the rise in thrombin activity (Vaughan et al., 1994; Riek-Burchardt et al., 2002). This results in a less efficient inhibitory system by the serpins in modulating the increasing levels of thrombin during pathological condition.

1.6.4 Function in brain

Many of the thrombin actions in the brain are mediated via PARs, which are ubiquitous in the brain (Junge et al., 2004). Thrombin acts as a mitogen in cultured microglia and astrocytes and also as a neuroinflammatory agent through the activation of PARs (Moller et al., 2000; Meli et al., 2001; Suo et al., 2002; Wang et al., 2002a; Wang et al., 2002b; Nicole et al., 2005; Wang et al., 2007). Thrombin is found to play a role in the disease development of

PD, AD and stroke patients. For example, thrombin mediates the loss of striatal neurons in the striatum and dopaminergic neuron in the substantia nigra through activation of cFos and extracellular signal-regulated kinase (Erk1/2) pathway via by PAR-4 while thrombin may also induce neuroprotection via activation of PAR-1 in PD rat models (Cannon et al., 2005; Lee et al., 2005; Cannon et al., 2006; Herrera et al., 2008). Not only so, thrombin also takes part in the formation of amyloid plaques, characteristic of AD patients. Thrombin is involved in the release and the processing of amyloid precursor protein (APP) to beta amyloid in amyloid plaques (Igarashi et al., 1992; Li et al., 1998b). In addition, it is also observed that thrombin can result in neuronal death, glial scarring and cognitive deficits. On the other hand, it is notable that thrombin is able to promote neuronal cell survival in AD animal models (Akiyama et al., 1992; Russo et al., 2002; Mhatre et al., 2004; Arai et al., 2006; Luo and Grammas, 2010). Indeed, depending on the concentration, thrombin can lead to beneficial or deleterious outcomes (Vaughan et al., 1995; Pike et al., 1996; Turgeon and Houenou, 1997; Turgeon et al., 1998; Choi et al., 2003; Suo et al., 2003; Cannon et al., 2006; Xi et al., 2006; Yang et al., 2008; Hua et al., 2009).

In particular, low concentrations of thrombin (10 pM-10 nM) are neuroprotective in ischemic brain and can protect hippocampal neurons and astrocytes from cell death in response to oxygen-glucose deprivation (OGD), hypoglycemia, growth supplement deprivation and oxidative stress through the activation of PAR-1 (Vaughan et al., 1995; Striggow et al., 2000; Wang et al., 2007). Thus, thrombin is investigated if it serves as another form of ischemic preconditioning (thrombin preconditioning) and exerts a neuroprotective effect in ischemic stroke. Low doses of thrombin improve the outcome to subsequent stroke condition via activation of PAR-1 (Xi et al., 1999; Masada et al., 2000; Henrich-Noack et al., 2006; Granziera et al., 2007). However at high concentration (500 nM), thrombin causes brain damage and also exacerbates OGD-induced neuronal death via PAR-1 and PAR-4 (Striggow et al., 2000; Junge et al., 2003; Olson et al., 2004; Cuomo et al., 2007; Thevenet et al., 2009;

Mao et al., 2010). It also induces delayed neuronal injury in cerebral cortex and shrinkage of the striatum *in vitro* and *in vivo* (Fujimoto et al., 2006; Fujimoto et al., 2007).

1.7 Proteases interaction with NMDA receptors

One of the mechanisms through which thrombin and PAR-1 mediates excitotoxicity in the brain is proposed to involve the release of glutamate from glial cells, which activates the NMDA receptors on neighboring neurons (Lee et al., 2007). Recently, many proteases are observed to interact directly or indirectly with the NMDA receptors and modulate the function of NMDA receptors. Indirect interaction requires proteases to interact with other proteins to modulate the NMDA receptors. Direct interaction involves the proteolysis of NMDA receptors to change the NMDA receptor function. Proteolysis of the NMDA receptors becomes a novel form of post-translational modification of the receptors.

1.7.1 Cysteine proteases

An example of cysteine proteases is calpain. Calpain proteolyzes the NR2 subunits at the CTD. NR2 proteolysis by calpain is phosphorylation-dependent and is also dependent on the MAGUKs the NR2 subunits are binding to (Bi et al., 1998a; Bi et al., 1998b; Bi et al., 2000; Guttmann et al., 2001; Rong et al., 2001; Simpkins et al., 2003; Wu et al., 2007; Yuen et al., 2008). Calpain also cleaves the NMDA receptor binding proteins such as PSD-95, cytoskeletal protein spectrin and collapsin response mediator proteins (CRMPs). These proteins anchor NMDA receptors at the synapse and are also required for modulating the microtubule dynamics at the synapse (Vanderklish et al., 1995; Vinade et al., 2001; Bretin et al., 2006). Thus, although calpain does not change NMDA receptor function, it may regulate the turnover of NMDA receptors at the synaptic and extrasynaptic region and affect the number of functional receptors expressed on the surface (Vinade et al., 2001; Dong et al., 2004; Wu et al., 2005; Bretin et al., 2006). As a Ca^{2+}-dependent protease, calpain is activated by the NMDA receptors. Thus calpain cleavage may represent an autoregulation of NMDA receptors during ischemic condition or other pathologies (Gascon et al., 2008; Nimmrich et al., 2008).

1.7.2 Matrix metalloproteinases (MMPs)

MMP-3 and MMP-7 cleave the NR1 at the LBD (Pauly et al., 2008; Szklarczyk et al., 2008). MMP-7 cleavage of the NR1 and NR2A decrease the NMDA-mediated Ca^{2+} flux and alter the translocation of the NMDA receptors (Szklarczyk et al., 2008). MMPs also modulate NMDA receptor function without proteolytic action on the NMDA receptors. MMP-9 interacts with PKC and accelerates the desensitization and deactivation kinetics without affecting the current amplitude (Gorkiewicz et al., 2009). MMP-9 also interacts with the β1-integrin and increases the surface expression of NMDA receptors through the β1-integrin signaling pathway (Michaluk et al., 2009). Interestingly, thrombin also activates pro-MMP9 and is more prominent in mediating cell death in intracerebral hemorrhage (ICH) compared to PAR-1 (Xue et al., 2006; Xue et al., 2009).

1.7.3 Serine proteases

Two other serine proteases, tPA and plasmin, that are involved in the modulating the blood hemostasis like thrombin, are also found in the CNS. tPA interacts with the liproprotein receptor-related protein (LRP1) from the low density lipoprotein receptor family (LDLR). The tPA-LRP1 entity interacts with the NMDA receptors via PSD-95 (Martin et al., 2008). This enhances the receptor function, with an increase in the surface NMDA receptors expression and also an increase in NMDA receptors signaling (Pawlak et al., 2005b; Martin et al., 2008; Samson et al., 2008). Enhancement of NMDA receptors function through the NR2B and NR2D mediates the neurotoxicity and stress condition via the Erk1/2 and inducible NOS (iNOS) (Kilic et al., 2005; Pawlak et al., 2005a; Pawlak et al., 2005b; Norris and Strickland, 2007; Martin et al., 2008; Baron et al., 2010). Proteolytic action of tPA also modulates the NMDA receptors through cleavage of NR1 and plasminogen (Nicole et al., 2001; Fernandez-Monreal et al., 2004; Pawlak et al., 2005b; Benchenane et al., 2007).

Activation of plasminogen by tPA generates plasmin which modulates the NMDA receptor function through direct cleavage of NMDA receptors or by modulating the interacting proteins of NMDA receptors. Plasmin can cleave the NR1, NR2A and NR2B and

cause a decrease in the number of surface NMDA receptors expressed and change the number of dendritic spines under stress condition (Pawlak et al., 2005a; Pawlak et al., 2005b). Plasmin cleaves the NR1 at the Lys^{316} and the Arg^{704} (Samson et al., 2008). It also cleaves the NR2A ATD at Lys^{317}. Removal of the ATD up to Lys^{317} eliminates the high affinity Zn^{2+} inhibition. As a result, the NMDA receptor response is also enhanced (Yuan et al., 2009b). Plasmin also interacts with PAR-1 to enhance NMDA receptor function through a similar mechanism as thrombin, i.e. by activating PAR-1 which results in the release of glutamate that can subsequently activates the NMDA receptors (Lee et al., 2007; Mannaioni et al., 2008).

Thrombin activation of PAR-1 expressed on astrocytes stimulates the release of Ca^{2+} from astrocytic intracellular Ca^{2+} stores. The Ca^{2+} then induces the release of glutamate from the astrocytes which activates the NMDA receptors (Bowser and Khakh, 2007; Lee et al., 2007). As a result, this activates the NMDA receptor-mediated component of the synaptic miniature excitatory postsynaptic currents (mEPSCs), evoked EPSCs (eEPSCs) and evoked excitatory postsynaptic potentials (eEPSPs) in a Mg^{2+}-dependent manner. Sustained release of glutamate tonically activates the perisynaptic NMDA receptors. These receptors remain blocked by tonic Mg^{2+} until the EPSPs in neighboring synapses lead to significant depolarization at the spine head. Thus unblocking the perisynaptic NMDA receptors appears as an enhancement of NMDA receptor function (Gingrich et al., 2000; Lee et al., 2007; Shigetomi et al., 2008). Activation of Src by PAR-1 may also modulate the phosphorylation states of NMDA receptor, thereby modulating its activity (Sharp et al., 2008). Enhancement of NMDA receptors by PAR-1 mediates the penumbral injury observed in middle cerebral artery occlusion (MCAO) rat model and may also play a part in emotionally motivated learning (Almonte et al., 2007; Hamill et al., 2009). Thrombin can also interact directly and cleave the NR1 but not the NR2A (Gingrich et al., 2000). Thrombin can cleave NR1 from cerebellum, cortex, hippocampus, brain stem and striatum after one hour of incubation with

high concentration of thrombin (1000-3000 nM). The cleavage of NR1 is likely to be near the CTD (Gingrich et al., 2000).

1.8 Objectives of the study

The NMDA receptors have been the focus for drug development in the treatment of neurological disease such as ischemic stroke. However, these drugs have never succeeded in clinical trials for stroke treatment. The failure in correlating with animal studies is incomprehensible. Proteases such as thrombin have been observed to modulate the NMDA receptors through direct and indirect interactions with the receptors. However, direct interaction with NMDA receptors by thrombin is not characterized and determined.

To address this knowledge gap, the objectives of this study are:

1) To examine if thrombin interact with the NMDA receptors, e.g. NR2B.
2) To investigate the putative interaction site of the NMDA receptor subunits with thrombin.
3) To determine if the interaction occur in the *ex vivo* system.
4) To determine the possible changes in the NMDA receptor properties upon thrombin cleavage.

In this study, the possibility of direct interaction with other members of the NMDA receptors, e.g. NR2B was investigated. Proteins from rat brain lysate (RBL) and synaptic plasma membrane (SPM) were used for the cleavage study. NR2B was cleaved by thrombin. Next, the putative cleavage site was determined using NR2B recombinant protein fused to the maltose binding protein (MBP). Using primary cortical neuronal culture and *Xenopus laevis* oocytes, it was examined if the cleavage of NR2B by thrombin occurs in the native conformation. The functional consequences of thrombin cleavage on heterologously expressing NR1/NR2B in *Xenopus Laevis* oocytes was also elucidated using two-electrode voltage clamp (TEVC). Taken together, this study provides insights into the consequences of thrombin cleavage and how cleavage may affect the NMDA receptor functions.

Chapter 2

Direct interaction of thrombin with NMDA receptors

2 Direct interaction of thrombin with NMDA receptors

2.1 Background and objectives

Emerging evidence have shown the expression of prothrombin (the zymogen form of thrombin), FX (the prothrombin activator), PN-1 and antithrombin (the thrombin inhibitors) and PARs (the thrombin receptors) in the CNS (Choi et al., 1990; Deschepper et al., 1991; Dihanich et al., 1991; Shikamoto and Morita, 1999; Junge et al., 2004). These indicate the presence and a role of thrombin in the CNS. During pathological condition such as ischemic stroke, expression and activity of thrombin are increased as demonstrated in *in vitro* and *in vivo* ischemic models (Hua et al., 2003; Karabiyikoglu et al., 2004; de Castro Ribeiro et al., 2006; Cuomo et al., 2007). This could be due to (1) an increase in thrombin (by increase in expression and activation) but an absence of increase in its inhibitors levels and/or (2) an extravasation of prothrombin, FX and thrombin when the blood brain barrier is compromised (Vaughan et al., 1994; Gingrich and Traynelis, 2000; Riek-Burchardt et al., 2002; Sinnreich et al., 2004; Sokolova and Reiser, 2008). Thrombin has been observed to interact with the NMDA receptors, either indirectly through PAR-1 or directly via cleavage of NR1 (at very high concentration of thrombin, 1000-3000 nM) (Gingrich et al., 2000; Lee et al., 2007). NMDA receptors are the major mediators in excitotoxicity during ischemic stroke (Dirnagl et al., 1999; Szydlowska and Tymianski, 2010). Interestingly, NR2B-expressing NMDA receptors are found to mediate the excitotoxicity (Liu et al., 2007; Chen et al., 2008b). Many ischemic drug researches have been made targeting the NR2B subunits. Modulators of the NR2B have been relatively well-studied due to their specificity on NR2B. The subtype selectivity of these drugs is highly preferred for their ability to minimize the inhibition of all NMDA receptors, which under physiological condition, also play an important role in neurological development and learning and memory. These NR2B modulators, although successful in animal stroke model, are not effective in providing a positive outcome in ischemic stroke clinical trials (Nikam and Meltzer, 2002; Gogas, 2006). Up to date, there have been observations of various proteases acting as modulators of the NMDA receptors through direct interaction with the NMDA receptors in the form of cleavage (Bi et al., 1998b;

Gingrich et al., 2000; Guttmann et al., 2001; Nicole et al., 2001; Guttmann et al., 2002; Simpkins et al., 2003; Fernandez-Monreal et al., 2004; Wu et al., 2005; Samson et al., 2008; Szklarczyk et al., 2008; Yuan et al., 2009b). But there is a lack of investigation with regards to thrombin direct interaction with NMDA receptors and if it can be a new form of modulator of the NR2B subunits.

To address this knowledge gap, the objective of this study is to use rat brain lysate (RBL) (to examine all NR2B subunits population) or synaptic plasma membrane (SPM) (to examine NR2B subunits population expressing on the synaptic membrane surface) from Sprague Dawley rats as a source of native NMDA receptors for the investigation of interaction with thrombin. Firstly, I sought to establish a method to ensure activity of thrombin would be comparable and maintain the same throughout all experiments. Next I aim to investigate the possibility of interaction between thrombin and NR2B. Thirdly, the site of interaction would be investigated.

2.2 Materials and methods

Materials

6-8 weeks old male adult Sprague Dawley rats were obtained from the National University of Singapore (NUS) Laboratory Animals Centre (LAC) (Singapore). All procedures involving animals were approved by the NUS Institutional Animal Care and Use Committee (IACUC). Phenylmethylsulphonyl fluoride (PMSF) was purchased from BDH (Dorset, UK). Pepstatin A was purchased from Sigma (St Louis, MO, USA). Leupeptin hemisulfate was purchased from US Biological (Swampscott, MA, USA). Bicinchoninic acid (BCA) protein assay kit was purchased from Pierce (Rockford, IL, USA). pMAL-c2-ATD2B was previously constructed by F.M. Ng from our laboratory (Ng et al., 2007). Mutants K318A and R292A were previously constructed from the pMAL-c2 ATD2B by J.T. Chen and N. Anthony from our laboratory. Amylose resin column was purchased from New England Biolabs (Beverly, MA, USA). Thrombin was purchased from Calbiochem (San Diego, CA, USA) and Novagen (Madison, WI, USA). Chromogenic substrate of thrombin (Spectrozyme®TH) was purchased from American Diagnostica (Greenwich, CT, USA). Thrombin inhibitor D-Phe-Pro-Arg-chloromethylketone (PPACK) was purchased from Biomol (Plymouth Meeting, PA, USA). Protein molecular marker was purchased from Bio-Rad Laboratories (Hercules, CA, USA). Anti-NR1 mouse monoclonal antibody (recognizing amino acid residues 660-811 of NR1) was purchased from BD Pharmingen (San Diego, CA, USA). N-terminal anti-NR2B rabbit polyclonal antibody (recognizing amino acid residues 27-76 of human NR2B) was purchased from Santa Cruz Biotechnology (Santa Cruz, CA, USA). C-terminal anti-NR2B rabbit polyclonal antibody (recognizing amino acid residues 1437-1456 of mature mouse NR2B) was purchased from Upstate Biotechnology (Lake Placid, NY, USA). Anti-βIII tubulin mouse monoclonal antibody was purchased from Chemicon International Inc. (Temecula, CA, USA). For the secondary antibodies, both the goat anti-rabbit and goat anti-mouse immunoglobulin G (IgG) horseradish peroxidase antibodies were purchased from Santa Cruz Biotechnology (Santa Cruz, CA, USA). Enhanced chemiluminescence (ECL) Plus Western

blotting detection reagent was purchased from Amersham (Buckinghamshire, UK). All other chemicals are purchased from Sigma-Aldrich (St Louis, MO, USA).

RBL preparation

Brain lysate was obtained by homogenizing Sprague Dawley rat brain in radioimmunoprecipitation assay (RIPA) buffer (150 mM NaCl, 1 % Nonidet P-40, 0.5 % deoxycholic acid, 50 mM Tris, pH 7.5) in the presence of protease inhibitor (1.5 µM pepstatin A and 4.4 µM leupeptin hemisulfate). The brain lysate was then centrifuged at 14000 *g* for 30 minutes (min). Supernatant was collected and was centrifuged again at 14000 *g* for 30 min to completely remove debris.

SPM preparation

SPM preparation protocol was adapted from Rogers *et al*. (1991) (Rogers et al., 1991). Briefly, SPM was prepared from 3-4 g of rat brain blended with 9 volume of dissection buffer (10 % (w/v) sucrose, 5 mM EDTA, 50 mM Tris acetate, pH 7.4, 1 mM PMSF, 10 µM leupeptin hemisulfate, 1 µM pepstatin A) using a variable speed homogenizer (Glas Col, Terre Haute, IN, USA) at 900 revolutions per minute (rpm) for 12-15 strokes. The suspension was centrifuged at 800 *g* for 20 min at 4ºC. The pellet (A) was kept on ice and the supernatant was centrifuged in Beckman Type 45 Ti rotor at 16000 *g* for 30 min at 4ºC. The pellet (B) obtained was resuspended in 20 ml of 20 mM HEPES buffer, pH 7.4 and centrifuged at 16000 *g* for 4 min at 4ºC. The pellet (C) obtained from this centrifugation step was pooled together with pellet (A) and resuspended in 6 volume of lysis buffer (5 mM Tris-acetate, pH 8.1, 10 µM leupeptin, 1 µM pepstatin). The suspension was left at 4°C for 45 min with constant mixing followed by homogenization at 900 rpm for 12-15 strokes using the Glas Col variable speed homogenizer. Sucrose and Tris acetate were carefully added to the homogenate to get a

final concentration of 34 % (w/w) sucrose and 50 mM Tris acetate, pH 7.4. Homogenate was overlaid with an equal volume of 50 mM Tris acetate, pH 7.4 containing 28.5 % (w/w) sucrose and a third volume of 50 mM Tris acetate, pH 7.4 containing 10 % (w/w) sucrose in a 94-ml tube. The tube was centrifuged at 60000 *g* for 2 h at 4ºC. The interface between 28.5 % and 34 % was collected as SPM. This fraction was diluted to 10 % sucrose with 2 volume of 50 mM Tris acetate, pH 7.4 and was centrifuged at 48000 *g* for 30 min at 4ºC. The pellet collected was resuspended in 50 mM Tris acetate, pH 7.4, stored at -80ºC and used as SPM homogenate.

Expression, purification and concentration of MBP-ATD2B fusion protein and its mutants

Glycerol stock of MBP-ATD2B, MBP-ATD2B(K318A) and MBP-ATD2B(R292A) were prepared by F.M. Ng, J.T. Chen and N. Anthony from our laboratory. Mutant constructs were verified by sequencing. Bacteria culture was precultured from the glycerol stock in Luria-Bertani (LB) broth overnight at 37ºC at 220 rpm. An aliquot of the preculture was inoculated into an appropriate volume of LB broth (ratio of preculture to LB broth is 1:10). Bacteria was cultured at 37ºC at 220 rpm and the growth of cells were monitored using optical density at 600 (OD_{600}). When OD_{600} was between 0.6-0.8, culture was induced with 1 mM IPTG for 5 h at 18ºC at 220 rpm. Bacterial cells were lyzed by sonication and the extracts were separated by centrifugation at 14000 *g* for 30 min at 4°C into soluble (supernatant) and insoluble (inclusion bodies) fractions. These fractions were analyzed by Coomassie brilliant blue-stained 15 % sodium dodecyl sulfate polyacrylamide gel (SDS-PAGE) gels. The soluble fractions were then purified. Typically, 10 mg of protein was loaded into an amylose resin column for purification and the bound protein was eluted with 10 mM maltose. The purified protein was analyzed by Coomassie brilliant blue-stained 15 % SDS-PAGE gels.

Measurement of protein concentration

The protein concentration of RBL or SPM was determined by the BCA protein assay according to the manufacturer's protocol. Bovine serum albumin (BSA) standard (0.025-2 mg/ml) was reconstituted in the buffer of RBL or SPM (RIPA buffer, pH 7.4 or 50 mM Tris Acetate, pH 7.4 respectively). Absorbance was measured at 562 nm. A protein calibration graph was generated. Protein concentration of RBL and SPM was based on the calibration graph generated.

The protein concentration of purified MBP-ATD2B was determined by the Bradford protein assay. Absorbance was measured at 280 nm. A protein calibration graph was generated using 0.2-1 mg/ml BSA. Protein concentration of MBP-ATD2B was based on the calibration graph generated.

Thrombin concentration determination

Lyophilized thrombin was reconstituted using thrombin diluent buffer (10 mM HEPES, 100 mM NaCl, pH 8.2). Activity of thrombin was measured using the chromogenic substrate, Spectrozyme®TH, according to the manufacturer's protocol. Readings were taken at $\lambda_{405\ nm}$ every 30 seconds (s) over a period of 31 min at room temperature. Thrombin concentration between 0.1 U/ml to 5 U/ml (i.e. 1 nM to 50 nM) were used to plot a calibration curve of initial rate against concentration of thrombin. All subsequent thrombin preparations' activity prior use will be measured and activity will be based on this calibration curve to ensure the consistency in the thrombin's activity used for all experiments. Thrombin in U/ml was converted to nM as described by Gingrich *et al.* (2000) previously.

Thrombin cleavage

60 µg of RBL or 50 µg of SPM homogenates or 2-5 µg of purified MBP-ATD2B, MBP-ATD2B(K318A) and MBP-ATD2B(R292A) were incubated with thrombin (0.1-1000 nM) in the presence of cleavage buffer (0.15 M NaCl, 2.5 mM $CaCl_2$, 20 mM Tris-HCl, pH 8.4) at 37°C. 24 h of thrombin treatment was performed (unless otherwise specified) to ensure complete cleavage. Experimental reactions were stopped by boiling in sample buffer (50 mM dithiothreitol (DTT), 5% glycerol, 1% SDS, 30 mM Tris-HCl, pH 6.8, 0.0005% bromophenol blue).

SDS-PAGE, immunoblotting and densitometry analysis

Protein was separated by denaturing Laemmli SDS-PAGE using the Hoefer Mighty Small Vertical Electrophoresis System (San Francisco, CA, USA). Reactions that were treated with thrombin were separated on 8.5 % or 15 % SDS-PAGE gel. Protein was stained and visualized using Coomassie brilliant blue R-250. For Western blotting, protein was electrophoresed and transferred onto polyvinyldine difluoride (PVDF) membranes in transfer buffer (10 % methanol, 25 mM Tris, 192 mM glycine) for 19 h at 30 V at 4°C. Membranes were blocked in 5% non-fat milk in Tris-buffered saline containing 0.1% Tween-20 for 1 h on a shaker at room temperature. They were incubated with either N-terminal anti-NR2B (1 : 200) or C-terminal anti-NR2B (1 : 800) or anti-NR1 antibody (1 : 2000) or anti-βIII tubulin antibody (1 : 1000) primary antibodies. Membranes were washed 3 times, each time of 10 min, in Tris-buffered saline containing 0.1% Tween-20. They were then incubated with anti-rabbit IgG horseradish peroxidase (1 : 20000) or anti-mouse IgG horseradish peroxidase (1 : 5000), washed again, and subsequently detected by ECL Plus. Densitometry analysis was done using UN-SCAN-IT gel (Version 6.1).

Sequencing of $NR2B_{ATD}$ Thrombin Cleavage Products

The protein was separated by gel electrophoresis, blotted onto PVDF membrane, and stained with Coomassie Brilliant Blue R-250. The N-terminal sequence after thrombin cleavage was determined using Edman degradation in a protein sequencer (Perkin Elmer Applied Biosystems, Foster City, CA, USA) performed by Midwest Analytical (St Louis, MO, USA).

Illustration of crystal structure of NR2B ATD

The apo-crystal structure of NR2B ATD (Protein Data Bank code 3JPW) provided the structural template to create the images using Protein Workshop (Karakas et al., 2009).

Data analysis

Data were expressed as mean ± standard error of the mean (S.E.M.) and analyzed statistically using one-way analysis of variance (ANOVA) followed by post-hoc Dunnett test. Significance for all tests was set at $P < 0.05$. Error bars in figures were S.E.M. Graphs were plotted using GraphPad PRISM® Version 4.

2.3 Results

Thrombin activity calibration

In order to ensure that thrombin concentration was comparable across experiments, a thrombin calibration curve was generated. Chromogenic substrate specific for thrombin was used (Sonder and Fenton, 1986). Initial rate of the hydrolysis of the substrates was determined from the linear portion of the saturation-kinetics plots (Fig. 2.1A). The initial rate of hydrolysis was the slope gradient of the linear phase. A range of thrombin concentration (from 0.05-500 nM) was used. However, hydrolysis rates of the chromogenic substrates by 0.05 nM, 0.1 nM, 0.5 nM thrombin were too low for detection (Fig. 2.1A). For 100 nM, 500 nM, 750 nM, 1000 nM and 5000 nM of thrombin, the hydrolysis rates were too fast to be accurately measured (Fig. 2.1A). Thus only the linear slope gradients of 1-50 nM of thrombin were used for generating the thrombin calibration graph (Fig. 2.1A and Fig. 2.1B). As the rate of hydrolysis was proportional to the concentration of the reactant (thrombin), a first order reaction graph was produced (Fig. 2.1B). Using the equation of the plot, $y = 1.5 \times 10^{-5} x - 6.8 \times 10^{-6}$ (whereby y is the rate of hydrolysis and x is the concentration of thrombin), the concentration of every new vial of thrombin to be used can be deduced based the rate of hydrolysis measured. With this, all thrombin used, regardless of batch, could be kept similar for all experiments.

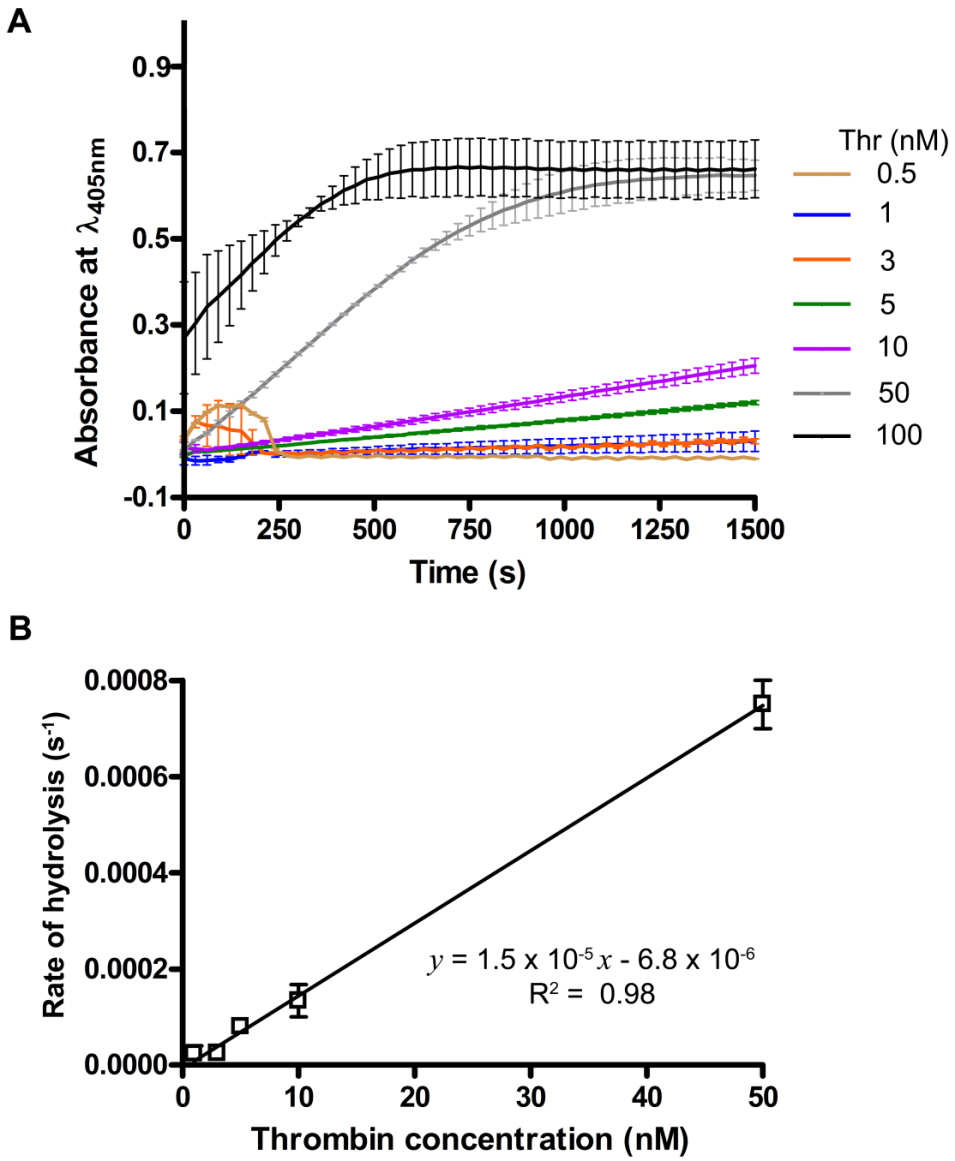

Fig. 2.1. Generation of thrombin calibration curve. (A) Saturation-kinetics plot of different concentration of thrombin. Only the first 1500 s were shown for clearer presentation. Thr indicates thrombin. Concentration of thrombin is as color coded. Some of the reactions required some time to stabilize (e.g. 0.5 nM and 3 nM of thrombin). Rate of hydrolysis of the substrates was taken from the linear phase, i.e. 250 s and after. Rate of hydrolysis was too low and too high to be measured accurately at 0.5 nM and 100 nM thrombin respectively. Thus, only 1-50 nM thrombin were used for the generation of the thrombin calibration curve. (B) Rate of hydrolysis was plotted against thrombin concentration. Values were mean ± S.E.M.

Interaction of thrombin and NR2B

RBL was incubated in increasing concentration of thrombin (0.1-1000 nM) for 24 h and analyzed by Western blots using an C-terminal and an N-terminal anti-NR2B (Fig. 2.4A) (Rao et al., 1998; Wong et al., 2005). We showed thrombin, in a concentration-dependent manner, caused (1) a decrease in the immunoreactivity of the full-length 180 kDa NR2B band, and (2) an increase in the immunoreactivity of a new ~150 kDa band detected by the C-terminal anti-NR2B (at 1 nM and higher thrombin concentrations; n=3; Fig. 2.4B, top panel). Concurrently, the other cleaved ~30 kDa fragment was detected with an N-terminal anti-NR2B (Fig. 2.4B, middle panel). Their parallel increase in immunoreactivity corresponded to the decrease in full-length NR2B immunoreactivity. At low thrombin concentration (1 nM), up to 80 % of the full-length NR2B was cleaved (Fig. 2.4C). At a high concentration (1000 nM thrombin), it was observed that the 150 kDa and 30 kDa smaller fragments also decreased in intensity. This may be a result of non-specific cleavage by high concentration of thrombin (1000 nM) for long exposure (24 h). However, it should be taken into consideration that the generation of the two smaller fragments, 150 kDa and 30 kDa fragments, is thrombin specific as saturated concentration of 120 μM thrombin irreversible inhibitor, PPACK, completely blocked thrombin-induced cleavage of NR2B, validating that the specificity of thrombin proteolytic action (Fig. 2.2 and Fig. 2.4B).

We also investigated if thrombin can cleave the NR2B localized on the synaptic membrane. The SPM that was to be used for investigation was characterized. As expected, NMDA receptors (NR1 and NR2B) were more enriched in the SPM fraction compared to the RBL (Fig. 2.3) (Perez-Otano et al., 2006). Thrombin also cleaved NR2B localized at the synaptic membrane and in a time dependent manner as indicated by the decrease in full length NR2B immunoreactivity with increasing time of incubation in 10 nM of thrombin (Fig. 2.4D). Based on the molecular weight of the cleaved fragments detected with C-terminal and N-terminal anti-NR2B, the thrombin cleavage of the NR2B subunit were deduced to occur at the extracellular N-terminal within the first 300 amino acids of the ATD (Fig. 2.4A).

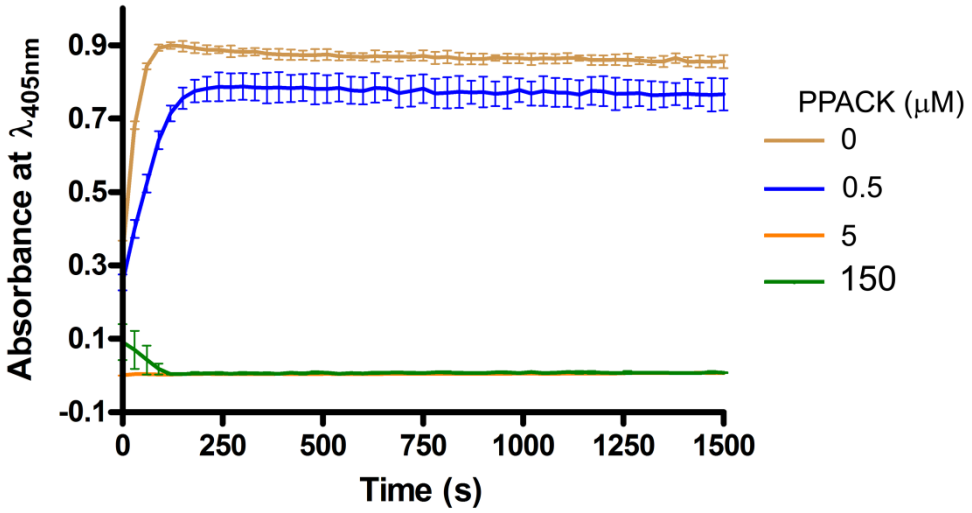

Fig. 2.2. Characterization of thrombin inhibitor. PPACK inhibited the action of thrombin. Only the first 1500 s were shown for clearer presentation. 5 μM of PPACK was sufficient in inhibiting the hydrolysis action of the chromogenic substrates by 10 nM thrombin. Values were mean ± S.E.M.

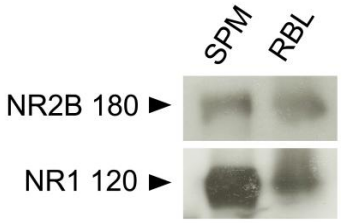

Fig. 2.3. Characterization of SPM. Equal amount (50 µg) of SPM and RBL were analyzed by western blot. NR1 and NR2B were more enriched in SPM fraction compared to RBL. Molecular weight (in kDa) of each protein is as indicated.

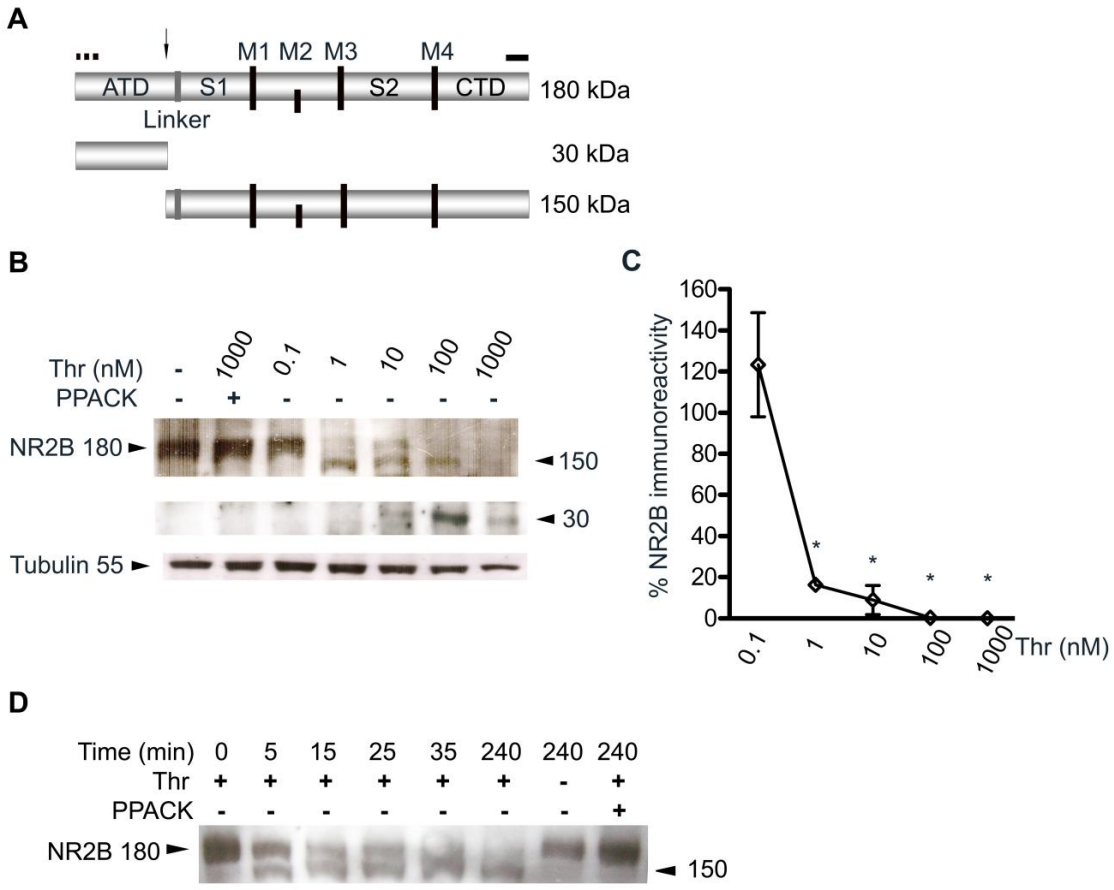

Fig. 2.4. Thrombin cleaves the NR2B subunit from RBL and SPM. (A) Diagram showing the cleavage site (arrow) based on the fragment sizes. The dotted line and the solid line represent the epitope to which the N-terminal and C-terminal anti-NR2B recognized respectively. Gray rectangular box indicates the linker between ATD and S1. Black rectangular boxes indicate the transmembrane domain (M1, M3 and M4) and the re-entrant loop (M2). Domains are as indicated. Molecular weight (in kDa) of the NR2B protein and the cleaved of fragments are indicated. (B-D) Thrombin is indicated as Thr. Molecular weight (in kDa) of the NR2B protein and the fragments are as indicated. (B) Thrombin cleaved NR2B protein in RBL. A 150 kDa (top panel) and a 30 kDa (middle panel) fragments were detected with an C-terminal and N-terminal anti-NR2B respectively upon 24 h of thrombin treatment. Cleavage was blocked by PPACK (120 μM) (n=3). (Bottom panel) Tubulin acted as the loading control. (C) Immunoreactivity quantification of full-length NR2B for the indicated treatment. Data (mean ± S.E.M.) were expressed in terms of percentage of initial substrate densitometry. * indicated $P < 0.01$ (one-way ANOVA, post-hoc Dunnett test). (D) Thrombin cleaved NR2B from SPM in a time-dependent manner. SPM was incubated in 10 nM of thrombin with increasing time of incubation. A smaller band of 150 kDa was detected by an C-terminal anti-NR2B. Thrombin action on NR2B was blocked by inhibitor PPACK (6 μM) (n=2).

Identification of cleavage site

Based on epitope mapping and the fragment sizes observed, it is hypothesized that the cleavage site is at the ATD (Fig. 2.4A). To investigate the thrombin cleavage site on NR2B, soluble recombinant fusion MBP-ATD2B protein (~85 kDa) was subjected to the same cleavage conditions as the RBL. At low concentration of thrombin (1 nM), MBP-ATD2B was cleaved, yielding a ~75 kDa band that could be detected by the N-terminal anti-NR2B. This cleavage was blocked by PPACK (Fig. 2.5A, upper panel). We isolated the smaller fragment (~10 kDa) (Fig. 2.5A, lower panel) and subjected the protein fragment to N-terminal sequencing. Sequencing results showed peptides matching NR2B subunit downstream of Lys^{318} (S^{319}SCYNTHE; Fig. 2.5B; underlined and italic amino acids). This observation suggested thrombin cleaved $NR2B_{ATD}$ after residue 318 (Fig. 2.5C). To verify that Lys^{318} is the thrombin cleavage site on ATD of NR2B, Lys^{318} was mutated to alanine on MBP-ATD2B (MBP-ATD2B(K318A)) and subjected to thrombin cleavage. At the highest thrombin concentration tested (10 nM), there was no detectable cleavage of recombinant MBP-ATD2B(K318A) protein and no detection of the ~75 kDa band (Fig. 2.5D). Previously, Perin-Dureau *et al.* (2002) speculated that Arg^{292} could be a putative thrombin cleavage site (Perin-Dureau et al., 2002b). Under the same thrombin treatment conditions as MBP-ATD2B, MBP-ATD2B(R292A) mutant fusion protein produced the same cleaved off fragment (~75 kDa) as the wild-type MBP-ATD2B, thus suggesting that Arg^{292} may not be a thrombin cleavage site on NR2B ATD (Fig. 2.5E). This is also consistent with the crystal structure of the ATD NR2B, where the Arg^{292} is hidden inside the cleft, inaccessible to thrombin interaction (Fig. 2.6A).

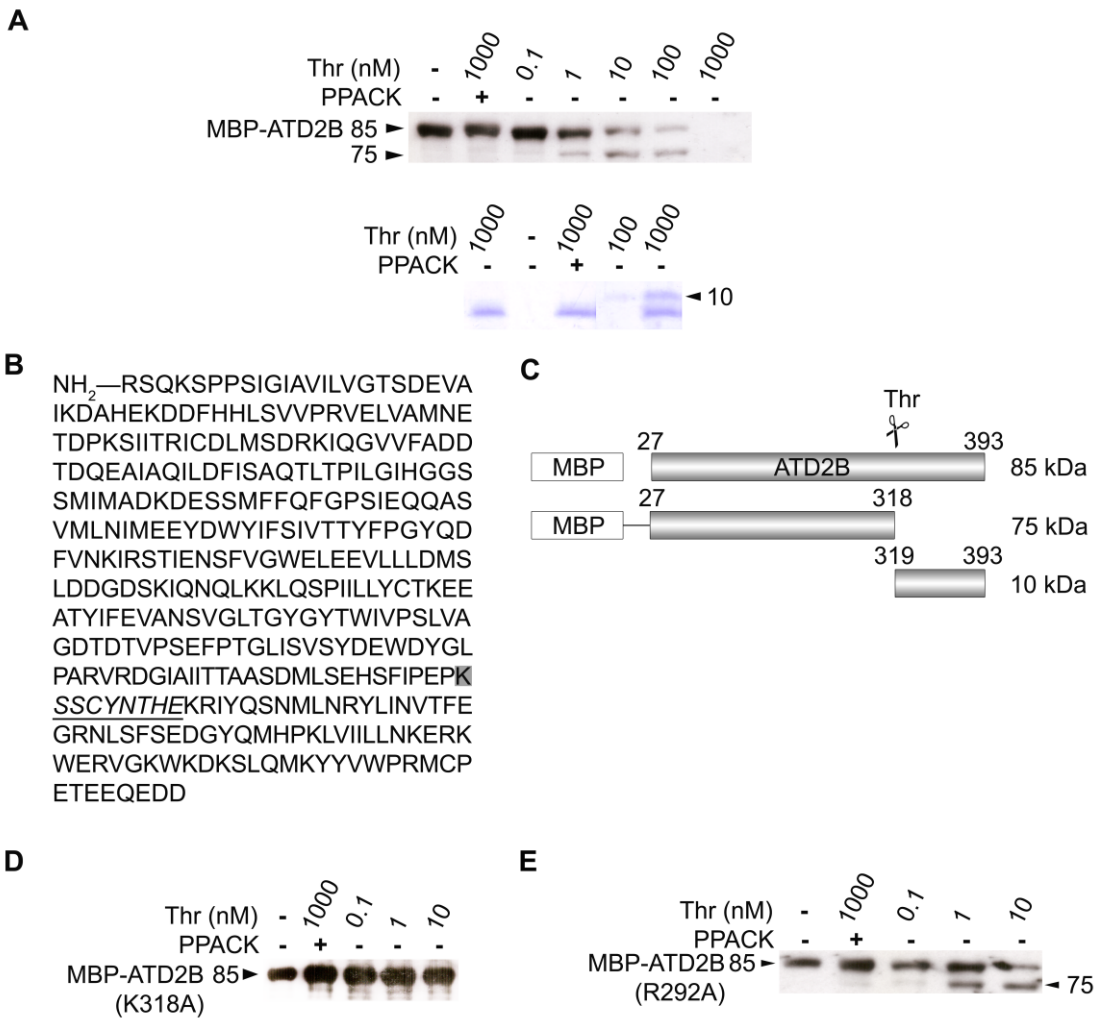

Fig. 2.5. Thrombin cleaves $NR2B_{ATD}$ recombinant protein. (A-E) Thrombin is represented as Thr. Molecular weight (in kDa) of the protein and the fragments are as indicated. (A) (Top panel) Cleavage of MBP-ATD2B yielded a smaller fragment of 75 kDa detected by N-terminal anti-NR2B (n=3). (Bottom panel) Coomassie blue-stained gel showed the other smaller fragment of 10 kDa (n=2). The band below the 10 kDa fragment was contributed by 1000 nM of thrombin. (B) Lys^{318} (highlighted in gray) was the thrombin cleavage site. The underlined and italic amino acids were determined from N-terminal sequencing on the cleaved 10 kDa protein fragment (see Fig. 2.5A, bottom panel). (C) Diagram of the recombinant MBP-ATD2B fusion protein and the thrombin-cleaved fragments. ✂ indicates the thrombin cleavage site. (D) Absence of thrombin cleavage on MBP-ATD2B(K318A) mutant protein (n=3). (E) Cleavage of MBP-ATD2B(R292A) yielded a smaller fragment of 75 kDa (n=3) indicating that Arg^{292} was not the thrombin cleavage site.

Thus far, the identified thrombin cleavage site (Lys^{318}) on NR2B ATD was consistent with other thrombin substrates where thrombin cleavage sites were mostly basic and positively charged (Fig. 2.5B and Table 2.1) (Leavis et al., 1978; Francois et al., 1995; Ishihara et al., 1997; Huntington, 2005). Coincidentally, all known critical residues that exert major influence on ifenprodil- and benzimidazole derivative-mediated inhibitions of NMDA receptors, including Asp^{101}, Ile^{150}, Phe^{176}, Phe^{182} and Tyr^{231}, were located upstream and distant from the thrombin cleavage site Lys^{318} on NR2B ATD (Fig. 2.6A) (Perin-Dureau et al., 2002b; Mony et al., 2009c; Wee et al., 2010). Thus binding of ifenprodil or its analogue, RO25,6981, prior thrombin treatment did not affect thrombin cleavage on NR2B (Fig. 2.6B).

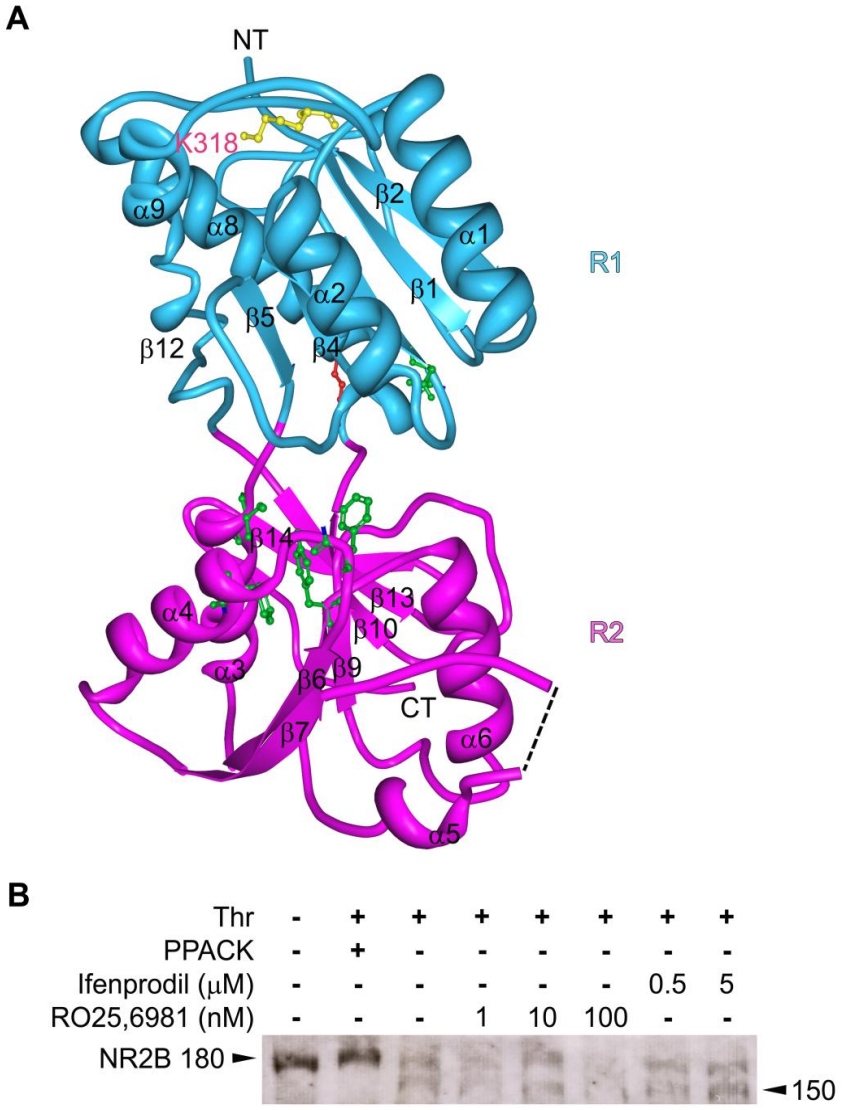

Fig. 2.6. Cleavage site is located away from the binding pocket of ifenprodil and its analogues. (A) Ribbon representation of the apo-NR2B ATD structure (3JPW) generated using Protein Workshop. The clam-shell structure of the NR2B ATD is made up of two domains, R1 (blue) and R2 (magenta). Secondary structures are as labeled (Karakas et al., 2009). NT indicates N-terminal while CT indicates C-terminal. The disordered region (residues 208-214) is indicated as a dotted line. Asp^{101}, Ile^{150}, Phe^{176}, Phe^{182} and Tyr^{231} involved in ifenprodil inhibition are colored green. Lys^{318} (yellow) is located at the top of R1. Arg^{292} (red) lies hidden inside the cleft. (B) NR2B antagonists binding to the pocket did not prevent cleavage by thrombin. NR2B specific antagonists (ifenprodil and RO25,6981), at their respective concentration, were incubated with 50 µg of SPM for 30 min before the addition of 10 nM thrombin for 3 h cleavage treatment. Immunoblot was detected with an antibody recognizing the C-terminal of NR2B. A smaller band of 150 kDa was observed. Thrombin is indicated as Thr. Molecular weight (in kDa) of the protein and the fragments are as indicated.

2.4 Discussion

Possibility of interaction: localization

Thrombin cleaved the Lys^{318} of the NR2B ATD located extracellularly. The possibility for contact between thrombin and NR2B becomes crucial. Cleavage of NR2B by thrombin is possible only if thrombin is located extracellularly in the brain parenchyma. Immunoreactivity for prothrombin has been observed in pyramidal neurons in the temporal cortex, capillaries of brain tissue and astrocytes (Deschepper et al., 1991; Arai et al., 2006; Yin et al., 2010). Thrombin activity is observed in serum-free culture medium bathing hippocampal slices (Thevenet et al., 2009). Modeling after the hepatocytes, the major site of prothrombin synthesis, prothrombin is proposed to be released by neurons and astrocytes in the CNS and subsequently activated by FX to thrombin (Deschepper et al., 1991; Saucan and Palade, 1994; Bristol et al., 1996; Yamada and Nagai, 1996; Davie and Kulman, 2006). The method of prothrombin release at the CNS, i.e. constitutive or regulated, is currently unknown, but the level of extracellular, active thrombin is regulated by CNS-derived ATIII or PNI (Choi et al., 1990; Deschepper et al., 1991; Vaughan et al., 1994; Niclou et al., 1998). In particular, extracellular thrombin activity increases significantly after OGD and ICH (Gong et al., 2008; Thevenet et al., 2009). In addition to local synthesis and secretion from neurons, astrocytes and endothelial cells, thrombin originating from the blood, may also enter into the brain parenchyma in the form of prothrombin in the cerebrospinal fluid (CSF) (Smirnova et al., 1997; Lewczuk et al., 1998). Thus, the localization of extracellular, active thrombin makes it possible for the cleavage of NR2B ATD at Lys^{318}.

Possibility of interaction: molecular recognition

The ability of thrombin to recognize Lys^{318} on NR2B is also important for successful cleavage. Thrombin recognizes molecular patterns for cleavage (Table 1.2). Basic, positive residues such as Arg (R) or Lys (K) at the P1 site forms an ionic interaction with Asp^{199} at the

S1 subsite of thrombin, determining the specificity (Davie and Kulman, 2006). However, based on thrombin crystal structure analysis and mutagenesis studies, the active site groove is surrounded by the 60 loop and the γ-loop, restricting access to potential substrates (Bode et al., 1989; Bode et al., 1992; Le Bonniec et al., 1992; Le Bonniec et al., 1993). Thus, the kinetic behavior is largely contributed by the side chain of surrounding amino acids on the substrates (Lottenberg et al., 1983). Looking at the two amino acids adjacent to the cleavage recognition site of NR2B, i.e. P2 and P1', they are well conserved and consistent with other P2 and P1' of other thrombin substrates (Table 2.1) (Leavis et al., 1978; Francois et al., 1995; Ishihara et al., 1997; Huntington, 2005). The pyrrolidine ring of Pro^{317} (P) of NR2B (P2 position), like many natural substrates of thrombin, allows excellent packing by the phenolic side chain of Tyr60A at the 60 loop (Table 2.1). Larger residues will not pack favorably into the S2 subsite of the thrombin cavity and smaller residues (e.g. Gly) will not fit as well (Bode et al., 1992; Huntington, 2005). In particular, the S1' site is restricted by the 60 loop, preferring small residues with polar side chain. Ser^{319} (S) at P1' position of NR2B ATD is a small residue with polar side chains (Lottenberg et al., 1983; Bode et al., 1989; Bode et al., 1992; Rezaie and Olson, 1997). This may explain that although the Lys^{317} is conserved in NR2A, no cleavage of NR2A by thrombin was observed due to the absence of Pro at the 316^{th} residue and the presence of a non, polar Ala at the 318^{th} residue of NR2A (Gingrich et al., 2000).

Thrombin

NH_2...P4—P3—P2—P1—P1'—P2'—P3'...COOH

Substrates/position	P4	P3	P2	P1	P1'	P2'	P3'
$NR2B_{ATD}$	P	E	P	K	S	S	C
PAR-3	L	P	I	K	T	F	R
PAR-1	L	D	P	R	S	F	L
Factor VIII (740)	I	E	P	R	S	F	S
Factor VIII (1689)	Q	S	P	R	S	F	Q
Heparin cofactor II	F	M	P	L	S	T	Q
PAR-4	P	A	P	R	G	Y	P
Factor V (1018)	L	S	P	R	T	F	H
Factor XIII	G	V	P	R	G	V	N
Factor XI	I	K	P	R	I	V	G
Protein C	V	D	P	R	L	I	D
Thrombin-activated fibrinolysis inhibitor (TAFI)	V	S	P	R	A	S	A
Factor V(709)	L	G	I	R	S	F	R
Factor V (1545)	W	Y	L	R	S	N	N
Factor VIII (372)	I	Q	I	R	S	V	A
Antithrombin	I	A	G	R	S	L	N
Fibrinogen (A chain)	G	G	V	R	G	P	R
Fibrinogen (B chain)	F	S	A	R	G	H	R
Troponin C (TH1)	A	E	I	F	R	A	S
Troponin C (TH3)	A	E	I	F	R	I	F

Table 2.1. Alignment of thrombin cleavage sites of known natural substrates. The terms P4, P3, P2, P1, P1', P2' and P3' describe the substrate peptide amino acid positions relative to the P1–P1' bond. Amino acids are represented by their one-letter amino acid code. Thrombin recognizes basic and positive residues (yellow) and cleaves at the bond between P1 and P1'. Pro (P) (cyan) are conserved at P2 and Ser (S) (orange) are small residue with polar side chains that are conserved at the P1'.

Possibility for interaction: structure

I have shown thrombin cleavage of NR2B in brain homogenate, SPM fraction and recombinant proteins. NR2B from such preparations may give an outlook on the possibility for interaction. It also allows us to identify the site of interaction (Lys^{318}) accurately. However it may misrepresent the real situation. Bearing in mind, NR2B exists as a quaternary structure, forming a heterotetramer complex with NR1 subunits. Based on the recent quaternary crystal structure of a close relative of the NMDA receptors, GluR2, there are numerous interface within a dimer, between two dimers and also between domains (Sobolevsky et al., 2009). From the analysis on the heterodimer of NR1-NR2A LBD crystal structure, the heterodimer buries 2640 Å of solvent accessible surface area (Furukawa et al., 2005). Mutagenesis studies also demonstrate contacts are formed between domain, e.g. ATD with LBD (Zheng et al., 2001; Gielen et al., 2008; Gielen et al., 2009; Yuan et al., 2009a). In the event that Lys^{318} of NR2B is located at such solvent inaccessible surface, interaction with thrombin would become unfeasible. Homogenizing procedures in lysis buffer could have disrupted the NR2B structure exposing cleavage sites that may be natively inaccessible to thrombin. Thus, it is crucial to carry out investigations on whether thrombin interaction with NR2B occurs in the *ex vivo* system when NR2B is expressed in its heteromeric receptor form.

Chapter 3

Ex vivo and electrophysiological demonstration of thrombin interaction with NR2B

3 *Ex vivo* and electrophysiological demonstration of thrombin interaction with NR2B

3.1 Background and objectives

In Chapter 2, I have reported the direct thrombin cleavage of NR2B at the Lys^{318} at the ATD. This was demonstrated using RBL, SPM and recombinant $NR2B_{ATD}$ proteins. The use of detergents to solubilize the NR2B subunits from RBL and also the expression of solely the ATD of NR2B produce NR2B subunits that may not be full representations of how NR2B exists in a quaternary NMDA receptor structure. Thus, an objective of the study would be to determine if the cleavage by thrombin occurs on NR2B expressed in a NMDA receptor complex in cortical neuronal cultures.

NR2B-expressing NMDA receptors are important mediators of excitotoxicity in ischemic stroke (Liu et al., 2007; Chen et al., 2008a). During ischemic stroke, a decrease in the blood flow will lead to an increase in synaptic glutamate levels and a reducing milieu (Yager et al., 1991; Anderson et al., 1999; Chen and Shi, 2008). To briefly illustrate, the redox environment is determined by the overall states contributed by the oxidized and reduced states of a number of redox couples, such as i) $NADP^+$ and NADPH, ii) NAD^+ and NADH and iii) GSSG and GSH (Mayevsky and Chance, 2007; Kakaç et al., 2010). Indeed, during ischemic stroke, a situation that results in a low glucose and oxygen supply to the brain, the reduced states of these redox couples are found to be increased, resulting in a reducing milieu (Tanaka et al., 1986; Yager et al., 1991; Anderson et al., 1999; Shi and Liu, 2006). It is observed that a reducing milieu changes the NMDA receptors through the modulation at the redox sites (Aizenman et al., 1989; Tang and Aizenman, 1993; Brimecombe et al., 1999; Choi et al., 2001; Takahashi et al., 2007). This may have an implication on the interaction with thrombin. Thus, in this study, we also mimic the reducing condition during ischemic stroke using a reducing agent, DTT, and investigate if under such conditions, thrombin would interact with NR2B expressed heterologously in *Xenopus laevis* oocytes.

3.2 Materials and methods

E18 Sprague Dawley rat embryos were obtained from LAC (Singapore) with procedures approval by IACUC (Singapore). Trypsin, deoxyribonuclease (DNase), dialyzed heat-inactivated fetal bovine serum (FBS), Hank's balanced salts solution (HBSS), penicillin-streptomycin, poly-D-lysine, cytosine-β-D-arabino-furanoside, BSA, Gel Mount, ethyl 3-aminobenzoate methanesulfonate salt (MS-222), collagenase, glutamate and ifenprodil were purchased from Sigma (St Louis, MO, USA). Neurobasal medium, B27 supplement, sodium pyruvate and HEPES were purchased from Invitrogen (Carlsbad, CA, USA). GlutaMAX-1 was purchased from Gibco (Eggenstein, Germany). Anti-βIII tubulin TUJ1 mouse monoclonal antibody was purchased from Covance (Madison, WI, USA). Anti-glial fibrillary acidic protein (GFAP) rabbit polyclonal antibody was purchased from DAKO (Carpinteria, CA, USA). Anti-NR1 goat polyclonal antibody (recognizing the C-terminus of human NR1) was purchased from Santa Cruz (Santa Cruz, CA, USA). N-terminal anti-NR2B rabbit polyclonal (recognizing amino acid residues 323-337 of rat NR2B) for immunocytochemistry was purchased from Alomone Labs (Jerusalem, Israel). C-terminal anti-NR2B rabbit polyclonal antibody (recognizing amino acid residues 1437-1456 of mature mouse NR2B) for western blot was purchased from Upstate Biotechnology (Lake Placid, NY, USA). Anti-glyceraldehyde-3-phosphate dehydrogenase (GAPDH) mouse monoclonal antibody was purchased from Chemicon International Inc. (Temecula, CA, USA). For the secondary antibodies used in immunocytochemistry, donkey anti-rabbit Alexa Fluor 488, donkey anti-goat Alexa Fluor 594 and donkey anti-mouse Alexa Fluor 647 were purchased from Molecular Probes (Eugene, OR, USA). For the secondary antibodies used in western blot, both the goat anti-rabbit and goat anti-mouse IgG horseradish peroxidase antibodies were purchased from Santa Cruz Biotechnology (Santa Cruz, CA, USA). Thrombin was purchased from Calbiochem (San Diego, CA, USA). Protein molecular marker and DTT were purchased from Bio-Rad Laboratories (Hercules, CA, USA). ECL Plus was purchased from Amersham (Buckinghamshire, UK). *Xenopus laevis* frogs were obtained from Xenopus Express (Vernassal, France). pCIneo NR1-1a and pcDNA1 NR2B were gifts from Dr. S.F.

Heinemann. pcDNA1 NR2B(K318A) was constructed by J.T. Chen and N. Anthony from our laboratory. Restriction enzymes were purchased from New England Biolabs (Beverly, MA, USA). QIAquick gel extraction kit was purchased from Qiagen (Valencia, CA, USA). mMESSAGE mMACHINE T7 kit was purchased from Ambion (Austin, TX, USA). RNA ladder was purchased from Fermentas (Vilnius, Lithuania). Glycine was purchased from AppliChem (Darmstadt, Germany). Chromogenic substrate of thrombin (Spectrozyme®TH), PMSF, pepstatin A and leupeptin hemisulfate were purchased from companies as stated in Chapter 2. All chemicals were purchased from Sigma-Aldrich (St Louis, MO, USA).

Cortical neuronal culture

Primary cultures of cerebrocortical neurons were obtained from E18 Sprague Dawley rat embryos. Cortices were aseptically dissected from the brains. The meninges and the choroid plexus were carefully removed under a dissecting microscope (Nikon SMZ645, Tokyo, Japan) performed in a Class I laminar flow hood. Cortical tissues were digested in 0.2 mg/ml trypsin and 40 µg/ml of DNase in HBSS supplemented with 7.4 mM glucose, 1 mM sodium pyruvate, 10 mM HEPES, 4.2 mM $NaHCO_3$, 1.2 mM $MgSO_4$ and 0.3 % (w/v) BSA at 37°C for 5 min followed by mechanical trituration. Dissociated cells were harvested by centrifugation and resuspended in Neurobasal medium supplemented with 10 % (v/v) dialyzed heat-inactivated FBS, 2.5 % (v/v) B27 supplement, 2 mM GlutaMAX-1 and 1 % (v/v) penicillin-streptomycin. Cells were seeded at a density of 0.5 x 10^6 cells in 24-well plates or nitric-acid treated glass coverslips, both coated with 0.1 mg/ml poly-D-lysine before plating. Cells were then cultured at 37°C in a humidified 5 % CO_2 incubator. Culture medium was replaced with the above Neurobasal medium and their supplements but in the absence of FBS a day later. 10 µM of cytosine-β-D-arabino-furanoside was added on day-in-vitro 4 (DIV4). Cultures were used for treatment on DIV11.

Immunocytochemistry

DIV11 cultures were fixed in 4 % (w/v) paraformaldehyde for 15 min at 4°C. The cells were washed in phosphate buffered saline supplemented with 0.1 % (v/v) Triton X-100 (PBS-Tx). This was followed by blocking in 3 % (w/v) BSA in PBS-Tx for 1 h at room temperature. Subsequently, the cells were incubated with anti-βIII tubulin TUJ1 (1 : 500) or anti-GFAP (1 : 2000) or anti-NR1 (1 : 100) or N-terminal anti-NR2B (1 : 100) for 24 h at 4°C and washed 3 times, each time of 5 min in PBS-Tx. The cells were then incubated with anti-rabbit Alexa Fluor 488 (1 : 400) or anti-goat Alexa Fluor 594 (1 : 400) or anti-mouse Alexa Fluor 647 (1 : 400) in the dark for 1 h at room temperature. The cells were washed again and mounted on glass slides using Gel Mount aqueous mounting medium.

Confocal microscopy

Fluorescent images were viewed and captured using a Zeiss LSM510 confocal microscope (Carl Zeiss, Göttingen, Germany) equipped with an Argon laser of 488 nm, HeNe laser of 543 nm and 633 nm. Alexa Fluor 488 was viewed with 505-530 nm BP filters. Alexa Fluor 594 was viewed using 560-615 nm BP filters and Alexa Fluor 647 was viewed using 650 nm BP filters. Images were viewed using a pinhole of 1.0 Airy units and objectives of 20x (0.5 NA), 40x (1.3 NA) or 63x (1.4 NA). Addition of scale bars and image brightness/contrast adjustments were performed on the Zeiss LSM Image Browser Software, version 4.0.0.157. Images were subsequently exported to TIFF format and assembled by Adobe Photoshop.

Thrombin concentration determination

Lyophilized thrombin was reconstituted and activity was measured using Spectrozyme®TH as depicted in Chapter 2. Initial rate of hydrolysis was determined from the linear portion of the saturation kinetics plot. Concentration of the newly constituted vial of thrombin was

determined using the plot and the equation $y = 1.5 \times 10^{-5} x - 6.8 \times 10^{-6}$ obtained in Chapter 2 (Fig. 2.1B), where *y* is the rate of hydrolysis and *x* is the concentration of thrombin.

Thrombin treatment on neuronal culture

Cultures were treated with thrombin (0.l-1000 nM) on DIV 11 in balanced salt solution (in mM): 140 NaCl, 5 KCl, 2 $CaCl_2$, 10 HEPES, 3 D-glucose, pH 7.4 for 2 h at 37°C. Cells were washed three times with phosphate buffered saline (PBS, pH 7.4), removed using rubber cell scraper, centrifuged at 14000 *g* for 5 min and the cell pellet was lyzed in RIPA (contents described in Chapter 2) to obtain the whole cell homogenate. Protein concentration was measured. Protein was analyzed on 8.5 % SDS-PAGE and western blot. Negative controls that had thrombin replaced by thrombin diluents (contents described in Chapter 2) and thrombin inhibitor, PPACK, were included.

Measurement of protein concentration

Measurement of protein concentration of cortical neuronal homogenate was performed using BCA protein assay as described in Chapter 2. BSA standard was reconstituted in RIPA. Absorbance was measured at 562 nm.

SDS-PAGE and immunoblotting

The protein was separated by SDS-PAGE and analyzed by immunoblotting as described in Chapter 2. Immunoblotting was performed using C-terminal anti-NR2B (1 : 800) or anti-GAPDH (1 : 50000). Detection of primary antibodies was performed using anti-rabbit IgG horseradish (1 : 20000) or anti-mouse IgG horseradish peroxidase (1 : 50000) followed by ECL Plus.

Harvesting Xenopus laevis oocytes

Stage V/VI oocytes were surgically removed from the ovaries of *Xenopus laevis* frogs anesthetized with 1 g/l MS-222. Clusters of oocytes were incubated with 2 mg/ml collagenase for 2 h in Ca^{2+}-free solution comprised of (in mM) 115 NaCl, 2.5 KCl, and 10 HEPES, pH 7.5, with slow agitation to remove the follicular cell layer. Oocytes were then washed extensively in the same solution supplemented with 1.8 mM $CaCl_2$ and maintained in Barth's solution comprised of (in mM): 88 NaCl, 1 KCl, 24 $NaHCO_3$, 10 HEPES, 0.82 $MgSO_4$, 0.33 $Ca(NO_3)_2$, and 0.91 $CaCl_2$ and supplemented with 100 mg/ml gentamycin, 40 mg/ml streptomycin, and 50 mg/ml penicillin in a 17°C incubator.

Expression of NR1/NR2 receptors in Xenopus oocytes

pCIneo NR1-1a, pcDNA1 NR2B and pcDNA1 NR2B(K318A) plasmid DNA were linearized using NotI. Linearized DNA was analyzed in preparative 0.8 % agarose gel electrophoresis and purified using QIAquick gel extraction kit according the manufacturer's protocol. Purified, linearized DNA was used to generate RNA using the mMESSAGE mMACHINE T7 kit according to the manufacturer's protocol. Quality of RNA was analyzed using analytical 0.6 % agarose gel electrophoresis and quantity was measured using ND-1000 spectrophotometer (NanoDrop Technologies, Montchanin, DE, USA). Oocytes were injected under the magnification of SMZ435 dissecting scope (Nikon, Tokyo, Japan) after 24 h of isolation. Oocytes were injected with 10-15 ng of RNA in a 50 nl volume using oocyte microinjection pipet (Drummond Scientific, Broomall, PA, USA) mounted on a Marzhauser MM33 micromanipulator (SDR, Sydney, Australia). The ratio of NR1 to NR2 was at 3:7. Following injection, oocytes were incubated at 17°C in Barth's solution.

Two-Electrode Voltage-Clamp (TEVC) Recordings from Xenopus Oocytes

TEVC recordings on oocytes were as described previously (Traynelis et al., 1998; Low et al., 2000). Recordings were performed 2-8 days post injection at room temperature using oocyte clamp OC-725C (Warner Instruments, Hamden, CT, USA). Oocytes were placed in a custom-made dual-track recording chamber with a single perfusion line that split to perfuse two oocytes. The bath clamps communicated across Ag-$AgCl_2$ pellets (Warner Instruments, Hamden, CT, USA) placed at each side of the recording chamber, both of which were assumed to be at a reference potential of 0 mV. The recording solution contained (in mM): 90 NaCl, 1 KCl, 10 HEPES, 0.5 $BaCl_2$, pH adjusted to 7.3 with 5 N NaOH. Solution exchange was computer-controlled through a 8-modular valve positioner (Hamilton, Reno, NV, USA) using the EasyOocyte software (a gift from Dr. S.F. Traynelis). Voltage and current electrodes had a resistance of 2-8 MΩ when filled with 0.3 and 3.0 M KCl, respectively. Saturating concentration of glutamate and glycine (30-100 μM) and 0.03-10 μM ifenprodil were used in all oocytes experiments unless otherwise stated. Current responses were elicited with agonists, in the presence or absence of ifenprodil for 1 min and recorded at a holding potential of -20 to -60 mV. Only currents greater than 50 nA were included in the analysis. Steady-state currents were obtained for 0.3–10 μM ifenprodil and near steady-state currents were obtained for 0.03-0.1 μM ifenprodil (Perin-Dureau et al., 2002b). Ifenprodil inhibition data points were fitted to the equation:

$$\textit{Percent response} = (100 - \textit{minimum}) / (1 + ([\text{ifenprodil}]/IC_{50})^{n}) + \textit{minimum}$$

obtaining the ifenprodil inhibition curves where *minimum* is a residual current response, IC_{50} is the concentration of ifenprodil that produces 50 % of the maximal inhibition and *n* is the Hill slope. Data points were collected from at least two different *Xenopus laevis* frogs.

Determination of thrombin activity in the presence of DTT

Rate of hydrolysis of thrombin in the presence and absence of DTT were also determined in the same manner as above. However, thrombin was incubated with 3 mM DTT before the addition of Spectrozyme®TH. The vehicle for DTT was ultrapure water. 3 mM DTT did not interfere with Spectrozyme®TH. 3 mM DTT (saturating concentration for inducing reduction action on NMDA receptors) was used to investigate interference on thrombin activity (Tang and Aizenman, 1993).

Thrombin treatment on oocytes

Oocytes were treated with ±thrombin/±DTT, followed by a wash out of drugs as stated in (Fig. 3.3A). Vehicle for DTT was the recording solution and that for thrombin was the thrombin diluent. Treatment was carried out with TEVC recording in real time. % maximum response was carried out in saturating concentration of glutamate and glycine (100 µM each) and 0.1 µM, 1 µM and 10 µM of ifenprodil.

Illustration of crystal structure of NR2B ATD

The apo-crystal structure of NR2B ATD (Protein Data Bank code 3JPW) provided the structural template to create the images using Protein Workshop (Karakas et al., 2009).

Data analysis

Data were expressed as mean ± S.E.M. and analyzed statistically using paired T-test or one-way ANOVA followed by post-hoc Tukey test. Significance for all tests was set at $P < 0.05$. Error bars in figures were S.E.M. Graphs were plotted using GraphPad PRISM® Version 4.

3.3 Results

In situ proteolysis of native NR2B in primary rat cortical neurons

To investigate if thrombin can interact and cleave the NR2B ATD in the native quaternary heteromeric structure, E18 cortical neuronal culture was used. E18 cortical neuronal culture was chosen because cortical neurons have the highest expression of NR2B at that developmental stage (Monyer et al., 1994). Culturing condition was optimized such that it favored the growth and development of neurons with minimal contamination from glia (less than 5 % glia) (Fig. 3.1A) (Wee et al., 2010). DIV11 neuronal culture obtained also showed NR1 and NR2B receptors colocalizing with each other (Fig. 3.1B-E). They were surface receptors, with the ability to develop as clusters along dendrites, starting from the soma (Fig. 3.1F-G) (Li et al., 1998a; Rao et al., 1998; Cottrell et al., 2000; Washbourne et al., 2004). Thrombin treatment was performed on these cortical neuronal cultures by incubating neurons in increasing concentration of thrombin (0.1-1000 nM), *in situ*, for 2 h at 37°C. With increasing thrombin concentration, ~150 kDa protein fragments that were immunoreactive to C-terminal anti-NR2B were detected (Fig. 3.2) (albeit was less efficient compared to experiments with RBL, SPM and recombinant $NR2B_{ATD}$; Fig. 2.4B, Fig. 2.4C, Fig. 2.4D, Fig. 2.5A and Fig. 2.6B in Chapter 2). The appearance of the cleaved ~150 kDa fragment was accompanied by a decrease in immunoreactivity to the full-length NR2B (Fig. 3.2A, n=3). At 100 nM of thrombin, about 50 % of the full-length NR2B was cleaved (Fig. 3.2B). These observations demonstrated that thrombin can cleave NR2B in its native NMDA receptor complex that was expressed of the membrane surface.

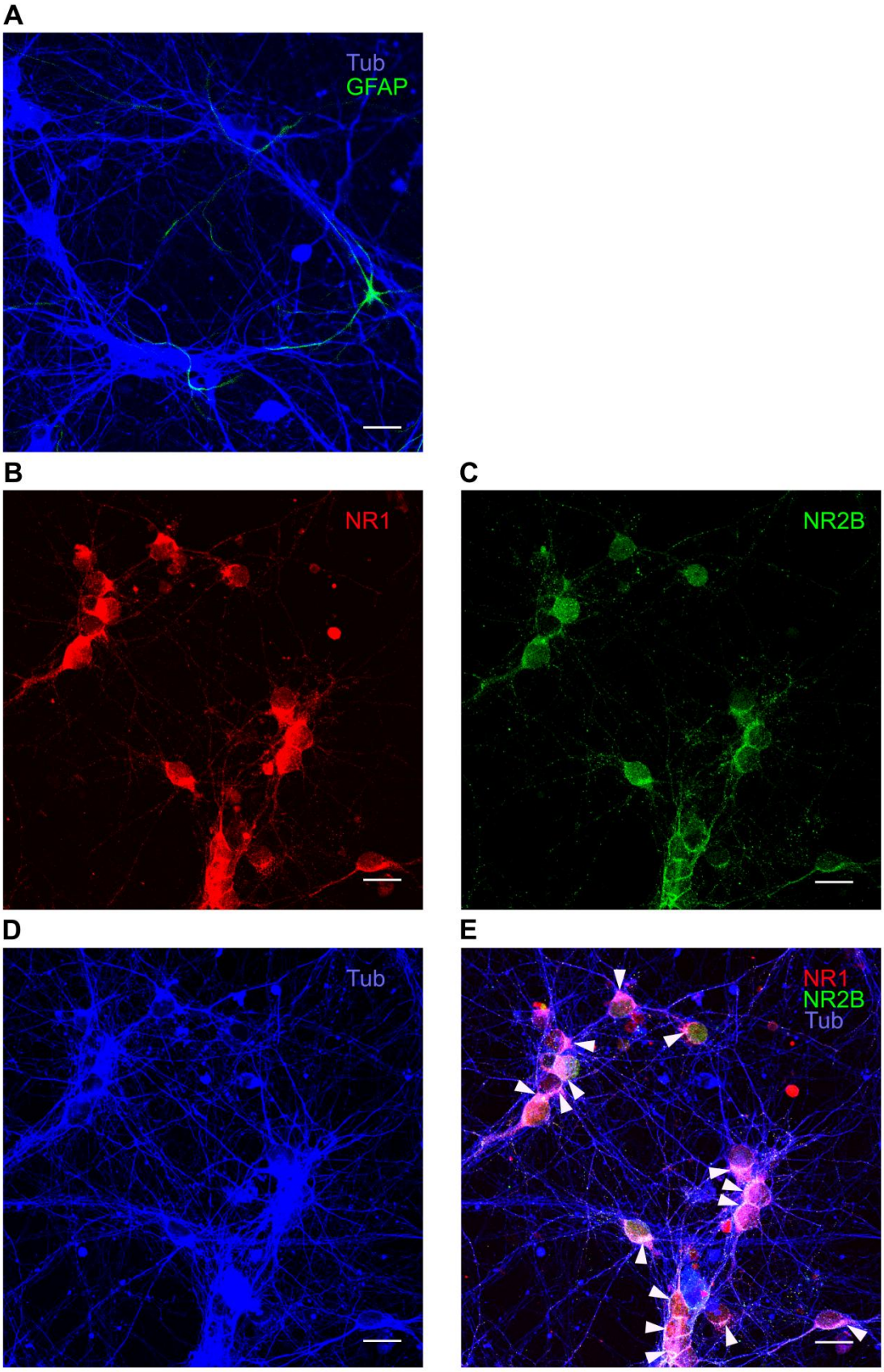
A
Tub
GFAP
B
NR1
C
NR2B
D
Tub
E
NR1
NR2B
Tub

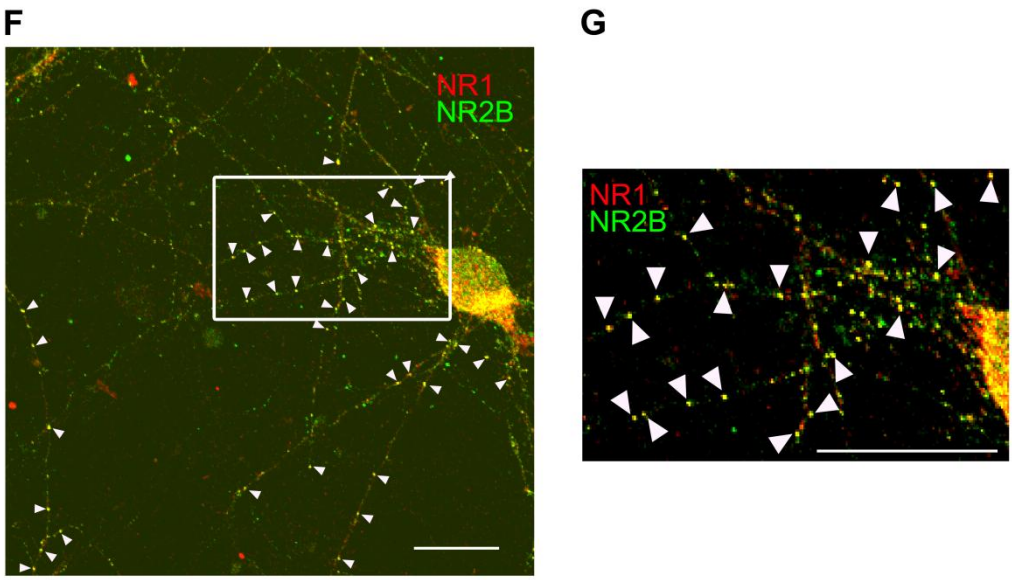

Fig. 3.1. Characterization of cultured cortical neurons using immunofluorescence microscopy. (A) Double immunolabeling with neuronal and astrocyte marker. Photomicrograph showed significantly more βIII tubulin (Tub)-positive neurons (blue) than GFAP-positive astrocytes (green). (B-D) Photomicrographs showing immunolabeling of NR1 (red), NR2B (green) and Tub (blue) in DIV11 cortical neuronal cells. (E) Merged immunofluorescence image showed co-localization of NR1 and NR2B in neurons (indicated by large arrowheads). (F) Photomicrographs showing NR1 (red) and NR2B (green) staining. Small arrow heads indicate clusters formed. The indicated segment of the image (white box) was magnified and showed in (G). (G) Both NR1 and NR2B subunits formed surface receptors and displayed as subunit cluster staining along dendrites (indicated by medium arrowheads) starting from the soma. Scale bar = 20 μm.

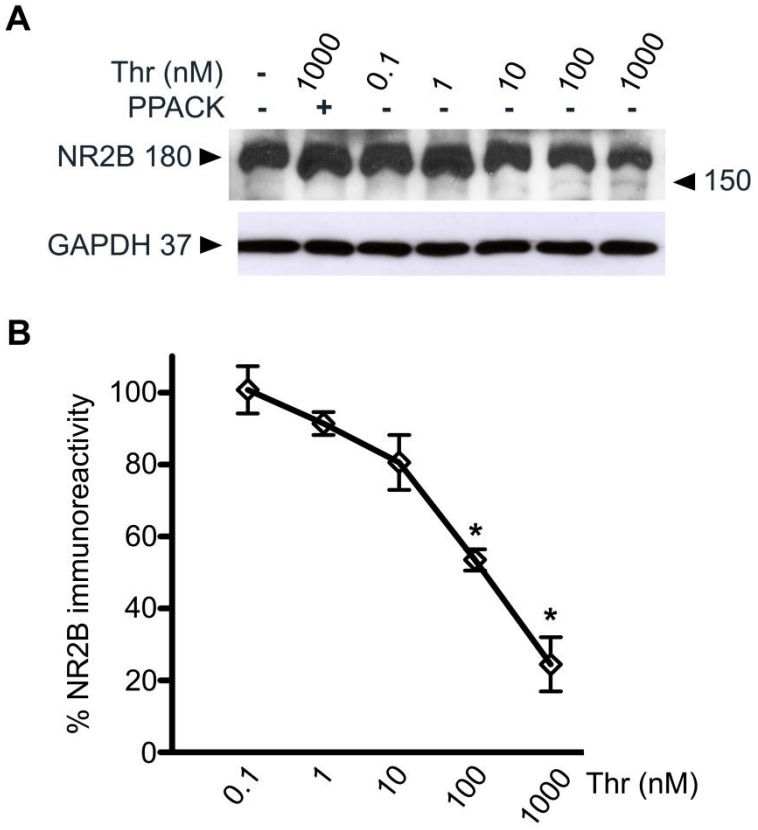

Fig. 3.2. Thrombin cleaves NR2B from NMDA receptor complex expressed on the membrane surface of cortical neurons. DIV11 cortical neurons were treated with thrombin for 2 h. (A) (Top panel) A 150 kDa fragment was detected with an C-terminal anti-NR2B upon 10 nM and higher concentrations of thrombin treatment (n=3). GAPDH was the loading control. Thrombin is indicated as Thr. Molecular weight (in kDa) of the protein and the fragments are as indicated. (B) Immunoreactivity quantification of full-length NR2B for the indicated treatment. Data (mean ± S.E.M.) were expressed in terms of percentage of initial substrate densitometry. * indicated $P < 0.01$ (one-way ANOVA, post-hoc Dunnett test).

Investigation of thrombin interaction with NR2B in the reducing environment experienced in ischemic stroke

The above results demonstrated the possibility of thrombin cleavage of NR2B in its native conformation expressed in the NMDA receptor complex. Considering that ifenprodil binds to the ATD of NR2B, a change in the ifenprodil sensitivity can be an indicator of thrombin cleavage at the ATD of NR2B in functional receptors (Perin-Dureau et al., 2002a; Mony et al., 2009b). Thus, to further verify that thrombin cleaves NR2B in functional NMDA receptors, thrombin treatment was performed on NR2B subunit heterologously expressed with NR1 in *Xenopus laevis* oocytes. After which, ifenprodil inhibition was measured. Oocytes were treated to 400 nM thrombin for 20 min to allow maximal interaction between thrombin and NR2B without affecting viability of oocytes (Fig. 3.3A). The ifenprodil IC_{50} of NR1/NR2B was 0.21 ± 0.05 μM (n=26) in the absence of thrombin treatment (Fig. 3.3B). Thus three ifenprodil concentrations (0.1 μM, 1 μM and 10 μM) were chosen as they would be sufficient in detecting any significant rightward shift in the IC_{50} of ifenprodil if there was successful reduction in ifenprodil sensitivity induced by thrombin cleavage at the NR2B ATD (Fig. 3.3A and Fig. 3.3B).

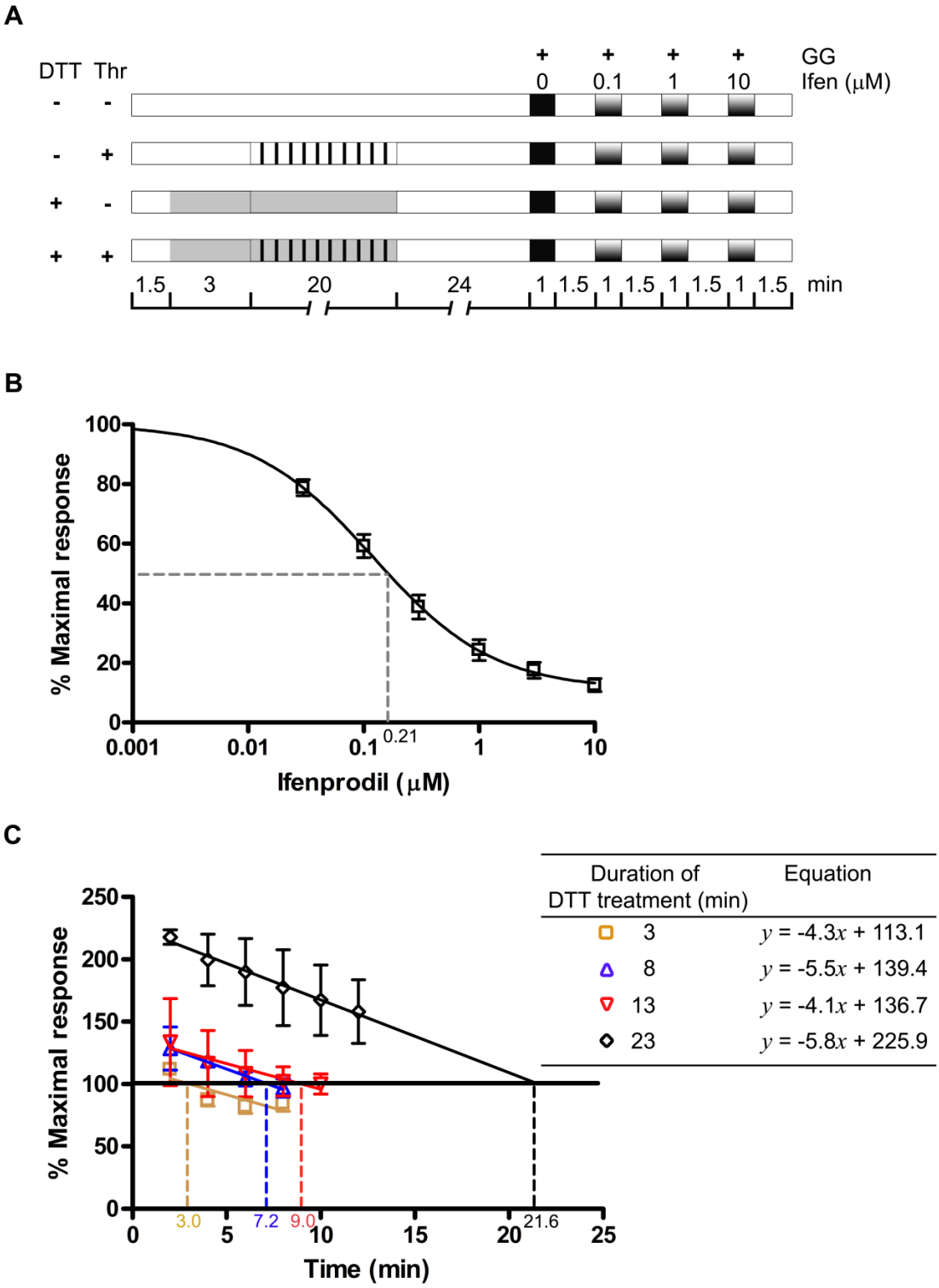

Fig. 3.3. Basis for treatment conditions for proposed experimental paradigm. (A) Experimental paradigm: Open field indicates wash perfusion with recording solution. Gray field indicates 3 mM DTT treatment. Vertical stripped field indicates 400 nM thrombin treatment. Black field indicates glutamate and glycine treatment (100 μM each). Gradient gray field indicates the respective concentration of ifenprodil treatment in the presence of glutamate and glycine (100 μM each). GG indicates glutamate and glycine. Ifen indicates ifenprodil. Thr indicates thrombin. Time line (in min) is indicated at the bottom. (B-C) Responses were presented as percentages of currents measured against the maximum current

elicited by saturating concentration of glutamate and glycine on NR1/NR2B receptors. Each data point was the mean ± S.E.M., n=2-26 oocytes recorded. (B) Range of ifenprodil concentration to be used. Ifenprodil dose-dependent response curve for NR1/NR2B was plotted. Ifenprodil IC_{50} of 0.21 ± 0.05 µM, n=26 was indicated. 0.1 µM to 10 µM ifenprodil produced a sufficient range for detecting a rightward shift in ifenprodil sensitivity upon possible thrombin cleavage. (C) Time required for reverting the effects of DTT. Receptors were more potentiated upon longer DTT treatment (as color coded). All returned to the original state (100 % maximal response) upon wash out with recording buffer. The equation was the best-fit of the data points. The time for wash out for each DTT treatment were calculated based on the best-fit equation and is indicated at the x-axis.

The probability of thrombin interaction with NR2B is the highest in pathological situations like stroke due to the increase in the level of thrombin during stroke condition (Karabiyikoglu et al., 2004; de Castro Ribeiro et al., 2006). In cerebral ischemic stroke, in addition to a change in the level of thrombin, the homeostatic environment is greatly disturbed. A reduction in oxygen in cerebral ischemic stroke would produce a reducing milieu in the affected brain area where proteolysis of NMDA receptors by thrombin could occur (Yager et al., 1991; Anderson et al., 1999; Chen and Shi, 2008). There are several redox sites at the NMDA receptors, which upon reduction, would result in potentiation of the NMDA receptors function through structural modification of the receptors via the disulfide bond at the redox sites (Table 1.1 in Chapter 1) (Tang and Aizenman, 1993; Sullivan et al., 1994; Brimecombe et al., 1999; Choi et al., 2001; Karakas et al., 2009). Thus I was interested in investigating whether such structural modification of the NMDA receptors during reducing condition would affect thrombin cleavage. I simulated the reducing environment by pre-incubating oocytes in recording solution containing a reducing agent DTT (3 mM) for 3 min followed by 20 min of thrombin (400 nM) treatment (Fig. 3.3A). Thrombin activity in 3 mM DTT was not statistically different ($6.5 \times 10^{-5} \pm 7.6 \times 10^{-6}$ s^{-1}, n=6) compared to that in the absence of 3 mM DTT ($6.2 \times 10^{-5} \pm 5.4 \times 10^{-6}$ s^{-1}, n=6) (Fig. 3.4) (Serejskaya et al., 1983; Rajesh Singh and Chang, 2003).

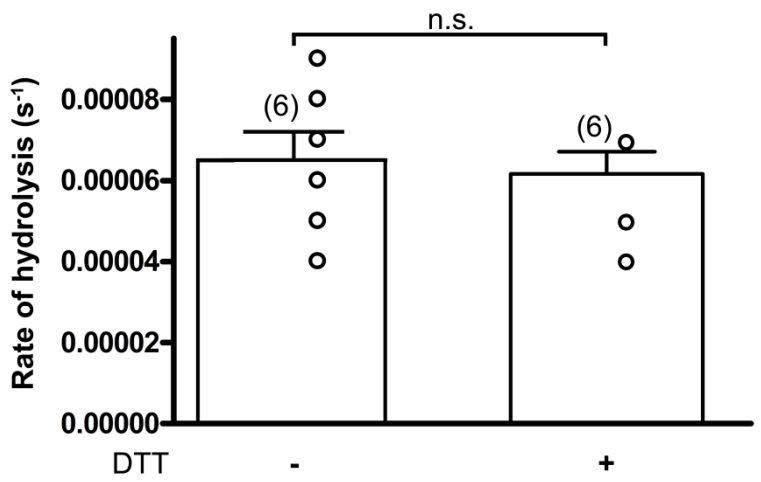

Fig. 3.4. Thrombin activity is not altered by 3 mM DTT. Rate of hydrolysis of chromogenic substrates by thrombin in the absence or presence of 3 mM DTT were not statistically different from each other (indicated as n.s.) Statistical test used was paired T-test. n=6 tests were performed (in parentheses). Values were mean ± S.E.M.

In order to eliminate the concern that DTT affects the ifenprodil binding and as a consequence, affects the analysis of thrombin cleavage based on ifenprodil sensitivity, complete wash out of the DTT had to be carried out, allowing for the spontaneous reversal of the DTT effect (i.e. 100 % maximal response) (Tang and Aizenman, 1993). Ifenprodil sensitivity was measured only after the DTT effect was reverted (Fig. 3.3A and Fig. 3.3C). It was observed that 2 min of 4 mM DTT treatment required 3 min of wash out period for spontaneous reversal of the DTT effect. In our study, the oocytes were pretreated to 3 mM of DTT followed by 20 min of thrombin treatment under reducing condition. As such, the oocytes would be under a total of 23 min of DTT treatment (Fig. 3.3A). Thus it was investigated if longer treatment of DTT would require longer wash out period. Indeed, with increasing time of DTT treatment, a longer time was required to spontaneously reverse the DTT effect. This was due to the larger DTT potentiation effect observed with longer DTT treatment (Fig. 3.3C). Using the best fitted line-plots, time required to revert back to the original state for different time of DTT treatment was calculated. For 23 min of DTT treatment, 21.6 min wash out was required (Fig. 3.3B). Considering the data obtained and the variations in the NMDA responses, a wash out time of 24 min was set to ensure all NMDA receptors revert to original state before ifenprodil sensitivity was measured. As such, the experimental paradigm was as depicted in (Fig. 3.3A). Ifenprodil sensitivity was evaluated as the percentage of maximal response at three different ifenprodil concentrations (0.1 μM, 1 μM and 10 μM; gradient gray field in Fig. 3.3A) observed at steady-state on glutamate and glycine (100 μM each) evoked oocyte currents against glutamate and glycine treatment only (with no ifenprodil) after the washout.

Thrombin-treated oocytes in the absence of reducing environment (-DTT) did not significantly decrease the ifenprodil (0.1 μM, 1 μM and 10 μM) sensitivity, an indication that NR2B may not be effectively cleaved under the specified experimental conditions (Table 3.1). Interestingly, thrombin-treated oocytes (in 3 mM DTT) shifted the ifenprodil concentration-response curve to the right as compared to no thrombin treatment (Fig. 3.5A).

This observation indicated that thrombin treatment had reduced the inhibitory effect of ifenprodil on the NR1/NR2B receptors. At 0.1 μM of ifenprodil, agonists-evoked response was significantly higher in thrombin (+DTT) group (54.8 ± 2.96 %, n=13 oocytes) as compared to no thrombin (+DTT) group (41.2 ± 3.87 %, n=12; $P < 0.05$; one-way ANOVA, post-hoc Tukey test), thrombin (-DTT) group (35.1 ± 6.13 %, n=6; $P < 0.01$; one-way ANOVA, post-hoc Tukey test) and no thrombin (-DTT) group (34.2 ± 2.46 %, n=7; $P < 0.01$; one-way ANOVA, post-hoc Tukey test) (Fig. 3.5B and Table 3.1). At 1 μM and 10 μM of ifenprodil, there was a trend of increase in the agonist-evoked responses in thrombin (+DTT) treatment group as compared to other treatment groups (Table 3.1). The shift in ifenprodil sensitivity was due to thrombin cleavage and was not contributed by DTT affecting ifenprodil binding as ifenprodil inhibition was not statistically different for oocytes treated with +DTT/-thrombin compared to –DTT/-thrombin treatment (Table 3.1). These results described, suggested that ifenprodil sensitivity was decreased by thrombin treatment under reducing condition.

Receptor	Treatment		Mean relative current (%)			
	DTT	Thrombin	Ifenprodil			
	(3 mM)	(400 nM)	0.1 μM	1 μM	10 μM	n
NR1/NR2B	-	-	34.2 ± 2.46 **	11.2 ± 2.21	6.60 ± 1.70	7
	-	+	35.1 ± 6.13 **	15.2 ± 4.10	10.9 ± 2.86	6
	+	-	41.2 ± 3.87 *	10.4 ± 3.47	5.32 ± 2.27	12
	+	+	54.8 ± 2.96	18.9 ± 3.46	12.3 ± 3.34	13

Table 3.1. Thrombin treatment alters NR1/NR2B receptors ifenprodil inhibition under reducing condition but not in non-reducing condition. Ifenprodil sensitivity was not statistically different between with and without thrombin treatment in the absence of DTT at the three concentration of ifenprodil (0.1, 1 and 10 μM ifenprodil) tested. * and ** represented $P < 0.05$ and $P < 0.01$ respectively when compared to thrombin treatment in the presence of 3 mM DTT. Statistical test used was one-way ANOVA, post-hoc Tukey test. n indicates the number of oocytes tested. Values represented mean ± S.E.M.

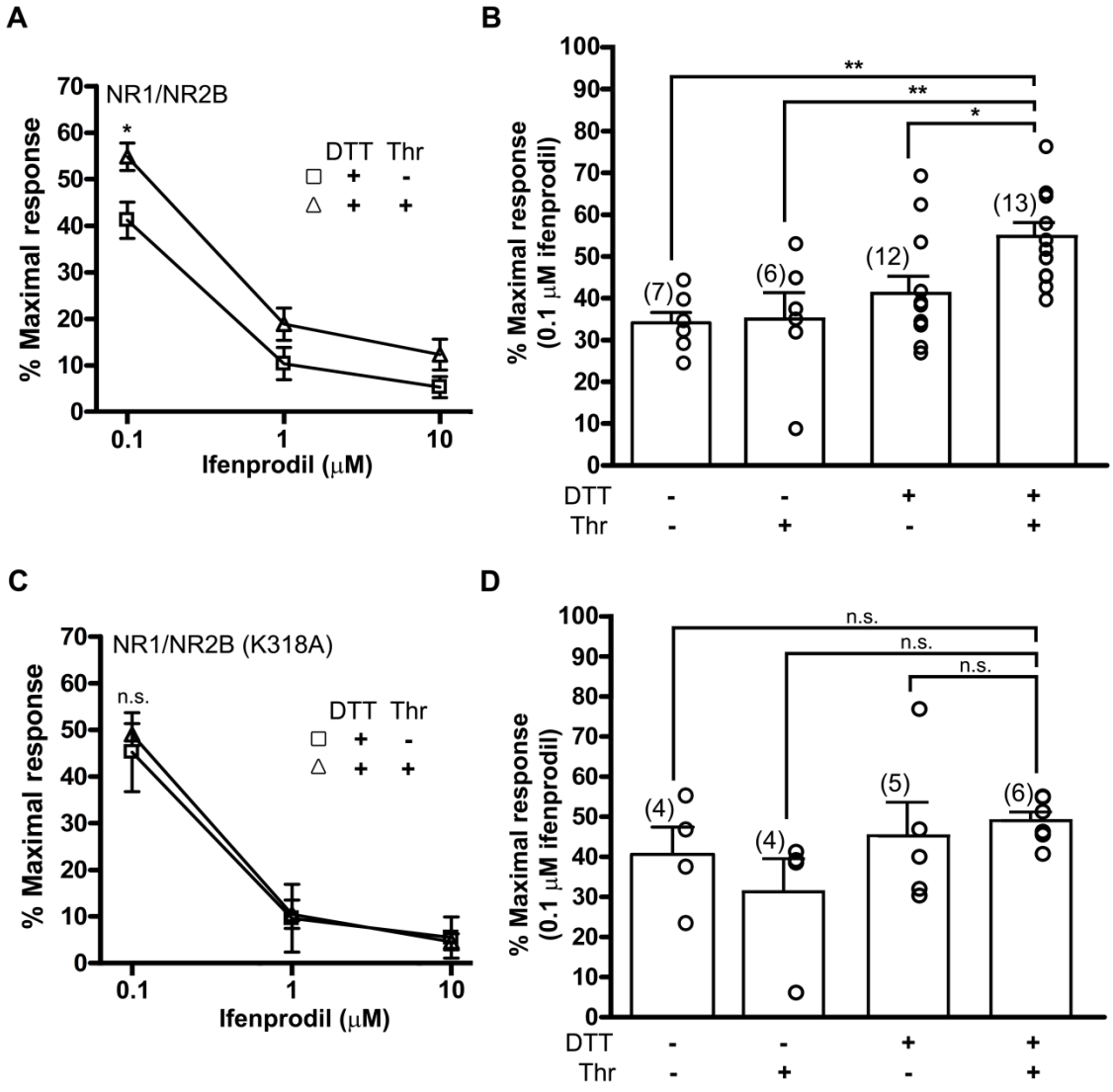

Fig. 3.5. Thrombin decreases ifenprodil inhibition of recombinant NR1/NR2B receptors but not NR1/NR2B(K318A) receptors under reducing condition. (A) % maximal responses produced by 0.1 μM, 1 μM and 10 μM of ifenprodil after -/+ thrombin (Thr) treatment in the presence of 3 mM DTT on NR1/NR2B receptors and (C) on NR1/NR2B(K318A) receptors. □ indicates +DTT/-Thr treatment. △ indicates +DTT/+Thr treatment. (B) % maximal responses in the presence of 0.1 μM of ifenprodil under four different treatment conditions depicted in Fig. 3.3A for NR1/NR2B and (D) for NR1/NR2B(K318A). ○ indicates value obtained from each experiment. * and ** represent $P < 0.05$ and $P < 0.01$, respectively. n.s. indicates that results were not statistically different. Statistical test used was one-way ANOVA, post-hoc Tukey test. n=4-13 oocytes recorded (in parentheses). Values were mean ± S.E.M.

To further confirm the hypothesis that the relief of ifenprodil inhibition observed in Fig. 3.5A was due to thrombin cleavage at Lys^{318} on the NR2B ATD, Lys^{318} was mutated to alanine (NR2B(K318A)). Ifenprodil inhibition was then measured from NR1/NR2B(K318A)-expressing oocytes in the same manner (±thrombin/±DTT) as described earlier for oocytes expressing heterologous NR1/NR2B receptors. Consistent with the hypothesis, we found that there was no rightward shift in the ifenprodil concentration-response curves (Fig. 3.5C) unlike that observed in thrombin treatment (+DTT) on wild-type NR1/NR2B (Fig. 3.5A). At 0.1 μM ifenprodil, the agonist-evoked response for thrombin treated under reducing condition (49.0 ± 2.33 %, n=6) was similar to that in the absence of thrombin under reducing condition (45.3 ± 8.43 %, n=5; $P > 0.05$; one-way ANOVA, post-hoc Tukey test) (Fig. 3.5D and Table 3.2). Taken together, these data suggest that thrombin-induced removal of ifenprodil inhibition of NR1/NR2B could be, at least in part, mediated through cleavage of the NR2B ATD at Lys^{318}.

Receptor	Treatment		Mean relative current (%)			
	DTT	Thrombin	Ifenprodil			
	(3 mM)	(400 nM)	0.1 μM	1 μM	10 μM	n
NR1/NR2B(K318A)	-	-	40.7 ± 6.77	9.35 ± 4.28	3.30 ± 1.92	4
	-	+	31.3 ± 8.39	9.90 ± 2.10	0.00 ± 0.00	4
	+	-	45.3 ± 8.43	9.62 ± 7.27	5.46 ± 4.40	5
	+	+	49.0 ± 2.33	10.5 ± 3.03	4.55 ± 1.70	6

Table 3.2. Thrombin treatment under reducing condition does not alter NR1/NR2B(K318A) receptors ifenprodil sensitivity. Ifenprodil sensitivity for the different treatment groups were not significantly different from each other at the ifenprodil concentration (0.1, 1 and 10 μM) tested. Statistical test used was one-way ANOVA, post-hoc Tukey test. n indicates the number of oocytes tested. Values represented mean ± S.E.M.

3.4 Discussion

The present study demonstrated that nanomolar concentration of thrombin can moderate NR2B-containing NMDA receptor's sensitivity to ifenprodil, at least in part in a reducing environment, by cleaving NR2B ATD at Lys^{318}. Importantly, if NR2B-selective antagonists targeted at the ATD were to be administered to reduce excitotoxicity, the efficacy of such drugs may be reduced by thrombin's proteolytic cleavage of NR2B at the ATD. Thus, the findings from this study hold implications for the design of new drug leads that are negative allosteric modulators of NMDA receptors binding at the ATD.

Structural implications of thrombin cleavage on NR2B

It is demonstrated that thrombin cleaved NR2B in a reducing environment but not in the non-reduced state (Fig. 3.5). Examining the crystal structure of the NR2B ATD (3JPW) that has recently been published, Lys^{318} is located approximately to the centre of a hypervariable loop (HVL) and is lying right above helix 1 and helix 2 (Fig. 3.6) (Karakas et al., 2009). The HVL of the ATD is made up of 18 amino acids and links helix 8 to helix 9. The HVL appears to be rigid as held by a disulfide bond formed between Cys^{86} on helix 1 and Cys^{321} on the HVL loop. The intraprotomer disulfide bond orientates the HVL in a way such that the loop appears to be a "lid" covering the R1 domain and renders Lys^{318} not as solvent accessible in the native conformation (Fig. 3.6A). This could also be the reason for the less efficient cleavage or an absence of cleavage under non-reducing conditions (Table 3.1, Fig. 3.5A and Fig. 3.5B). Since both apo- and Zn^{2+}-bound conformations (3JPW and 3JPY respectively) are similar to each other with root mean square (r.m.s.) deviation of only 0.56 Å over 356 Cα positions, we expect Lys^{318} to be relatively inaccessible to thrombin in both conformations (Karakas et al., 2009).

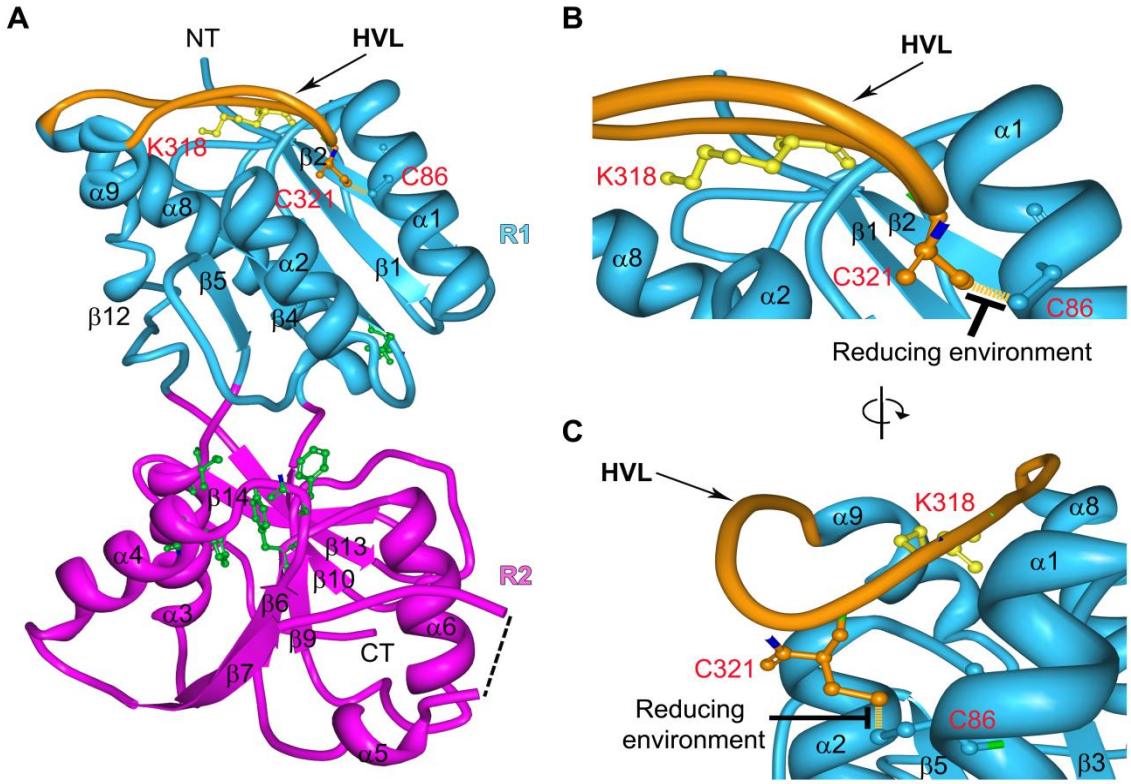

Fig. 3.6. Crystal structure of apo-NR2B ATD and location of Lys^{318}. (A) Ribbon representation of the apo-NR2B ATD structure (3JPW) generated using Protein Workshop. Secondary structures are as labeled (Karakas et al., 2009). N-terminal is indicated as NT while C-terminal is indicated as CT. The clam-shell structure of the NR2B ATD is made up of two domains, R1 (blue) and R2 (magenta). The disordered region (residues 208-214) is indicated as a black dotted line. Asp^{101}, Ile^{150}, Phe^{176}, Phe^{182} and Tyr^{231} involved in ifenprodil inhibition are colored green. The disulfide bond formed between Cys^{86} (blue) and Cys^{321} (orange) is highlighted as a pale orange dotted line. The disulfide bond is involved in holding the HVL (orange) in place such that the HVL covers the top of R1. Lys^{318} (yellow) lies on HVL. (B) Zoom in view of the spatial orientation of Lys^{318} on the HVL with respect to the disulfide bond. (C) NR2B ATD structure viewed from the front of the HVL. Reducing environment may disrupt the disulfide bond formation between Cys^{86} and Cys^{321}, affecting the intact structure of the HVL.

In ischemic stroke, many proteins are in a reduced state (Anderson et al., 1999; Chen and Shi, 2008). In such pathological condition, a disulfide bond between the Cys^{86} and Cys^{321} could be potentially reduced. Reduction of the disulfide bond between Cys^{86} and Cys^{321} to the respective thiol groups may render the HVL more flexible and may cause the Lys^{318} residue to be more solvent accessible (Fig. 3.6B and Fig. 3.6C). This hypothesis was further demonstrated through a molecular dynamics simulation carried out by our collaborator, Dr Zhang Bing. Simulating a reduction of the disulfide bond between Cys^{86} and Cys^{321}, it was shown in the molecular model that the Lys^{318} becomes exposed to the extracellular milieu (Fig. 3.7). Moreover, in the present study, it was also observed that point mutation at K318A was able to block the proteolytic effects of thrombin, which further supported the notion that thrombin could access the cleavage site (Lys^{318}) on NR2B ATD under reducing condition (Fig. 3.5). Interestingly, these Cys^{86} and Cys^{321} residues are highly conserved among NR1 and NR2 subunits (Fig. 3.8). From the structure, we envisaged that under reducing condition, the reduction of the disulfide bond would allow more flexibility at the HVL and cleavage of the HVL of the NR1 and the other NR2 subunits could concur in a similar way (Fig. 3.6C). However, due to the absence of molecular recognition motif in all other subunits, thrombin cleavage is less likely (Fig. 3.8) (also briefly discussed in Chapter 2) (Gingrich et al., 2000). However, HVL may, nevertheless, be prone to other proteases cleavage that has different molecular recognition motif from thrombin (Fig. 3.8) (Samson et al., 2008; Yuan et al., 2009b). Thus, the disulfide bond acts as a redox switch and plays a crucial role in determining the accessibility of residues like Lys^{318} on NR2B to proteases like thrombin (Lipton et al., 2002; Takahashi et al., 2007).

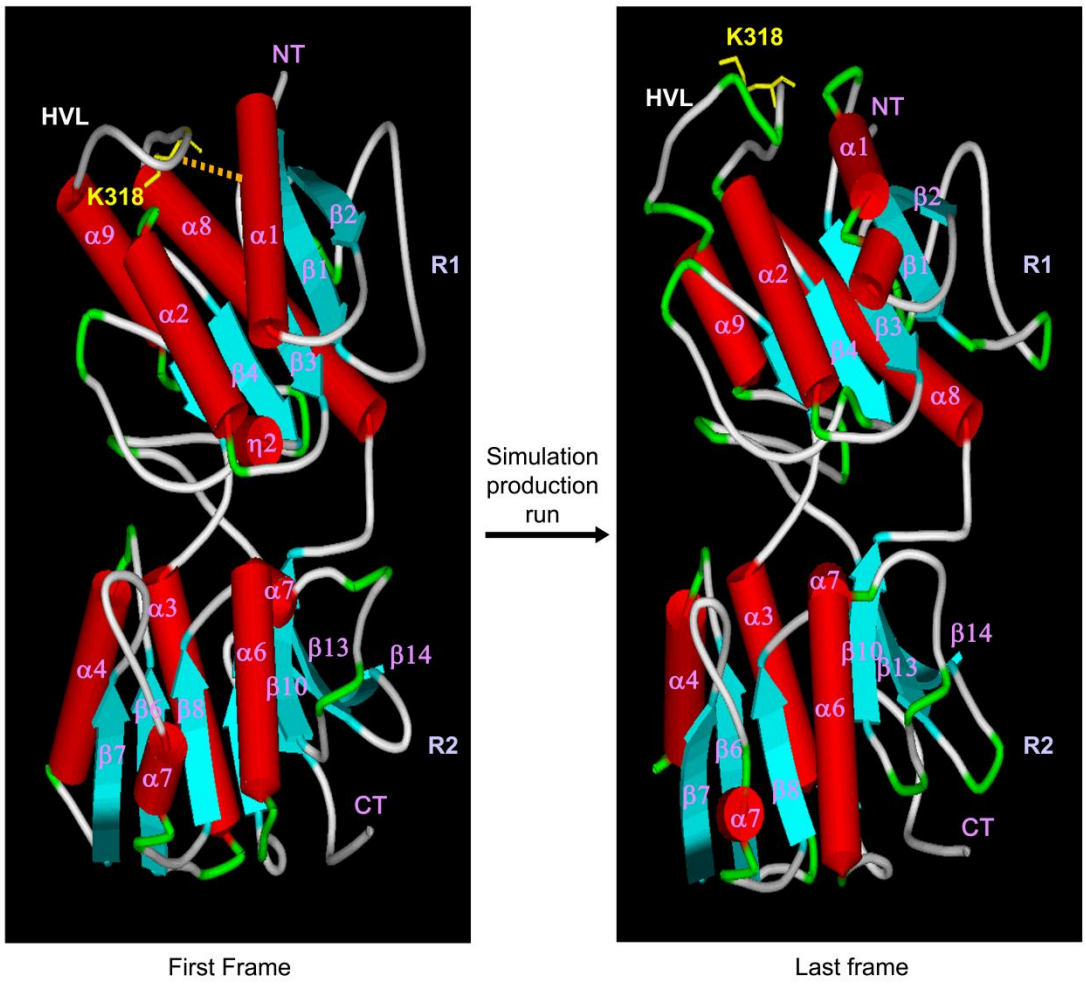

Fig. 3.7. Molecular dynamics simulation based on the NR2B ATD crystal structure (3JPY). The dynamics simulation and post-progressing sampling were carried out using the Amber10 program package. The dynamics simulation spanned over a period of 10 ns and snapshots of the conformation of the protein were sampled every 500 ps throughout the whole dynamic process. All the snapshots (in PDB format) were then superimposed onto and compared with the NR2B crystal structure (3JPY). Pictures of each conformation were taken and saved separately with Accelrys Discovery Studio. The first frame and the last frame of the simulation are presented here. Lys^{318} (yellow) in NR2B protein was minimized prior to the production run to reduce any possible clashes among the amino acids. Molecular simulation was performed on the NR2B C86A to mimic the absence of the disulfide bond between Cys^{86} and Cys^{321} (indicated as orange dotted line) during reducing condition. Lys^{318}, located at the HVL (as indicated), was shown to be exposed to the extracellular milieu upon reduction of the disulfide bond. The R1 domain, R2 domain and the secondary structures are as labeled (Karakas et al., 2009). NT indicates N-terminal while CT indicates C-terminal.

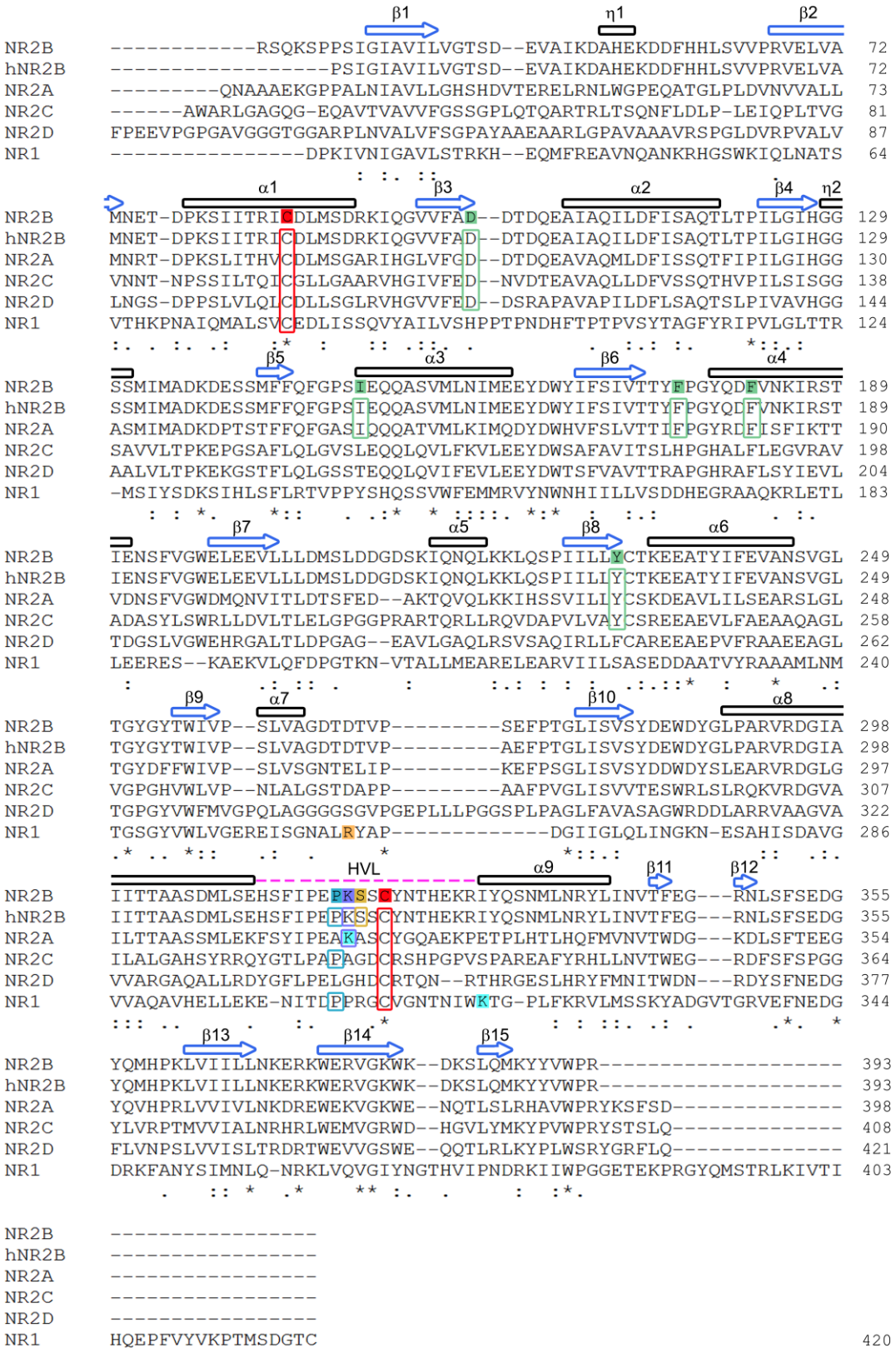

Fig. 3.8. NR1 and NR2 ATD sequence alignment. The ATD of NR2B, human NR2B (hNR2B), the different NR2 subunits (NR2A-D) and NR1 protein sequences are aligned using ClustalW (http://www.ebi.ac.uk/Tools/clustalw2/index.html). The cysteine residues that are involved in the disulfide bond in the NR2B crystal structure are highlighted in red. The

cleavage site Lys^{318} is highlighted in light purple. The P1 Pro^{317} is highlighted in light blue. The P1' Ser^{319} is highlighted in light brown. Plasmin cleavage sites are highlighted in cyan. tPA cleavage site is highlighted in orange. Residues that are important for binding to ifenprodil are highlighted in green. Conserved residues of the above mentioned sites are boxed up in their respective color. ***** indicates residues are conserved. **:** indicates conserved substitution. **.** indicates semi-conserved substitution. Secondary structures of NR2B ATD are indicated as blue arrows for β-strands and black boxes for α- and $\eta(3_{10})$-helices (Karakas et al., 2009). Hypervariable loop (HVL) is indicated as a pink dotted line.

Functional implications of thrombin cleavage on NR2B

The oocyte functional data showed significant decrease in ifenprodil inhibition at 0.1 μM but not 1 μM and 10 μM ifenprodil upon thrombin treatment in the presence of 3 mM DTT. We proposed that at 400 nM thrombin (20 min treatment in the presence of 3 mM DTT), the proportion of cleaved NR2B is at a low level. As concentrations of ifenprodil increases (1 μM and 10 μM in this study), the probability of ifenprodil molecules binding to the uncleaved NR2B increases. The resultant degree of inhibition by high concentrations of ifenprodil would resemble that of wild-type NR1/NR2B receptors and hence would not show significant difference between the cleaved and intact NR1/N2B receptors. Increasing the time of exposure and concentration of thrombin would likely cause more disruption in the ATD via cleavage and possibly a greater change in the ifenprodil inhibition (i.e. even at higher concentration of 1 μM and 10 μM ifenprodil). Unfortunately, from my experience, increasing time (up to 40min) and concentration (up to 500 nM) of thrombin treatment rendered oocytes unstable to prolonged TEVC recordings. Thus, it would be interesting to investigate how full cleavage of NR2B Lys^{318} affects the function of the NMDA receptors.

Clinical implications of thrombin cleavage on NR2B

It is shown in this study that 400 nM of thrombin can cleave Lys^{318} under reducing condition, one of the pathological conditions present in ischemic stroke. Cleavage at the Lys^{318} lowered the ifenprodil inhibition on NMDA receptors. Ifenprodil and their analogues had been investigated as potential drug leads in ischemic stroke. However, such clinical trials have failed due to adverse effects or absence of positive stroke outcome (Nikam and Meltzer, 2002; Gogas, 2006). One of the reasons for the lack of translational success from animal stroke models lies in the way such stroke models are conducted. Unlike typical stroke patients who are usually old and may suffer from other health complications, young and healthy rodents are used as subjects of stroke model. The typical animal ischemic stroke model, MCAO, does not

involve the formation of a blood clot to mimic ischemic stroke (Ginsberg, 1996; Hoyte et al., 2004; Fisher and Tatlisumak, 2005). Choosing the right method for inducing an ischemic stroke model in animal clinical trials is crucial considering a 50-μl clot, a typical inducer for ischemic stroke, produces 15 U thrombin per ml of plasma (150 nM of thrombin) (Seegers, 1962; Arand and Sawaya, 1986; Lee et al., 1996; Gingrich and Traynelis, 2000). Thus when the blood brain barrier becomes compromised during ischemic stroke, large quantity of thrombin may extravasate into the brain parenchyma to cleave NR2B. In the reducing condition of the ischemic stroke, cleavage at Lys^{318} renders NR2B less ifenprodil sensitive (Fig. 3.5). This may also be one of the reasons NR2B ATD binding drugs, e.g. ifenprodil and its analogues, have improved the outcome of MCAO animal stroke models but fail in improving that in stroke patients (Gotti et al., 1988; Di et al., 1997; Ikonomidou and Turski, 2002; Gogas, 2006). Considering the results on the cleavage of NR2B and also the recent data on other proteases cleaving the NMDA receptors, such cleavage of NMDA receptors can modulate sites of interaction with drug leads (Fig. 3.8) (Nicole et al., 2001; Fernandez-Monreal et al., 2004; Pauly et al., 2008; Samson et al., 2008; Szklarczyk et al., 2008; Yuan et al., 2009b). Hence, the approach of drug discovery for ischemic stroke has to be carefully reconsidered.

Chapter 4

Functional effects of thrombin cleavage on NR2B-containing receptors

4 Functional effects of thrombin cleavage on NR2B-containing receptors

4.1 Background and objectives

In Chapter 3, it was shown that thrombin can cleave NR2B in its native conformation. Two possible scenarios could be foreseen upon thrombin cleavage (Fig. 4.1). (1) Upon thrombin cleavage at Lys^{318} of NR2B ATD, the cleaved fragment up to residue Lys^{318} might be loosely associated to the rest of the receptors by Van der Waals forces and hydrogen bonds formed among the α-helices and β-sheets. There is disruption to the ATD but to a smaller extent compared to the second scenario. (2) The other possible scenario could be the complete dissociation of the fragment up to residue Lys^{318} from the NMDA receptor complex upon treatment by thrombin. In this study, we will investigate the effects of both scenarios on the function of NMDA receptors.

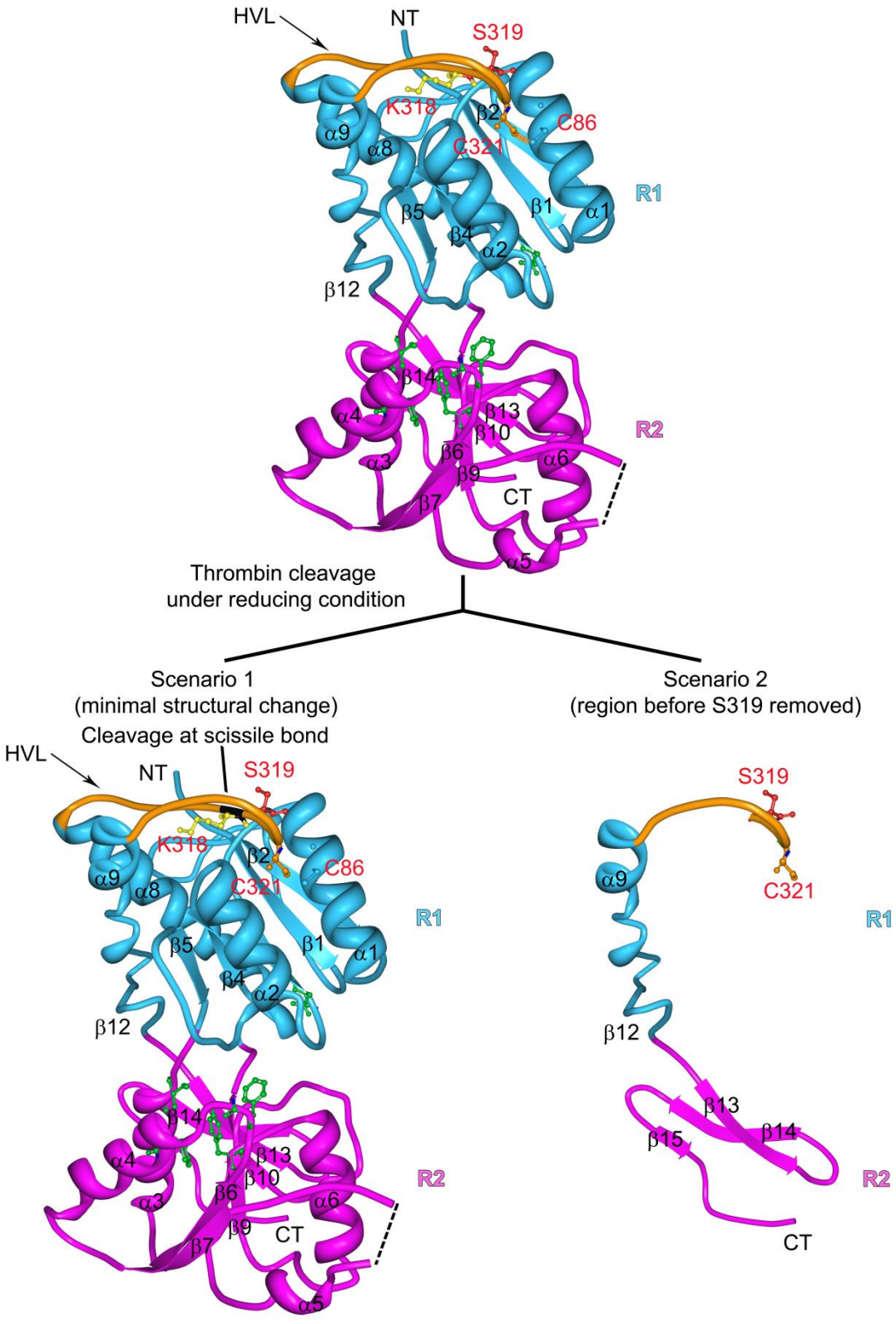

Fig. 4.1. Model illustrating two possible scenarios upon thrombin cleavage at Lys^{318} of NR2B based on the NR2B ATD crystal structure (3JPW). Ribbon representation of the apo-NR2B ATD structure (3JPW) generated using Protein Workshop. (Top panel) NR2B ATD structure illustrates the state of NR2B ATD before thrombin cleavage. Secondary structures are as labeled (Karakas et al., 2009). NT indicates N-terminal while CT indicates C-terminal. R1 and R2 domain are colored in blue and magenta respectively. The HVL (orange)

is held in place by the disulfide bond (dotted orange line) formed between the Cys^{86} (blue) and Cys^{321} (orange) and covers the top of R1. The disordered region (residues 208-214) is indicated as a dotted line. The respective positions of K318 and S319 are as indicated and residues are labeled yellow and red respectively. Residues interacting with ifenprodil (Asp^{101}, Ile^{150}, Phe^{176}, Phe^{182} and Tyr^{231}) are indicated in green. Upon thrombin cleavage, two scenarios are hypothesized. (Left, bottom panel) Scenario 1 is shown in which there is minimal change in the overall structure. Black color indicates the bond between K318 and S319 where thrombin proteolyze at. Cleavage at Lys^{318} may induce changes in the structure of the loop, changing the distance between the Cys^{86} and Cys^{321}, affecting its ability to form disulfide bond (further illustrated in Fig. 4.2). (Right, bottom panel) Scenario 2 is shown in which the ATD region up to Lys^{318} is completely removed.

In scenario one where the cleaved fragment is loosely attached to the rest of the receptors, the disulfide bond may be less likely to form due to the increase in the distance between Cys^{86} and Cys^{321} (Fig. 4.2). Formation of disulfide bonds requires a minimum distance of 6.4 Å and an angle of ~115° between the side chains of two cysteine residues. Formation of the disulfide bond also takes into consideration that water molecule cannot pass between them owing to excluded volume (Colonna-Cesari and Sander, 1990; Dombkowski and Crippen, 2000; Seeger et al., 2008). The disulfide bonds between the various cysteine pairs in the NMDA receptors may maintain important structural configuration that is crucial for governing the sensitivity of the receptors to modulators and to agonists (Table 1.1 in Chapter 1) (Tang and Aizenman, 1993; Sullivan et al., 1994; Gozlan and Ben-Ari, 1995; Choi et al., 2001; Kaye et al., 2007; Karakas et al., 2009). Thus, one of the objectives of the study is to utilize substitution mutants to investigate how a failure in forming the intraprotomer disulfide bond between Cys^{86} and Cys^{321} would affect the function of NMDA receptors. As the ATD is involved in binding to the modulator ifenprodil, the sensitivity to ifenprodil would be investigated (Perin-Dureau et al., 2002a; Mony et al., 2009b). It is also evident that the ATD modulates the action of the LBD, thus, the sensitivity to the agonist glutamate and co-agonist glycine would be examined (Zheng et al., 2001; Madry et al., 2007a; Gielen et al., 2008).

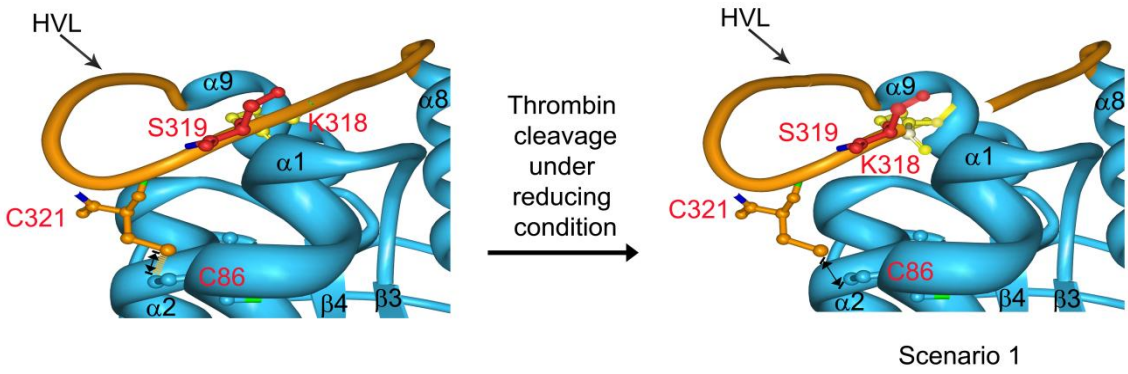

Fig. 4.2. Enlarged representation of scenario 1. Upon thrombin cleavage under reducing condition at K318 (yellow residue), the peptide bond (pale yellow) between K318 and S319 (red) is cleaved, leaving a broken HVL (orange). The disrupted HVL structure may increase the distance and change the angle between the Cys^{86} and Cys^{321} indicated by the double-headed arrows. Secondary structures are as indicated (Karakas et al., 2009). Figure is generated using Protein Workshop.

In scenario two, the functional consequences in the situation when the portion of the ATD region up to Lys^{318} is removed would be determined. In addition to the importance of binding to modulators such as ifenprodil, the ATD of NR2 subunits are also important in allosterically modulating the binding of agonists at the LBD (Zheng et al., 2001; Perin-Dureau et al., 2002a; Madry et al., 2007a; Mony et al., 2009b). Recently, it is also observed that the ATD is important for the modulation of channel kinetics (Gielen et al., 2009; Yuan et al., 2009a). Thus in this study, we would like to investigate how the removal of a big portion of the ATD (up to Lys^{318}), as in the case upon cleavage at Lys^{318}, would affect the properties of the NMDA receptors.

4.2 Materials and methods

pCIneo NR1-1a and pcDNA1 NR2B were gifts from Dr. S.F. Heinemann. pCIneo NR2B(C86A), pCIneo NR2B(C321A), pCIneo NR2B(C86A/C321A) double cysteine mutant and pCIneo NR2B(C232A) were constructed by F.M. Ng from our laboratory. pcDNA1 NR2B-ΔATD-K318 was constructed by J.T. Chen, N. Anthony and Y. Zhang from our laboratory. SP6 NR1-1a(A652C) was a gift from Dr. S.F. Traynelis. Restriction enzymes, QIAquick gel extraction kit, mMESSAGE mMACHINE T7 kit, RNA ladder, *Xenopus laevis* frogs, PMSF, pepstatin A, leupeptin hemisulfate, protein marker, ECL Plus, glutamate, glycine and ifenprodil were purchased from companies as described in Chapter 3. mMESSAGE mMACHINE SP6 kit was purchased from Ambion (Austin, TX, USA). Anti-NR1 mouse monoclonal antibody (recognizing the amino acids 660-881 of rat NR1) was purchased from BD Pharmingen (San Diego, CA, USA). C-terminal anti-NR2B rabbit polyclonal antibody (recognizing amino acid residues 1437-1456 of mature mouse NR2B) was purchased from Upstate Biotechnology (Lake Placid, NY, USA). For secondary antibodies, both the goat anti-rabbit and goat anti-mouse IgG horseradish peroxidase antibodies were purchased from Santa Cruz Biotechnology (Santa Cruz, CA, USA). D-cycloserine was purchased from Sigma (St Louis, MO, USA). 2-aminoethyl methanethiosulfonate hydrobromide (MTSEA) was purchased from Toronto Research Chemicals (Ontario, Canada). All chemicals were purchased from Sigma-Aldrich (St Louis, MO. USA).

Harvesting Xenopus laevis oocytes

Stage V/VI oocytes were obtained from the ovaries of *Xenopus laevis* frogs and maintained in a 17°C incubator as described in Chapter 3.

Expression of NR1/NR2 receptors in Xenopus oocyte injection

pCIneo NR1-1a, pcDNA1 NR2B, pCIneo NR2B(C86A), pCIneo NR2B(C321A), pCIneo NR2B(C86A/C321A), pCIneo NR2B(C232A) and pcDNA1 NR2B-ΔATD-K318 were linearized using NotI. SP6 NR1-1a(A652C) was linearized using MluI. Linearized DNA were analyzed and purified as described in Chapter 3. With the exception of SP6 NR1-1a(A652C), all RNA were generated from their respective linearized DNA using mMESSAGE mMACHINE T7 kit according to the manufacturer's protocol. SP6 NR1-1a(A652C) RNA was generated from the linearized DNA using mMESSAGE mMACHINE SP6 kit. Quality of RNA was analyzed using analytical 0.6 % agarose gel electrophoresis and quantity was measured using ND-1000 spectrophotometer (NanoDrop Technologies, Montchanin, DE, USA). Oocytes were injected under the magnification of SMZ435 dissecting scope (Nikon, Tokyo, Japan) after 24 h of isolation. Oocytes were injected with 10-25 ng of RNA in a 50 nl volume using oocyte microinjection pipet (Drummond Scientific, Broomall, PA, USA) mounted on a Marzhauser MM33 micromanipulator (SDR, Sydney, Australia). The ratio of NR1 to NR2 was at 3:7. Following injection, oocytes were incubated at 17°C in Barth's solution.

Homogenization of oocytes

At 3-8 days after RNA injection, total protein was obtained by lyzing 20 oocytes in 400 µl of homogenization buffer (100 mM NaCl, 1 % Triton X-100, 20 mM Tris-HCl, pH 7.4) in the presence of protease inhibitors (1 mM PMSF, 1.5 µM pepstatin A and 4.4 µM leupeptin hemisulfate). The homogenate was then centrifuged at 14000 *g* for 1 min. Supernatant was collected and analyzed on 8.5 % SDS-PAGE and immunoblotting.

Measurement of protein concentration

Measurement of protein concentration of oocyte homogenate was performed using BCA protein assay as described in Chapter 2. BSA standard was reconstituted in homogenization buffer. Absorbance was measured at 562 nm.

SDS-PAGE and immunoblotting

The proteins were separated by SDS-PAGE and analyzed by immunoblotting as described in Chapter 2. Immunoblotting was performed using C-terminal anti-NR2B (1 : 800) or anti-NR1 (1 : 2000). Detection of primary antibodies was performed using anti-rabbit IgG horseradish (1 : 20000) or anti-mouse IgG horseradish peroxidase (1 : 5000) followed by ECL Plus.

TEVC recordings from Xenopus oocytes

Recordings were performed as described in Chapter 3. Saturating concentration of glutamate and glycine (30-100 μM) and 0.03-10 μM of ifenprodil or 0.01-1000 μM of D-cycloserine were used in all oocytes experiments unless otherwise stated. Glutamate (50 μM), glycine (30 μM) and 0.2 mM MTSEA were used to investigate the P_{OPEN} of receptors. MTSEA was prepared fresh and used within 20 min. Data points were collected from at least two different Xenopus laevis frogs.

For the antagonist ifenprodil, experimental points were fitted with the following equation for:

$$Percent\ response = (100 - minimum) / (1 + ([\text{ifenprodil}]/IC_{50})^{n}) + minimum$$

obtaining the ifenprodil inhibition curves, where *minimum* is a residual current response, IC_{50} is the concentration of ifenprodil that produces 50 % of the maximal inhibition and *n* is the Hill slope.

For the agonist (glutamate), co-agonist (glycine) and partial agonist (D-cycloserine), data points were fitted to the following equation:

$$\textit{Percent response} = 100 \times \textit{relative efficacy} / (1 + (EC_{50}/[\text{agonist}])^{n})$$

obtaining the full agonist curves where *relative efficacy* is the response at maximally effective concentration relative to the maximal response of glutamate or glycine (as indicated in the respective experiment), EC_{50} is the concentration of agonist that produces 50% maximum activation and *n* is the Hill slope.

Illustration of crystal structure of NR2B ATD

The apo-crystal structure of NR2B ATD (Protein Data Bank code 3JPW) provided the structural template to create the images using Protein Workshop (Karakas et al., 2009).

Data analysis

Data were expressed as mean ± S.E.M. and analyzed statistically using unpaired T-test or one-way ANOVA followed by Dunnett test. Significance for all tests was set at $P < 0.05$. Error bars in figures were S.E.M. Graphs were plotted using GraphPad PRISM® Version 4.

4.3 Results

Disruption in the disulfide bond formation between Cys^{86} and Cys^{321} affects the function of NMDA receptors minimally

The cleavage at Lys^{318} observed suggested two possible scenarios. One of which could be the failure to reinstate the disulfide bond between Cys^{86} and Cys^{321} due to the increase in distance introduced by the cleavage at Lys^{318} at the HVL of ATD NR2B (Fig. 4.2). Using NR2B(C86A), NR2B(C321A) and NR2B(C86A/C321A) double cysteine mutants, we investigated how the absence of the disulfide bond affect the function of the NMDA receptors. NR2B(C232A) was also included as a form of control in the investigation as it is the only other cysteine in the ATD and it is not involved in the formation of the disulfide bond (Karakas et al., 2009). Considering that the ATD is directly involved in the binding of ifenprodil, the IC_{50} of ifenprodil was measured. The IC_{50} of ifenprodil were not significantly altered among the cysteine mutants compared to the wild-type (Table 4.1). The IC_{50} ranged from 0.07 to 0.17 μM, i.e. close to the IC_{50} of wild-type NR1/NR2B (0.21 ± 0.05 μM, n=26; $P > 0.05$; one-way ANOVA, post-hoc Dunnett test) (Table 4.1). The sensitivities of these cysteine mutants to the agonist glutamate and co-agonist glycine were also investigated. The glutamate EC_{50} and glycine EC_{50} were not significantly changed among the wild-type and cysteine mutants (Table 4.1). For the glutamate EC_{50}, it ranged from 0.54 to 1.75 μM and that for glycine ranged from 0.25 to 0.39 μM for the cysteine mutants tested (Table 4.1). These values were similar to those of the wild-type NR1/NR2B glutamate EC_{50} (1.28 ± 0.19 μM, n=19; $P > 0.05$; one-way ANOVA, post-hoc Dunnett test) and glycine EC_{50} (0.29 ± 0.03 μM, n=20; $P > 0.05$; one-way ANOVA, post-hoc Dunnett test). These indicated that the failure in forming the disulfide bond (possibly induced by thrombin cleavage) does not affect the agonist binding. This suggested that the failure in forming the disulfide bond between Cys^{86} and Cys^{321} did not cause a major change in the structure of the NMDA receptors and did not affect the properties of the ATD binding site and the ATD-LBD interaction.

Receptors	Ifenprodil		Glutamate		Glycine	
	IC_{50} (μM)	n	EC_{50} (μM)	n	EC_{50} (μM)	n
NR1/NR2B	0.21 ± 0.05	26	1.28 ± 0.19	19	0.29 ± 0.03	20
NR1/NR2B(C86A)	0.08 ± 0.01	5	0.54 ± 0.05	3	0.39 ± 0.08	5
NR1/NR2B(C321A)	0.08 ± 0.01	3	1.19 ± 0.21	7	0.34 ± 0.03	6
NR1/NR2B(C86A/C321A)	0.07 ± 0.01	4	1.75 ± 0.40	3	0.30 ± 0.00	2
NR1/NR2B(C232A)	0.17 ± 0.03	5	1.17 ± 0.18	5	0.25 ± 0.04	5

Table 4.1. Ifenprodil IC_{50}, glutamate EC_{50} and glycine EC_{50} are not altered in NR2B ATD cysteine mutants. IC_{50} of ifenprodil were obtained by co-application of 0.03-10 μM of ifenprodil in the presence of 30-100 μM glutamate and glycine. Glutamate and glycine EC_{50} were determined in the presence of saturating glycine or glutamate respectively (30-100 μM). Ifenprodil IC_{50}, glutamate EC_{50} and glycine EC_{50} of cysteine mutants were not significantly altered as compared to wild-type NR1/NR2B. Statistical test used was one-way ANOVA, post-hoc Dunnett test. n indicates the number of oocytes tested. Values represent means ± S.E.M.

Deletion of $NR2B_{ATD}$ at Lys^{318} is functional but ifenprodil-insensitive in oocytes

Thrombin cleavage at Lys^{318} also raised the possibility that a population of NMDA receptors may exist where the ATD of NR2B is truncated at Lys^{318} after coming into contact with thrombin and this receptor species is functional but resistant to ifenprodil inhibition (scenario two) (Fig. 4.1). To evaluate if there are functional changes of these receptors, a NR2B DNA plasmid with the NR2B ATD up to Lys^{318} deleted (NR2B-ΔATD-K318) was generated. This was achieved by inserting two BglII cut sites between Ser^{28}-Ser^{31} and Glu^{316}-Ser^{319} sequentially using QuikChange site directed mutagenesis on pcDNA1 NR2B wild-type plasmid template as previously reported in (Yuan et al., 2009b) (Fig. 4.3A). This NR2B-ΔATD-K318 was co-expressed with wild-type NR1 in oocytes (Fig. 4.3B). Dose-response curves for ifenprodil (0.03-10 μM) inhibition were generated from recombinant wild-type NR1/NR2B and NR1/NR2B-ΔATD-K318 receptors expressed in oocytes in the presence of a saturating concentration of glutamate and glycine. The high affinity ifenprodil inhibition was significantly reduced in NR1/NR2B-ΔATD-K318 receptors (estimated IC_{50} > 100 μM, n=4) (Fig. 4.4B, Fig. 4.4C and Table 4.2) as compared to wild-type receptors (IC_{50} 0.21 ± 0.05 μM, n=26) (Fig. 4.4A, Fig. 4.4C and Table 4.2). Coincidentally, all known critical residues that exert major influence on ifenprodil- and benzimidazole derivative-mediated inhibitions of NMDA receptors, including Asp^{101}, Ile^{150}, Phe^{176}, Phe^{182} and Tyr^{231}, are located upstream from the thrombin cleavage site Lys^{318} on NR2B ATD (Fig. 4.1 top and bottom right panel) (Perin-Dureau et al., 2002b; Mony et al., 2009c; Wee et al., 2010). This explained the relief of ifenprodil inhibition in NR1/NR2B-ΔATD-K318 receptors.

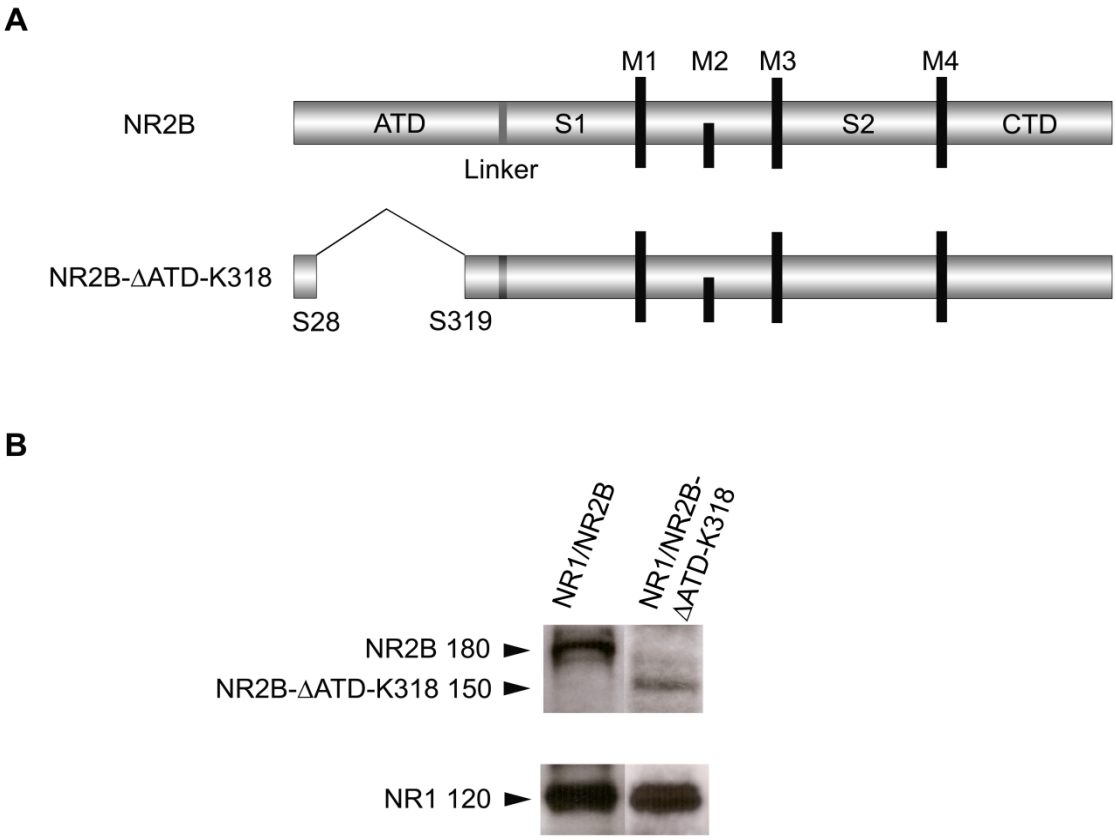

Fig. 4.3. Construction and expression of the truncated mutant NR2B-ΔATD-K318. (A) Schematic diagram showing the construction of NR2B-ΔATD-K318 from the wild-type NR2B plasmid by joining Ser^{28} to Ser^{319}. This construct included the first 28 residues of NR2B which are the signal peptides. Gray rectangular box indicates the linker between ATD and S1. Black rectangular boxes indicate the transmembrane domain (M1, M3 and M4) and the re-entrant loop (M2). Domains are as indicated. (B) NR2B-ΔATD-K318 DNA translated into a ~150 kDa truncated NR2B subunit when co-expressed with NR1 in *Xenopus* oocytes. Homogenate of NR1/NR2B or NR1/NR2B-ΔATD-K318 injected oocytes were analyzed on western blot. Molecular weight (in kDa) of each protein is indicated.

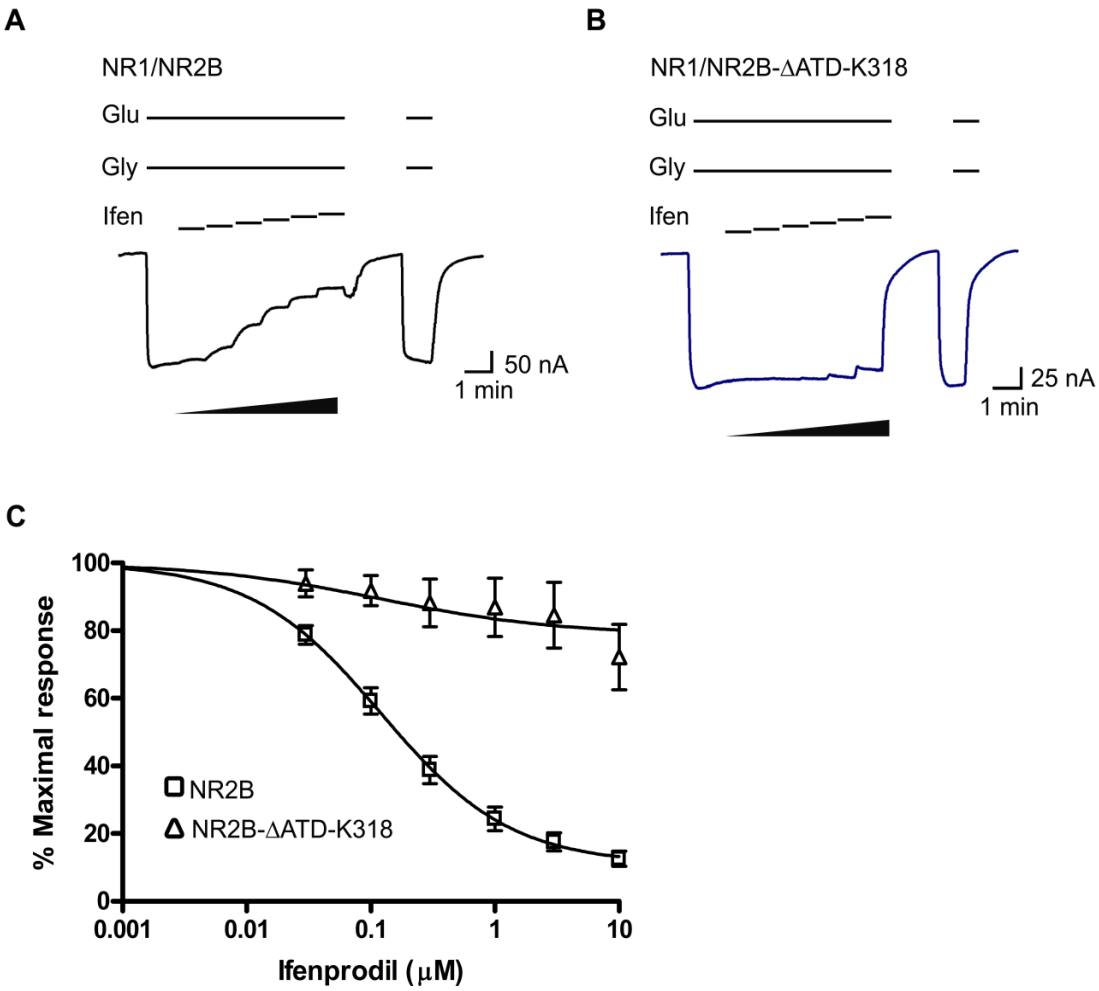

Fig. 4.4. NR2B-ΔATD-K318 abolishes high-affinity ifenprodil inhibition. Representative current traces recorded from *Xenopus* oocytes co-expressing rat (A) NR1/NR2B and (B) NR1/NR2B-ΔATD-K318 upon ifenprodil (Ifen) and saturating glutamate (Glu) and glycine (Gly) treatment. The horizontal short lines show applications of 0.03, 0.1, 0.3, 1, 3 and 10 μM ifenprodil. (C) Dose-dependent inhibition curves for ifenprodil. Maximal response (%) represented the percentage of current measured at each ifenprodil concentration tested to the maximum current elicited by saturating concentration of glutamate and glycine. □ indicates NR1/NR2B-injected oocytes. △ indicates NR1/NR2B-ΔATD-K318-injected oocytes. Each data point was the mean ± S.E.M., n=4-26 oocytes recorded.

NR2B-ΔATD-K318 affects glycine but not glutamate EC_{50}

As the ATD can allosterically modulate the function of LBD, the truncated mutant NR2B-ΔATD-K318 was also employed to investigate the effects of removing region of the ATD up to Lys^{318} on the glutamate and glycine EC_{50} values, which are ligands binding to the LBD of NR2 and NR1 respectively (Zheng et al., 2001; Gielen et al., 2008). Here, we assumed that glycine and glutamate are full agonists and produce maximal receptor activation. The EC_{50} of glutamate measured in the presence of saturating concentration of glycine on NR1/NR2B-ΔATD-K318 receptors (1.12 ± 0.09 μM, n=6) (Fig. 4.5B, Fig. 4.5C and Table 4.2) was similar to that of wild-type NR1/NR2B (1.28 ± 0.19 μM, n=19; $P > 0.05$; unpaired T-test) (Fig. 4.5A, Fig. 4.5C and Table 4.2). The NR1/NR2B-ΔATD-K318 receptor EC_{50} for glycine was, however, significantly higher by 14-fold (4.27 ± 0.50 μM, n=5) (Fig. 4.6B, Fig. 4.6C and Table 4.2) as compared to NR1/NR2B (0.29 ± 0.03 μM, n=20; $P < 0.0001$; unpaired T-test) (Fig. 4.6B, Fig. 4.6C and Table 4.2).

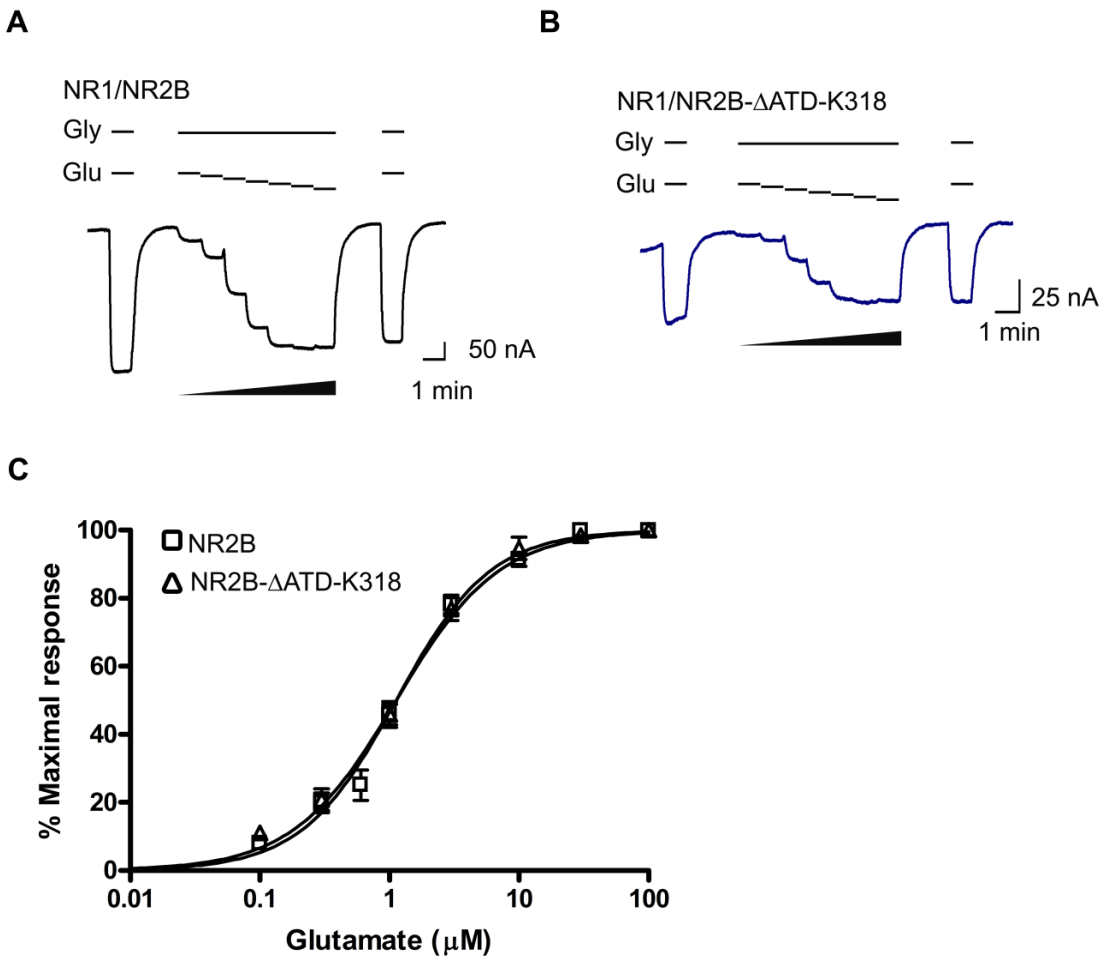

Fig. 4.5. NR2B-ΔATD-K318 does not alter glutamate EC_{50}. Representative current traces recorded from *Xenopus* oocytes co-expressing rat (A) NR1/NR2B and (B) NR1/NR2B-ΔATD-K318 upon glutamate (Glu) and saturating glycine (Gly) treatment. The horizontal short lines show applications of 0.1, 0.3 1, 3, 10, 30 and 100 μM glutamate. (C) Dose-dependent activation curves for glutamate. Maximal response (%) represented the percentage of current measured at each glutamate concentration tested to the maximum current elicited by saturating concentration of glycine. □ indicates NR1/NR2B-injected oocytes. △ indicates NR1/NR2B-ΔATD-K318-injected oocytes. Each data point was the mean ± S.E.M., n=6-19 oocytes recorded.

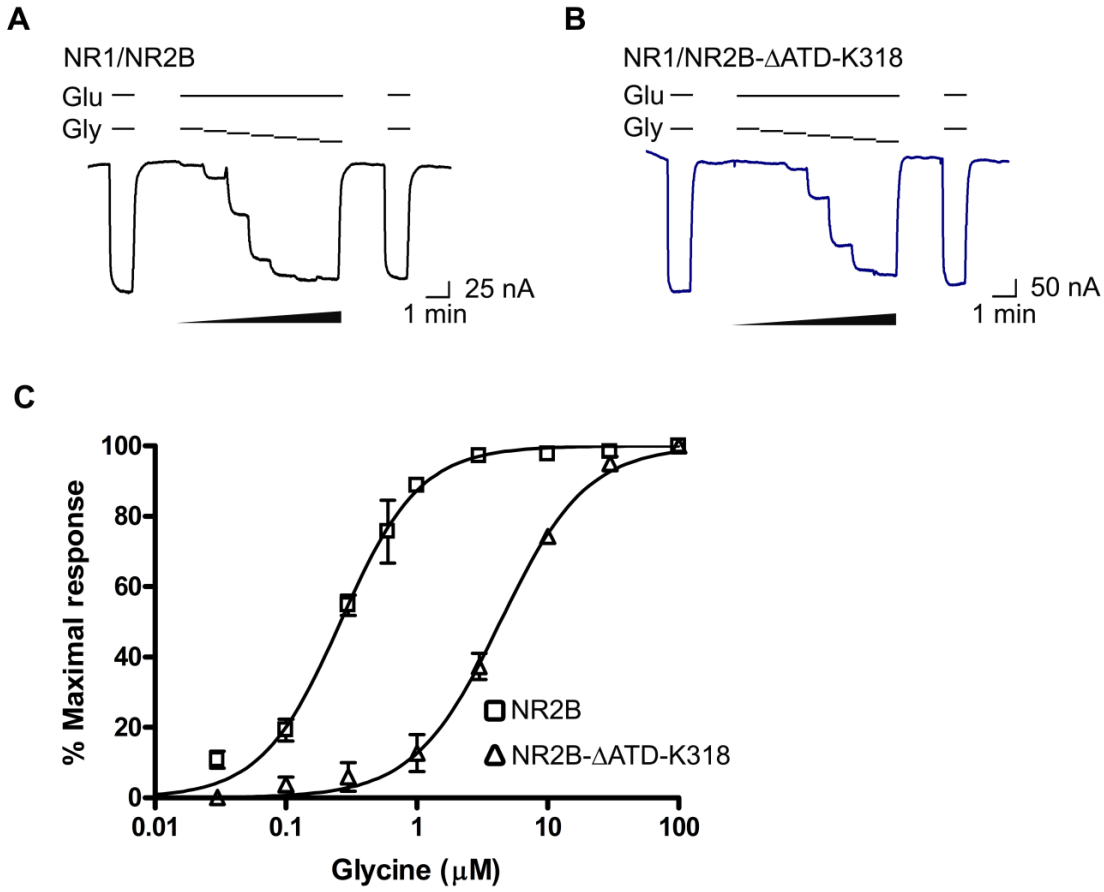

Fig. 4.6. NR2B-ΔATD-K318 reduces glycine EC_{50} significantly (P < 0.0001). Representative current traces recorded from *Xenopus* oocytes co-expressing rat (A) NR1/NR2B and (B) NR1/NR2B-ΔATD-K318 upon glycine (Gly) and saturating glutamate (Glu) treatment. The horizontal short lines show applications of 0.1, 0.3, 1, 3, 10, 30 or 100 μM glutamate. (C) Dose-dependent activation curves for glycine. Maximal response (%) represented the percentage of current measured at each glycine concentration tested to the maximum current elicited by saturating concentration of glutamate. □ indicates NR1/NR2B-injected oocytes. △ indicates NR1/NR2B-ΔATD-K318-injected oocytes. Each data point was the mean ± S.E.M., n=5-20 oocytes recorded.

NR2B-ΔATD-K318 changes partial agonist efficacy

Co-agonist glycine binds to the NR1 LBD of the NMDA receptors. Interestingly, removal of the ATD region up to Lys^{318} of the NR2B subunit caused a change in the EC_{50} of glycine (Fig. 4.6). Thus it was hypothesized the binding of NR1 partial agonist could be affected. Although the NR1/NR2B-ΔATD-K318 receptors only yielded a small EC_{50} reduction for D-cycloserine (EC_{50} 3.86 ± 0.81 μM, n=10) (Fig. 4.7B, Fig. 4.7C and Table 4.2) as compared to the wild-type receptors (EC_{50} 4.83 ± 0.98 μM, n=7; $P > 0.05$; unpaired T-test) (Fig. 4.7A, Fig. 4.7C and Table 4.2), the relative efficacy of D-cycloserine was increased from 44.3 to ± 3.95 % (n=7) of glycine in NR1/NR2B receptors (Fig. 4.7A and Fig. 4.7C) to 83.4 ± 4.90 % (n=10) in NR1/NR2B-ΔATD-K318 receptors (Fig. 4.7B and Fig. 4.7C) ($P < 0.0001$; unpaired T-test). These results suggested that the ATD may be involved in regulating co-agonist binding site and that there may be multiple factors responsible for the differences in D-cycloserine and glycine relative efficacy (Chen et al., 2008b; Dravid et al., 2010).

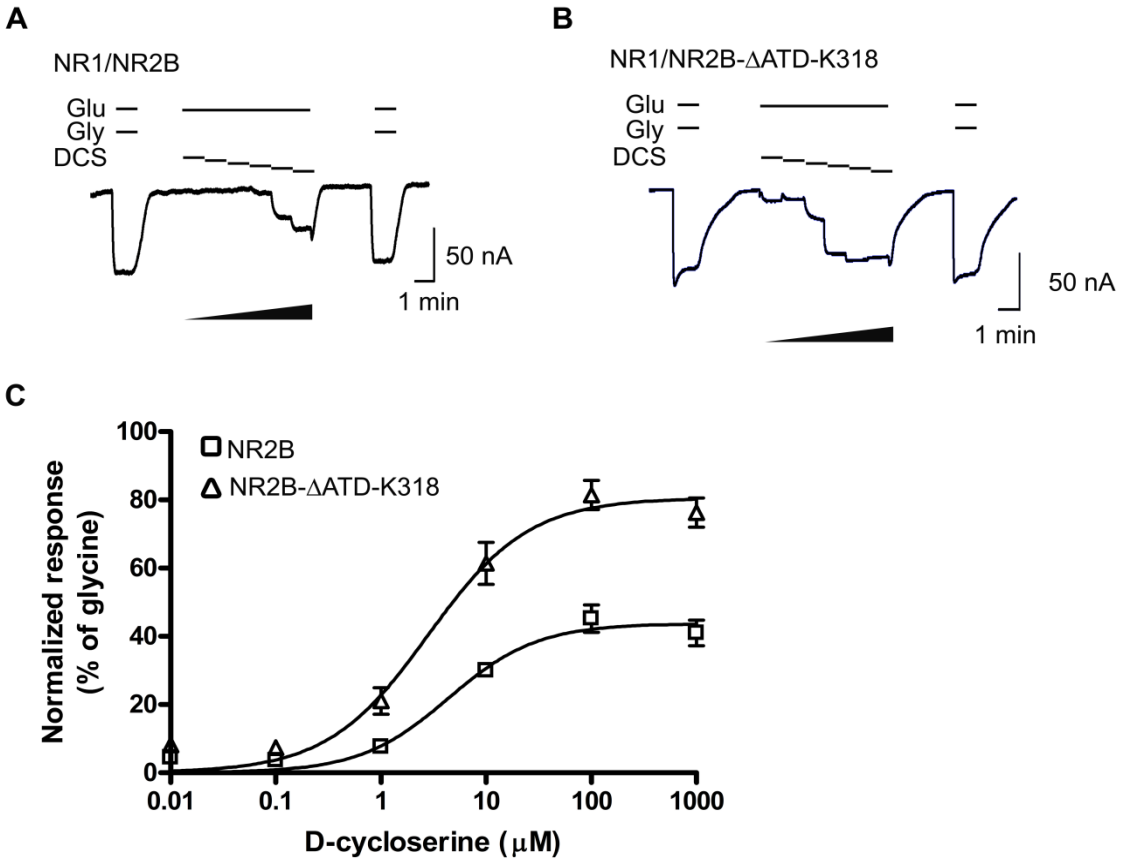

Fig. 4.7. NR2B-ΔATD-K318 increases partial agonist D-cycloserine efficacy (E_{max}) (*P* < 0.0001). Representative current traces recorded from *Xenopus* oocytes co-expressing rat (A) NR1/NR2B and (B) NR1/NR2B-ΔATD-K318. 0.01, 0.1, 1, 10, 100 or 1000 μM D-cycloserine (DCS) (represented by horizontal short lines) was co-applied with 100 μM glutamate (Glu). Relative efficacy of D-cycloserine was compared to saturating concentration of glutamate and glycine (Gly). (C) Dose-dependent activation curves for DCS. % of response induced by D-cycloserine was normalized as a percentage of the maximal response obtained at saturating glycine and glutamate. □ indicates NR1/NR2B-injected oocytes. △ indicates NR1/NR2B-ΔATD-K318-injected oocytes. Each data point was the mean ± S.E.M., n= 7-10 oocytes recorded.

	NR1/NR2B	NR1/NR2B-ΔATD-K318
Ifenprodil IC_{50} (μM)	0.21 ± 0.05 (26)	>100 (4)
Glutmate EC_{50} (μM)	1.28 ± 0.19 (19)	1.12 ± 0.09 (6)
Glycine EC_{50} (μM)	0.29 ± 0.03 (20)	4.27 ± 0.50 (5) *
D-cycloserine EC_{50} (μM)	4.83 ± 0.98 (7)	3.86 ± 0.81 (10)

Table 4.2. NR2B-ΔATD-K318 alters the glycine EC_{50} and ifenprodil IC_{50} but not glutamate EC_{50} and D-cycloserine EC_{50} of NMDA receptors. The IC_{50} value for the ifenprodil binding on NR1/NR2B-ΔATD-K318 was estimated from the plot. There was a significant increase in the glycine EC_{50} between wild type and NR2B-ΔATD-K318. * represents $P < 0.0001$. Statistical test used was unpaired T-test. n=4-26 oocytes recorded (in parentheses). Values were mean ± S.E.M.

Deletion of NR2B ATD does not alter NR1/NR2B channel P_{OPEN}

The ATD of NR2B binds to ifenprodil resulting in the closure of the ATD cleft (Perin-Dureau et al., 2002a; Mony et al., 2009b). This in turn leads to receptor inhibition through interaction with the LBD interface (Gielen et al., 2008). In short, the ATD has two conformations, a ligand-free open state of the receptors and a ligand-bound close state of the receptors (Karakas et al., 2009) (Fig. 4.9 top panel). Thus it was hypothesized that the removal of ATD region up to Lys^{318} could play a role in modulating the channel opening. We investigated the channel P_{OPEN} of the NR2B-ΔATD-K318-containing receptors as P_{OPEN} is one of fundamental differences among the NR2 subtypes (Chen et al., 1999; Erreger et al., 2005). We estimated P_{OPEN} using a method based on the covalent modification by the thiol-modifying reagent (MTSEA) on a cysteine introduced in the NR1 subunit (NR1(A652C)). This residue is one of the residues of the highly conserved motif (SYTANLAAF) located at the M3 of the NR1. Upon activation of the receptors and opening of the NMDA receptor channel pore, extracellular MTSEA becomes accessible to NR1(A652C) and covalently modifies the NR1(A652C), locking open the NMDA receptor channel (Jones et al., 2002). Although, this method does not give the absolute P_{OPEN} of the receptors, it can report relative differences in channel activity. MTSEA potentiates NMDA receptor current which is inversely related to the channel P_{OPEN} (Erreger et al., 2004; Yuan et al., 2005). From the results obtained, co-application of 0.2 mM MTSEA with agonists potentiated the currents for NR1(A652C)/NR2B to a similar degree as previously reported (Fig. 4.8A) (Yuan et al., 2005). Application of MTSEA to NR1(A652C)/NR2B-ΔATD-K318 receptors (27.2 ± 4.90-fold, n=5) (Fig. 4.8B and Fig. 4.8C) produced similar degree of potentiation as compared to that of the NR1(A652C)/NR2B receptors (30.4 ± 2.85-fold, n=10; $P > 0.05$; unpaired T-test) (Fig. 4.8A and Fig. 4.8C).

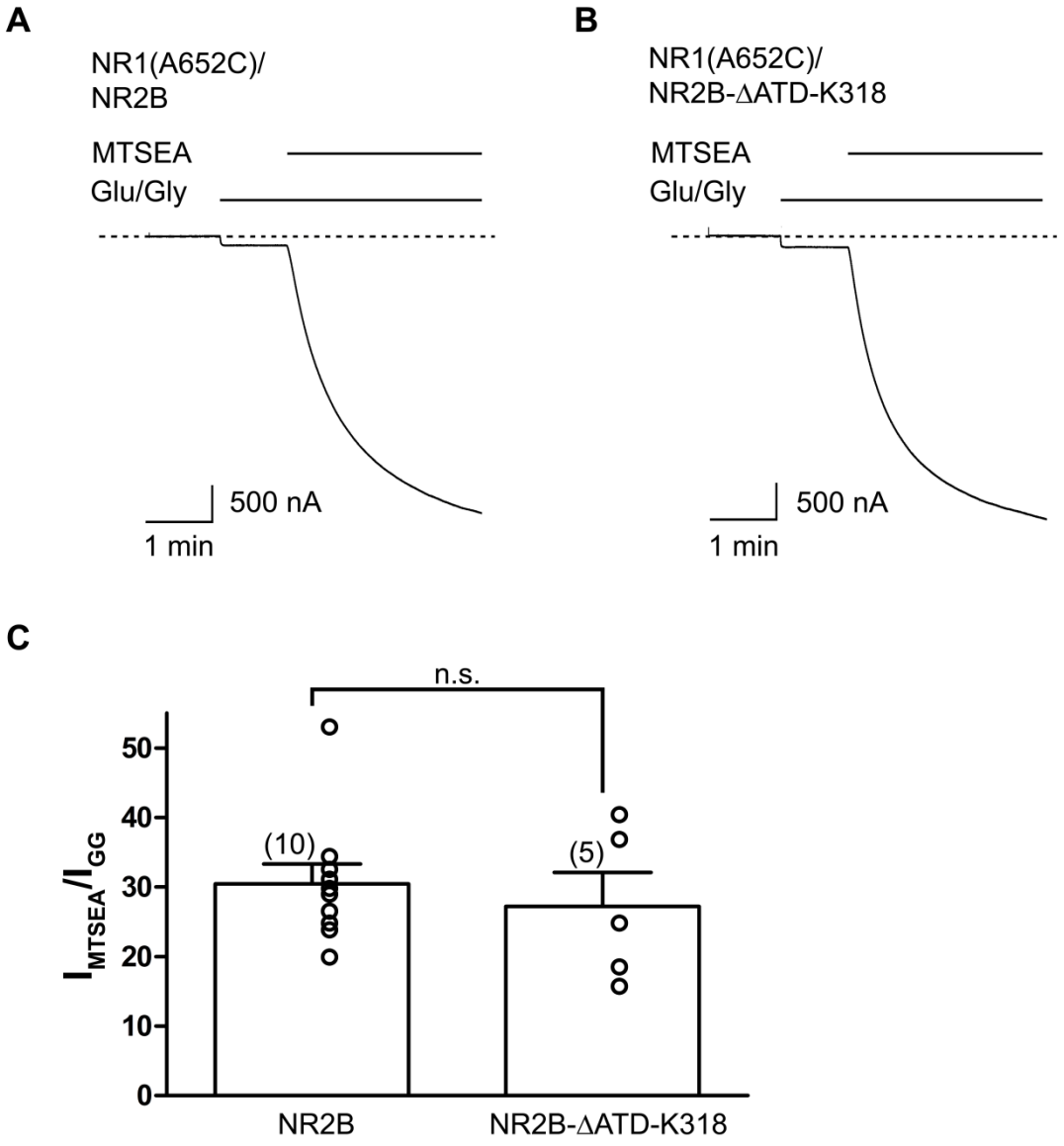

Fig. 4.8. NR2B-ΔATD-K318-expressing receptors does not alter P_{OPEN}. (A) Glu/Gly represented glutamate (50 μM) and glycine (30 μM). 0.2 mM MTSEA potentiated the agonist-evoked NMDA receptor for NR1(A652C) co-expressed with (A) NR2B or (B) NR2B-ΔATD-K318. (C) Summary of the MTSEA potentiation of NR1(A652C)/NR2B and NR1(A652C)/NR2B-ΔATD-K318. I_{GG} and I_{MTSEA} represent the maximal currents evoked by the agonists (glutamate and glycine) and MTSEA + agonists (glutamate and glycine) respectively. I_{MTSEA}/I_{GG} responses between wild-type and NR2B-ΔATD-K318 were not statistically different (indicated as n.s.). O indicates value obtained from each experiment. Statistical test used was unpaired T-test. n=5-10 oocytes recorded (in parentheses). Values were mean ± S.E.M.

4.4 Discussion

Scenario one versus scenario two

In this study, we have explored two possible consequences of the thrombin cleavage of NR2B at Lys^{318} to the NMDA receptors, i.e. consequences of the (1) missing intraprotomer disulfide bond on the ATD NR2B of the NMDA receptors and (2) removal of the ATD region up to Lys^{318} at the NR2B. In scenario one, the strategy chosen was to mutate the NR2B ATD cysteine residues (that are involved in the disulfide bond) to alanine and analyze the changes to the function of the NMDA receptors. For scenario one, the absence of the intraprotomer disulfide bond, as demonstrated by NR2B(C86A), NR2B(C321A) and the double mutant NR2B(C86A/C321A), did not appear to be crucial for the function of the NMDA receptors in terms of ligand binding as it did not affect the IC_{50} of ifenprodil and EC_{50} of glutamate and glycine (Table 4.1). This indicated that upon thrombin cleavage at Lys^{318}, a change in the HVL structure could occur and affect the disulfide bond formation. However, the failure in forming the disulfide bond between Cys^{86} and Cys^{321} is not sufficient in affecting the apparent binding properties of the ATD and the ATD-LBD interaction. Analyzing the recent ATD NR2B crystal structure, the disulfide bond is located at the top of the R1, a distant away from the cleft for the ifenprodil binding (Fig. 4.1 top panel) (Perin-Dureau et al., 2002a; Karakas et al., 2009; Mony et al., 2009b). This could explain the failure to induce a change in the ifenprodil IC_{50}. Although the ATD is also observed to be involved in the allosteric modulation of the LBD, changing the glutamate apparent binding and crucial in modulating the glycine apparent binding, the absence of the disulfide bond between Cys^{86} and Cys^{321} did not change the EC_{50} of glutamate and glycine (Zheng et al., 2001; Madry et al., 2007b; Gielen et al., 2008). Inter-domain and/or inter-subunit interface was proposed to be at the bottom of the R2 of the ATD, due to the observation of a hydrophobic patch at that region (Karakas et al., 2009). The disulfide bond between Cys^{86} and Cys^{321} at the R1 would be less effective in inducing a change in the glutamate and glycine EC_{50}. These results correlated with some of the earlier studies in which homologous residues Cys^{79} and Cys^{308} residing at NR1 and the homologous residues Cys^{87} and Cys^{320} at NR2A, upon mutation to alanine, did not

significantly affect the EC_{50} of glutamate and glycine (Laube et al., 1993; Choi et al., 2001). The double mutant NR2A(C87A/C320A) was also ineffective in inducing a significant change in the Zn^{2+} IC_{50} (Choi et al., 2001). Thus upon cleavage at Lys^{318} of NR2B, progression to scenario one would induce minimal changes to the NMDA receptors function.

In the second scenario, the removal of the ATD region up to Lys^{318} caused a change in the IC_{50} of ifenprodil. This correlated with our earlier results and proposition from Chapter 3, whereby thrombin cleavage at Lys^{318} of NR2B under reducing condition and the resultant shift in the ifenprodil sensitivity would be due to cleavage of NR2B subunits (Fig. 3.5 in Chapter 3). As proposed in Chapter 3, the complete removal of the region up to Lys^{318}, as demonstrated in this Chapter, caused an almost complete removal of the high-affinity ifenprodil inhibition (Fig. 4.4 and Table 4.2). Thus, we proposed that upon cleavage at Lys^{318}, progression to scenario two could be more likely than scenario one, as scenario one did not induce any change in the ifenprodil IC_{50}. However more experiments would be required to confirm such a hypothesis.

Role of ATD in NMDA receptor function

Removal of the ATD region up to Lys^{318} as demonstrated in scenario two also gave a glimpse of the importance of the ATD in the NMDA receptors.

Assembly

Unlike the ATD of NR2A and NR2B, the ATD of other iGluRs and mGluRs does not bind to modulators to allosterically regulate the function of the receptors. Rather, the ATD of these receptors, are important for the proper assembly of the receptors (Kuusinen et al., 1999; Leuschner and Hoch, 1999; Ayalon and Stern-Bach, 2001; Meddows et al., 2001). However, in our investigation, it was observed that the removal of a big portion of the ATD (NR2B-

ΔATD-K318), functional receptors were nonetheless expressed. This correlated with earlier results in which the removal of the entire ATD of NR1 and NR2 are functional (Fayyazuddin et al., 2000; Hu and Zheng, 2005b; Madry et al., 2007a; Gielen et al., 2009; Yuan et al., 2009a). Thus, in NMDA receptors, ATD may not be a crucial determinant for the assembly of the receptors.

Pharmacological properties

Removing the ATD region up to Lys^{318} of NR2B (NR2B-ΔATD-K318) did not result in a change in the glutamate EC_{50} (Fig. 4.5 and Table 4.2). It was also observed previously that ATD deletion constructs did not influence glutamate EC_{50} (Madry et al., 2007a; Yuan et al., 2009a). However using NR2 ATD chimeras, Yuan et al. (2009) observed that the ATD contributed to the high and low glutamate EC_{50} of the NR2A and NR2D respectively, suggesting the importance of the ATD in determining the glutamate binding. The discrepancies between studies of the deletion mutants and chimera mutants reflect different effects of experimentally modulating the intra- and inter-subunit allosteric interactions.

It was also observed in this study that the NR2B-ΔATD-K318 also showed a significant increase in the EC_{50} of glycine. This correlated with earlier studies in which the removal of the ATD of NR2 subunits increases the EC_{50} of glycine, indicating the importance of NR2 regulation of glycine binding at the NR1 subunit (Madry et al., 2007a; Yuan et al., 2009a). Recently, Sobolevsky and colleagues suggest that the NR1 and NR2, could assume a similar architecture as GluR2, ie. with subunits arranged in a 1-2-1-2 pattern, where there are intra- and inter-ATD dimer interface in a NMDA receptor complex (Sobolevsky et al., 2009). Thus, disrupting the ATD of NR2B via thrombin proteolytic cleavage may have upset the inter- and intra-domains allosteric interactions as shown by the change in EC_{50} glycine (Fig. 4.6 and Fig. 4.9) (Zheng et al., 2001; Gielen et al., 2008).

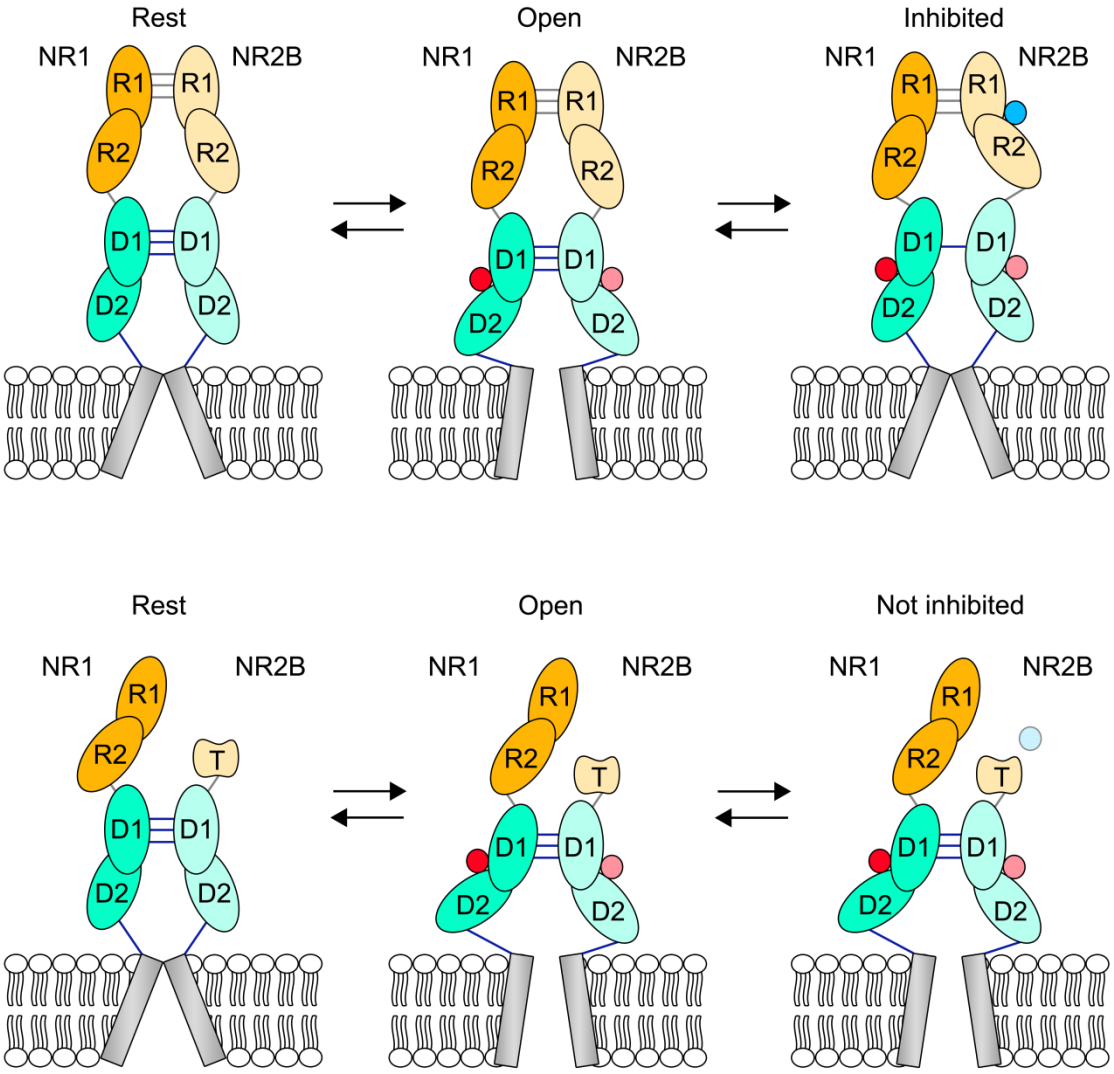

Fig. 4.9. Model illustrating the conformational changes proposed to occur in scenario two. R1 and R2 form the cleft of the ATD (orange) while D1 and D2 form the cleft of the LBD (green). (Top panel) Upon binding of glutamate (pink) and glycine/D-cycloserine (red) to NR2B and NR1 respectively, the channel (gray) opens. Binding of ifenprodil (blue) at the ATD pulls the LBD apart and triggers the closure of the channel, inducing inhibition. (Bottom panel) Upon cleavage at Lys^{318} of NR2B, a truncated fragment of ATD (indicated by T) is left attached to the rest of the NR2B subunit. A slight change in the conformation is created due to the truncated ATD NR2B. Glutmate and glycine/D-cycloserine can bind to the receptor, albeit in a slightly different conformation, making different interdomain or intersubunit contacts compared to the non-cleaved NR2B-expressing receptors (top panel). Ifenprodil (light blue) cannot bind to the truncated NR2B ATD and is not able to inhibit the receptor.

Interestingly, it was also observed that the efficacy of the the partial agonist, D-cycloserine, specific for binding to NR1, was increased significantly when the ATD region up to Lys^{318} of NR2B was removed (Fig. 4.7 and Table 4.2). It is observed that the efficacy of D-cycloserine at different NR1/NR2 subunit combinations is dependent on the NR2 subunit (Sheinin et al., 2001; Dravid et al., 2010). Dependency on the NR2 subtype suggests that the intersubunit communication must occur, which concurs with our results that the NR2B-ΔATD-K318 resulted in a change in the D-cycloserine efficacy. However, LBD dimer interface interactions between the NR1 and NR2B-ΔATD-K318 could be different compared to NR2B, resulting in a higher relative efficacy for NR1/NR2B-ΔATD-K318 receptors (Fig. 4.7). This change could have been induced by the shorter remaining ATD (Fig. 4.9). This somewhat correlated with observations by Dravid et al. (2010) that the ATD cold be one of the multiple factors responsible for the differential D-cycloserine efficacy (Dravid et al., 2010).

Kinetics

It was also observed that the removal of the ATD region up to Lys^{318} did not change the P_{OPEN} of the receptors. However, recent data had shown that the ATD is important for the regulation of the P_{OPEN} and the determination of the different P_{OPEN} observed among the NR2 subunits (Erreger et al., 2005; Gielen et al., 2009; Yuan et al., 2009a). Looking closely at the data obtained in this Chapter, the discrepancies suggested that the region between Ser^{319} and the LBD harbors the important determinant for modulating the P_{OPEN}. Indeed, it has been observed that the linker (Pro^{392}-Asp^{404} of NR2B) works together with the ATD to control the gating of the NMDA receptors (Gielen et al., 2009; Yuan et al., 2009a).

Clinical relevance

Considering the importance of the ATD in regulating numerous aspects of the NMDA receptor function and properties, cleavage by thrombin at Lys^{318} of NR2B may be a form of modulation on the NMDA receptors. This is also supported by a recent report that plasmin cleavage at a homologous residue Lys^{317} of NR2A removes the Zn^{2+} sensitivity and shifts the EC_{50} of glycine slightly to the right, i.e. a higher EC_{50} of glycine (Yuan et al., 2009b). Such protease modification of the NMDA receptors is also observed in other protease systems. For example, upon overactivation of NMDA receptors, calpain, a Ca^{2+}-dependent protease, becomes activated and cleaves the CTD of NR2 subunits, regulating the NMDA receptor turnover at the synapses (Dong et al., 2004; Wu et al., 2005; Bretin et al., 2006). Thus, the downregulation of NMDA receptors at the synapse provide a neuroprotective mechanism against NMDA receptor overstimulation accompanying ischemia and stroke (Gascon et al., 2008).

During ischemic stroke, thrombin cleavage at Lys^{318} of NR2B may also become a form of neuroprotective mechanism. The removal of the region before this portion of the ATD caused an increase in EC_{50} of glycine by 14-fold, i.e. from an EC_{50} of 0.29 ± 0.03 μM in

wild-type receptors to 4.27 ± 0.50 μM in NR2B-ΔATD-K318 receptors (Table 4.2). Glycine concentration is observed to be about 6 μM in the CSF obtained through microdialysis experiment (Thomson et al., 1989; Whitehead et al., 2001). However, it should be noted the neurotransmitter levels, such as that of glycine, are highly regulated by uptake mechanism, inhibitor systems and enzymatic degradation to inactive metabolites (Swartz et al., 1990; Russi et al., 1992; Betz et al., 2006). With that in consideration, glycine sites at the NMDA receptors may not be at saturation (Wilcox et al., 1996; Berger et al., 1998; Bergeron et al., 1998; Chen et al., 2003; Hayashi et al., 2006; Li et al., 2009). Thus, it may be possible that the increase in glycine EC_{50} induced by thrombin cleavage at Lys^{318} of NR2B is a mechanism of protection from excitotoxicity. Bearing in mind that the endogenous NR1 binding ligand in the brain is D-serine, it would be interesting to investigate if cleavage at the Lys^{318} could affect the interaction of D-serine with the NMDA receptors (Shleper et al., 2005).

Chapter 5

Conclusion and future studies

5 Conclusion and future studies

5.1 Conclusion

In this thesis, the interaction between the serine protease thrombin and the NMDA receptors and the possible consequences of the interaction were studied (Fig. 5.1). Firstly, by using RBL and SPM as the NMDA receptors sources, the interaction between thrombin and the NR2B subunit was determined. The interaction was in the form of direct and specific cleavage of NR2B by thrombin. Using site directed mutagenesis on the recombinant MBP-ATD2B protein and N-terminal sequencing of the cleaved off product, the cleavage site was identified to be at Lys^{318} of NR2B. It was also observed that thrombin could cleave NR2B existing in NMDA receptors complex expressed on the membrane surface of E18 cortical neuronal culture. I further demonstrated, electrophysiologically, the thrombin cleavage on NR2B ATD using TEVC recordings on *Xenopus* oocytes. The reduction in ifenprodil inhibition upon thrombin cleavage under reducing conditions validated that thrombin cleaves at the ATD, affecting the apparent binding of ifenprodil to the ATD and ultimately the sensitivity of the cleaved receptors to ifenprodil. However, it was also observed that the thrombin cleavage on NR2B existing in a functional receptors was less efficient and required a reducing environment. By analyzing the relative position of Lys^{318} on the NR2B ATD crystal structure and performing a molecular dynamics simulation, we have provided insight into how a reducing environment exposes the Lys^{318} to the extracellular milieu allowing for interaction with thrombin.

In addition, the possible effects of the thrombin cleavage on NR2B-expressing receptors were explored. The deletion construct, with the ATD region up to Lys^{318} removed, decreases the apparent ifenprodil binding and increases the glycine EC_{50} and the efficacy of D-cycloserine. Thus the observation reported herein provides an understanding for (1) a less explored mechanism for the modulation of the NMDA receptors via thrombin cleavage and (2) the importance of the ATD in the function of the NMDA receptors.

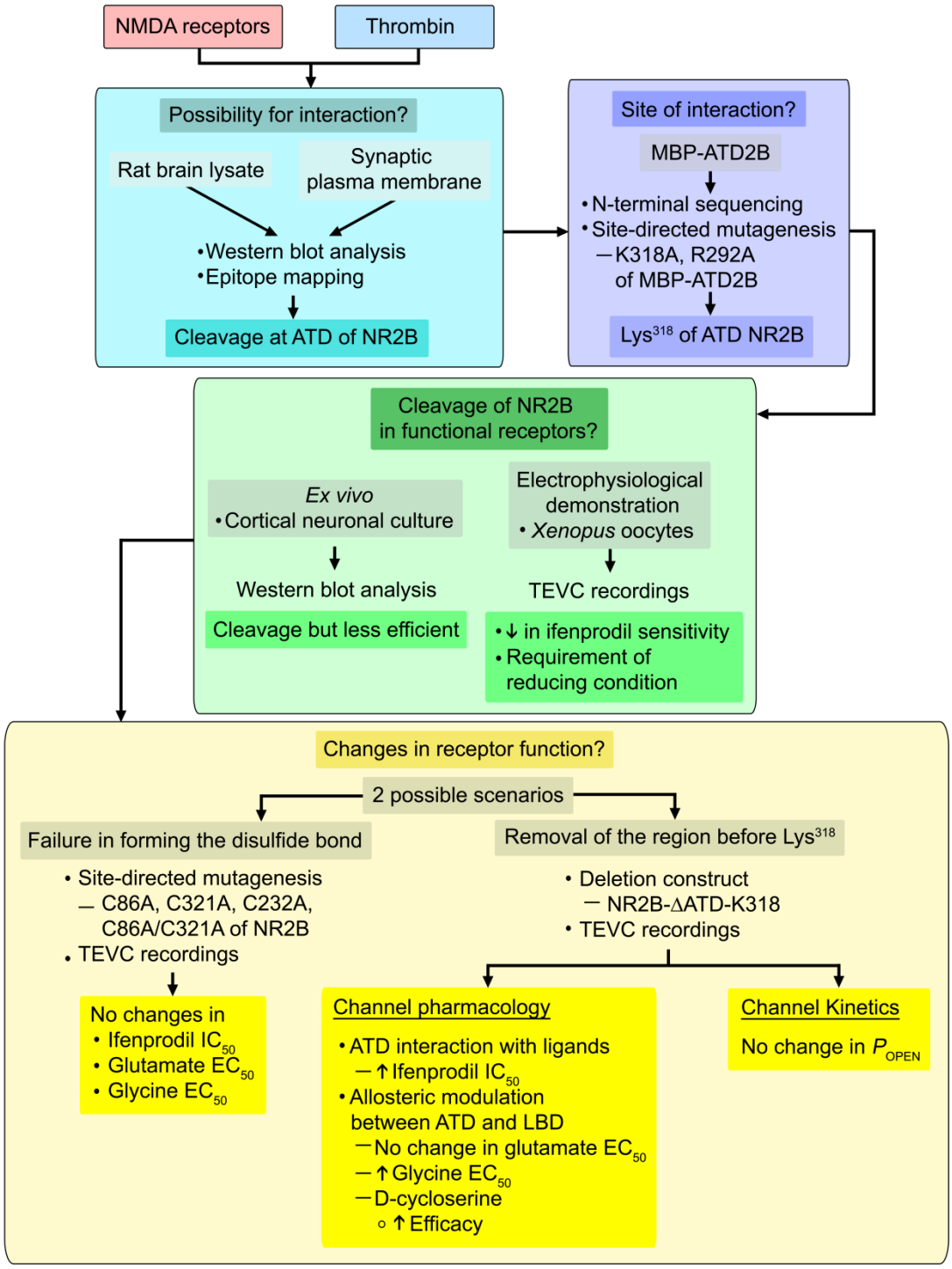

Fig. 5.1. Summary of the work done in this study. TEVC indicates two-electrode voltage clamp.

5.2 Future studies

Based on the observations in this thesis, several areas would be of interest for future studies (Fig. 5.2).

State of NR2B-expressing receptors after thrombin cleavage

The study presented above proposes two possible scenarios of the NR2B-expressing receptors upon thrombin cleavage. One scenario demonstrates minimal disruption to the structure and function of the receptors when the truncated fragment remains associated to the rest of the receptors via bonds formed between the α-helices and β-sheets. The other scenario demonstrates major disruption of the structure and function of the receptors when the truncated fragment is completely detached away from the rest of the receptors. Our results from Chapter 3, which demonstrate a decrease in ifenprodil sensitivity (Fig. 3.5), suggested that the second scenario may be more probable (Fig. 4.1 in Chapter 4). However, more experiments will be needed to verify these observations (Fig. 5.2). As described previously in this study, it would be optimal to identify protease cleavage when the substrates are in their native forms. NR2B from cortical neuronal cells or NR2B co-transfected with NR1 in cell-lines can act as substrates. Upon thrombin cleavage, if the ATD region up to Lys^{318} of NR2B is detached away from the receptors, it will be shed and will accumulate in conditioned medium. The conditioned medium could be analyzed for the presence of the cleaved off 30 kDa through liquid chromatography (Overall and Blobel, 2007).

What is the fate of the 30 kDa that has been shedded off? Is it targeted for degradation? Or would it present as a likely antigen for the generation of autoantibodies against the NMDA receptors (Fig. 5.2)? NMDA receptors autoantibodies have been observed in the CSF and serum of patients suffering from encephalitis, systemic lupus erythematosus (SLE), epilepsy and craniocerebral trauma (Boldyrev et al., 2004; Miglio et al., 2005; Goryunova et al., 2007; Efthimiou and Blanco, 2009; Gable et al., 2009; Kashihara et al.,

2009; Sorokina et al., 2009; Zandi et al., 2009; Hughes et al., 2010; Irani et al., 2010). These autoantibodies recognize the extracellular domain of the NR1 and/or NR2 subunits, with exception to the autoantibodies from Rasmussen's encephalitis which recognize the CTD (Shefner et al., 1991; Katz et al., 1994; Gaynor et al., 1997; Takahashi et al., 2005; Dalmau et al., 2007; Steup-Beekman et al., 2007; Arinuma et al., 2008; Dalmau et al., 2008). The production and the presence of the autoantibodies correlate with the development of the diseases (Dambinova et al., 2002; Ishikawa et al., 2007; Irani et al., 2010). The autoantibodies produced from the diseases bind to the NMDA receptors resulting in differential effects. For example, autoantibodies from encephalitis bind to NMDA receptors and reversibly reduce the number NMDA receptors at the synapse while binding to autoantibodies from SLE causes neuronal death. These actions contribute to the neurobehavioral and cognitive impairment observed in encephalitis or SLE patients (DeGiorgio et al., 2001; Omdal et al., 2005; Kowal et al., 2006; Lapteva et al., 2006; Levite and Ganor, 2008). The mechanisms for the production of these antibodies may involve two possible ways. (1) Memory B cells are postulated to cross the blood brain barrier and are able to undergo restimulation, antigen-driven affinity maturation, clonal expansion and differentiation into antibody-secreting plasma cells (Hauser et al., 2008). (2) Like in encephalitis which has paraneoplastic manifestation of a tumor, such tumor expresses neuronal proteins such as NMDA receptors, resulting in production of autoantibodies. These autoantibodies enter the CNS when the blood brain barrier is compromised (Kowal et al., 2006). Interestingly, autoantibodies are also observed from the serum of patients suffering from transient ischemic attack and ischemic stroke. These antibodies recognize the extracellular domain (Dambinova et al., 1998; Dambinova et al., 2002; Dambinova et al., 2003; Saenger and Christenson, 2010). Thus would the 30 kDa be one of the antigens for the production of autoantibodies in ischemic stroke? This could be investigated by collecting serum samples, or possibly CSF samples, from rat ischemic stroke model or patients suffering from ischemic stroke. As previously discussed in the Discussion section in Chapter 3, the rat ischemic stroke model that mimic closely to a focal embolic stroke would be optimal. Focal embolic stroke model can be

performed by the injection of a pre-formed clot into middle cerebral artery (MCA) (Wang et al., 2001; Wang et al., 2003). This may take into account of thrombin cleavage on NMDA receptors. Serum or CSF collected from these ischemic model rats can be analyzed using liquid chromatography for the presence of the 30 kDa fragment antigen. The analysis for the presence of autoantibodies can also be performed using immunohistochemistry with rat and human brain, immunostaining of live, non-permeabilized neuronal cultures and immunolabeling of human embryonic kidney 293 (HEK293) cell-lines transfected with NR1/NR2B and NR1/NR2B-ΔATD-K318. These methods are used previously for the identification of autoantibodies in CSF of encephalitis patients (Dalmau et al., 2008; Hughes et al., 2010).

In the case that the ATD region up to Lys^{318} is completely removed, leaving the remaining 150 kDa localized on the surface membrane, what is the relative stability of this population of receptors as compared to an uncleaved NR2B-expressing NMDA receptors (Fig. 5.2)? Although the internalization motif of the NR2B is located in the CTD, it is observed that glycine can prime the NMDA receptors for internalization by binding to the LBD of the NMDA receptors (Roche et al., 2001; Nong et al., 2003). Compared to the glycine concentration required for activation of the NMDA receptors, that required for the priming effect is 20-100 times higher (Nong et al., 2003). The removal of the ATD region up to Lys^{318} of the NR2B ATD increases the EC_{50} glycine possibly through a change in the interaction between the ATD and LBD domain of NR1 and NR2B (in an intrasubunit or intersubunit interacting manner). Would the priming effect be altered in a similar way? If the glycine priming effect is altered, does it affect the endocytosis of these cleaved, truncated receptors? These effects can be first investigated by electrophysiology. For example, whole cell voltage recording can be performed on NR2B-ΔATD-K318-expressing receptors expressed on HEK293 cells or oocytes that had been primed with glycine, followed by exposure to agonist stimulation over several minutes. Observation can be made, investigating if such glycine priming induces a rapid, use-dependent rundown of NR2B-ΔATD-K318-expessing NMDA

receptors similar to that of the wild-type NR2B-expressing receptors (Vissel et al., 2001). The mEPSCs, particularly the NMDA receptor component, can also be measured upon thrombin cleavage on hippocampal neurons from primary culture, to investigate if cleaved synaptic NMDA receptors are internalized in a different manner (Nong et al., 2003; Prybylowski et al., 2005). Such cultures can be obtained from PAR-1 knockout mice to exclude the indirect effects from PAR-1 on NMDA receptors (Lee et al., 2007). This allows solely the study of the possible effects of thrombin cleavage on NR2B-containing NMDA receptors endocytosis.

Recent evidences have shown the importance of ATD of the NR2 subunits in the modulation of the channel kinetics, such as deactivation time courses, mean open and the P_{OPEN} (Gielen et al., 2009; Yuan et al., 2009a). In this study, it was demonstrated that the P_{OPEN} of NR1/NR2B-ΔATD-K318 was not statistically different from that of wild-type NR1/NR2B receptors (Fig. 4.8). This correlated with studies that the ATD, together with the linker between the ATD and S1 of the LBD, are crucial in determining the P_{OPEN} (Gielen et al., 2009). Thus, how would the deactivation rate and mean open duration be changed for the NR2B-expressing NMDA receptors if the region before the Lys^{318} of NR2B is removed by thrombin (Fig. 5.2)? Will these properties be unchanged, similar to that of the P_{OPEN}, since the linker between ATD and the S1 of the LBD remains intact in the NR2B-ΔATD-K318? How will the overall current density of the receptor be affected? These questions can be answered through electrophysiology recordings. One of which is single channel recordings from outside-out patches expressing NR1/NR2B-ΔATD-K318 for the investigation of current density, the mean open duration and the deactivation time course (Das et al., 1998; Zhang et al., 2008; Yuan et al., 2009a).

Importance of ATD

The electrophysiological data that are obtained using the NR1/NR2B-ΔATD-K318 receptors demonstrated that, through a disruption in the ATD (in the form of removing the first 318

residues of the NR2B ATD), the interaction between the LBD of NR1 and its ligands are altered. This suggests that in addition to binding to the allosteric modulators such as ifenprodil, ATD of the NR2B can affect agonists binding to NR1(Madry et al., 2007a). This may involve intrasubunit or intersubunit interactions yet identified (Fig. 5.2). These information can be more clearly refined with the generation of heteromeric crystal structure similar to that generated for GluR2 (Sobolevsky et al., 2009). Currently, the only available structure of the NMDA receptors that can give an insight on the subunit interaction is the heterodimer crystal structure of the NR1 and NR2A LBD (Furukawa et al., 2005). This does not give information on which part of the NR2B ATD is crucial in the interaction and affects the NR1 LBD. However, homology modeling and electrophysiological data can provide an indication of the interface involved (Chen et al., 2005; Kaczor et al., 2009). Homology modeling can give an idea of the possible sites of interaction. Site of interaction at the ATD can be confirmed through site-directed mutagenesis. Changes in the glycine binding, demonstrated by the glycine EC_{50} through electrophysiological means, can be analyzed from such mutants. For example, the hydrophobic patch at the NR2B R2 may be involved in the interdomain or intersubunit interaction (Karakas et al., 2009). Residues at this region can be mutated to hydrophilic residues and any changes in the EC_{50} glycine may confirm this region as mediators of allosteric regulation. Engineered disulfide bridges introduced at appropriate positions in the form of cysteine pairs can also identify possible sites of interaction (Sobolevsky et al., 2002a; Furukawa et al., 2005; Blanke and VanDongen, 2008; Sobolevsky et al., 2009). Such cysteines are easily manipulated through redox action or the introduction of bulky thiol-modifying agent such as MTSEA. These manipulations can easily alter the state of interaction and will aid in the study intersubunit or intradomain interactions and how NR2B ATD modulate the NR1 LBD in agonist binding (Gielen et al., 2008).

Other than playing a role in modulating the pharmacological properties and the channel kinetics of the NMDA receptors, the ATD may be involved in non-ionotropic properties of the receptors (Dalva et al., 2000; Madry et al., 2007a; Gielen et al., 2009; Yuan

et al., 2009a). Evidences have suggested that the ATD of NR1 is involved in interacting with ephrinB receptors (EphB). Upon stimulation by the ligand ephrinB, postsynaptically localized EphB interacts with the ATD of the NR1, resulting in clustering of the NMDA receptors through the redistribution of NR1 receptors at the synapse (Dalva et al., 2000; Grunwald et al., 2001; Henderson et al., 2001). Clusters are usually the initiation of synapse formation (Rao et al., 1998). EphB also leads to potentiation of the NMDA receptors and the ultimate enhancement of the NMDA receptor gene expression through tyrosine phosphorylation of the Src family of tyrosine kinases (Takasu et al., 2002). This indicates that the ATD of NR1 may be a crucial determinant for the interaction with extracellular molecules that may affect synapse formation, maturation and plasticity (Grunwald et al., 2001; Henderson et al., 2001; Grunwald et al., 2004). Recently, the ATD of GluRδ2, another member of the glutamate receptor family (orphan receptor), is also observed to interact with the extracellular molecule Cbln1 (from granule cells) for forming synapses *in vitro* and *in vivo* (Kakegawa et al., 2009; Matsuda et al., 2010; Matsuda and Yuzaki, 2010). Moreover, the absence of the ATD, induced by MMP-7 cleavage at the LBD domain of NR1, resulted in the translocation of NMDA receptors, an indication that proteases cleavage may modulate the location of NMDA receptors at the synapse and eventually affect synapse formation (Szklarczyk et al., 2008). Does thrombin have the similar effect in modulating synapse formation through the cleavage of NR2B at the ATD (Fig. 5.2)? This can be investigated using confocal microscopy techniques and electron microscopy for observing the changes in synapse formation upon changes in the ATD induced by thrombin. Alternatively, the ATD region up to Lys^{318} can be fused to the immunoglobulin Fc fragment. This enables the coupling of the ATD to protein G beads. If such beads colocalize with presynaptic marker such as synapsin or FM4-64, it may indicate the ATD's involvement in making synapses (Matsuda et al., 2010).

Relative importance activation of PAR-1 versus cleavage on NR2B of NMDA receptors

The modulation of the NMDA receptors by thrombin can occur via two mechanisms. One is via the activation of the PAR-1 receptors at the astrocytes resulting in release of astrocytic glutamate. The glutamate then activates the NMDA receptors and may potentiate of the perisynaptic NMDA receptors (Gingrich et al., 2000; Lee et al., 2007). This is the indirect pathway. The study presented here demonstrates the direct pathway whereby cleavage of the NR2B affected the ifenprodil inhibition (Fig. 4.4). The removal of the region before the cleavage site (Lys^{318}) of NR2B also changes the agonist and partial agonist binding to NR1 (Fig. 4.6 and Fig. 4.7). The indirect pathway involves the activation and potentiation of the receptors while the direct pathway involves the increase in glycine EC_{50} of the NMDA receptors and results in the NMDA receptors requiring higher concentration of glycine for activation. The two pathways exhibit opposite effects on the NMDA receptors and may affect the amount of Ca^{2+} influx through the NMDA receptors in opposing ways. What is the significance of each pathway? Does one pathway favor over the other? How would the excitotoxicity and the outcome of ischemic stroke be affected through the different progression of pathway (Fig. 5.2)? One pathway overriding the other has also been observed when thrombin activates both PAR-1 and MMP in intracerebral hemorrhage but it is the MMP which is more prominent in inducing death (Xue et al., 2006; Xue et al., 2009). If such predominance of one pathway over the other exists, what governs it? Is it dependent on thrombin concentration? This is because PAR-1 requires a lower concentration for the activation of NMDA receptors compared to that required for cleavage of the NMDA receptors (Gingrich et al., 2000; Lee et al., 2007). We can employ the use of PAR-1 knockout mice neurons and neurons overexpressed with NR1/NR2B(K318A) and compare the Ca^{2+} influx through NMDA receptors by Ca^{2+} imaging. The excitotoxicity effects caused by the differential activation of the NMDA receptors can also be investigated and compared using these neurons.

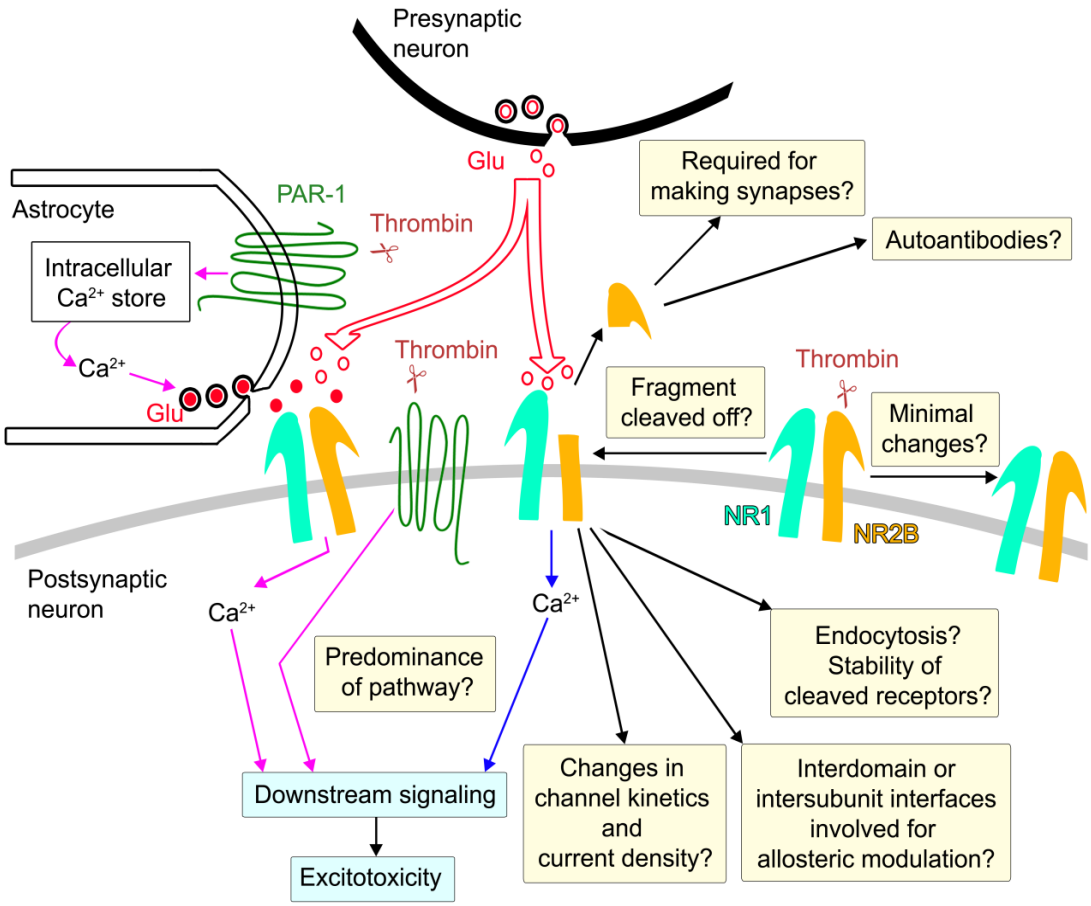

Fig. 5.2. Summary of the future studies. Thrombin (maroon), PAR-1 (green), NR1 (light green) and NR2B (orange) are indicated and as color coded. Glu indicates glutamate (red). Red circles indicate glutamate from astrocytes while open, red circles indicate glutamate from presynaptic neuron. Glutamate is stored in vesicles (open black circles) and is released when vesicles fuse with the membrane. Thrombin can initiate downstream signaling through two pathways. One is the indirect pathway (pink) through PAR-1 activation while the other is the direct pathway (blue) through cleavage of the NR2B of NMDA receptors. Refer to the text for explanation.

6 References

Aizenman E, Potthoff WK (1999) Lack of interaction between nitric oxide and the redox modulatory site of the NMDA receptor. Br J Pharmacol 126:296-300.

Aizenman E, Lipton SA, Loring RH (1989) Selective modulation of NMDA responses by reduction and oxidation. Neuron 2:1257-1263.

Akiyama H, Ikeda K, Kondo H, McGeer PL (1992) Thrombin accumulation in brains of patients with Alzheimer's disease. Neurosci Lett 146:152-154.

Al-Hallaq RA, Conrads TP, Veenstra TD, Wenthold RJ (2007) NMDA di-heteromeric receptor populations and associated proteins in rat hippocampus. J Neurosci 27:8334-8343.

Al-Hallaq RA, Jarabek BR, Fu Z, Vicini S, Wolfe BB, Yasuda RP (2002) Association of NR3A with the N-methyl-D-aspartate receptor NR1 and NR2 subunits. Mol Pharmacol 62:1119-1127.

Alanine A, Bourson A, Buttelmann B, Gill R, Heitz MP, Mutel V, Pinard E, Trube G, Wyler R (2003) 1-Benzyloxy-4,5-dihydro-1H-imidazol-2-yl-amines, a novel class of NR1/2B subtype selective NMDA receptor antagonists. Bioorg Med Chem Lett 13:3155-3159.

Albers GW, Goldstein LB, Hall D, Lesko LM (2001) Aptiganel hydrochloride in acute ischemic stroke: a randomized controlled trial. JAMA 286:2673-2682.

Almonte AG, Hamill CE, Chhatwal JP, Wingo TS, Barber JA, Lyuboslavsky PN, David Sweatt J, Ressler KJ, White DA, Traynelis SF (2007) Learning and memory deficits in mice lacking protease activated receptor-1. Neurobiol Learn Mem 88:295-304.

Anderson RE, Tan WK, Martin HS, Meyer FB (1999) Effects of glucose and PaO2 modulation on cortical intracellular acidosis, NADH redox state, and infarction in the ischemic penumbra. Stroke 30:160-170.

Andersson O, Stenqvist A, Attersand A, von Euler G (2001) Nucleotide sequence, genomic organization, and chromosomal localization of genes encoding the human NMDA receptor subunits NR3A and NR3B. Genomics 78:178-184.

Arai T, Miklossy J, Klegeris A, Guo JP, McGeer PL (2006) Thrombin and prothrombin are expressed by neurons and glial cells and accumulate in neurofibrillary tangles in Alzheimer disease brain. J Neuropathol Exp Neurol 65:19-25.

Arand AG, Sawaya R (1986) Intraoperative chemical hemostasis in neurosurgery. Neurosurgery 18:223-233.

Araneda RC, Lan JY, Zheng X, Zukin RS, Bennett MV (1999) Spermine and arcaine block and permeate N-methyl-D-aspartate receptor channels. Biophys J 76:2899-2911.

Arinuma Y, Yanagida T, Hirohata S (2008) Association of cerebrospinal fluid anti-NR2 glutamate receptor antibodies with diffuse neuropsychiatric systemic lupus erythematosus. Arthritis Rheum 58:1130-1135.

Arundine M, Tymianski M (2003) Molecular mechanisms of calcium-dependent neurodegeneration in excitotoxicity. Cell Calcium 34:325-337.

Ascher P, Nowak L (1988) The role of divalent cations in the N-methyl-D-aspartate responses of mouse central neurones in culture. J Physiol 399:247-266.

Ascher P, Bregestovski P, Nowak L (1988) N-methyl-D-aspartate-activated channels of mouse central neurones in magnesium-free solutions. J Physiol 399:207-226.

Asztely F, Gustafsson B (1996) Ionotropic glutamate receptors. Their possible role in the expression of hippocampal synaptic plasticity. Mol Neurobiol 12:1-11.

Ayalon G, Stern-Bach Y (2001) Functional assembly of AMPA and kainate receptors is mediated by several discrete protein-protein interactions. Neuron 31:103-113.

Backes BJ, Harris JL, Leonetti F, Craik CS, Ellman JA (2000) Synthesis of positional-scanning libraries of fluorogenic peptide substrates to define the extended substrate specificity of plasmin and thrombin. Nat Biotechnol 18:187-193.

Bajaj G, Zhang Y, Schimerlik MI, Hau AM, Yang J, Filtz TM, Kioussi C, Ishmael JE (2009) N-methyl-D-aspartate receptor subunits are non-myosin targets of myosin regulatory light chain. J Biol Chem 284:1252-1266.

Banke TG, Traynelis SF (2003) Activation of NR1/NR2B NMDA receptors. Nat Neurosci 6:144-152.

Banke TG, Dravid SM, Traynelis SF (2005) Protons trap NR1/NR2B NMDA receptors in a nonconducting state. J Neurosci 25:42-51.

Baron A, Montagne A, Casse F, Launay S, Maubert E, Ali C, Vivien D (2010) NR2D-containing NMDA receptors mediate tissue plasminogen activator-promoted neuronal excitotoxicity. Cell Death Differ 17:860-871.

Baron JC (2001) Perfusion thresholds in human cerebral ischemia: historical perspective and therapeutic implications. Cerebrovasc Dis 11 Suppl 1:2-8.

Beck C, Wollmuth LP, Seeburg PH, Sakmann B, Kuner T (1999) NMDAR channel segments forming the extracellular vestibule inferred from the accessibility of substituted cysteines. Neuron 22:559-570.

Benchenane K, Castel H, Boulouard M, Bluthe R, Fernandez-Monreal M, Roussel BD, Lopez-Atalaya JP, Butt-Gueulle S, Agin V, Maubert E, Dantzer R, Touzani O, Dauphin F, Vivien D, Ali C (2007) Anti-NR1 N-terminal-domain vaccination unmasks the crucial action of tPA on NMDA-receptor-mediated toxicity and spatial memory. J Cell Sci 120:578-585.

Bendel O, Meijer B, Hurd Y, von Euler G (2005) Cloning and expression of the human NMDA receptor subunit NR3B in the adult human hippocampus. Neurosci Lett 377:31-36.

Benveniste M, Mayer ML (1991) Kinetic analysis of antagonist action at N-methyl-D-aspartic acid receptors. Two binding sites each for glutamate and glycine. Biophys J 59:560-573.

Benveniste M, Mayer ML (1993) Multiple effects of spermine on N-methyl-D-aspartic acid receptor responses of rat cultured hippocampal neurones. J Physiol 464:131-163.

Benveniste M, Clements J, Vyklicky L, Jr., Mayer ML (1990) A kinetic analysis of the modulation of N-methyl-D-aspartic acid receptors by glycine in mouse cultured hippocampal neurones. J Physiol 428:333-357.

Berger AJ, Dieudonne S, Ascher P (1998) Glycine uptake governs glycine site occupancy at NMDA receptors of excitatory synapses. J Neurophysiol 80:3336-3340.

Bergeron R, Meyer TM, Coyle JT, Greene RW (1998) Modulation of N-methyl-D-aspartate receptor function by glycine transport. Proc Natl Acad Sci U S A 95:15730-15734.

Besancon E, Guo S, Lok J, Tymianski M, Lo EH (2008) Beyond NMDA and AMPA glutamate receptors: emerging mechanisms for ionic imbalance and cell death in stroke. Trends in Pharmacological Sciences 29:268-275.

Betz H, Gomeza J, Armsen W, Scholze P, Eulenburg V (2006) Glycine transporters: essential regulators of synaptic transmission. Biochem Soc Trans 34:55-58.

Bi R, Bi X, Baudry M (1998a) Phosphorylation regulates calpain-mediated truncation of glutamate ionotropic receptors. Brain Res 797:154-158.

Bi R, Rong Y, Bernard A, Khrestchatisky M, Baudry M (2000) Src-mediated tyrosine phosphorylation of NR2 subunits of N-methyl-D-aspartate receptors protects from calpain-mediated truncation of their C-terminal domains. J Biol Chem 275:26477-26483.

Bi X, Rong Y, Chen J, Dang S, Wang Z, Baudry M (1998b) Calpain-mediated regulation of NMDA receptor structure and function. Brain Res 790:245-253.

Blanke ML, VanDongen AM (2008) Constitutive activation of the N-methyl-D-aspartate receptor via cleft-spanning disulfide bonds. J Biol Chem 283:21519-21529.

Blanpied TA, Boeckman FA, Aizenman E, Johnson JW (1997) Trapping channel block of NMDA-activated responses by amantadine and memantine. J Neurophysiol 77:309-323.

Bliss TV, Collingridge GL (1993) A synaptic model of memory: long-term potentiation in the hippocampus. Nature 361:31-39.

Bode W, Turk D, Karshikov A (1992) The refined 1.9-A X-ray crystal structure of D-Phe-Pro-Arg chloromethylketone-inhibited human alpha-thrombin: structure analysis, overall structure, electrostatic properties, detailed active-site geometry, and structure-function relationships. Protein Sci 1:426-471.

Bode W, Mayr I, Baumann U, Huber R, Stone SR, Hofsteenge J (1989) The refined 1.9 A crystal structure of human alpha-thrombin: interaction with D-Phe-Pro-Arg chloromethylketone and significance of the Tyr-Pro-Pro-Trp insertion segment. EMBO J 8:3467-3475.

Boissel JP, Le Bonniec B, Rabiet MJ, Labie D, Elion J (1984) Covalent structures of beta and gamma autolytic derivatives of human alpha-thrombin. J Biol Chem 259:5691-5697.

Boldyrev AA, Kazey VI, Leinsoo TA, Mashkina AP, Tyulina OV, Johnson P, Tuneva JO, Chittur S, Carpenter DO (2004) Rodent lymphocytes express functionally active glutamate receptors. Biochem Biophys Res Commun 324:133-139.

Boven LA, Vergnolle N, Henry SD, Silva C, Imai Y, Holden J, Warren K, Hollenberg MD, Power C (2003) Up-regulation of proteinase-activated receptor 1 expression in astrocytes during HIV encephalitis. J Immunol 170:2638-2646.

Bovill EG, Tracy RP, Hayes TE, Jenny RJ, Bhushan FH, Mann KG (1995) Evidence that meizothrombin is an intermediate product in the clotting of whole blood. Arterioscler Thromb Vasc Biol 15:754-758.

Bowser DN, Khakh BS (2007) Two forms of single-vesicle astrocyte exocytosis imaged with total internal reflection fluorescence microscopy. Proc Natl Acad Sci U S A 104:4212-4217.

Brackley P, Goodnow Jr R, Nakanishi K, Sudan HL, Usherwood PNR (1990) Spermine and philanthotoxin potentiate excitatory amino acid responses of Xenopus oocytes injected with rat and chick brain RNA. Neuroscience Letters 114:51-56.

Brenman JE, Chao DS, Gee SH, McGee AW, Craven SE, Santillano DR, Wu Z, Huang F, Xia H, Peters MF, Froehner SC, Bredt DS (1996) Interaction of nitric oxide synthase with the postsynaptic density protein PSD-95 and alpha1-syntrophin mediated by PDZ domains. Cell 84:757-767.

Bretin S, Rogemond V, Marin P, Maus M, Torrens Y, Honnorat J, Glowinski J, Premont J, Gauchy C (2006) Calpain product of WT-CRMP2 reduces the amount of surface NR2B NMDA receptor subunit. J Neurochem 98:1252-1265.

Brimecombe JC, Boeckman FA, Aizenman E (1997) Functional consequences of NR2 subunit composition in single recombinant N-methyl-D-aspartate receptors. Proc Natl Acad Sci U S A 94:11019-11024.

Brimecombe JC, Potthoff WK, Aizenman E (1999) A critical role of the N-methyl-D-aspartate (NMDA) receptor subunit (NR) 2A in the expression of redox sensitivity of NR1/NR2A recombinant NMDA receptors. J Pharmacol Exp Ther 291:785-792.

Bristol JA, Ratcliffe JV, Roth DA, Jacobs MA, Furie BC, Furie B (1996) Biosynthesis of prothrombin: intracellular localization of the vitamin K-dependent carboxylase and the sites of gamma-carboxylation. Blood 88:2585-2593.

Brose N, Gasic GP, Vetter DE, Sullivan JM, Heinemann SF (1993) Protein chemical characterization and immunocytochemical localization of the NMDA receptor subunit NMDA R1. J Biol Chem 268:22663-22671.

Brothwell SL, Barber JL, Monaghan DT, Jane DE, Gibb AJ, Jones S (2008) NR2B- and NR2D-containing synaptic NMDA receptors in developing rat substantia nigra pars compacta dopaminergic neurones. J Physiol 586:739-750.

Brufatto N, Nesheim ME (2003) Analysis of the kinetics of prothrombin activation and evidence that two equilibrating forms of prothrombinase are involved in the process. J Biol Chem 278:6755-6764.

Buttelmann B, Alanine A, Bourson A, Gill R, Heitz MP, Mutel V, Pinard E, Trube G, Wyler R (2003) 2-(3,4-Dihydro-1H-isoquinolin-2yl)-pyridines as a novel class of NR1/2B subtype selective NMDA receptor antagonists. Bioorg Med Chem Lett 13:829-832.

Cannon JR, Keep RF, Hua Y, Richardson RJ, Schallert T, Xi G (2005) Thrombin preconditioning provides protection in a 6-hydroxydopamine Parkinson's disease model. Neurosci Lett 373:189-194.

Cannon JR, Keep RF, Schallert T, Hua Y, Richardson RJ, Xi G (2006) Protease-activated receptor-1 mediates protection elicited by thrombin preconditioning in a rat 6-hydroxydopamine model of Parkinson's disease. Brain Res 1116:177-186.

Carlisle HJ, Kennedy MB (2005) Spine architecture and synaptic plasticity. Trends Neurosci 28:182-187.

Chang HR, Kuo CC (2008) The activation gate and gating mechanism of the NMDA receptor. J Neurosci 28:1546-1556.

Chang JY (1986) The structures and proteolytic specificities of autolysed human thrombin. Biochem J 240:797-802.

Chatterton JE, Awobuluyi M, Premkumar LS, Takahashi H, Talantova M, Shin Y, Cui J, Tu S, Sevarino KA, Nakanishi N, Tong G, Lipton SA, Zhang D (2002) Excitatory glycine receptors containing the NR3 family of NMDA receptor subunits. Nature 415:793-798.

Chen BS, Roche KW (2007) Regulation of NMDA receptors by phosphorylation. In: Neuropharmacology, 2007/07/24 Edition, pp 362-368.

Chen BS, Roche KW (2009) Growth factor-dependent trafficking of cerebellar NMDA receptors via protein kinase B/Akt phosphorylation of NR2C. Neuron 62:471-478.

Chen H, Shi H (2008) A reducing environment stabilizes HIF-2alpha in SH-SY5Y cells under hypoxic conditions. FEBS Lett 582:3899-3902.

Chen HS, Pellegrini JW, Aggarwal SK, Lei SZ, Warach S, Jensen FE, Lipton SA (1992) Open-channel block of N-methyl-D-aspartate (NMDA) responses by memantine: therapeutic advantage against NMDA receptor-mediated neurotoxicity. J Neurosci 12:4427-4436.

Chen HS, Wang YF, Rayudu PV, Edgecomb P, Neill JC, Segal MM, Lipton SA, Jensen FE (1998) Neuroprotective concentrations of the N-methyl-D-aspartate open-channel blocker memantine are effective without cytoplasmic vacuolation following post-ischemic administration and do not block maze learning or long-term potentiation. Neuroscience 86:1121-1132.

Chen L, Muhlhauser M, Yang CR (2003) Glycine tranporter-1 blockade potentiates NMDA-mediated responses in rat prefrontal cortical neurons in vitro and in vivo. J Neurophysiol 89:691-703.

Chen M, Lu TJ, Chen XJ, Zhou Y, Chen Q, Feng XY, Xu L, Duan WH, Xiong ZQ (2008a) Differential roles of NMDA receptor subtypes in ischemic neuronal cell death and ischemic tolerance. Stroke 39:3042-3048.

Chen N, Moshaver A, Raymond LA (1997) Differential sensitivity of recombinant N-methyl-D-aspartate receptor subtypes to zinc inhibition. Mol Pharmacol 51:1015-1023.

Chen N, Luo T, Raymond LA (1999) Subtype-dependence of NMDA receptor channel open probability. J Neurosci 19:6844-6854.

Chen N, Li B, Murphy TH, Raymond LA (2004a) Site within N-Methyl-d-aspartate Receptor Pore Modulates Channel Gating. Molecular Pharmacology 65:157-164.

Chen PE, Johnston AR, Mok MH, Schoepfer R, Wyllie DJ (2004b) Influence of a threonine residue in the S2 ligand binding domain in determining agonist potency and deactivation rate of recombinant NR1a/NR2D NMDA receptors. J Physiol 558:45-58.

Chen PE, Geballe MT, Stansfeld PJ, Johnston AR, Yuan H, Jacob AL, Snyder JP, Traynelis SF, Wyllie DJ (2005) Structural features of the glutamate binding site in recombinant NR1/NR2A N-methyl-D-aspartate receptors determined by site-directed mutagenesis and molecular modeling. Mol Pharmacol 67:1470-1484.

Chen PE, Geballe MT, Katz E, Erreger K, Livesey MR, O'Toole KK, Le P, Lee CJ, Snyder JP, Traynelis SF, Wyllie DJ (2008b) Modulation of glycine potency in rat recombinant NMDA receptors containing chimeric NR2A/2D subunits expressed in Xenopus laevis oocytes. J Physiol 586:227-245.

Cho KK, Khibnik L, Philpot BD, Bear MF (2009) The ratio of NR2A/B NMDA receptor subunits determines the qualities of ocular dominance plasticity in visual cortex. Proc Natl Acad Sci U S A 106:5377-5382.
Choi BH, Suzuki M, Kim T, Wagner SL, Cunningham DD (1990) Protease nexin-1. Localization in the human brain suggests a protective role against extravasated serine proteases. Am J Pathol 137:741-747.
Choi DW, Koh JY (1998) Zinc and brain injury. Annu Rev Neurosci 21:347-375.
Choi SH, Joe EH, Kim SU, Jin BK (2003) Thrombin-induced microglial activation produces degeneration of nigral dopaminergic neurons in vivo. J Neurosci 23:5877-5886.
Choi Y, Chen HV, Lipton SA (2001) Three pairs of cysteine residues mediate both redox and zn2+ modulation of the nmda receptor. J Neurosci 21:392-400.
Choi YB, Lipton SA (1999) Identification and mechanism of action of two histidine residues underlying high-affinity Zn2+ inhibition of the NMDA receptor. Neuron 23:171-180.
Choi YB, Tenneti L, Le DA, Ortiz J, Bai G, Chen HS, Lipton SA (2000) Molecular basis of NMDA receptor-coupled ion channel modulation by S-nitrosylation. Nat Neurosci 3:15-21.
Christine CW, Choi DW (1990) Effect of zinc on NMDA receptor-mediated channel currents in cortical neurons. J Neurosci 10:108-116.
Chung HJ, Huang YH, Lau LF, Huganir RL (2004) Regulation of the NMDA receptor complex and trafficking by activity-dependent phosphorylation of the NR2B subunit PDZ ligand. J Neurosci 24:10248-10259.
Ciabarra AM, Sullivan JM, Gahn LG, Pecht G, Heinemann S, Sevarino KA (1995) Cloning and characterization of chi-1: a developmentally regulated member of a novel class of the ionotropic glutamate receptor family. J Neurosci 15:6498-6508.
Claiborne CF et al. (2003) Orally efficacious NR2B-selective NMDA receptor antagonists. Bioorg Med Chem Lett 13:697-700.
Clarke RJ, Johnson JW (2006) NMDA receptor NR2 subunit dependence of the slow component of magnesium unblock. J Neurosci 26:5825-5834.
Clements JD, Westbrook GL (1991) Activation kinetics reveal the number of glutamate and glycine binding sites on the N-methyl-D-aspartate receptor. Neuron 7:605-613.
Clements JD, Westbrook GL (1994) Kinetics of AP5 dissociation from NMDA receptors: evidence for two identical cooperative binding sites. J Neurophysiol 71:2566-2569.
Colonna-Cesari F, Sander C (1990) Excluded volume approximation to protein-solvent interaction. The solvent contact model. Biophys J 57:1103-1107.
Cote A, Chiasson M, Peralta MR, 3rd, Lafortune K, Pellegrini L, Toth K (2005) Cell type-specific action of seizure-induced intracellular zinc accumulation in the rat hippocampus. J Physiol 566:821-837.
Cottrell JR, Dube GR, Egles C, Liu G (2000) Distribution, density, and clustering of functional glutamate receptors before and after synaptogenesis in hippocampal neurons. J Neurophysiol 84:1573-1587.
Cousins SL, Papadakis M, Rutter AR, Stephenson FA (2008) Differential interaction of NMDA receptor subtypes with the post-synaptic density-95 family of membrane associated guanylate kinase proteins. J Neurochem 104:903-913.
Cregan EF, Peeling J, Corbett D, Buchan AM, Saunders J, Auer RN, Gao M, McCarthy DJ, Eisman MS, Campbell TM, Murray RJ, Stagnitto ML, Palmer GC (1997) -(S)-Alpha-phenyl-2-pyridine-ethanamine Dihydrochloride-, a low affinity uncompetitive N-methyl-D-aspartic acid antagonist, is effective in rodent models of global and focal ischemia. J Pharmacol Exp Ther 283:1412-1424.
Cull-Candy SG, Usowicz MM (1987) Multiple-conductance channels activated by excitatory amino acids in cerebellar neurons. Nature 325:525-528.
Cuomo O, Pignataro G, Gala R, Scorziello A, Gravino E, Piazza O, Tufano R, Di Renzo G, Annunziato L (2007) Antithrombin reduces ischemic volume, ameliorates neurologic deficits, and prolongs animal survival in both transient and permanent focal ischemia. Stroke 38:3272-3279.

Dalmau J, Gleichman AJ, Hughes EG, Rossi JE, Peng X, Lai M, Dessain SK, Rosenfeld MR, Balice-Gordon R, Lynch DR (2008) Anti-NMDA-receptor encephalitis: case series and analysis of the effects of antibodies. Lancet Neurol 7:1091-1098.

Dalmau J, Tuzun E, Wu HY, Masjuan J, Rossi JE, Voloschin A, Baehring JM, Shimazaki H, Koide R, King D, Mason W, Sansing LH, Dichter MA, Rosenfeld MR, Lynch DR (2007) Paraneoplastic anti-N-methyl-D-aspartate receptor encephalitis associated with ovarian teratoma. Ann Neurol 61:25-36.

Dalva MB, Takasu MA, Lin MZ, Shamah SM, Hu L, Gale NW, Greenberg ME (2000) EphB receptors interact with NMDA receptors and regulate excitatory synapse formation. Cell 103:945-956.

Dambinova SA, Khounteev GA, Skoromets AA (2002) Multiple panel of biomarkers for TIA/stroke evaluation. Stroke 33:1181-1182.

Dambinova SA, Granstrem OK, Tourov A, Salluzzo R, Castello F, Izykenova GA (1998) Monitoring of brain spiking activity and autoantibodies to N-terminus domain of GluR1 subunit of AMPA receptors in blood serum of rats with cobalt-induced epilepsy. J Neurochem 71:2088-2093.

Dambinova SA, Khounteev GA, Izykenova GA, Zavolokov IG, Ilyukhina AY, Skoromets AA (2003) Blood test detecting autoantibodies to N-methyl-D-aspartate neuroreceptors for evaluation of patients with transient ischemic attack and stroke. Clin Chem 49:1752-1762.

Dang QD, Sabetta M, Di Cera E (1997) Selective loss of fibrinogen clotting in a loop-less thrombin. J Biol Chem 272:19649-19651.

Das S, Sasaki YF, Rothe T, Premkumar LS, Takasu M, Crandall JE, Dikkes P, Conner DA, Rayudu PV, Cheung W, Chen HS, Lipton SA, Nakanishi N (1998) Increased NMDA current and spine density in mice lacking the NMDA receptor subunit NR3A. Nature 393:377-381.

Davie EW, Kulman JD (2006) An overview of the structure and function of thrombin. Semin Thromb Hemost 32 Suppl 1:3-15.

Davis SM, Albers GW, Diener HC, Lees KR, Norris J (1997) Termination of Acute Stroke Studies Involving Selfotel Treatment. ASSIST Steering Committed. Lancet 349:32.

Davis SM, Lees KR, Albers GW, Diener HC, Markabi S, Karlsson G, Norris J (2000) Selfotel in acute ischemic stroke : possible neurotoxic effects of an NMDA antagonist. Stroke 31:347-354.

de Castro Ribeiro M, Badaut J, Price M, Meins M, Bogousslavsky J, Monard D, Hirt L (2006) Thrombin in ischemic neuronal death. Exp Neurol 198:199-203.

De Silva DA, Brekenfeld C, Ebinger M, Christensen S, Barber PA, Butcher KS, Levi CR, Parsons MW, Bladin CF, Donnan GA, Davis SM (2010) The benefits of intravenous thrombolysis relate to the site of baseline arterial occlusion in the Echoplanar Imaging Thrombolytic Evaluation Trial (EPITHET). Stroke 41:295-299.

DeGiorgio LA, Konstantinov KN, Lee SC, Hardin JA, Volpe BT, Diamond B (2001) A subset of lupus anti-DNA antibodies cross-reacts with the NR2 glutamate receptor in systemic lupus erythematosus. Nat Med 7:1189-1193.

Deschepper CF, Bigornia V, Berens ME, Lapointe MC (1991) Production of thrombin and antithrombin III by brain and astroglial cell cultures. Brain Res Mol Brain Res 11:355-358.

Di Fabio R, Capelli AM, Conti N, Cugola A, Donati D, Feriani A, Gastaldi P, Gaviraghi G, Hewkin CT, Micheli F, Missio A, Mugnaini M, Pecunioso A, Quaglia AM, Ratti E, Rossi L, Tedesco G, Trist DG, Reggiani A (1997) Substituted indole-2-carboxylates as in vivo potent antagonists acting as the strychnine-insensitive glycine binding site. J Med Chem 40:841-850.

Di X, Bullock R, Watson J, Fatouros P, Chenard B, White F, Corwin F (1997) Effect of CP101,606, a novel NR2B subunit antagonist of the N-methyl-D-aspartate receptor, on the volume of ischemic brain damage off cytotoxic brain edema after middle cerebral artery occlusion in the feline brain. Stroke 28:2244-2251.

Diener HC, AlKhedr A, Busse O, Hacke W, Zingmark PH, Jonsson N, Basun H (2002) Treatment of acute ischaemic stroke with the low-affinity, use-dependent NMDA antagonist AR-R15896AR. A safety and tolerability study. J Neurol 249:561-568.
Dihanich M, Kaser M, Reinhard E, Cunningham D, Monard D (1991) Prothrombin mRNA is expressed by cells of the nervous system. Neuron 6:575-581.
Dingledine R, Borges K, Bowie D, Traynelis SF (1999) The glutamate receptor ion channels. Pharmacol Rev 51:7-61.
Dirnagl U, Iadecola C, Moskowitz MA (1999) Pathobiology of ischaemic stroke: an integrated view. Trends Neurosci 22:391-397.
Disorders TNIoN, Stroke rt-PA Stroke Study Group (1995) Tissue Plasminogen Activator for Acute Ischemic Stroke. N Engl J Med 333:1581-1588.
Docagne F, Nicole O, Marti HH, MacKenzie ET, Buisson A, Vivien D (1999) Transforming growth factor-beta1 as a regulator of the serpins/t-PA axis in cerebral ischemia. FASEB J 13:1315-1324.
Dombkowski AA, Crippen GM (2000) Disulfide recognition in an optimized threading potential. Protein Eng 13:679-689.
Dong YN, Waxman EA, Lynch DR (2004) Interactions of postsynaptic density-95 and the NMDA receptor 2 subunit control calpain-mediated cleavage of the NMDA receptor. J Neurosci 24:11035-11045.
Donnan GA, Fisher M, Macleod M, Davis SM (2008) Stroke. The Lancet 371:1612-1623.
Dravid SM, Burger PB, Prakash A, Geballe MT, Yadav R, Le P, Vellano K, Snyder JP, Traynelis SF (2010) Structural determinants of D-cycloserine efficacy at the NR1/NR2C NMDA receptors. J Neurosci 30:2741-2754.
Dravid SM, Erreger K, Yuan H, Nicholson K, Le P, Lyuboslavsky P, Almonte A, Murray E, Mosely C, Barber J, French A, Balster R, Murray TF, Traynelis SF (2007) Subunit-specific mechanisms and proton sensitivity of NMDA receptor channel block. J Physiol 581:107-128.
Dunah AW, Standaert DG (2003) Subcellular segregation of distinct heteromeric NMDA glutamate receptors in the striatum. J Neurochem 85:935-943.
Dunah AW, Luo J, Wang YH, Yasuda RP, Wolfe BB (1998) Subunit composition of N-methyl-D-aspartate receptors in the central nervous system that contain the NR2D subunit. Mol Pharmacol 53:429-437.
Durand GM, Bennett MV, Zukin RS (1993) Splice variants of the N-methyl-D-aspartate receptor NR1 identify domains involved in regulation by polyamines and protein kinase C. Proc Natl Acad Sci U S A 90:6731-6735.
Dyker AG, Lees KR (1999) Remacemide hydrochloride: a double-blind, placebo-controlled, safety and tolerability study in patients with acute ischemic stroke. Stroke 30:1796-1801.
Efthimiou P, Blanco M (2009) Pathogenesis of neuropsychiatric systemic lupus erythematosus and potential biomarkers. Mod Rheumatol 19:457-468.
Ehlers MD, Zhang S, Bernhadt JP, Huganir RL (1996) Inactivation of NMDA receptors by direct interaction of calmodulin with the NR1 subunit. Cell 84:745-755.
Erreger K, Traynelis SF (2005) Allosteric interaction between zinc and glutamate binding domains on NR2A causes desensitization of NMDA receptors. J Physiol 569:381-393.
Erreger K, Chen PE, Wyllie DJ, Traynelis SF (2004) Glutamate receptor gating. Crit Rev Neurobiol 16:187-224.
Erreger K, Dravid SM, Banke TG, Wyllie DJ, Traynelis SF (2005) Subunit-specific gating controls rat NR1/NR2A and NR1/NR2B NMDA channel kinetics and synaptic signalling profiles. J Physiol 563:345-358.
Erreger K, Geballe MT, Kristensen A, Chen PE, Hansen KB, Lee CJ, Yuan H, Le P, Lyuboslavsky PN, Micale N, Jorgensen L, Clausen RP, Wyllie DJ, Snyder JP, Traynelis SF (2007) Subunit-specific agonist activity at NR2A-, NR2B-, NR2C-, and NR2D-containing N-methyl-D-aspartate glutamate receptors. Mol Pharmacol 72:907-920.

Ewald RC, Van Keuren-Jensen KR, Aizenman CD, Cline HT (2008) Roles of NR2A and NR2B in the development of dendritic arbor morphology in vivo. J Neurosci 28:850-861.

Fayyazuddin A, Villarroel A, Le Goff A, Lerma J, Neyton J (2000) Four residues of the extracellular N-terminal domain of the NR2A subunit control high-affinity Zn2+ binding to NMDA receptors. Neuron 25:683-694.

Fernandez-Monreal M, Lopez-Atalaya JP, Benchenane K, Cacquevel M, Dulin F, Le Caer JP, Rossier J, Jarrige AC, Mackenzie ET, Colloc'h N, Ali C, Vivien D (2004) Arginine 260 of the amino-terminal domain of NR1 subunit is critical for tissue-type plasminogen activator-mediated enhancement of N-methyl-D-aspartate receptor signaling. J Biol Chem 279:50850-50856.

Fischer G, Mutel V, Trube G, Malherbe P, Kew JN, Mohacsi E, Heitz MP, Kemp JA (1997) Ro 25-6981, a highly potent and selective blocker of N-methyl-D-aspartate receptors containing the NR2B subunit. Characterization in vitro. J Pharmacol Exp Ther 283:1285-1292.

Fisher M, Tatlisumak T (2005) Use of animal models has not contributed to development of acute stroke therapies: con. Stroke 36:2324-2325.

Francois JM, Sheng Z, Szczesna D, Potter JD (1995) The functional role of the domains of troponin-C investigated with thrombin fragments of troponin-C reconstituted into skinned muscle fibers. J Biol Chem 270:19287-19293.

Fujimoto S, Katsuki H, Kume T, Akaike A (2006) Thrombin-induced delayed injury involves multiple and distinct signaling pathways in the cerebral cortex and the striatum in organotypic slice cultures. Neurobiol Dis 22:130-142.

Fujimoto S, Katsuki H, Ohnishi M, Takagi M, Kume T, Akaike A (2007) Thrombin induces striatal neurotoxicity depending on mitogen-activated protein kinase pathways in vivo. Neuroscience 144:694-701.

Fukaya M, Hayashi Y, Watanabe M (2005) NR2 to NR3B subunit switchover of NMDA receptors in early postnatal motoneurons. Eur J Neurosci 21:1432-1436.

Furukawa H, Gouaux E (2003) Mechanisms of activation, inhibition and specificity: crystal structures of the NMDA receptor NR1 ligand-binding core. EMBO J 22:2873-2885.

Furukawa H, Singh SK, Mancusso R, Gouaux E (2005) Subunit arrangement and function in NMDA receptors. Nature 438:185-192.

Gable MS, Gavali S, Radner A, Tilley DH, Lee B, Dyner L, Collins A, Dengel A, Dalmau J, Glaser CA (2009) Anti-NMDA receptor encephalitis: report of ten cases and comparison with viral encephalitis. Eur J Clin Microbiol Infect Dis 28:1421-1429.

Gallagher MJ, Huang H, Pritchett DB, Lynch DR (1996) Interactions between ifenprodil and the NR2B subunit of the N-methyl-D-aspartate receptor. J Biol Chem 271:9603-9611.

Gallagher MJ, Huang H, Grant ER, Lynch DR (1997) The NR2B-specific interactions of polyamines and protons with the N-methyl-D-aspartate receptor. J Biol Chem 272:24971-24979.

Gardoni F (2008) MAGUK proteins: new targets for pharmacological intervention in the glutamatergic synapse. Eur J Pharmacol 585:147-152.

Gardoni F, Di Luca M (2006) New targets for pharmacological intervention in the glutamatergic synapse. Eur J Pharmacol 545:2-10.

Gascon S, Sobrado M, Roda JM, Rodriguez-Pena A, Diaz-Guerra M (2008) Excitotoxicity and focal cerebral ischemia induce truncation of the NR2A and NR2B subunits of the NMDA receptor and cleavage of the scaffolding protein PSD-95. Mol Psychiatry 13:99-114.

Gaynor B, Putterman C, Valadon P, Spatz L, Scharff MD, Diamond B (1997) Peptide inhibition of glomerular deposition of an anti-DNA antibody. Proc Natl Acad Sci U S A 94:1955-1960.

Gibb AJ, Colquhoun D (1991) Glutamate activation of a single NMDA receptor-channel produces a cluster of channel openings. Proc Biol Sci 243:39-45.

Gibb AJ, Colquhoun D (1992) Activation of N-methyl-D-aspartate receptors by L-glutamate in cells dissociated from adult rat hippocampus. J Physiol 456:143-179.

Gielen M, Siegler Retchless B, Mony L, Johnson JW, Paoletti P (2009) Mechanism of differential control of NMDA receptor activity by NR2 subunits. Nature 459:703-707.

Gielen M, Le Goff A, Stroebel D, Johnson JW, Neyton J, Paoletti P (2008) Structural rearrangements of NR1/NR2A NMDA receptors during allosteric inhibition. Neuron 57:80-93.

Giffard RG, Monyer H, Christine CW, Choi DW (1990) Acidosis reduces NMDA receptor activation, glutamate neurotoxicity, and oxygen-glucose deprivation neuronal injury in cortical cultures. Brain Res 506:339-342.

Gilling K, Jatzke C, Wollenburg C, Vanejevs M, Kauss V, Jirgensons A, Parsons CG (2007) A novel class of amino-alkylcyclohexanes as uncompetitive, fast, voltage-dependent, N-methyl-D-aspartate (NMDA) receptor antagonists--in vitro characterization. J Neural Transm 114:1529-1537.

Gingrich MB, Traynelis SF (2000) Serine proteases and brain damage - is there a link? Trends Neurosci 23:399-407.

Gingrich MB, Junge CE, Lyuboslavsky P, Traynelis SF (2000) Potentiation of NMDA receptor function by the serine protease thrombin. J Neurosci 20:4582-4595.

Ginsberg MD (1996) The validity of rodent brain-ischemia models is self-evident. Arch Neurol 53:1065-1067; discussion 1070.

Gogas KR (2006) Glutamate-based therapeutic approaches: NR2B receptor antagonists. Curr Opin Pharmacol 6:68-74.

Gong Y, Xi G, Hu H, Gu Y, Huang F, Keep RF, Hua Y (2008) Increase in brain thrombin activity after experimental intracerebral hemorrhage. Acta Neurochir Suppl 105:47-50.

Gorkiewicz T, Szczuraszek K, Wyrembek P, Michaluk P, Kaczmarek L, Mozrzymas JW (2009) Matrix metalloproteinase-9 reversibly affects the time course of NMDA-induced currents in cultured rat hippocampal neurons. Hippocampus.

Goryunova AV, Bazarnaya NA, Sorokina EG, Semenova NY, Globa OV, Semenova Zh B, Pinelis VG, Roshal LM, Maslova OI (2007) Glutamate receptor autoantibody concentrations in children with chronic post-traumatic headache. Neurosci Behav Physiol 37:761-764.

Gotti B, Duverger D, Bertin J, Carter C, Dupont R, Frost J, Gaudilliere B, MacKenzie ET, Rousseau J, Scatton B, et al. (1988) Ifenprodil and SL 82.0715 as cerebral anti-ischemic agents. I. Evidence for efficacy in models of focal cerebral ischemia. J Pharmacol Exp Ther 247:1211-1221.

Gozlan H, Ben-Ari Y (1995) NMDA receptor redox sites: are they targets for selective neuronal protection? Trends Pharmacol Sci 16:368-374.

Grammas P, Samany PG, Thirumangalakudi L (2006) Thrombin and inflammatory proteins are elevated in Alzheimer's disease microvessels: implications for disease pathogenesis. J Alzheimers Dis 9:51-58.

Grant ER, Bacskai BJ, Anegawa NJ, Pleasure DE, Lynch DR (1998) Opposing contributions of NR1 and NR2 to protein kinase C modulation of NMDA receptors. J Neurochem 71:1471-1481.

Granziera C, Thevenet J, Price M, Wiegler K, Magistretti PJ, Badaut J, Hirt L (2007) Thrombin-induced ischemic tolerance is prevented by inhibiting c-jun N-terminal kinase. Brain Res 1148:217-225.

Green AR, Shuaib A (2006) Therapeutic strategies for the treatment of stroke. Drug Discov Today 11:681-693.

Groc L, Bard L, Choquet D (2009) Surface trafficking of N-methyl-D-aspartate receptors: physiological and pathological perspectives. Neuroscience 158:4-18.

Grosshans DR, Clayton DA, Coultrap SJ, Browning MD (2002) LTP leads to rapid surface expression of NMDA but not AMPA receptors in adult rat CA1. Nat Neurosci 5:27-33.

Grunwald IC, Korte M, Wolfer D, Wilkinson GA, Unsicker K, Lipp HP, Bonhoeffer T, Klein R (2001) Kinase-independent requirement of EphB2 receptors in hippocampal synaptic plasticity. Neuron 32:1027-1040.

Grunwald IC, Korte M, Adelmann G, Plueck A, Kullander K, Adams RH, Frotscher M, Bonhoeffer T, Klein R (2004) Hippocampal plasticity requires postsynaptic ephrinBs. Nat Neurosci 7:33-40.

Guttmann RP, Baker DL, Seifert KM, Cohen AS, Coulter DA, Lynch DR (2001) Specific proteolysis of the NR2 subunit at multiple sites by calpain. J Neurochem 78:1083-1093.

Guttmann RP, Sokol S, Baker DL, Simpkins KL, Dong Y, Lynch DR (2002) Proteolysis of the N-methyl-d-aspartate receptor by calpain in situ. J Pharmacol Exp Ther 302:1023-1030.

Haley EC, Jr., Thompson JL, Levin B, Davis S, Lees KR, Pittman JG, DeRosa JT, Ordronneau P, Brown DL, Sacco RL (2005) Gavestinel does not improve outcome after acute intracerebral hemorrhage: an analysis from the GAIN International and GAIN Americas studies. Stroke 36:1006-1010.

Hamill CE, Mannaioni G, Lyuboslavsky P, Sastre AA, Traynelis SF (2009) Protease-activated receptor 1-dependent neuronal damage involves NMDA receptor function. Exp Neurol 217:136-146.

Han X, Tomitori H, Mizuno S, Higashi K, Full C, Fukiwake T, Terui Y, Leewanich P, Nishimura K, Toida T, Williams K, Kashiwagi K, Igarashi K (2008) Binding of spermine and ifenprodil to a purified, soluble regulatory domain of the N-methyl-D-aspartate receptor. J Neurochem 107:1566-1577.

Hansen KB, Furukawa H, Traynelis SF (2010) Control of assembly and function of glutamate receptors by the amino-terminal domain. Molecular Pharmacology:-.

Hatton CJ, Paoletti P (2005) Modulation of triheteromeric NMDA receptors by N-terminal domain ligands. Neuron 46:261-274.

Hauser J, Sveshnikova N, Wallenius A, Baradaran S, Saarikettu J, Grundstrom T (2008) B-cell receptor activation inhibits AID expression through calmodulin inhibition of E-proteins. Proc Natl Acad Sci U S A 105:1267-1272.

Hawkins LM, Chazot PL, Stephenson FA (1999) Biochemical evidence for the co-association of three N-methyl-D-aspartate (NMDA) R2 subunits in recombinant NMDA receptors. J Biol Chem 274:27211-27218.

Hayashi Y, Ishibashi H, Hashimoto K, Nakanishi H (2006) Potentiation of the NMDA receptor-mediated responses through the activation of the glycine site by microglia secreting soluble factors. Glia 53:660-668.

Henderson JT, Georgiou J, Jia Z, Robertson J, Elowe S, Roder JC, Pawson T (2001) The receptor tyrosine kinase EphB2 regulates NMDA-dependent synaptic function. Neuron 32:1041-1056.

Henrich-Noack P, Striggow F, Reiser G, Reymann KG (2006) Preconditioning with thrombin can be protective or worsen damage after endothelin-1-induced focal ischemia in rats. J Neurosci Res 83:469-475.

Herrera AJ, de Pablos RM, Carreno-Muller E, Villaran RF, Venero JL, Tomas-Camardiel M, Cano J, Machado A (2008) The intrastriatal injection of thrombin in rat induced a retrograde apoptotic degeneration of nigral dopaminergic neurons through synaptic elimination. J Neurochem 105:750-762.

Hestrin S, Nicoll RA, Perkel DJ, Sah P (1990) Analysis of excitatory synaptic action in pyramidal cells using whole-cell recording from rat hippocampal slices. J Physiol 422:203-225.

Hofsteenge J, Braun PJ, Stone SR (1988) Enzymatic properties of proteolytic derivatives of human alpha-thrombin. Biochemistry 27:2144-2151.

Hollmann M, Heinemann S (1994) Cloned glutamate receptors. Annu Rev Neurosci 17:31-108.

Honer M, Benke D, Laube B, Kuhse J, Heckendorn R, Allgeier H, Angst C, Monyer H, Seeburg PH, Betz H, Mohler H (1998) Differentiation of glycine antagonist sites of

N-methyl-D-aspartate receptor subtypes. Preferential interaction of CGP 61594 with NR1/2B receptors. J Biol Chem 273:11158-11163.
Horak M, Wenthold RJ (2009) Different roles of C-terminal cassettes in the trafficking of full-length NR1 subunits to the cell surface. J Biol Chem 284:9683-9691.
Hoyte L, Kaur J, Buchan AM (2004) Lost in translation: taking neuroprotection from animal models to clinical trials. Exp Neurol 188:200-204.
Hu B, Zheng F (2005a) Molecular determinants of glycine-independent desensitization of NR1/NR2A receptors. J Pharmacol Exp Ther 313:563-569.
Hu B, Zheng F (2005b) Differential effects on current kinetics by point mutations in the lurcher motif of NR1/NR2A receptors. J Pharmacol Exp Ther 312:899-904.
Hua Y, Keep RF, Hoff JT, Xi G (2007) Brain injury after intracerebral hemorrhage: the role of thrombin and iron. Stroke 38:759-762.
Hua Y, Keep RF, Gu Y, Xi G (2009) Thrombin and brain recovery after intracerebral hemorrhage. Stroke 40:S88-89.
Hua Y, Wu J, Keep RF, Hoff JT, Xi G (2003) Thrombin exacerbates brain edema in focal cerebral ischemia. Acta Neurochir Suppl 86:163-166.
Huettner JE, Bean BP (1988) Block of N-methyl-D-aspartate-activated current by the anticonvulsant MK-801: selective binding to open channels. Proc Natl Acad Sci U S A 85:1307-1311.
Hughes EG, Peng X, Gleichman AJ, Lai M, Zhou L, Tsou R, Parsons TD, Lynch DR, Dalmau J, Balice-Gordon RJ (2010) Cellular and synaptic mechanisms of anti-NMDA receptor encephalitis. J Neurosci 30:5866-5875.
Hung AY, Sheng M (2002) PDZ domains: structural modules for protein complex assembly. J Biol Chem 277:5699-5702.
Huntington JA (2005) Molecular recognition mechanisms of thrombin. J Thromb Haemost 3:1861-1872.
Husi H, Ward MA, Choudhary JS, Blackstock WP, Grant SG (2000) Proteomic analysis of NMDA receptor-adhesion protein signaling complexes. Nat Neurosci 3:661-669.
Igarashi K, Murai H, Asaka J (1992) Proteolytic processing of amyloid beta protein precursor (APP) by thrombin. Biochem Biophys Res Commun 185:1000-1004.
Ignarro LJ (1990) Biosynthesis and metabolism of endothelium-derived nitric oxide. Annu Rev Pharmacol Toxicol 30:535-560.
Ikonomidou C, Turski L (2002) Why did NMDA receptor antagonists fail clinical trials for stroke and traumatic brain injury? Lancet Neurol 1:383-386.
Irani SR, Bera K, Waters P, Zuliani L, Maxwell S, Zandi MS, Friese MA, Galea I, Kullmann DM, Beeson D, Lang B, Bien CG, Vincent A (2010) N-methyl-D-aspartate antibody encephalitis: temporal progression of clinical and paraclinical observations in a predominantly non-paraneoplastic disorder of both sexes. Brain 133:1655-1667.
Ishida Y, Nagai A, Kobayashi S, Kim SU (2006) Upregulation of protease-activated receptor-1 in astrocytes in Parkinson disease: astrocyte-mediated neuroprotection through increased levels of glutathione peroxidase. J Neuropathol Exp Neurol 65:66-77.
Ishihara H, Connolly AJ, Zeng D, Kahn ML, Zheng YW, Timmons C, Tram T, Coughlin SR (1997) Protease-activated receptor 3 is a second thrombin receptor in humans. Nature 386:502-506.
Ishii T, Moriyoshi K, Sugihara H, Sakurada K, Kadotani H, Yokoi M, Akazawa C, Shigemoto R, Mizuno N, Masu M, et al. (1993) Molecular characterization of the family of the N-methyl-D-aspartate receptor subunits. J Biol Chem 268:2836-2843.
Ishikawa N, Tajima G, Hyodo S, Takahashi Y, Kobayashi M (2007) Detection of autoantibodies against NMDA-type glutamate receptor in a patient with recurrent optic neuritis and transient cerebral lesions. Neuropediatrics 38:257-260.
Izumi Y, Auberson YP, Zorumski CF (2006) Zinc modulates bidirectional hippocampal plasticity by effects on NMDA receptors. J Neurosci 26:7181-7188.
Jackson MF, Konarski JZ, Weerapura M, Czerwinski W, MacDonald JF (2006) Protein kinase C enhances glycine-insensitive desensitization of NMDA receptors

independently of previously identified protein kinase C sites. J Neurochem 96:1509-1518.
Jahr CE, Stevens CF (1987) Glutamate activates multiple single channel conductances in hippocampal neurons. Nature 325:522-525.
Jahr CE, Stevens CF (1990) A quantitative description of NMDA receptor-channel kinetic behavior. J Neurosci 10:1830-1837.
Jeffrey RA, Ch'ng TH, O'Dell TJ, Martin KC (2009) Activity-dependent anchoring of importin alpha at the synapse involves regulated binding to the cytoplasmic tail of the NR1-1a subunit of the NMDA receptor. J Neurosci 29:15613-15620.
Jin L, Miyazaki M, Mizuno S, Takigawa M, Hirose T, Nishimura K, Toida T, Williams K, Kashiwagi K, Igarashi K (2008) The pore region of N-methyl-D-aspartate receptors differentially influences stimulation and block by spermine. J Pharmacol Exp Ther 327:68-77.
Johnson JW, Kotermanski SE (2006) Mechanism of action of memantine. Curr Opin Pharmacol 6:61-67.
Jones KS, VanDongen HM, VanDongen AM (2002) The NMDA receptor M3 segment is a conserved transduction element coupling ligand binding to channel opening. J Neurosci 22:2044-2053.
Junge CE, Sugawara T, Mannaioni G, Alagarsamy S, Conn PJ, Brat DJ, Chan PH, Traynelis SF (2003) The contribution of protease-activated receptor 1 to neuronal damage caused by transient focal cerebral ischemia. Proc Natl Acad Sci U S A 100:13019-13024.
Junge CE, Lee CJ, Hubbard KB, Zhang Z, Olson JJ, Hepler JR, Brat DJ, Traynelis SF (2004) Protease-activated receptor-1 in human brain: localization and functional expression in astrocytes. Exp Neurol 188:94-103.
Kaczor AA, Kijkowska-Murak UA, Kronbach C, Unverferth K, Matosiuk D (2009) Modeling of glutamate GluR6 receptor and its interactions with novel noncompetitive antagonists. J Chem Inf Model 49:1094-1104.
Kakaç S, Kosoy B, Li D, Pramuanjaroenkij A, SpringerLink (Online service) (2010) Microfluidics Based Microsystems Fundamentals and Applications. In: NATO Science for Peace and Security Series A: Chemistry and Biology,. Dordrecht: Springer Science+Business Media B.V.
Kakegawa W, Miyazaki T, Kohda K, Matsuda K, Emi K, Motohashi J, Watanabe M, Yuzaki M (2009) The N-terminal domain of GluD2 (GluRdelta2) recruits presynaptic terminals and regulates synaptogenesis in the cerebellum in vivo. J Neurosci 29:5738-5748.
Kaku DA, Giffard RG, Choi DW (1993) Neuroprotective effects of glutamate antagonists and extracellular acidity. Science 260:1516-1518.
Kampa BM, Clements J, Jonas P, Stuart GJ (2004) Kinetics of Mg2+ unblock of NMDA receptors: implications for spike-timing dependent synaptic plasticity. J Physiol 556:337-345.
Karabiyikoglu M, Hua Y, Keep RF, Ennis SR, Xi G (2004) Intracerebral hirudin injection attenuates ischemic damage and neurologic deficits without altering local cerebral blood flow. J Cereb Blood Flow Metab 24:159-166.
Karakas E, Simorowski N, Furukawa H (2009) Structure of the zinc-bound amino-terminal domain of the NMDA receptor NR2B subunit. EMBO J 28:3910-3920.
Kashihara K, Kawada S, Takahashi Y (2009) Autoantibodies to glutamate receptor GluRepsilon2 in a patient with limbic encephalitis associated with relapsing polychondritis. J Neurol Sci 287:275-277.
Kashiwagi K, Fukuchi J, Chao J, Igarashi K, Williams K (1996) An aspartate residue in the extracellular loop of the N-methyl-D-aspartate receptor controls sensitivity to spermine and protons. Mol Pharmacol 49:1131-1141.
Kashiwagi K, Pahk AJ, Masuko T, Igarashi K, Williams K (1997) Block and modulation of N-methyl-D-aspartate receptors by polyamines and protons: role of amino acid

residues in the transmembrane and pore-forming regions of NR1 and NR2 subunits. Mol Pharmacol 52:701-713.
Katz JB, Limpanasithikul W, Diamond B (1994) Mutational analysis of an autoantibody: differential binding and pathogenicity. J Exp Med 180:925-932.
Kay AR (2003) Evidence for chelatable zinc in the extracellular space of the hippocampus, but little evidence for synaptic release of Zn. J Neurosci 23:6847-6855.
Kay AR (2006) Imaging synaptic zinc: promises and perils. Trends Neurosci 29:200-206.
Kaye SL, Sansom MS, Biggin PC (2007) In silico mutation of cysteine residues in the ligand-binding domain of an N-methyl-D-aspartate receptor. Biochemistry 46:2136-2145.
Keana JF, Kher SM, Cai SX, Dinsmore CM, Glenn AG, Guastella J, Huang JC, Ilyin V, Lu Y, Mouser PL, et al. (1995) Synthesis and structure-activity relationships of substituted 1,4-dihydroquinoxaline-2,3-diones: antagonists of N-methyl-D-aspartate (NMDA) receptor glycine sites and non-NMDA glutamate receptors. J Med Chem 38:4367-4379.
Kendrick SJ, Dichter MA, Wilcox KS (1998) Characterization of desensitization in recombinant N-methyl-D-aspartate receptors: comparison with native receptors in cultured hippocampal neurons. Brain Res Mol Brain Res 57:10-20.
Kew JN, Kemp JA (1998) An allosteric interaction between the NMDA receptor polyamine and ifenprodil sites in rat cultured cortical neurones. J Physiol 512 (Pt 1):17-28.
Kew JN, Trube G, Kemp JA (1996) A novel mechanism of activity-dependent NMDA receptor antagonism describes the effect of ifenprodil in rat cultured cortical neurones. The Journal of Physiology 497:761-772.
Kilic E, Kilic U, Bahr M, Hermann DM (2005) Tissue plasminogen activator-induced ischemic injury is reversed by NMDA antagonist MK-801 in vivo. Neurodegener Dis 2:49-55.
Kim JH, Liao D, Lau LF, Huganir RL (1998) SynGAP: a synaptic RasGAP that associates with the PSD-95/SAP90 protein family. Neuron 20:683-691.
Kim MJ, Dunah AW, Wang YT, Sheng M (2005) Differential roles of NR2A- and NR2B-containing NMDA receptors in Ras-ERK signaling and AMPA receptor trafficking. Neuron 46:745-760.
Kim WK, Choi YB, Rayudu PV, Das P, Asaad W, Arnelle DR, Stamler JS, Lipton SA (1999) Attenuation of NMDA receptor activity and neurotoxicity by nitroxyl anion, NO. Neuron 24:461-469.
Kleckner NW, Dingledine R (1988) Requirement for glycine in activation of NMDA-receptors expressed in Xenopus oocytes. Science 241:835-837.
Klee CB, Crouch TH, Krinks MH (1979) Calcineurin: a calcium- and calmodulin-binding protein of the nervous system. Proc Natl Acad Sci U S A 76:6270-6273.
Kohda K, Wang Y, Yuzaki M (2000) Mutation of a glutamate receptor motif reveals its role in gating and delta2 receptor channel properties. Nat Neurosci 3:315-322.
Kohr G, Eckardt S, Luddens H, Monyer H, Seeburg PH (1994) NMDA receptor channels: subunit-specific potentiation by reducing agents. Neuron 12:1031-1040.
Komiyama NH, Watabe AM, Carlisle HJ, Porter K, Charlesworth P, Monti J, Strathdee DJ, O'Carroll CM, Martin SJ, Morris RG, O'Dell TJ, Grant SG (2002) SynGAP regulates ERK/MAPK signaling, synaptic plasticity, and learning in the complex with postsynaptic density 95 and NMDA receptor. J Neurosci 22:9721-9732.
Kowal C, Degiorgio LA, Lee JY, Edgar MA, Huerta PT, Volpe BT, Diamond B (2006) Human lupus autoantibodies against NMDA receptors mediate cognitive impairment. Proc Natl Acad Sci U S A 103:19854-19859.
Kraut J (1977) Serine proteases: structure and mechanism of catalysis. Annu Rev Biochem 46:331-358.
Krishnaswamy S, Church WR, Nesheim ME, Mann KG (1987) Activation of human prothrombin by human prothrombinase. Influence of factor Va on the reaction mechanism. J Biol Chem 262:3291-3299.

Krupp JJ, Vissel B, Heinemann SF, Westbrook GL (1996) Calcium-dependent inactivation of recombinant N-methyl-D-aspartate receptors is NR2 subunit specific. Mol Pharmacol 50:1680-1688.
Krupp JJ, Vissel B, Heinemann SF, Westbrook GL (1998) N-terminal domains in the NR2 subunit control desensitization of NMDA receptors. Neuron 20:317-327.
Krupp JJ, Vissel B, Thomas CG, Heinemann SF, Westbrook GL (1999) Interactions of calmodulin and alpha-actinin with the NR1 subunit modulate Ca2+-dependent inactivation of NMDA receptors. J Neurosci 19:1165-1178.
Krupp JJ, Vissel B, Thomas CG, Heinemann SF, Westbrook GL (2002) Calcineurin acts via the C-terminus of NR2A to modulate desensitization of NMDA receptors. Neuropharmacology 42:593-602.
Kulagowski JJ, Baker R, Curtis NR, Leeson PD, Mawer IM, Moseley AM, Ridgill MP, Rowley M, Stansfield I, Foster AC, et al. (1994) 3'-(Arylmethyl)- and 3'-(aryloxy)-3-phenyl-4-hydroxyquinolin-2(1H)-ones: orally active antagonists of the glycine site on the NMDA receptor. J Med Chem 37:1402-1405.
Kuner T, Wollmuth LP, Karlin A, Seeburg PH, Sakmann B (1996) Structure of the NMDA receptor channel M2 segment inferred from the accessibility of substituted cysteines. Neuron 17:343-352.
Kupper J, Ascher P, Neyton J (1996) Probing the pore region of recombinant N-methyl-D-aspartate channels using external and internal magnesium block. Proc Natl Acad Sci U S A 93:8648-8653.
Kury P, Schaeren-Wiemers N, Monard D (1997) Protease nexin-1 is expressed at the mouse met-/mesencephalic junction and FGF signaling regulates its promoter activity in primary met-/mesencephalic cells. Development 124:1251-1262.
Kuryatov A, Laube B, Betz H, Kuhse J (1994) Mutational analysis of the glycine-binding site of the NMDA receptor: structural similarity with bacterial amino acid-binding proteins. Neuron 12:1291-1300.
Kuusinen A, Abele R, Madden DR, Keinanen K (1999) Oligomerization and ligand-binding properties of the ectodomain of the alpha-amino-3-hydroxy-5-methyl-4-isoxazole propionic acid receptor subunit GluRD. J Biol Chem 274:28937-28943.
Lan JY, Skeberdis VA, Jover T, Grooms SY, Lin Y, Araneda RC, Zheng X, Bennett MV, Zukin RS (2001) Protein kinase C modulates NMDA receptor trafficking and gating. Nat Neurosci 4:382-390.
Lapteva L, Nowak M, Yarboro CH, Takada K, Roebuck-Spencer T, Weickert T, Bleiberg J, Rosenstein D, Pao M, Patronas N, Steele S, Manzano M, van der Veen JW, Lipsky PE, Marenco S, Wesley R, Volpe B, Diamond B, Illei GG (2006) Anti-N-methyl-D-aspartate receptor antibodies, cognitive dysfunction, and depression in systemic lupus erythematosus. Arthritis Rheum 54:2505-2514.
Lau CG, Zukin RS (2007) NMDA receptor trafficking in synaptic plasticity and neuropsychiatric disorders. Nat Rev Neurosci 8:413-426.
Laube B, Kuhse J, Betz H (1998) Evidence for a tetrameric structure of recombinant NMDA receptors. J Neurosci 18:2954-2961.
Laube B, Kuryatov A, Kuhse J, Betz H (1993) Glycine-glutamate interactions at the NMDA receptor: role of cysteine residues. FEBS Lett 335:331-334.
Laughlin TM, Kitto KF, Wilcox GL (1999) Redox manipulation of NMDA receptors in vivo: alteration of acute pain transmission and dynorphin-induced allodynia. Pain 80:37-43.
Laurie DJ, Seeburg PH (1994a) Regional and developmental heterogeneity in splicing of the rat brain NMDAR1 mRNA. J Neurosci 14:3180-3194.
Laurie DJ, Seeburg PH (1994b) Ligand affinities at recombinant N-methyl-D-aspartate receptors depend on subunit composition. Eur J Pharmacol 268:335-345.
Layton ME, Kelly MJ, 3rd, Rodzinak KJ (2006) Recent advances in the development of NR2B subtype-selective NMDA receptor antagonists. Curr Top Med Chem 6:697-709.
Le Bonniec BF, MacGillivray RT, Esmon CT (1991) Thrombin Glu-39 restricts the P'3 specificity to nonacidic residues. J Biol Chem 266:13796-13803.

Le Bonniec BF, Guinto ER, Esmon CT (1992) Interaction of thrombin des-ETW with antithrombin III, the Kunitz inhibitors, thrombomodulin and protein C. Structural link between the autolysis loop and the Tyr-Pro-Pro-Trp insertion of thrombin. J Biol Chem 267:19341-19348.

Le Bonniec BF, Guinto ER, MacGillivray RT, Stone SR, Esmon CT (1993) The role of thrombin's Tyr-Pro-Pro-Trp motif in the interaction with fibrinogen, thrombomodulin, protein C, antithrombin III, and the Kunitz inhibitors. J Biol Chem 268:19055-19061.

Le Bonniec BF, Myles T, Johnson T, Knight CG, Tapparelli C, Stone SR (1996) Characterization of the P2' and P3' specificities of thrombin using fluorescence-quenched substrates and mapping of the subsites by mutagenesis. Biochemistry 35:7114-7122.

Leavis PC, Rosenfeld S, Lu RC (1978) Cleavage of a specific bond in troponin C by thrombin. Biochim Biophys Acta 535:281-286.

Lee CJ, Mannaioni G, Yuan H, Woo DH, Gingrich MB, Traynelis SF (2007) Astrocytic control of synaptic NMDA receptors. J Physiol 581:1057-1081.

Lee DY, Oh YJ, Jin BK (2005) Thrombin-activated microglia contribute to death of dopaminergic neurons in rat mesencephalic cultures: dual roles of mitogen-activated protein kinase signaling pathways. Glia 51:98-110.

Lee KR, Colon GP, Betz AL, Keep RF, Kim S, Hoff JT (1996) Edema from intracerebral hemorrhage: the role of thrombin. J Neurosurg 84:91-96.

Lees KR, Dyker AG, Sharma A, Ford GA, Ardron ME, Grosset DG (2001) Tolerability of the low-affinity, use-dependent NMDA antagonist AR-R15896AR in stroke patients: a dose-ranging study. Stroke 32:466-472.

Lees KR, Asplund K, Carolei A, Davis SM, Diener HC, Kaste M, Orgogozo JM, Whitehead J (2000) Glycine antagonist (gavestinel) in neuroprotection (GAIN International) in patients with acute stroke: a randomised controlled trial. GAIN International Investigators. Lancet 355:1949-1954.

Legendre P, Westbrook GL (1990) The inhibition of single N-methyl-D-aspartate-activated channels by zinc ions on cultured rat neurones. J Physiol 429:429-449.

Lei SZ, Pan ZH, Aggarwal SK, Chen HS, Hartman J, Sucher NJ, Lipton SA (1992) Effect of nitric oxide production on the redox modulatory site of the NMDA receptor-channel complex. Neuron 8:1087-1099.

Lerma J (1992) Spermine regulates N-methyl-D-aspartate receptor desensitization. Neuron 8:343-352.

Lerma J, Zukin RS, Bennett MV (1990) Glycine decreases desensitization of N-methyl-D-aspartate (NMDA) receptors expressed in Xenopus oocytes and is required for NMDA responses. Proc Natl Acad Sci U S A 87:2354-2358.

Lester RA, Jahr CE (1992) NMDA channel behavior depends on agonist affinity. J Neurosci 12:635-643.

Lester RA, Tong G, Jahr CE (1993) Interactions between the glycine and glutamate binding sites of the NMDA receptor. J Neurosci 13:1088-1096.

Lester RA, Clements JD, Westbrook GL, Jahr CE (1990) Channel kinetics determine the time course of NMDA receptor-mediated synaptic currents. Nature 346:565-567.

Leszkiewicz D, Aizenman E (2002) A role for the redox site in the modulation of the NMDA receptor by light. J Physiol 545:435-440.

Leszkiewicz DN, Kandler K, Aizenman E (2000) Enhancement of NMDA receptor-mediated currents by light in rat neurones in vitro. J Physiol 524 Pt 2:365-374.

Leuschner WD, Hoch W (1999) Subtype-specific assembly of alpha-amino-3-hydroxy-5-methyl-4-isoxazole propionic acid receptor subunits is mediated by their n-terminal domains. J Biol Chem 274:16907-16916.

Levite M, Ganor Y (2008) Autoantibodies to glutamate receptors can damage the brain in epilepsy, systemic lupus erythematosus and encephalitis. Expert Rev Neurother 8:1141-1160.

Lewczuk P, Reiber H, Ehrenreich H (1998) Prothrombin in normal human cerebrospinal fluid originates from the blood. Neurochem Res 23:1027-1030.
Li B, Otsu Y, Murphy TH, Raymond LA (2003) Developmental decrease in NMDA receptor desensitization associated with shift to synapse and interaction with postsynaptic density-95. J Neurosci 23:11244-11254.
Li JH, Wang YH, Wolfe BB, Krueger KE, Corsi L, Stocca G, Vicini S (1998a) Developmental changes in localization of NMDA receptor subunits in primary cultures of cortical neurons. Eur J Neurosci 10:1704-1715.
Li QX, Whyte S, Tanner JE, Evin G, Beyreuther K, Masters CL (1998b) Secretion of Alzheimer's disease Abeta amyloid peptide by activated human platelets. Lab Invest 78:461-469.
Li W, Johnson DJ, Esmon CT, Huntington JA (2004) Structure of the antithrombin-thrombin-heparin ternary complex reveals the antithrombotic mechanism of heparin. Nat Struct Mol Biol 11:857-862.
Li Y, Krupa B, Kang JS, Bolshakov VY, Liu G (2009) Glycine site of NMDA receptor serves as a spatiotemporal detector of synaptic activity patterns. J Neurophysiol 102:578-589.
Liao GY, Wagner DA, Hsu MH, Leonard JP (2001) Evidence for direct protein kinase-C mediated modulation of N-methyl-D-aspartate receptor current. Mol Pharmacol 59:960-964.
Lin JW, Wyszynski M, Madhavan R, Sealock R, Kim JU, Sheng M (1998) Yotiao, a novel protein of neuromuscular junction and brain that interacts with specific splice variants of NMDA receptor subunit NR1. J Neurosci 18:2017-2027.
Lipton SA (1993) Prospects for clinically tolerated NMDA antagonists: open-channel blockers and alternative redox states of nitric oxide. Trends Neurosci 16:527-532.
Lipton SA (2006) Paradigm shift in neuroprotection by NMDA receptor blockade: memantine and beyond. Nat Rev Drug Discov 5:160-170.
Lipton SA, Choi YB, Takahashi H, Zhang D, Li W, Godzik A, Bankston LA (2002) Cysteine regulation of protein function--as exemplified by NMDA-receptor modulation. Trends Neurosci 25:474-480.
Lipton SA, Choi YB, Pan ZH, Lei SZ, Chen HS, Sucher NJ, Loscalzo J, Singel DJ, Stamler JS (1993) A redox-based mechanism for the neuroprotective and neurodestructive effects of nitric oxide and related nitroso-compounds. Nature 364:626-632.
Liu X, Chen C (2008) Different roles for AMPA and NMDA receptors in transmission at the immature retinogeniculate synapse. J Neurophysiol 99:629-643.
Liu Y, Wong TP, Aarts M, Rooyakkers A, Liu L, Lai TW, Wu DC, Lu J, Tymianski M, Craig AM, Wang YT (2007) NMDA receptor subunits have differential roles in mediating excitotoxic neuronal death both in vitro and in vivo. J Neurosci 27:2846-2857.
Logan SM, Rivera FE, Leonard JP (1999) Protein kinase C modulation of recombinant NMDA receptor currents: roles for the C-terminal C1 exon and calcium ions. J Neurosci 19:974-986.
Lottenberg R, Hall JA, Blinder M, Binder EP, Jackson CM (1983) The action of thrombin on peptide p-nitroanilide substrates. Substrate selectivity and examination of hydrolysis under different reaction conditions. Biochim Biophys Acta 742:539-557.
Low CM, Wee KS (2010) New insights into the not-so-new NR3 subunits of N-methyl-D-aspartate receptor: localization, structure, and function. Mol Pharmacol 78:1-11.
Low CM, Zheng F, Lyuboslavsky P, Traynelis SF (2000) Molecular determinants of coordinated proton and zinc inhibition of N-methyl-D-aspartate NR1/NR2A receptors. Proc Natl Acad Sci U S A 97:11062-11067.
Low CM, Lyuboslavsky P, French A, Le P, Wyatte K, Thiel WH, Marchan EM, Igarashi K, Kashiwagi K, Gernert K, Williams K, Traynelis SF, Zheng F (2003) Molecular determinants of proton-sensitive N-methyl-D-aspartate receptor gating. Mol Pharmacol 63:1212-1222.

Lu WY, Jackson MF, Bai D, Orser BA, MacDonald JF (2000) In CA1 pyramidal neurons of the hippocampus protein kinase C regulates calcium-dependent inactivation of NMDA receptors. J Neurosci 20:4452-4461.

Luo J, Grammas P (2010) Endothelin-1 is elevated in Alzheimer's disease brain microvessels and is neuroprotective. J Alzheimers Dis 21:887-896.

Maccaferri G, Dingledine R (2002) Control of feedforward dendritic inhibition by NMDA receptor-dependent spike timing in hippocampal interneurons. J Neurosci 22:5462-5472.

MacDermott AB, Mayer ML, Westbrook GL, Smith SJ, Barker JL (1986) NMDA-receptor activation increases cytoplasmic calcium concentration in cultured spinal cord neurones. Nature 321:519-522.

MacDonald JF, Jackson MF, Beazely MA (2006) Hippocampal long-term synaptic plasticity and signal amplification of NMDA receptors. Crit Rev Neurobiol 18:71-84.

Madry C, Mesic I, Betz H, Laube B (2007a) The N-terminal domains of both NR1 and NR2 subunits determine allosteric Zn2+ inhibition and glycine affinity of N-methyl-D-aspartate receptors. Mol Pharmacol 72:1535-1544.

Madry C, Mesic I, Betz H, Laube B (2007b) The N-Terminal Domains of both NR1 and NR2 Subunits Determine Allosteric Zn2+ Inhibition and Glycine Affinity of N-Methyl-D-aspartate Receptors. Mol Pharmacol 72:1535-1544.

Mannaioni G, Orr AG, Hamill CE, Yuan H, Pedone KH, McCoy KL, Berlinguer Palmini R, Junge CE, Lee CJ, Yepes M, Hepler JR, Traynelis SF (2008) Plasmin potentiates synaptic N-methyl-D-aspartate receptor function in hippocampal neurons through activation of protease-activated receptor-1. J Biol Chem 283:20600-20611.

Mansuy IM, van der Putten H, Schmid P, Meins M, Botteri FM, Monard D (1993) Variable and multiple expression of Protease Nexin-1 during mouse organogenesis and nervous system development. Development 119:1119-1134.

Mao Y, Zhang M, Tuma RF, Kunapuli SP (2010) Deficiency of PAR4 attenuates cerebral ischemia/reperfusion injury in mice. J Cereb Blood Flow Metab.

Maren S, Baudry M (1995) Properties and mechanisms of long-term synaptic plasticity in the mammalian brain: relationships to learning and memory. Neurobiol Learn Mem 63:1-18.

Marinelli L, Cosconati S, Steinbrecher T, Limongelli V, Bertamino A, Novellino E, Case DA (2007) Homology modeling of NR2B modulatory domain of NMDA receptor and analysis of ifenprodil binding. ChemMedChem 2:1498-1510.

Markus R, Reutens DC, Kazui S, Read S, Wright P, Pearce DC, Tochon-Danguy HJ, Sachinidis JI, Donnan GA (2004) Hypoxic tissue in ischaemic stroke: persistence and clinical consequences of spontaneous survival. Brain 127:1427-1436.

Marque PE, Spuntarelli R, Juliano L, Aiach M, Le Bonniec BF (2000) The role of Glu(192) in the allosteric control of the S(2)' and S(3)' subsites of thrombin. J Biol Chem 275:809-816.

Martin AM, Kuhlmann C, Trossbach S, Jaeger S, Waldron E, Roebroek A, Luhmann HJ, Laatsch A, Weggen S, Lessmann V, Pietrzik CU (2008) The functional role of the second NPXY motif of the LRP1 beta-chain in tissue-type plasminogen activator-mediated activation of N-methyl-D-aspartate receptors. J Biol Chem 283:12004-12013.

Martorell L, Martinez-Gonzalez J, Rodriguez C, Gentile M, Calvayrac O, Badimon L (2008) Thrombin and protease-activated receptors (PARs) in atherothrombosis. Thromb Haemost 99:305-315.

Masada T, Xi G, Hua Y, Keep RF (2000) The effects of thrombin preconditioning on focal cerebral ischemia in rats. Brain Res 867:173-179.

Masuko T, Kashiwagi K, Kuno T, Nguyen ND, Pahk AJ, Fukuchi J, Igarashi K, Williams K (1999) A regulatory domain (R1-R2) in the amino terminus of the N-methyl-D-aspartate receptor: effects of spermine, protons, and ifenprodil, and structural similarity to bacterial leucine/isoleucine/valine binding protein. Mol Pharmacol 55:957-969.

Masuko T, Kusama-Eguchi K, Sakata K, Kusama T, Chaki S, Okuyama S, Williams K, Kashiwagi K, Igarashi K (2003) Polyamine transport, accumulation, and release in brain. J Neurochem 84:610-617.
Matsuda K, Yuzaki M (2010) Cbln1 and the Delta2 Glutamate Receptor-An Orphan Ligand and an Orphan Receptor Find Their Partners. Cerebellum.
Matsuda K, Kamiya Y, Matsuda S, Yuzaki M (2002) Cloning and characterization of a novel NMDA receptor subunit NR3B: a dominant subunit that reduces calcium permeability. Brain Res Mol Brain Res 100:43-52.
Matsuda K, Fletcher M, Kamiya Y, Yuzaki M (2003) Specific assembly with the NMDA receptor 3B subunit controls surface expression and calcium permeability of NMDA receptors. J Neurosci 23:10064-10073.
Matsuda K, Miura E, Miyazaki T, Kakegawa W, Emi K, Narumi S, Fukazawa Y, Ito-Ishida A, Kondo T, Shigemoto R, Watanabe M, Yuzaki M (2010) Cbln1 is a ligand for an orphan glutamate receptor delta2, a bidirectional synapse organizer. Science 328:363-368.
Mayer ML (2006) Glutamate receptors at atomic resolution. Nature 440:456-462.
Mayer ML, Westbrook GL (1987) Permeation and block of N-methyl-D-aspartic acid receptor channels by divalent cations in mouse cultured central neurones. J Physiol 394:501-527.
Mayer ML, Westbrook GL, Guthrie PB (1984) Voltage-dependent block by Mg2+ of NMDA responses in spinal cord neurones. Nature 309:261-263.
Mayer ML, Vyklicky L, Jr., Clements J (1989) Regulation of NMDA receptor desensitization in mouse hippocampal neurons by glycine. Nature 338:425-427.
Mayevsky A, Chance B (2007) Oxidation-reduction states of NADH in vivo: from animals to clinical use. Mitochondrion 7:330-339.
McCauley JA et al. (2004) NR2B-selective N-methyl-D-aspartate antagonists: synthesis and evaluation of 5-substituted benzimidazoles. J Med Chem 47:2089-2096.
McGee AW, Bredt DS (2003) Assembly and plasticity of the glutamatergic postsynaptic specialization. Curr Opin Neurobiol 13:111-118.
McGurk JF, Bennett MV, Zukin RS (1990) Polyamines potentiate responses of N-methyl-D-aspartate receptors expressed in xenopus oocytes. Proc Natl Acad Sci U S A 87:9971-9974.
Meddows E, Le Bourdelles B, Grimwood S, Wafford K, Sandhu S, Whiting P, McIlhinney RA (2001) Identification of molecular determinants that are important in the assembly of N-methyl-D-aspartate receptors. J Biol Chem 276:18795-18803.
Medina I, Filippova N, Charton G, Rougeole S, Ben-Ari Y, Khrestchatisky M, Bregestovski P (1995) Calcium-dependent inactivation of heteromeric NMDA receptor-channels expressed in human embryonic kidney cells. J Physiol 482 (Pt 3):567-573.
Meli R, Raso GM, Cicala C, Esposito E, Fiorino F, Cirino G (2001) Thrombin and PAR-1 activating peptide increase iNOS expression in cytokine-stimulated C6 glioma cells. J Neurochem 79:556-563.
Mhatre M, Nguyen A, Kashani S, Pham T, Adesina A, Grammas P (2004) Thrombin, a mediator of neurotoxicity and memory impairment. Neurobiol Aging 25:783-793.
Michaluk P, Mikasova L, Groc L, Frischknecht R, Choquet D, Kaczmarek L (2009) Matrix metalloproteinase-9 controls NMDA receptor surface diffusion through integrin beta1 signaling. J Neurosci 29:6007-6012.
Miglio G, Varsaldi F, Lombardi G (2005) Human T lymphocytes express N-methyl-D-aspartate receptors functionally active in controlling T cell activation. Biochem Biophys Res Commun 338:1875-1883.
Moller T, Hanisch UK, Ransom BR (2000) Thrombin-induced activation of cultured rodent microglia. J Neurochem 75:1539-1547.
Mony L, Kew JN, Gunthorpe MJ, Paoletti P (2009a) Allosteric modulators of NR2B-containing NMDA receptors: molecular mechanisms and therapeutic potential. Br J Pharmacol 157:1301-1317.

Mony L, Krzaczkowski L, Leonetti M, Le Goff A, Alarcon K, Neyton J, Bertrand H-O, Acher F, Paoletti P (2009b) Structural Basis of NR2B-Selective Antagonist Recognition by N-Methyl-D-aspartate Receptors. Mol Pharmacol 75:60-74.
Mony L, Krzaczkowski L, Leonetti M, Le Goff A, Alarcon K, Neyton J, Bertrand HO, Acher F, Paoletti P (2009c) Structural basis of NR2B-selective antagonist recognition by N-methyl-D-aspartate receptors. Mol Pharmacol 75:60-74.
Monyer H, Burnashev N, Laurie DJ, Sakmann B, Seeburg PH (1994) Developmental and regional expression in the rat brain and functional properties of four NMDA receptors. Neuron 12:529-540.
Monyer H, Sprengel R, Schoepfer R, Herb A, Higuchi M, Lomeli H, Burnashev N, Sakmann B, Seeburg PH (1992) Heteromeric NMDA receptors: molecular and functional distinction of subtypes. Science 256:1217-1221.
Moriyoshi K, Masu M, Ishii T, Shigemoto R, Mizuno N, Nakanishi S (1991) Molecular cloning and characterization of the rat NMDA receptor. Nature 354:31-37.
Mosesson MW (2005) Fibrinogen and fibrin structure and functions. J Thromb Haemost 3:1894-1904.
Mott DD, Doherty JJ, Zhang S, Washburn MS, Fendley MJ, Lyuboslavsky P, Traynelis SF, Dingledine R (1998) Phenylethanolamines inhibit NMDA receptors by enhancing proton inhibition. Nat Neurosci 1:659-667.
Mulligan LP, Rosenblatt DE, Toms R, Johnson D (1991) Protease nexin-1 activity in cultured Schwann cells. Neurosci Lett 128:42-46.
Nahum-Levy R, Lipinski D, Shavit S, Benveniste M (2001) Desensitization of NMDA receptor channels is modulated by glutamate agonists. Biophys J 80:2152-2166.
Nahum-Levy R, Tam E, Shavit S, Benveniste M (2002) Glutamate but not glycine agonist affinity for NMDA receptors is influenced by small cations. J Neurosci 22:2550-2560.
Nakanishi S (1992) Molecular diversity of glutamate receptors and implications for brain function. Science 258:597-603.
Nesheim ME, Taswell JB, Mann KG (1979) The contribution of bovine Factor V and Factor Va to the activity of prothrombinase. J Biol Chem 254:10952-10962.
Ng FM, Soh W, Geballe MT, Low CM (2007) Improving solubility of NR2B amino-terminal domain of N-methyl-d-aspartate receptor expressed in Escherichia coli. Biochem Biophys Res Commun 362:69-74.
Niclou S, Suidan HS, Brown-Luedi M, Monard D (1994) Expression of the thrombin receptor mRNA in rat brain. Cell Mol Biol (Noisy-le-grand) 40:421-428.
Niclou SP, Suidan HS, Pavlik A, Vejsada R, Monard D (1998) Changes in the expression of protease-activated receptor 1 and protease nexin-1 mRNA during rat nervous system development and after nerve lesion. Eur J Neurosci 10:1590-1607.
Nicole O, Docagne F, Ali C, Margaill I, Carmeliet P, MacKenzie ET, Vivien D, Buisson A (2001) The proteolytic activity of tissue-plasminogen activator enhances NMDA receptor-mediated signaling. Nat Med 7:59-64.
Nicole O, Goldshmidt A, Hamill CE, Sorensen SD, Sastre A, Lyuboslavsky P, Hepler JR, McKeon RJ, Traynelis SF (2005) Activation of protease-activated receptor-1 triggers astrogliosis after brain injury. J Neurosci 25:4319-4329.
Nikam SS, Meltzer LT (2002) NR2B selective NMDA receptor antagonists. Curr Pharm Des 8:845-855.
Nimmrich V, Szabo R, Nyakas C, Granic I, Reymann KG, Schroder UH, Gross G, Schoemaker H, Wicke K, Moller A, Luiten P (2008) Inhibition of Calpain Prevents N-Methyl-D-aspartate-Induced Degeneration of the Nucleus Basalis and Associated Behavioral Dysfunction. J Pharmacol Exp Ther 327:343-352.
Nishi M, Hinds H, Lu HP, Kawata M, Hayashi Y (2001) Motoneuron-specific expression of NR3B, a novel NMDA-type glutamate receptor subunit that works in a dominant-negative manner. J Neurosci 21:RC185.
Niswender CM, Conn PJ (2010) Metabotropic glutamate receptors: physiology, pharmacology, and disease. Annu Rev Pharmacol Toxicol 50:295-322.

Nong Y, Huang YQ, Ju W, Kalia LV, Ahmadian G, Wang YT, Salter MW (2003) Glycine binding primes NMDA receptor internalization. Nature 422:302-307.
Norris EH, Strickland S (2007) Modulation of NR2B-regulated contextual fear in the hippocampus by the tissue plasminogen activator system. Proc Natl Acad Sci U S A 104:13473-13478.
Nowak L, Bregestovski P, Ascher P, Herbet A, Prochiantz A (1984) Magnesium gates glutamate-activated channels in mouse central neurones. Nature 307:462-465.
Okabe S, Miwa A, Okado H (1999) Alternative splicing of the C-terminal domain regulates cell surface expression of the NMDA receptor NR1 subunit. J Neurosci 19:7781-7792.
Olson EE, Lyuboslavsky P, Traynelis SF, McKeon RJ (2004) PAR-1 deficiency protects against neuronal damage and neurologic deficits after unilateral cerebral hypoxia/ischemia. J Cereb Blood Flow Metab 24:964-971.
Omdal R, Brokstad K, Waterloo K, Koldingsnes W, Jonsson R, Mellgren SI (2005) Neuropsychiatric disturbances in SLE are associated with antibodies against NMDA receptors. Eur J Neurol 12:392-398.
Orgogozo JM, Rigaud AS, Stoffler A, Mobius HJ, Forette F (2002) Efficacy and safety of memantine in patients with mild to moderate vascular dementia: a randomized, placebo-controlled trial (MMM 300). Stroke 33:1834-1839.
Ossovskaya VS, Bunnett NW (2004) Protease-activated receptors: contribution to physiology and disease. Physiol Rev 84:579-621.
Overall CM, Blobel CP (2007) In search of partners: linking extracellular proteases to substrates. Nat Rev Mol Cell Biol 8:245-257.
Paoletti P, Neyton J (2007) NMDA receptor subunits: function and pharmacology. Curr Opin Pharmacol 7:39-47.
Paoletti P, Ascher P, Neyton J (1997) High-affinity zinc inhibition of NMDA NR1-NR2A receptors. J Neurosci 17:5711-5725.
Paoletti P, Perin-Dureau F, Fayyazuddin A, Le Goff A, Callebaut I, Neyton J (2000) Molecular organization of a zinc binding n-terminal modulatory domain in a NMDA receptor subunit. Neuron 28:911-925.
Pauly T, Ratliff M, Pietrowski E, Neugebauer R, Schlicksupp A, Kirsch J, Kuhse J (2008) Activity-dependent shedding of the NMDA receptor glycine binding site by matrix metalloproteinase 3: a PUTATIVE mechanism of postsynaptic plasticity. PLoS One 3:e2681.
Pawlak R, Melchor JP, Matys T, Skrzypiec AE, Strickland S (2005a) Ethanol-withdrawal seizures are controlled by tissue plasminogen activator via modulation of NR2B-containing NMDA receptors. Proc Natl Acad Sci U S A 102:443-448.
Pawlak R, Rao BS, Melchor JP, Chattarji S, McEwen B, Strickland S (2005b) Tissue plasminogen activator and plasminogen mediate stress-induced decline of neuronal and cognitive functions in the mouse hippocampus. Proc Natl Acad Sci U S A 102:18201-18206.
Pechik I, Madrazo J, Mosesson MW, Hernandez I, Gilliland GL, Medved L (2004) Crystal structure of the complex between thrombin and the central "E" region of fibrin. Proc Natl Acad Sci U S A 101:2718-2723.
Perez-Otano I, Schulteis CT, Contractor A, Lipton SA, Trimmer JS, Sucher NJ, Heinemann SF (2001) Assembly with the NR1 subunit is required for surface expression of NR3A-containing NMDA receptors. J Neurosci 21:1228-1237.
Perez-Otano I, Lujan R, Tavalin SJ, Plomann M, Modregger J, Liu XB, Jones EG, Heinemann SF, Lo DC, Ehlers MD (2006) Endocytosis and synaptic removal of NR3A-containing NMDA receptors by PACSIN1/syndapin1. Nat Neurosci 9:611-621.
Perin-Dureau F, Rachline J, Neyton J, Paoletti P (2002a) Mapping the Binding Site of the Neuroprotectant Ifenprodil on NMDA Receptors. J Neurosci 22:5955-5965.
Perin-Dureau F, Rachline J, Neyton J, Paoletti P (2002b) Mapping the binding site of the neuroprotectant ifenprodil on NMDA receptors. J Neurosci 22:5955-5965.

Petrassi HM, Williams JA, Li J, Tumanut C, Ek J, Nakai T, Masick B, Backes BJ, Harris JL (2005) A strategy to profile prime and non-prime proteolytic substrate specificity. Bioorg Med Chem Lett 15:3162-3166.

Pike CJ, Vaughan PJ, Cunningham DD, Cotman CW (1996) Thrombin attenuates neuronal cell death and modulates astrocyte reactivity induced by beta-amyloid in vitro. J Neurochem 66:1374-1382.

Pike RN, Buckle AM, le Bonniec BF, Church FC (2005) Control of the coagulation system by serpins. Getting by with a little help from glycosaminoglycans. FEBS J 272:4842-4851.

Pina-Crespo JC, Talantova M, Micu I, States B, Chen HS, Tu S, Nakanishi N, Tong G, Zhang D, Heinemann SF, Zamponi GW, Stys PK, Lipton SA (2010) Excitatory glycine responses of CNS myelin mediated by NR1/NR3 "NMDA" receptor subunits. J Neurosci 30:11501-11505.

Pinard E, Alanine A, Bourson A, Buttelmann B, Heitz M, Mutela Ramanjit Gill V, Trube G, Wyler R (2002) 4-Aminoquinolines as a novel class of NR1/2B subtype selective NMDA receptor antagonists. Bioorg Med Chem Lett 12:2615-2619.

Planells-Cases R, Montoliu C, Humet M, Fernandez AM, Garcia-Martinez C, Valera E, Merino JM, Perez-Paya E, Messeguer A, Felipo V, Ferrer-Montiel A (2002) A novel N-methyl-D-aspartate receptor open channel blocker with in vivo neuroprotectant activity. J Pharmacol Exp Ther 302:163-173.

Popescu G, Auerbach A (2003) Modal gating of NMDA receptors and the shape of their synaptic response. Nat Neurosci 6:476-483.

Popescu G, Robert A, Howe JR, Auerbach A (2004) Reaction mechanism determines NMDA receptor response to repetitive stimulation. Nature 430:790-793.

Premkumar LS, Auerbach A (1996) Identification of a high affinity divalent cation binding site near the entrance of the NMDA receptor channel. Neuron 16:869-880.

Premkumar LS, Auerbach A (1997) Stoichiometry of recombinant N-methyl-D-aspartate receptor channels inferred from single-channel current patterns. J Gen Physiol 110:485-502.

Prybylowski K, Wenthold RJ (2004) N-Methyl-D-aspartate receptors: subunit assembly and trafficking to the synapse. J Biol Chem 279:9673-9676.

Prybylowski K, Chang K, Sans N, Kan L, Vicini S, Wenthold RJ (2005) The synaptic localization of NR2B-containing NMDA receptors is controlled by interactions with PDZ proteins and AP-2. Neuron 47:845-857.

Qiu S, Zhang XM, Cao JY, Yang W, Yan YG, Shan L, Zheng J, Luo JH (2009) An endoplasmic reticulum retention signal located in the extracellular amino-terminal domain of the NR2A subunit of N-Methyl-D-aspartate receptors. J Biol Chem 284:20285-20298.

Quesada O, Hirsch J, Ben-Ari Y, Bernard C (1996) Redox sites of NMDA receptors can modulate epileptiform activity in hippocampal slices from kainic acid-treated rats. Neurosci Lett 212:171-174.

Rachline J, Perin-Dureau F, Le Goff A, Neyton J, Paoletti P (2005) The micromolar zinc-binding domain on the NMDA receptor subunit NR2B. J Neurosci 25:308-317.

Rajesh Singh R, Chang JY (2003) Structural stability of human alpha-thrombin studied by disulfide reduction and scrambling. Biochim Biophys Acta 1651:85-92.

Rambhadran A, Gonzalez J, Jayaraman V (2010) Subunit arrangement in NMDA receptors. J Biol Chem.

Ransom RW, Deschenes NL (1990) Polyamines regulate glycine interaction with the N-methyl-D-aspartate receptor. Synapse 5:294-298.

Rao A, Kim E, Sheng M, Craig AM (1998) Heterogeneity in the molecular composition of excitatory postsynaptic sites during development of hippocampal neurons in culture. J Neurosci 18:1217-1229.

Regalado MP, Villarroel A, Lerma J (2001) Intersubunit cooperativity in the NMDA receptor. Neuron 32:1085-1096.

Reisberg B, Doody R, Stoffler A, Schmitt F, Ferris S, Mobius HJ (2003) Memantine in moderate-to-severe Alzheimer's disease. N Engl J Med 348:1333-1341.
Ren H, Honse Y, Karp BJ, Lipsky RH, Peoples RW (2003) A site in the fourth membrane-associated domain of the N-methyl-D-aspartate receptor regulates desensitization and ion channel gating. J Biol Chem 278:276-283.
Rezaie AR, Olson ST (1997) Contribution of lysine 60f to S1' specificity of thrombin. Biochemistry 36:1026-1033.
Riek-Burchardt M, Striggow F, Henrich-Noack P, Reiser G, Reymann KG (2002) Increase of prothrombin-mRNA after global cerebral ischemia in rats, with constant expression of protease nexin-1 and protease-activated receptors. Neurosci Lett 329:181-184.
Roche KW, Standley S, McCallum J, Dune Ly C, Ehlers MD, Wenthold RJ (2001) Molecular determinants of NMDA receptor internalization. Nat Neurosci 4:794-802.
Rock DM, Macdonald RL (1992a) The polyamine spermine has multiple actions on N-methyl-D-aspartate receptor single-channel currents in cultured cortical neurons. Mol Pharmacol 41:83-88.
Rock DM, MacDonald RL (1992b) Spermine and related polyamines produce a voltage-dependent reduction of N-methyl-D-aspartate receptor single-channel conductance. Mol Pharmacol 42:157-164.
Rock DM, Macdonald RL (1995) Polyamine regulation of N-methyl-D-aspartate receptor channels. Annu Rev Pharmacol Toxicol 35:463-482.
Rogers SW, Hughes TE, Hollmann M, Gasic GP, Deneris ES, Heinemann S (1991) The characterization and localization of the glutamate receptor subunit GluR1 in the rat brain. J Neurosci 11:2713-2724.
Rong Y, Lu X, Bernard A, Khrestchatisky M, Baudry M (2001) Tyrosine phosphorylation of ionotropic glutamate receptors by Fyn or Src differentially modulates their susceptibility to calpain and enhances their binding to spectrin and PSD-95. J Neurochem 79:382-390.
Rosenmund C, Feltz A, Westbrook GL (1995) Calcium-dependent inactivation of synaptic NMDA receptors in hippocampal neurons. J Neurophysiol 73:427-430.
Rumbaugh G, Prybylowski K, Wang JF, Vicini S (2000) Exon 5 and spermine regulate deactivation of NMDA receptor subtypes. J Neurophysiol 83:1300-1306.
Russi P, Alesiani M, Lombardi G, Davolio P, Pellicciari R, Moroni F (1992) Nicotinylalanine increases the formation of kynurenic acid in the brain and antagonizes convulsions. J Neurochem 59:2076-2080.
Russo C, Dolcini V, Salis S, Venezia V, Zambrano N, Russo T, Schettini G (2002) Signal transduction through tyrosine-phosphorylated C-terminal fragments of amyloid precursor protein via an enhanced interaction with Shc/Grb2 adaptor proteins in reactive astrocytes of Alzheimer's disease brain. J Biol Chem 277:35282-35288.
Rycroft BK, Gibb AJ (2004) Regulation of single NMDA receptor channel activity by alpha-actinin and calmodulin in rat hippocampal granule cells. J Physiol 557:795-808.
Saenger AK, Christenson RH (2010) Stroke biomarkers: progress and challenges for diagnosis, prognosis, differentiation, and treatment. Clin Chem 56:21-33.
Samson AL, Nevin ST, Croucher D, Niego B, Daniel PB, Weiss TW, Moreno E, Monard D, Lawrence DA, Medcalf RL (2008) Tissue-type plasminogen activator requires a co-receptor to enhance NMDA receptor function. J Neurochem 107:1091-1101.
Saucan L, Palade GE (1994) Membrane and secretory proteins are transported from the Golgi complex to the sinusoidal plasmalemma of hepatocytes by distinct vesicular carriers. J Cell Biol 125:733-741.
Seeger MA, von Ballmoos C, Eicher T, Brandstatter L, Verrey F, Diederichs K, Pos KM (2008) Engineered disulfide bonds support the functional rotation mechanism of multidrug efflux pump AcrB. Nat Struct Mol Biol 15:199-205.
Seegers WH (1962) Prothrombin. Cambridge, Mass.,: Published for the Commonwealth Fund by Harvard University Press.
Serejskaya AA, Zubak SV, Osadchuk TW, Serebryani SB (1983) Enzymic activity of thrombin with partially reduced disulfide bonds. Thromb Res 32:147-154.

Sessoms-Sikes S, Honse Y, Lovinger DM, Colbran RJ (2005) CaMKIIalpha enhances the desensitization of NR2B-containing NMDA receptors by an autophosphorylation-dependent mechanism. Mol Cell Neurosci 29:139-147.

Sharma TA, Reynolds IJ (1999) Characterization of the effects of polyamines on [125I]MK-801 binding to recombinant N-methyl-D-aspartate receptors. J Pharmacol Exp Ther 289:1041-1047.

Sharp F, Liu DZ, Zhan X, Ander BP (2008) Intracerebral hemorrhage injury mechanisms: glutamate neurotoxicity, thrombin, and Src. Acta Neurochir Suppl 105:43-46.

Sheehan JP, Sadler JE (1994) Molecular mapping of the heparin-binding exosite of thrombin. Proc Natl Acad Sci U S A 91:5518-5522.

Shefner R, Kleiner G, Turken A, Papazian L, Diamond B (1991) A novel class of anti-DNA antibodies identified in BALB/c mice. J Exp Med 173:287-296.

Sheinin A, Shavit S, Benveniste M (2001) Subunit specificity and mechanism of action of NMDA partial agonist D-cycloserine. Neuropharmacology 41:151-158.

Sheng M, Pak DT (2000) Ligand-gated ion channel interactions with cytoskeletal and signaling proteins. Annu Rev Physiol 62:755-778.

Sheng M, Cummings J, Roldan LA, Jan YN, Jan LY (1994) Changing subunit composition of heteromeric NMDA receptors during development of rat cortex. Nature 368:144-147.

Shi H, Liu KJ (2006) Effects of glucose concentration on redox status in rat primary cortical neurons under hypoxia. Neurosci Lett 410:57-61.

Shigetomi E, Bowser DN, Sofroniew MV, Khakh BS (2008) Two forms of astrocyte calcium excitability have distinct effects on NMDA receptor-mediated slow inward currents in pyramidal neurons. J Neurosci 28:6659-6663.

Shikamoto Y, Morita T (1999) Expression of factor X in both the rat brain and cells of the central nervous system. FEBS Lett 463:387-389.

Shleper M, Kartvelishvily E, Wolosker H (2005) D-serine is the dominant endogenous coagonist for NMDA receptor neurotoxicity in organotypic hippocampal slices. J Neurosci 25:9413-9417.

Simpkins KL, Guttmann RP, Dong Y, Chen Z, Sokol S, Neumar RW, Lynch DR (2003) Selective activation induced cleavage of the NR2B subunit by calpain. J Neurosci 23:11322-11331.

Sinnreich M, Meins M, Niclou SP, Suidan HS, Monard D (2004) Prothrombin overexpressed in post-natal neurones requires blood factors for activation in the mouse brain. J Neurochem 88:1380-1388.

Smirnova IV, Salazar A, Arnold PM, Glatt S, Handler M, Festoff BW (1997) Thrombin and its precursor in human cerebrospinal fluid. Thromb Haemost 78:1473-1479.

Smirnova IV, Ma JY, Citron BA, Ratzlaff KT, Gregory EJ, Akaaboune M, Festoff BW (1996) Neural thrombin and protease nexin I kinetics after murine peripheral nerve injury. J Neurochem 67:2188-2199.

Sobolevsky AI, Rooney L, Wollmuth LP (2002a) Staggering of subunits in NMDAR channels. Biophys J 83:3304-3314.

Sobolevsky AI, Beck C, Wollmuth LP (2002b) Molecular rearrangements of the extracellular vestibule in NMDAR channels during gating. Neuron 33:75-85.

Sobolevsky AI, Rosconi MP, Gouaux E (2009) X-ray structure, symmetry and mechanism of an AMPA-subtype glutamate receptor. Nature 462:745-756.

Sokolova E, Reiser G (2008) Prothrombin/thrombin and the thrombin receptors PAR-1 and PAR-4 in the brain: localization, expression and participation in neurodegenerative diseases. Thromb Haemost 100:576-581.

Sonder SA, Fenton JW, 2nd (1986) Thrombin specificity with tripeptide chromogenic substrates: comparison of human and bovine thrombins with and without fibrinogen clotting activities. Clin Chem 32:934-937.

Sornarajah L, Vasuta OC, Zhang L, Sutton C, Li B, El-Husseini A, Raymond LA (2008) NMDA receptor desensitization regulated by direct binding to PDZ1-2 domains of PSD-95. J Neurophysiol 99:3052-3062.

Sorokina EG, Semenova Zh B, Bazarnaya NA, Meshcheryakov SV, Reutov VP, Goryunova AV, Pinelis VG, Granstrem OK, Roshal LM (2009) Autoantibodies to glutamate receptors and products of nitric oxide metabolism in serum in children in the acute phase of craniocerebral trauma. Neurosci Behav Physiol 39:329-334.

Spruston N, Jonas P, Sakmann B (1995) Dendritic glutamate receptor channels in rat hippocampal CA3 and CA1 pyramidal neurons. J Physiol 482 (Pt 2):325-352.

Standaert DG, Testa CM, Young AB, Penney JB, Jr. (1994) Organization of N-methyl-D-aspartate glutamate receptor gene expression in the basal ganglia of the rat. J Comp Neurol 343:1-16.

Standley S, Roche KW, McCallum J, Sans N, Wenthold RJ (2000) PDZ domain suppression of an ER retention signal in NMDA receptor NR1 splice variants. Neuron 28:887-898.

Steinhoff M, Buddenkotte J, Shpacovitch V, Rattenholl A, Moormann C, Vergnolle N, Luger TA, Hollenberg MD (2005) Proteinase-activated receptors: transducers of proteinase-mediated signaling in inflammation and immune response. Endocr Rev 26:1-43.

Stern-Bach Y, Bettler B, Hartley M, Sheppard PO, O'Hara PJ, Heinemann SF (1994) Agonist selectivity of glutamate receptors is specified by two domains structurally related to bacterial amino acid-binding proteins. Neuron 13:1345-1357.

Stern P, Behe P, Schoepfer R, Colquhoun D (1992) Single-channel conductances of NMDA receptors expressed from cloned cDNAs: comparison with native receptors. Proc Biol Sci 250:271-277.

Stern P, Cik M, Colquhoun D, Stephenson FA (1994) Single channel properties of cloned NMDA receptors in a human cell line: comparison with results from Xenopus oocytes. J Physiol 476:391-397.

Steup-Beekman G, Steens S, van Buchem M, Huizinga T (2007) Anti-NMDA receptor autoantibodies in patients with systemic lupus erythematosus and their first-degree relatives. Lupus 16:329-334.

Striggow F, Riek M, Breder J, Henrich-Noack P, Reymann KG, Reiser G (2000) The protease thrombin is an endogenous mediator of hippocampal neuroprotection against ischemia at low concentrations but causes degeneration at high concentrations. Proc Natl Acad Sci U S A 97:2264-2269.

Sucher NJ, Akbarian S, Chi CL, Leclerc CL, Awobuluyi M, Deitcher DL, Wu MK, Yuan JP, Jones EG, Lipton SA (1995) Developmental and regional expression pattern of a novel NMDA receptor-like subunit (NMDAR-L) in the rodent brain. J Neurosci 15:6509-6520.

Sullivan JM, Traynelis SF, Chen HS, Escobar W, Heinemann SF, Lipton SA (1994) Identification of two cysteine residues that are required for redox modulation of the NMDA subtype of glutamate receptor. Neuron 13:929-936.

Sun L, Margolis FL, Shipley MT, Lidow MS (1998) Identification of a long variant of mRNA encoding the NR3 subunit of the NMDA receptor: its regional distribution and developmental expression in the rat brain. FEBS Lett 441:392-396.

Suo Z, Wu M, Citron BA, Palazzo RE, Festoff BW (2003) Rapid tau aggregation and delayed hippocampal neuronal death induced by persistent thrombin signaling. J Biol Chem 278:37681-37689.

Suo Z, Wu M, Ameenuddin S, Anderson HE, Zoloty JE, Citron BA, Andrade-Gordon P, Festoff BW (2002) Participation of protease-activated receptor-1 in thrombin-induced microglial activation. J Neurochem 80:655-666.

Swartz KJ, During MJ, Freese A, Beal MF (1990) Cerebral synthesis and release of kynurenic acid: an endogenous antagonist of excitatory amino acid receptors. J Neurosci 10:2965-2973.

Swartz KJ, Koroshetz WJ, Rees AH, Huettner JE (1992) Competitive antagonism of glutamate receptor channels by substituted benzazepines in cultured cortical neurons. Mol Pharmacol 41:1130-1141.

Szklarczyk A, Ewaleifoh O, Beique JC, Wang Y, Knorr D, Haughey N, Malpica T, Mattson MP, Huganir R, Conant K (2008) MMP-7 cleaves the NR1 NMDA receptor subunit and modifies NMDA receptor function. FASEB J 22:3757-3767.

Szydlowska K, Tymianski M (2010) Calcium, ischemia and excitotoxicity. Cell Calcium 47:122-129.

Takahashi H, Shin Y, Cho SJ, Zago WM, Nakamura T, Gu Z, Ma Y, Furukawa H, Liddington R, Zhang D, Tong G, Chen HS, Lipton SA (2007) Hypoxia enhances S-nitrosylation-mediated NMDA receptor inhibition via a thiol oxygen sensor motif. Neuron 53:53-64.

Takahashi Y, Mori H, Mishina M, Watanabe M, Kondo N, Shimomura J, Kubota Y, Matsuda K, Fukushima K, Shiroma N, Akasaka N, Nishida H, Imamura A, Watanabe H, Sugiyama N, Ikezawa M, Fujiwara T (2005) Autoantibodies and cell-mediated autoimmunity to NMDA-type GluRepsilon2 in patients with Rasmussen's encephalitis and chronic progressive epilepsia partialis continua. Epilepsia 46 Suppl 5:152-158.

Takasu MA, Dalva MB, Zigmond RE, Greenberg ME (2002) Modulation of NMDA receptor-dependent calcium influx and gene expression through EphB receptors. Science 295:491-495.

Tanaka K, Dora E, Greenberg JH, Reivich M (1986) Cerebral glucose metabolism during the recovery period after ischemia--its relationship to NADH-fluorescence, blood flow, EcoG and histology. Stroke 17:994-1004.

Tang CM, Dichter M, Morad M (1990) Modulation of the N-methyl-D-aspartate channel by extracellular H+. Proc Natl Acad Sci U S A 87:6445-6449.

Tang LH, Aizenman E (1993) The modulation of N-methyl-D-aspartate receptors by redox and alkylating reagents in rat cortical neurones in vitro. J Physiol 465:303-323.

Tariot PN, Farlow MR, Grossberg GT, Graham SM, McDonald S, Gergel I (2004) Memantine treatment in patients with moderate to severe Alzheimer disease already receiving donepezil: a randomized controlled trial. JAMA 291:317-324.

Taverna F, Xiong ZG, Brandes L, Roder JC, Salter MW, MacDonald JF (2000) The Lurcher mutation of an alpha-amino-3-hydroxy-5-methyl- 4-isoxazolepropionic acid receptor subunit enhances potency of glutamate and converts an antagonist to an agonist. J Biol Chem 275:8475-8479.

Thevenet J, Angelillo-Scherrer A, Price M, Hirt L (2009) Coagulation factor Xa activates thrombin in ischemic neural tissue. J Neurochem 111:828-836.

Thomson AM, Walker VE, Flynn DM (1989) Glycine enhances NMDA-receptor mediated synaptic potentials in neocortical slices. Nature 338:422-424.

Tingley WG, Roche KW, Thompson AK, Huganir RL (1993) Regulation of NMDA receptor phosphorylation by alternative splicing of the C-terminal domain. Nature 364:70-73.

Tong G, Jahr CE (1994) Regulation of glycine-insensitive desensitization of the NMDA receptor in outside-out patches. J Neurophysiol 72:754-761.

Tong G, Shepherd D, Jahr CE (1995) Synaptic desensitization of NMDA receptors by calcineurin. Science 267:1510-1512.

Tong G, Takahashi H, Tu S, Shin Y, Talantova M, Zago W, Xia P, Nie Z, Goetz T, Zhang D, Lipton SA, Nakanishi N (2008) Modulation of NMDA receptor properties and synaptic transmission by the NR3A subunit in mouse hippocampal and cerebrocortical neurons. J Neurophysiol 99:122-132.

Tovar KR, Westbrook GL (1999) The incorporation of NMDA receptors with a distinct subunit composition at nascent hippocampal synapses in vitro. J Neurosci 19:4180-4188.

Traynelis SF, Cull-Candy SG (1990) Proton inhibition of N-methyl-D-aspartate receptors in cerebellar neurons. Nature 345:347-350.

Traynelis SF, Hartley M, Heinemann SF (1995) Control of proton sensitivity of the NMDA receptor by RNA splicing and polyamines. Science 268:873-876.

Traynelis SF, Burgess MF, Zheng F, Lyuboslavsky P, Powers JL (1998) Control of voltage-independent zinc inhibition of NMDA receptors by the NR1 subunit. J Neurosci 18:6163-6175.

Tsiang M, Jain AK, Dunn KE, Rojas ME, Leung LL, Gibbs CS (1995) Functional mapping of the surface residues of human thrombin. J Biol Chem 270:16854-16863.

Tu W, Xu X, Peng L, Zhong X, Zhang W, Soundarapandian MM, Balel C, Wang M, Jia N, Lew F, Chan SL, Chen Y, Lu Y (2010) DAPK1 interaction with NMDA receptor NR2B subunits mediates brain damage in stroke. Cell 140:222-234.

Turgeon VL, Houenou LJ (1997) The role of thrombin-like (serine) proteases in the development, plasticity and pathology of the nervous system. Brain Res Brain Res Rev 25:85-95.

Turgeon VL, Lloyd ED, Wang S, Festoff BW, Houenou LJ (1998) Thrombin perturbs neurite outgrowth and induces apoptotic cell death in enriched chick spinal motoneuron cultures through caspase activation. J Neurosci 18:6882-6891.

Ulbrich MH, Isacoff EY (2008) Rules of engagement for NMDA receptor subunits. Proc Natl Acad Sci U S A 105:14163-14168.

van Zundert B, Yoshii A, Constantine-Paton M (2004) Receptor compartmentalization and trafficking at glutamate synapses: a developmental proposal. Trends Neurosci 27:428-437.

Vanderklish P, Saido TC, Gall C, Arai A, Lynch G (1995) Proteolysis of spectrin by calpain accompanies theta-burst stimulation in cultured hippocampal slices. Brain Res Mol Brain Res 32:25-35.

Vargas-Caballero M, Robinson HP (2003) A slow fraction of Mg2+ unblock of NMDA receptors limits their contribution to spike generation in cortical pyramidal neurons. J Neurophysiol 89:2778-2783.

Vargas-Caballero M, Robinson HP (2004) Fast and slow voltage-dependent dynamics of magnesium block in the NMDA receptor: the asymmetric trapping block model. J Neurosci 24:6171-6180.

Vaughan PJ, Su J, Cotman CW, Cunningham DD (1994) Protease nexin-1, a potent thrombin inhibitor, is reduced around cerebral blood vessels in Alzheimer's disease. Brain Res 668:160-170.

Vaughan PJ, Pike CJ, Cotman CW, Cunningham DD (1995) Thrombin receptor activation protects neurons and astrocytes from cell death produced by environmental insults. J Neurosci 15:5389-5401.

Vicini S, Wang JF, Li JH, Zhu WJ, Wang YH, Luo JH, Wolfe BB, Grayson DR (1998) Functional and pharmacological differences between recombinant N-methyl-D-aspartate receptors. J Neurophysiol 79:555-566.

Villarroel A, Regalado MP, Lerma J (1998) Glycine-independent NMDA receptor desensitization: localization of structural determinants. Neuron 20:329-339.

Vinade L, Petersen JD, Do K, Dosemeci A, Reese TS (2001) Activation of calpain may alter the postsynaptic density structure and modulate anchoring of NMDA receptors. Synapse 40:302-309.

Vissel B, Krupp JJ, Heinemann SF, Westbrook GL (2001) A use-dependent tyrosine dephosphorylation of NMDA receptors is independent of ion flux. Nat Neurosci 4:587-596.

Vissel B, Krupp JJ, Heinemann SF, Westbrook GL (2002) Intracellular domains of NR2 alter calcium-dependent inactivation of N-methyl-D-aspartate receptors. Mol Pharmacol 61:595-605.

Vogt K, Mellor J, Tong G, Nicoll R (2000) The actions of synaptically released zinc at hippocampal mossy fiber synapses. Neuron 26:187-196.

Vyklicky L, Jr. (1993) Calcium-mediated modulation of N-methyl-D-aspartate (NMDA) responses in cultured rat hippocampal neurones. J Physiol 470:575-600.

Vyklicky L, Jr., Benveniste M, Mayer ML (1990) Modulation of N-methyl-D-aspartic acid receptor desensitization by glycine in mouse cultured hippocampal neurones. J Physiol 428:313-331.

Wang C, Wang HG, Xie H, Pitt GS (2008) Ca2+/CaM controls Ca2+-dependent inactivation of NMDA receptors by dimerizing the NR1 C termini. J Neurosci 28:1865-1870.
Wang CX, Yang T, Shuaib A (2001) An improved version of embolic model of brain ischemic injury in the rat. J Neurosci Methods 109:147-151.
Wang H, Ubl JJ, Reiser G (2002a) Four subtypes of protease-activated receptors, co-expressed in rat astrocytes, evoke different physiological signaling. Glia 37:53-63.
Wang H, Ubl JJ, Stricker R, Reiser G (2002b) Thrombin (PAR-1)-induced proliferation in astrocytes via MAPK involves multiple signaling pathways. Am J Physiol Cell Physiol 283:C1351-1364.
Wang X, Xu L, Wang H, Grzanna R, Zhan Y, Knabb RM, Luettgen JM, Bozarth TA, Galemmo RA, Wong PC, Bernard R, Vargas H, Chopp M, Friedman SM, Feuerstein GZ (2003) Inhibition of factor Xa reduces ischemic brain damage after thromboembolic stroke in rats. Stroke 34:468-474.
Wang Y, Luo W, Reiser G (2007) Activation of protease-activated receptors in astrocytes evokes a novel neuroprotective pathway through release of chemokines of the growth-regulated oncogene/cytokine-induced neutrophil chemoattractant family. Eur J Neurosci 26:3159-3168.
Wang YT, Salter MW (1994) Regulation of NMDA receptors by tyrosine kinases and phosphatases. Nature 369:233-235.
Warach S, Kaufman D, Chiu D, Devlin T, Luby M, Rashid A, Clayton L, Kaste M, Lees KR, Sacco R, Fisher M (2006) Effect of the Glycine Antagonist Gavestinel on cerebral infarcts in acute stroke patients, a randomized placebo-controlled trial: The GAIN MRI Substudy. Cerebrovasc Dis 21:106-111.
Washbourne P, Liu XB, Jones EG, McAllister AK (2004) Cycling of NMDA receptors during trafficking in neurons before synapse formation. J Neurosci 24:8253-8264.
Wee KS, Zhang Y, Khanna S, Low CM (2008) Immunolocalization of NMDA receptor subunit NR3B in selected structures in the rat forebrain, cerebellum, and lumbar spinal cord. J Comp Neurol 509:118-135.
Wee XK, Ng KS, Leung HW, Cheong YP, Kong KH, Ng FM, Soh W, Lam Y, Low CM (2010) Mapping the high-affinity binding domain of 5-substituted benzimidazoles to the proximal N-terminus of the GluN2B subunit of the NMDA receptor. Br J Pharmacol 159:449-461.
Wenzel A, Fritschy JM, Mohler H, Benke D (1997) NMDA receptor heterogeneity during postnatal development of the rat brain: differential expression of the NR2A, NR2B, and NR2C subunit proteins. J Neurochem 68:469-478.
Westphal RS, Tavalin SJ, Lin JW, Alto NM, Fraser ID, Langeberg LK, Sheng M, Scott JD (1999) Regulation of NMDA receptors by an associated phosphatase-kinase signaling complex. Science 285:93-96.
Whitehead KJ, Manning JP, Smith CG, Bowery NG (2001) Determination of the extracellular concentration of glycine in the rat spinal cord dorsal horn by quantitative microdialysis. Brain Res 910:192-194.
Wilcox KS, Fitzsimonds RM, Johnson B, Dichter MA (1996) Glycine regulation of synaptic NMDA receptors in hippocampal neurons. J Neurophysiol 76:3415-3424.
Williams K (1993) Ifenprodil discriminates subtypes of the N-methyl-D-aspartate receptor: selectivity and mechanisms at recombinant heteromeric receptors. Mol Pharmacol 44:851-859.
Williams K (1994) Mechanisms influencing stimulatory effects of spermine at recombinant N-methyl-D-aspartate receptors. Mol Pharmacol 46:161-168.
Williams K (1995) Pharmacological properties of recombinant N-methyl-D-aspartate (NMDA) receptors containing the epsilon 4 (NR2D) subunit. Neurosci Lett 184:181-184.
Williams K (1996) Separating dual effects of zinc at recombinant N-methyl-D-aspartate receptors. Neurosci Lett 215:9-12.
Williams K (1997a) Modulation and block of ion channels: a new biology of polyamines. Cell Signal 9:1-13.

Williams K (1997b) Interactions of polyamines with ion channels. Biochem J 325 (Pt 2):289-297.
Williams K (2001) Ifenprodil, a novel NMDA receptor antagonist: site and mechanism of action. Curr Drug Targets 2:285-298.
Williams K, Kashiwagi K, Fukuchi J, Igarashi K (1995) An acidic amino acid in the N-methyl-D-aspartate receptor that is important for spermine stimulation. Mol Pharmacol 48:1087-1098.
Williams K, Dawson VL, Romano C, Dichter MA, Molinoff PB (1990) Characterization of polyamines having agonist, antagonist, and inverse agonist effects at the polyamine recognition site of the NMDA receptor. Neuron 5:199-208.
Williams K, Pahk AJ, Kashiwagi K, Masuko T, Nguyen ND, Igarashi K (1998) The selectivity filter of the N-methyl-D-aspartate receptor: a tryptophan residue controls block and permeation of Mg2+. Mol Pharmacol 53:933-941.
Winblad B, Poritis N (1999) Memantine in severe dementia: results of the 9M-Best Study (Benefit and efficacy in severely demented patients during treatment with memantine). Int J Geriatr Psychiatry 14:135-146.
Wollmuth LP, Kuner T, Sakmann B (1998) Adjacent asparagines in the NR2-subunit of the NMDA receptor channel control the voltage-dependent block by extracellular Mg2+. J Physiol 506 (Pt 1):13-32.
Wollmuth LP, Kuner T, Seeburg PH, Sakmann B (1996) Differential contribution of the NR1- and NR2A-subunits to the selectivity filter of recombinant NMDA receptor channels. J Physiol 491 (Pt 3):779-797.
Wong E, Ng FM, Yu CY, Lim P, Lim LH, Traynelis SF, Low CM (2005) Expression and characterization of soluble amino-terminal domain of NR2B subunit of N-methyl-D-aspartate receptor. Protein Sci 14:2275-2283.
Wong EH, Kemp JA, Priestley T, Knight AR, Woodruff GN, Iversen LL (1986) The anticonvulsant MK-801 is a potent N-methyl-D-aspartate antagonist. Proc Natl Acad Sci U S A 83:7104-7108.
Wong HK, Liu XB, Matos MF, Chan SF, Perez-Otano I, Boysen M, Cui J, Nakanishi N, Trimmer JS, Jones EG, Lipton SA, Sucher NJ (2002) Temporal and regional expression of NMDA receptor subunit NR3A in the mammalian brain. J Comp Neurol 450:303-317.
Woodward RM, Huettner JE, Guastella J, Keana JF, Weber E (1995) In vitro pharmacology of ACEA-1021 and ACEA-1031: systemically active quinoxalinediones with high affinity and selectivity for N-methyl-D-aspartate receptor glycine sites. Mol Pharmacol 47:568-581.
Wu HY, Hsu FC, Gleichman AJ, Baconguis I, Coulter DA, Lynch DR (2007) Fyn-mediated phosphorylation of NR2B Tyr-1336 controls calpain-mediated NR2B cleavage in neurons and heterologous systems. J Biol Chem 282:20075-20087.
Wu HY, Yuen EY, Lu YF, Matsushita M, Matsui H, Yan Z, Tomizawa K (2005) Regulation of N-methyl-D-aspartate receptors by calpain in cortical neurons. J Biol Chem 280:21588-21593.
Wyllie DJ, Behe P, Colquhoun D (1998) Single-channel activations and concentration jumps: comparison of recombinant NR1a/NR2A and NR1a/NR2D NMDA receptors. J Physiol 510 (Pt 1):1-18.
Wyszynski M, Lin J, Rao A, Nigh E, Beggs AH, Craig AM, Sheng M (1997) Competitive binding of alpha-actinin and calmodulin to the NMDA receptor. Nature 385:439-442.
Xi G, Keep RF, Hoff JT (2006) Mechanisms of brain injury after intracerebral haemorrhage. Lancet Neurol 5:53-63.
Xi G, Keep RF, Hua Y, Xiang J, Hoff JT (1999) Attenuation of thrombin-induced brain edema by cerebral thrombin preconditioning. Stroke 30:1247-1255.
Xiong ZG, Raouf R, Lu WY, Wang LY, Orser BA, Dudek EM, Browning MD, MacDonald JF (1998) Regulation of N-methyl-D-aspartate receptor function by constitutively active protein kinase C. Mol Pharmacol 54:1055-1063.

Xue M, Hollenberg MD, Yong VW (2006) Combination of thrombin and matrix metalloproteinase-9 exacerbates neurotoxicity in cell culture and intracerebral hemorrhage in mice. J Neurosci 26:10281-10291.

Xue M, Hollenberg MD, Demchuk A, Yong VW (2009) Relative importance of proteinase-activated receptor-1 versus matrix metalloproteinases in intracerebral hemorrhage-mediated neurotoxicity in mice. Stroke 40:2199-2204.

Yager JY, Brucklacher RM, Vannucci RC (1991) Cerebral oxidative metabolism and redox state during hypoxia-ischemia and early recovery in immature rats. Am J Physiol 261:H1102-1108.

Yamada T, Nagai Y (1996) Immunohistochemical studies of human tissues with antibody to factor Xa. Histochem J 28:73-77.

Yang S, Song S, Hua Y, Nakamura T, Keep RF, Xi G (2008) Effects of thrombin on neurogenesis after intracerebral hemorrhage. Stroke 39:2079-2084.

Yao Y, Mayer ML (2006) Characterization of a soluble ligand binding domain of the NMDA receptor regulatory subunit NR3A. J Neurosci 26:4559-4566.

Yashiro K, Philpot BD (2008) Regulation of NMDA receptor subunit expression and its implications for LTD, LTP, and metaplasticity. Neuropharmacology 55:1081-1094.

Yin X, Wright J, Wall T, Grammas P (2010) Brain endothelial cells synthesize neurotoxic thrombin in Alzheimer's disease. Am J Pathol 176:1600-1606.

Yuan H, Erreger K, Dravid SM, Traynelis SF (2005) Conserved structural and functional control of N-methyl-D-aspartate receptor gating by transmembrane domain M3. J Biol Chem 280:29708-29716.

Yuan H, Hansen KB, Vance KM, Ogden KK, Traynelis SF (2009a) Control of NMDA receptor function by the NR2 subunit amino-terminal domain. J Neurosci 29:12045-12058.

Yuan H, Vance KM, Junge CE, Geballe MT, Snyder JP, Hepler JR, Yepes M, Low CM, Traynelis SF (2009b) The serine protease plasmin cleaves the amino-terminal domain of the NR2A subunit to relieve zinc inhibition of the N-methyl-D-aspartate receptors. J Biol Chem 284:12862-12873.

Yuen EY, Ren Y, Yan Z (2008) Postsynaptic density-95 (PSD-95) and calcineurin control the sensitivity of N-methyl-D-aspartate receptors to calpain cleavage in cortical neurons. Mol Pharmacol 74:360-370.

Zandi MS, Irani SR, Follows G, Moody AM, Molyneux P, Vincent A (2009) Limbic encephalitis associated with antibodies to the NMDA receptor in Hodgkin lymphoma. Neurology 73:2039-2040.

Zhang J, Diamond JS (2009) Subunit- and pathway-specific localization of NMDA receptors and scaffolding proteins at ganglion cell synapses in rat retina. J Neurosci 29:4274-4286.

Zhang S, Ehlers MD, Bernhardt JP, Su CT, Huganir RL (1998) Calmodulin mediates calcium-dependent inactivation of N-methyl-D-aspartate receptors. Neuron 21:443-453.

Zhang W, Howe JR, Popescu GK (2008) Distinct gating modes determine the biphasic relaxation of NMDA receptor currents. Nat Neurosci 11:1373-1375.

Zheng F, Gingrich MB, Traynelis SF, Conn PJ (1998) Tyrosine kinase potentiates NMDA receptor currents by reducing tonic zinc inhibition. Nat Neurosci 1:185-191.

Zheng F, Erreger K, Low CM, Banke T, Lee CJ, Conn PJ, Traynelis SF (2001) Allosteric interaction between the amino terminal domain and the ligand binding domain of NR2A. Nat Neurosci 4:894-901.

Zheng X, Zhang L, Durand GM, Bennett MV, Zukin RS (1994) Mutagenesis rescues spermine and Zn2+ potentiation of recombinant NMDA receptors. Neuron 12:811-818.